



Nuclear Hormone Receptors and Fibroblast Growth Factor Receptor
Signaling in *Echinococcus multilocularis*

Signalwege in *Echinococcus multilocularis* am Beispiel der Nukleären Hormonrezeptoren und
des *Fibroblast Growth Factor* Rezeptors

Doctoral thesis for a doctoral degree
at the Graduate School of Life Sciences,
Julius-Maximilians-Universität Würzburg,
Section Infection and Immunity

submitted by

Sabine Förster

from

Zeit

Würzburg 2012

Submitted on:
(Office stamp)

Members of the *Promotionskomitee*:

Chairperson: Prof. Dr. Jörg Schultz

Primary Supervisor: Prof. Dr. Klaus Brehm

Supervisor (Second): Prof. Dr. Roy Gross

Supervisor (Third): Dr. Nicolai Siegel

Date of Public Defense:

Date of receipt of Certificates:

Affidavit
(Eidesstattliche Erklärung)

I hereby declare that my thesis entitled

Nuclear Hormone Receptors and Fibroblast Growth Factor Receptor Signaling in
Echinococcus multilocularis

is the result of my own work. I did not receive any help or support from commercial consultants. All sources and / or materials are listed and specified in the thesis.

Furthermore, I verify that this thesis, has not yet been submitted as part of another examination process neither in identical nor in similar form.

Würzburg.....

Date

Signature

List of content

1.	Abstract	1
2.	Zusammenfassung	2
3.	Introduction	3
3.1.	The small fox-tapeworm <i>Echinococcus multilocularis</i>	3
3.1.1.	Phylogeny and epidemiology	3
3.1.2.	Biology and the life cycle of <i>E. multilocularis</i>	5
3.1.3.	Clinical manifestation – Alveolar Echinococcosis	6
3.2.	Host-parasite relationship	8
3.2.1.	Biochemical and molecular biological approaches	8
3.2.2.	Cultivation of <i>E. multilocularis</i>	8
3.2.3.	Evolutionary conserved signaling cascades in <i>E. multilocularis</i>	9
3.3.	Fibroblast growth factors (FGF) and FGF receptors (FGFRs)	11
3.3.1.	Diversity and function of FGF and FGFRs	11
3.3.2.	FGFRs in platyhelminthes and nematodes	12
3.4.	Nuclear hormone receptor (NHR) signaling	15
3.4.1.	Function and structure of NHRs	15
3.4.2.	NHRs in parasitichelminths	16
3.5.	Objectives	17
4.	Materials and Methods	18
4.1.	Material	18
4.1.1.	Equipment	18
4.1.2.	Consumables	19
4.1.3.	Chemicals, Enzymes and Solutions	19
4.1.4.	Commercial Kits	21
4.2.	Oligonucleotides	21
4.3.	Determination of nucleic acid concentration and purity	25
4.4.	RNA applications	25
4.4.1.	Isolation and purification of total RNA from <i>E. multilocularis</i>	25
4.4.2.	First strand cDNA synthesis	25
4.5.	DNA procedures	26
4.5.1.	Isolation and purification of chromosomal DNA from the metacestodes	26
4.5.2.	Isolation of plasmid DNA from <i>E. coli</i>	26
4.5.3.	Gel electrophoresis of DNA	26
4.5.4.	Purification and DNA precipitation	26
4.5.5.	Sequencing of DNA	27
4.5.6.	Amplification of DNA via PCR	27
4.5.7.	Rapid amplification of cDNA ends (RACE)	27
4.5.8.	Semi-quantitative RT PCR	28
4.5.9.	PCR based mutagenesis	28
4.5.10.	TA cloning	29
4.5.11.	Colony-PCR	29
4.5.12.	Restriction digest of DNA	29

4.5.13.	Ligation of DNA fragments	29
4.6.	Protein analysis	30
4.6.1.	Determination of protein concentration	30
4.6.2.	SDS-PAGE	30
4.6.3.	Coomassie staining of protein gels	31
4.6.4.	Silver staining of protein gels	31
4.6.5.	Western blotting	31
4.6.6.	Mass spectrometry	32
4.7.	Working with bacteria	33
4.7.1.	Bacteria strains and media	33
4.7.2.	Chemically competent <i>E. coli</i>	33
4.7.3.	<i>E. coli</i> transformation	34
4.7.4.	Heterologous expression in <i>E. coli</i> and purification of the recombinant proteins	34
4.8.	Working with yeast	36
4.8.1.	Yeast strains and media	36
	Yeast-two hybrid analysis	37
4.8.2.	Liquid culture β -galactosidase assay	38
4.9.	Working with mammalian cell lines	39
4.9.1.	Cell lines and media	39
4.9.2.	Cultivation of RH- cells under serum-free conditions: Panserin TM 401	39
4.9.3.	Transfection of HEK293 cells	39
4.10.	Transfection and treatment of <i>Xenopus laevis</i> oocytes	40
4.11.	Working with <i>E. multilocularis</i>	41
4.11.1.	<i>E. multilocularis</i> isolates	41
4.11.2.	In vivo cultivation of metacestode larvae and isolation from Mongolian jirds	41
4.11.3.	Isolation and activation of protoscoleces	41
4.11.4.	In vitro cultivation of metacestode larvae	42
4.11.5.	In vitro cultivation and treatment of activated protoscoleces	43
4.11.6.	Treatment of the metacestode vesicles	43
4.11.7.	Isolation and cultivation of <i>E. multilocularis</i> primary cells	43
4.11.8.	Treatment of <i>E. multilocularis</i> primary cells	44
4.11.9.	Verification of purity of <i>Echinococcus</i> material	44
4.11.10.	BrdU-Proliferation Assay	44
4.11.11.	siRNA knock-down of EmFR	45
4.12.	Computer analyses and statistics	46
4.12.1.	Iterative BLAST for the identification of putative <i>E. multilocularis</i> NHRs	46
4.13.	Ethics Statement	47
5.	Results	48
5.1.	FGFR signaling - EmFR	48
5.1.1.	EmFR expression analysis in <i>Echinococcus</i> larval stages	48
5.1.2.	Protein-protein-interactions studies of the intracellular domain of EmFR	49
5.1.3.	Host derived FGFs stimulate <i>de novo</i> DNA Synthesis in <i>Echinococcus</i> larvae in vitro	50
5.1.4.	Growth and development of <i>E. multilocularis</i> is stimulated by host FGFs in vitro – primary cells	51

5.1.5.	Targeting the FGF signaling pathway of <i>E. multilocularis</i> : BIBF1120– effects on metacestode vesicles and primary cells -----	52
5.1.6.	The effect of host FGFs and BIBF1120 on in vitro cultivated protoscoleces -----	55
5.1.7.	Targeting the FGF signaling pathway of <i>E. multilocularis</i> : SU5042– effects on metacestode vesicles and primary cells -----	58
5.1.8.	siRNA knock-down of EmFR – preliminary data -----	61
5.1.9.	EmFR is activated by aFGF and bFGF, leading to MAP-kinase signaling in <i>Xenopus laevis</i> oocytes -----	63
5.1.10.	Phosphorylation status of EmMPK1 in metacestodes and primary cells -----	65
5.1.11.	Phosphorylation status of EmAkt in metacestode vesicles and primary cells -----	67
5.1.12.	The <i>E. multilocularis</i> genome does not encode for own canonical FGFs -----	68
5.2.	NHR signaling – EmNHR1 -----	69
5.2.1.	Expression analysis of <i>Emnhr1</i> in <i>Echinococcus</i> larval stages -----	69
5.2.2.	Recombinantly expressed EmNHR1 – an attempt to raise a specific antibody -----	70
5.2.3.	Protein-protein interaction studies of EmNHR1 and its domains: LBD and DBD -----	71
5.2.4.	EmNHR1-LBD dimerization studies -----	72
5.2.5.	Effect of bile salts and conjugated bile salts on axenically cultivated metacestode vesicles -----	74
5.3.	NHR signaling – other putative EmNHRs -----	76
5.3.1.	<i>In silico</i> analysis and identification of putative <i>E. multilocularis</i> NHRs -----	76
5.3.2.	Expression of other EmNHRs in <i>Echinococcus</i> larval stages -----	81
5.4.	NHR signaling – EmHNF4 -----	82
5.4.1.	Isolation and characterization of the <i>Emhnf4</i> cDNA and the genomic locus -----	82
5.4.2.	Expression analysis <i>Emhnf4a</i> and <i>Emhnf4b</i> in <i>Echinococcus</i> larval stages -----	86
5.4.3.	Protein-protein interaction studies of EmHNF4 -----	86
5.5.	Serum-free cultivation of <i>E. multilocularis</i> -----	88
5.5.1.	Adaptation of RH- to serum free conditions -----	88
5.5.2.	Co-cultivation of <i>E. multilocularis</i> under serum-free conditions and in vivo passage --	90
5.5.3.	Axenic cultivation of metacestode vesicles and cultivation of primary cells under serum-free conditions -----	92
5.5.4.	Influence of insulin and serotonin on axenic metacestode vesicles cultured in Panserin™401 -----	93
5.5.5.	Cultivation of primary cells in serum-free Panserin™401 -----	97
5.5.6.	Mass spectrometry and Western blot analyses of pre-conditioned Panserin™401 ----	99
5.6.	EmMPK3 – a serum-responsive MAPK -----	101
5.6.1.	Phosphorylation of EmMPK3 is not induced by serum in metacestode vesicles, dormant and activated protoscoleces -----	101
5.6.2.	Expression analysis of <i>Emmpk3</i> -----	102
6.	Discussion -----	104
6.1.	FGFR signaling - EmFR -----	104
6.2.	NHR signaling – EmNHR1, EmHNF4 and other putative EmNHRs -----	109
6.3.	Serum-free cultivation of <i>E. multilocularis</i> -----	114
6.4.	EmMPK3 – a serum-responsive MAPK -----	115
7.	Supplement -----	117

7.1.	Full length cDNA sequence of <i>Emnhr1</i> (isolate H95)-----	117
7.2.	Full length cDNA sequences of <i>Emhnf4a</i> and <i>Emhnf4b</i> -----	118
7.3.	LBD sequences of <i>E. multilocularis</i> NHRs from <i>in silico</i> analysis -----	120
7.4.	Putative amino acid sequence of EmNDK -----	122
8.	List of Abbreviations -----	123
9.	References -----	127
10.	Acknowledgement – Danksagung -----	139
11.	Publications -----	141
11.1.	Original Publications-----	141
11.2.	Conference Contributions-----	142
11.2.1.	Talks -----	142
11.2.2.	Poster -----	143
12.	Curriculum Vitae -----	144

1. Abstract

Parasitic helminths share a large degree of common genetic heritage with their various hosts. This includes cell-cell-communication mechanisms mediated by small peptide cytokines and lipophilic/steroid hormones. These cytokines are candidate molecules for host-parasite cross-communication in helminth diseases. In this work the function of two evolutionary conserved signaling pathways in the model cestode *Echinococcus multilocularis* has been studied.

First, signaling mechanisms mediated through fibroblast growth factors (FGF) and their cognate receptors (FGFR) which influence a multitude of biological functions, like homeostasis and differentiation, were studied. I herein investigated the role of EmFR which is the only FGFR homolog in *E. multilocularis*. Functional analyses using the *Xenopus* oocyte expression system clearly indicate that EmFR can sense both acidic and basic FGF of human origin, resulting in an activation of the EmFR tyrosine kinase domain. In vitro experiments demonstrate that mammalian FGF significantly stimulates proliferation and development of *E. multilocularis* metacestode vesicles and primary cells. Furthermore, DNA synthesis and the parasite's Erk-like MAPK cascade module was stimulated in the presence of exogenously added mammalian FGF. By using the FGFR inhibitor BIBF1120 the activity of EmFR in the *Xenopus* oocyte system was effectively blocked. Addition of BIBF1120 to in vitro cultivated *Echinococcus* larval material led to detrimental effects concerning the generation of metacestode vesicles from parasite stem cells, the proliferation and survival of metacestode vesicles, and the dedifferentiation of protoscoleces towards the metacestode. In conclusion, these data demonstrate the presence of a functional EmFR-mediated signaling pathway in *E. multilocularis* that is able to interact with host-derived cytokines and that plays an important role in larval parasite development.

Secondly, the role of nuclear hormone receptor (NHR) signaling was addressed. Lipophilic and steroid hormone signaling contributes to the regulation of metazoan development. By means of *in silico* analyses I demonstrate that *E. multilocularis* expresses a set of 17 NHRs that broadly overlaps with that of the related flatworms *Schistosoma mansoni* and *S. japonicum*, but also contains several NHR encoding genes that are unique to this parasite. One of these, EmNHR1, is homolog to the DAF-12/HR-96 subfamily of NHRs which regulate cholesterol homeostasis in metazoans. Modified yeast-two hybrid analyses revealed that host serum contains a ligand which induces homodimerization of the EmNHR1 ligand-binding domain. Also, a HNF4-like homolog, EmHNF4, was characterized. Human HNF4 plays an important role in liver development. RT-PCR experiments showed that both isoforms of the EmHNF4 encoding gene are expressed stage-dependently suggesting distinct functions of the two isoforms in the parasite. Moreover, specific regulatory mechanisms on the convergence of NHR signaling and TGF- β /BMP signaling pathways in *E. multilocularis* have been identified. On the one hand, EmNHR1 directly interacted with the EmSmadC and on the other hand EmHNF4b interacted with EmSmadD, EmSmadE which are all downstream signaling components of the TGF- β /BMP signaling pathway. This suggests cross-communication in order to regulate target gene expression. With these results, further studies on the role of NHR signaling in the cestode will be facilitated.

Also, the first serum-free in vitro cultivation system for *E. multilocularis* was established using Panserin™401 as medium. Serum-free co-cultivation with RH-feeder cells and an axenic cultivation method have been established. With the help of this serum-free cultivation system investigations on the role of specific peptide hormones, like FGFs, or lipophilic/steroid hormones, like cholesterol, for the development of helminths will be much easier.

2. Zusammenfassung

Parasitäre Würmer weisen eine große genetische Verwandtschaft mit ihren Wirten auf. Diese schließt auch Zell-Zell-Kommunikationsmechanismen ein, die sowohl durch Peptidhormone als auch durch lipophile/steroidale Hormone vermittelt werden. Man vermutet, dass diese Stoffe eine wichtige Rolle bei der Wirt-Parasiten-Kreuzkommunikation spielen. Deshalb untersuchte diese Arbeit die Funktion von zwei konservierten Signalwegen im Modellorganismus *Echinococcus multilocularis*.

Der erste Teil dieser Arbeit beschäftigt sich mit den *Fibroblast Growth Factors* (FGF). Diese steuern durch die Bindung an spezifische FGF-Rezeptoren (FGFR) eine Vielzahl von biologischen Funktionen, wie beispielsweise Homöostase- und Differenzierungsprozesse. Zunächst wurde EmFR, das einzige FGFR-Homolog im Fuchsbandwurm in *Xenopus* Oozyten heterolog exprimiert. Dabei wurde nachgewiesen, dass der Rezeptor sowohl *acidic* als auch *basic* FGF erkennen kann und dies zur Aktivierung der Tyrosinkinasedomäne führt. Außerdem förderte im *in vitro* Experiment die exogene Zugabe dieser Wirtsfaktoren die Proliferation und Entwicklung von Metacestodenvesikeln und Primärzellen. Darüber hinaus wurden die DNA-Synthese und die Erk-MAPK-Kaskade des Parasiten stimuliert. Im Gegensatz dazu konnte durch die Hinzugabe des FGFR-Inhibitor BIBF1120 die Aktivität des Rezeptors im *Xenopus* Oozytensystem erfolgreich blockiert werden. Durch den Inhibitor wurde die Regeneration von Metacestodenvesikeln aus Stammzellen, die Proliferation und das Überleben von Metacestodenvesikeln verhindert und eine Dedifferenzierung von Protoskolizes verursacht. Zusammengefasst zeigen diese Daten, dass *E. multilocularis* einen funktionellen durch EmFR-vermittelten Signalweg besitzt, welcher in der Lage ist, mit Wirtszytokinen zu interagieren und eine wichtige Rolle bei der Entwicklung von *Echinococcus* Larvenstadien spielt.

Außerdem wurde die Bedeutung der Nukleären Hormon Rezeptoren (NHR) für den Parasiten untersucht. Lipophile und steroidale Hormone regulieren viele Entwicklungsprozesse in Metazoen. Mittels *in silico* Analyse konnten 17 Rezeptoren der NHR-Familie in *E. multilocularis* identifiziert werden, die größtenteils mit dem NHR Repertoire von *Schistosoma mansoni* und *S. japonicum* übereinstimmen. Allerdings wurden auch Rezeptoren identifiziert, die einzigartig für *E. multilocularis* sind. Einer dieser Rezeptoren, EmNHR1, ist homolog zur DAF-12/HR-96 Familie, die den Cholesterinstoffwechsel in Metazoen reguliert. Yeast-Two Hybrid Experimente zeigten, dass Wirtsserum den putativen Liganden von EmNHR1 enthält, da dessen Zugabe zur Homodimerisierung der EmNHR1-Liganden-bindungsdomäne führte. Außerdem wurde mit EmHNF4 ein weiterer Rezeptor charakterisiert, dessen humanes Homolog die Entwicklung der Leber beeinflusst. RT-PCR-Experimente zeigten, dass die zwei entdeckten Isoformen von EmHNF4 stadienspezifisch exprimiert werden, was auf mögliche Funktionsunterschiede deutet. Darüber hinaus wurde sowohl für EmNHR1, als auch für EmHNF4 beobachtet, dass die DNA-Bindungsdomänen mit Komponenten des TGF- β /BMP-Signalwegs direkte Proteininteraktionen eingehen. Während EmNHR1 mit EmSmadC interagiert, zeigte EmHNF4b eine Reaktion mit EmSmadD und EmSmadE, was auf eine Kreuzkommunikation zwischen beiden Signalwegen deutet. Diese Ergebnisse werden zukünftige Studien bezüglich der Funktion von NHR-Signalwegen in Zestoden deutlich erleichtern.

Weiterhin wurde in dieser Arbeit das erste serum-freie *in vitro* Kultivierungssystem für *E. multilocularis* etabliert. PanserinTM401 diente als Medium sowohl für die Kultur mit Fütterzellen als auch für eine axenische Kulturmethode. Mit Hilfe dieses Systems können in Zukunft Untersuchungen über die Rolle von Peptidhormonen wie FGF, oder lipophilen bzw. steroidal Substanzen, wie Cholesterin, bei der Parasitenentwicklung besser untersucht werden.

3. Introduction

3.1. The small fox-tapeworm *Echinococcus multilocularis*

3.1.1. Phylogeny and epidemiology

The small fox-tapeworm *Echinococcus multilocularis* belongs to the class of Cestoda (Fig. 1) and is the causative agent of Alveolar Echinococcosis (AE).

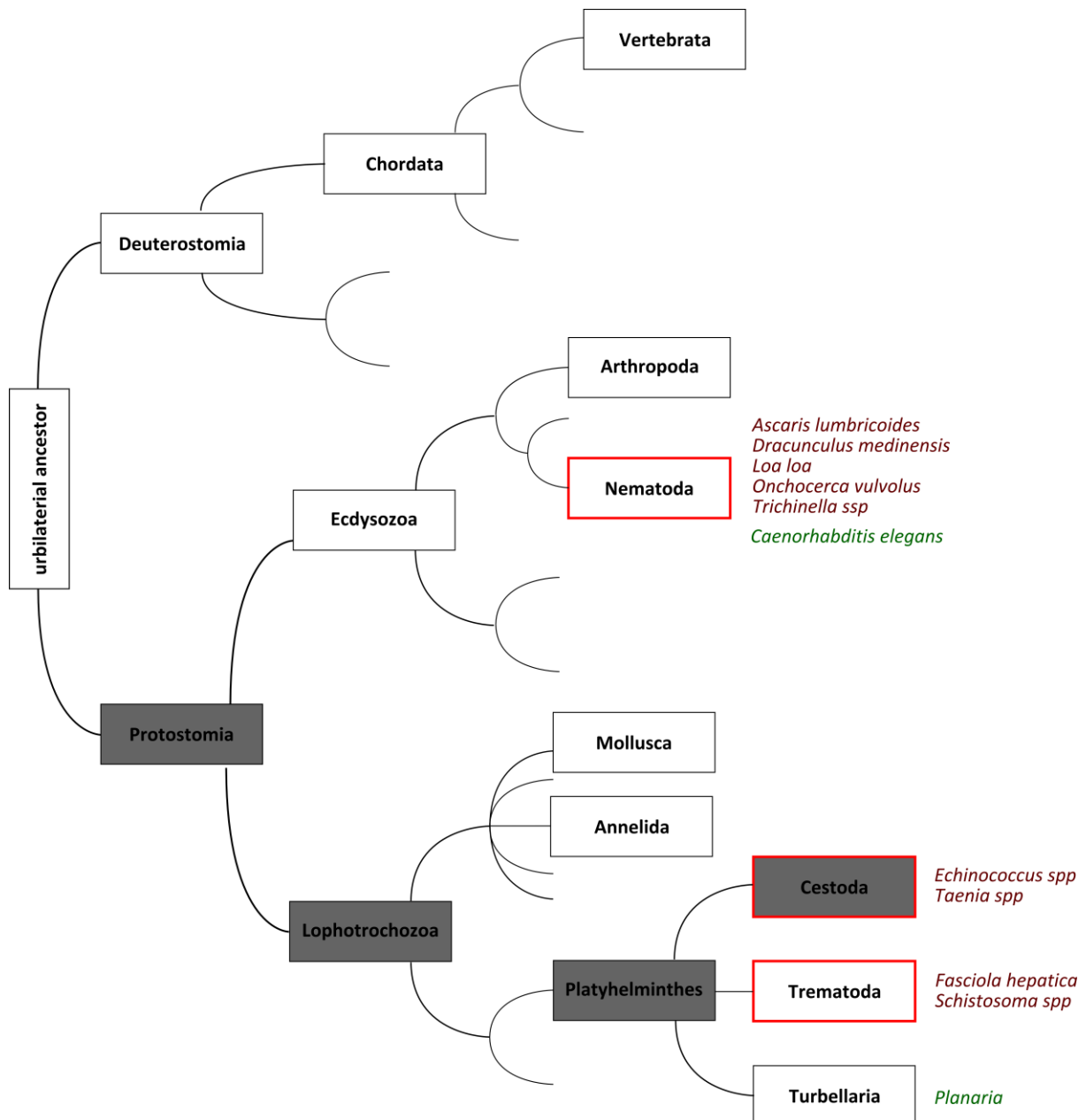


Fig. 1: Phylogenetic position of the genus *Echinococcus* in the tree of life. Species marked in pink are parasitic worms, in green free living worms. Squares in red illustrate the term “helminths”, with the exception of non-parasitic Nematoda [1].

Like all small tapeworms of the genus *Echinococcus*, the adult worm of *E. multilocularis* is an endoparasite residing in the intestine of vertebrates. Its body is segmented into proglottids and comprises adhesive structures like the rostellum or the scolex.

Echinococcus species belongs to the family of Taeniidae which is placed in the order of Cyclophyllidea and the subclass of Eucestoda. Overall, the phylum of Platyhelminthes consists of the classes Cestoda, Turbellaria and Trematoda. They share like all protostomes a bilateral symmetry, the development of three germ layers and during gastrulation the development of the mouth near the gut entrance. For the Turbellaria, all Platyhelminthes are parasites. Yet, the protostomes are divided into two branches: Ecdysozoa and Lophotrochozoa of which the Ecdysozoa include all moulting animals such as the arthropod *Drosophila melanogaster* and the nematode *Ceanorhabditis elegans*. In contrast, the Lophotrochozoa consist of flatworms (Platyhelminthes), Annelida and Mollusca. They are predominantly characterized by spiral cleavage and a prominent digestion system. In contrast to phylogenetic analyses the term “helminthes” is of historic origin and describes all endoparasitic living nematodes and platyhelminthes [1], like the study object of this thesis: *E. multilocularis*.

The genus *Echinococcus* consists of different species causing a variety of clinical outcomes in various final host species. However, only the small fox-tapeworm *E. multilocularis* and the dog-tapeworm *E. granulosus* cause severe zoonotic diseases in humans, that is AE and cystic echinococcosis (CE), respectively [2]. Other species are: *E. vogeli*, *E. shiquicus*, *E. oligarthrus*, *E. felidis* [3]. Throughout the last years, the taxonomic classification of the various *E. granulosus* strains (G1-G10) was extensively discussed and some strains are thought to be separate species [4]. In detail, *E. granulosus* strain G1 is termed *E. granulosus sensu stricto*, strain G4 *E. equinus* and strain G5 *E. ortleppi*, respectively [4,5]. Other strains like the cervid strain G10 and the pig strain G7 including G9 were grouped together with the non-European strains G6 in a single monophyletic group [2]. Yet, for the genotypes (G6, G7 and G9) the term *E. intermedius* and for G8/G10 *E. canadensis* has been proposed [6,7]. In contrast to the *E. granulosus* strains, there is no evidence for species differentiation in *E. multilocularis* which is considered to be genetically conservative [8,9].

E. multilocularis is endemic in arctic and temperate zones of the Northern Hemisphere, namely in Europe, North America and Asia [10]. As depicted in Fig. 2 *E. multilocularis*, *E. granulosus sensu stricto* and *E. granulosus* strain G7 are endemic in Europe, however with different geographic distributions [11].

Since the last decade of the 20th century it was reported that *E. multilocularis* spread from south-central Europe to central Europe including countries like Denmark, central France, northern Italy and the Balkan states. Most likely this recent spread is caused by high rabies vaccination rates in foxes which lead to an increase of survival rates and population density in foxes, resulting in a higher infection rate with *E. multilocularis* [11,12]. *E. granulosus sensu stricto* is present world-wide as concomitant of sheep farming and is present in Europe in the Mediterranean area, Wales and Bulgaria [11].



Fig. 2: Distribution of the genus *Echinococcus* in Europe. Endemic areas of *E. multilocularis* (A), *E. granulosus sensu stricto* (B) and *E. granulosus* G7(C) [11].

3.1.2. Biology and the life cycle of *E. multilocularis*

E. multilocularis is characterized by a hermaphroditic life cycle which involves two host switches (Fig.3).

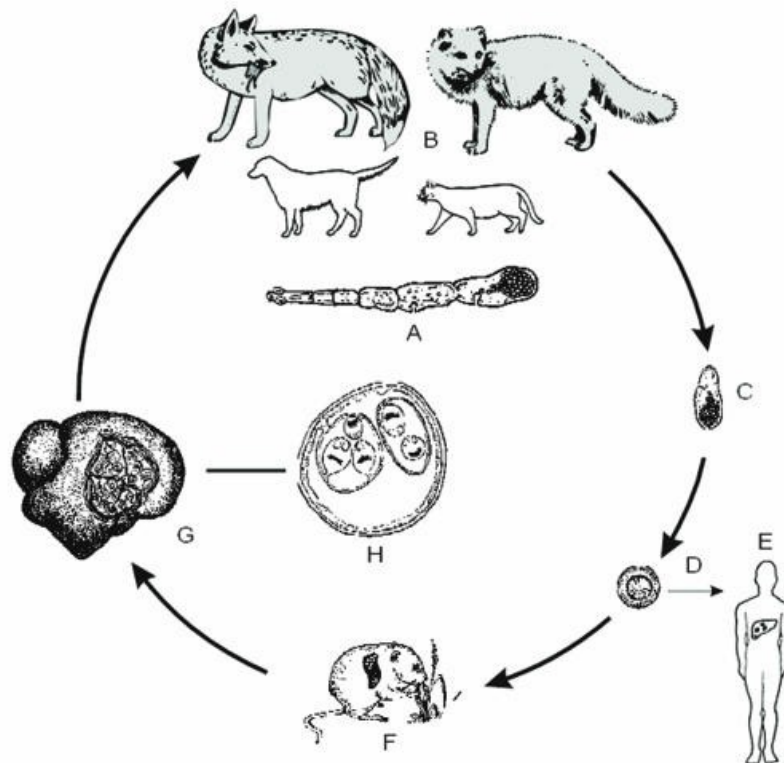


Fig. 3: Life cycle of *E. multilocularis*. The adult worm of *E. multilocularis* (A) resides within the intestine of the definitive host, such as foxes, dogs or cats (B). The segmented worm is producing fertilized, infective eggs (C) in the gravid proglottid. The infective eggs harbor the first larval stage, the oncosphere (D) and are shed with the feces of the final host. Normally these are ingested by an intermediate host (F), mostly small rodents. Then the oncosphere gets activated by the passage through the stomach and the gut. Subsequently it actively penetrates the gut epithelium, and reaches small mesenteric veins, eventually being transported in the blood flow to the liver, where it develops to the third larval stage, the metacestode vesicle (G). After some time, protoscoleces develop in the metacestode vesicle. Once the final host takes up the intermediate host as a prey, the protoscoleces are activated and attach to the gut epithelium and develop into an adult worm. Thus, the cycle is closed. The oncosphere can also be taken up accidentally by humans who are considered as dead end host (E). [2]. Schematic drawing taken from [2].

The adult worm resides within the intestine of the carnivore final host and is about 2 - 4 mm in size. The scolex (head region) is comprised of the rostellum and adhesive organs with which the adult worm attaches to the gut wall of red and arctic foxes (genus *Vulpes*), but also dogs and cats as final hosts have been described. The estimated survival time of the *E. multilocularis* in the intestine is approximately six to twelve months and one fox can be infected with up to 200,000 worms without showing any sign of disease [13]. Characteristically, the adult platyhelminth is segmented in five proglottids. The last proglottid is termed gravid proglottid. It is usually enlarged and produces fertilized eggs. These infective eggs which harbor the first larval stage, the so-called oncosphere, are shed with the feces of the definitive host. Upon ingestion of contaminated diet the intermediate host takes them up. Habitually small rodents, but also deer, moose, reindeer and bison have been reported as intermediate hosts [13]. After ingestion the oncosphere hatches from the egg. The oncosphere becomes activated by the passage through the stomach and the intestine. Most likely, the acidic pH and bile salts are involved in this activation process [14]. After activation it penetrates and invades the surrounding tissue and subsequently enters the mesenteric veins leading into the portal vein. From there, the oncosphere is transported by the blood flow to the liver. In the majority of all cases, the oncosphere develops within the liver to the second larval stage, the metacestode [15,16]. Characteristically, the metacestode is a fluid filled vesicle termed hydatid cyst which consists of an inner germinal layer and an outer acellular laminated layer. Main components of the laminated layer are carbohydrates [17,18] and high molecular weight glycans [19] which both are thought to be a protective shield against the intermediate host's immune response [2]. The cells of the germinal layer proliferate, leading to the growth of the metacestode vesicle. By exogenous budding daughter cysts appear [13,20]. This leads to an infiltrative growth in the surrounding tissue and causes the typical tumor-like appearance inside the infected organs. Within the metacestode vesicle approximately 6 weeks post-infection with the oncosphere the third larval stage, the protoscolex develops in a so-called brood capsule and is characterized by its invaginated head structures. Once the intermediate host is taken up by the final host, as they are in a predator-prey-relationship, the protoscolexes are activated and develop into the adult worm attached to the gut epithelium of the final host. The life cycle is closed. Signal triggering the evagination of protoscolexes are thought to be low pH and bile salts while passing through the stomach and the gut [15]. Around one week after settlement, the first proglottids are produced and the first oncospheres are synthesized after another five weeks [15].

3.1.3. Clinical manifestation – Alveolar Echinococcosis

When infective eggs are accidentally taken up by humans the life cycle is interrupted. Therefore, humans are considered as dead end hosts. Like in normal intermediate hosts the oncosphere will get activated by the passage through the stomach and the gut. Subsequently, it will manifest itself in the liver and develop into metacestode tissue, which is characterized by infiltrative, tumor-like growth, accompanied by metastasis formation in secondary organs like brain and lung during long-term infections [15,21]. Interestingly, only 10 % of all individuals exposed to *E. multilocularis* develop active AE [2]. However, for those that develop AE the lethality rate is about 96% if untreated [13]. The major obstacle in diagnosis of AE is that early infection appears clinically asymptomatic. Estimated time frame from infection to AE diagnosis is usually years to decades [13]. Therefore, the primary source of infection is hard to determine. People which have very high risk of transmission are individuals like hunters, farmers, and gardeners and particularly dog owners because of the close

contact to animals or contaminated material [22]. The prevalence of AE in central Europe is between two and 40 cases per 100,000 habitants [11].

While early infection is asymptomatic, the first signs of infection resemble that of a hepatic infection. Abdominal and pleural pain, vomiting, fever, anemia, weight loss and icterus are common symptoms. In this case, the metacestode tissue has extensively proliferated, has caused liver damage by inducing necrosis and has very likely formed metastasis. This phase of disease is characterized by an intensified inflammatory response of the immune system. While in the early stage of infection cytokines of a T_H1 profile are predominant, namely IL-12, TNF- α and INF- γ , in the late phase of infection a T_H2 immune response takes over with high levels of IL-4, IL-5, IL-6, IL-10 and INF- γ [2,23-26].

The probability to be cured profoundly depends on the time point of diagnosis and adequate treatment. If AE is diagnosed within the first 10 years after infection, survival rates are above 30 %, while after 15 years they are 0 % [13]. Diagnosis is usually based on imaging techniques, like ultrasound or computer tomography and serological methods[13]. The detection of parasite specific antigens is of utter importance for primary diagnosis. For example the antigen Em2 which was isolated from the metacestode cyst is successfully used for the detection of human AE via enzyme-linked immunosorbent assay (ELISA) [27].

Treatment options are very limited for AE patient. In the case of early diagnosis a radical surgery might be an option. However, due to the infiltrative growth of the metacestode tissue this solution is very complicated. Also liver transplantation harbors high risks, because residual material that might be present in the patient's body will show an accelerated growth due to the immunosuppressant medication going along with transplantation. On the other hand chemotherapy is based on benzimidazole compounds. Unfortunately those drugs, like mebendazole and albendazole are rather parasitostatic than parasitocidal. Hence medication must be administered lifelong, also in case of incomplete resection[28]. Yet, the patients have to be examined over a long period of time by aiming tests and suffer from enormous side effects of the drugs, e.g. neurological deficit, gastrointestinal disorders, decreased numbers of leukocytes and thrombocytes, fever, urticaria, and bone marrow toxicity [29].

3.2. Host-parasite relationship

3.2.1. Biochemical and molecular biological approaches

The clinical entity of AE was first described in 1852 and 1855 by the German pathologists Ludwig Buhl and Rudolf Virchow, respectively [30,31]. Virchow suggested AE to be of echinococcal origin, but did not recognize the causing agent as own *Echinococcus* species although the clinical manifestation was rather unusual. Later in 1863 Rudolf Leuckart stated the agent causing the pathology from the reported case by Virchow was a morphologically different form compared to the known echinococcosis disease and thus named it "*Echinococcus multilocularis*". Nonetheless, it took almost 140 years to get first insights into the molecular biology of *E. multilocularis*. First, investigations focused on the identification of diagnostic markers for AE. From these efforts, the recombinant antigens Em2, Em10, Em13, Em16 and Em18 were identified and verified as suitable indicators [32-35]. Later on, also molecular studies were conducted. The *Emelp* (*E. multilocularis* ezrin-radixin-moesin-like protein) gene locus was analyzed in 1999 and gave first knowledge about gene organization and expression of echinococcal genes [36]. EmElp, from which the recombinant antigens Em10, Em4, Em11/3 and Em18 derive, belongs to the ezrin-radixin-moesin (ERM) cytoskeleton family it is involved in the cytoskeletal organization and developmental processes dependent on Rho and PKB signal transduction [37,38]. In 2000, the mechanism of trans-splicing was described for *E. multilocularis* [39]. Next to the conventional cis-splicing process in which exons from a pre-mature mRNA are fused by excision of introns from the same RNA strand, trans-splicing is characterized by the fusion of a mini-exon of a small nucleolar pre-mRNA, the so-called spliced leader (SL) with the 5' end exon of a different mRNA. In *E. multilocularis* only one 36 bp long SL is present and approximately 30 % of all transcripts are recognized as trans-spliced entities. Trans-splicing was first reported in kinetoplastid protozoans in 1986 where all mRNA carry an identical SL [40]. In contrast, in the nematode *C. elegans* two different SL, SL1 and SL2, are present and found at the 5' end of 60% and 10% of the mRNAs, respectively [41-43]. Meanwhile, among cestodes trans-splicing has also been reported for *E. granulosus* and *T. solium* [39,44,45]. While for trypanosomes trans-splicing is clearly needed to resolve polycistronic transcription units into monocistronic transcripts it is yet unsolved what the particular function in flatworms is. The mechanism of trans-splicing might serve as a yet unknown process of gene regulation in these organisms. Recent, preliminary data from the *E. multilocularis* genome project, however, clearly indicated that polycistronic transcription units are also present in cestodes and exclusively affect trans-spliced genes (Kiss F, Brehm K, unpublished results).

3.2.2. Cultivation of *E. multilocularis*

The establishment of an in vitro cultivation system for *E. multilocularis* considerably facilitated the molecular analysis of the parasite and its interactions with the host. In 1996, the first in vitro cultivation system was introduced by Jura et al. [46], in which metacestode vesicles were grown in the presence of either rat or human hepatocytes surrounded by two layers of collagen. Later, in a similar system hepatoma cell lines were applied as feeder cells [47]. Host factors which were secreted by the hepatocytes or hepatoma cell lines helped the parasite to proliferate and to differentiate in vitro. Within one or two weeks small vesicles of 1 - 2 mm in diameter developed. The

development of brood capsules and eventually protoscolex formation took up to three months. On the one hand the step-wise development of the metacystode vesicle was clearly observed by means of this system. But on the other hand it was not possible to discriminate between direct and indirect effects as the feeder cells were always present. Once peptide hormones or steroid / lipophilic hormones are applied they might also influence the feeder cells. Therefore, investigations have been made to establish an axenic cultivation system devoid of these feeder cells [48]. In this modified system the metacystode vesicles were kept under low oxygen and mild reducing conditions. In addition the vesicles were grown in medium which was preconditioned by hepatocytes and allowed growth for several months. This system helps to investigate the effect caused by host derived substances on the developmental process of *E. multilocularis*. More recently a culture system for *E. multilocularis* primary cells was introduced [49,50]. Upon isolation of primary cells an incubation period of approximately five weeks either under axenic conditions or in the presence of physically separated feeder cells resulted in newly formed metacystode vesicles. Those vesicles were infective as they caused lesions when applied into the peritoneum of mice. In the future, primary cells could possibly be a target for genetic manipulation in order to generate transgenic parasites. Altogether the cultivation methods at hand significantly facilitate studies on host-parasite communication and parasite development under in vitro conditions.

3.2.3. Evolutionary conserved signaling cascades in *E. multilocularis*

Parasitichelminths like *E. multilocularis* share a large degree of common genetic heritage with their various vertebrate or non-vertebrate hosts. This includes basic cellular functions, proteins and also conserved cell-cell-communication mechanisms which involve cytokines and hormones. A basic set of cytokine/hormonal cell-cell-communication systems already evolved in the most primitive animals like sponges and is still used by many animals. Therefore, in recent years studies have been performed to investigate the molecular signaling mechanisms in various parasitichelminths. For *E. multilocularis* it has successfully been shown that signaling systems involve surface RTK like the insulin- or the epidermal growth factor (EGF) receptors and serine/threonine kinases like the transforming growth factor- β (TGF- β) receptors. Not surprisingly homologues of proteins which are responsible for down-stream transduction of external stimuli of these surface receptors were also identified. Small GTP-binding proteins, members of the MAPK cascade and multiple Smad molecules are of significance, respectively [51-60]. All mentioned pathways are well conserved within the metazoa and are key players in developmental processes. Thus the theory was established that they might also be essential for parasite-host-communication. Indeed it was demonstrated that there are direct interactions between parasite-receptors and corresponding host cytokines: EmIR, a member of the insulin-receptor family with host insulin (Brehm, personal communication), EmER (*E. multilocularis* epidermal growth factor receptor) with host EGF (Gelmedin, personal communication) and EmTR1, a member of the transforming growth factor- β receptor family with host BMP2 [59]. This clearly confirms that *E. multilocularis* utilizes conserved signaling pathways and is, at least in vitro, able to sense host-cytokines via these evolutionary conserved signaling mechanisms [53,56,60]. Moreover, members of the evolutionary conserved NHR family are present in *Echinococcus* as well (section: 3.4.2) [61,62]. Of course, also these proteins could play a role in sensing steroid/lipophilic hormones of the host and influence parasitic development. Hence it is of utmost importance to study conserved signaling pathways to broaden the understanding how host-

parasite interplay functions and thus it might explain the question how the parasite is able to survive within the host depending on host factors and the necessity to circumvent the host immune system.

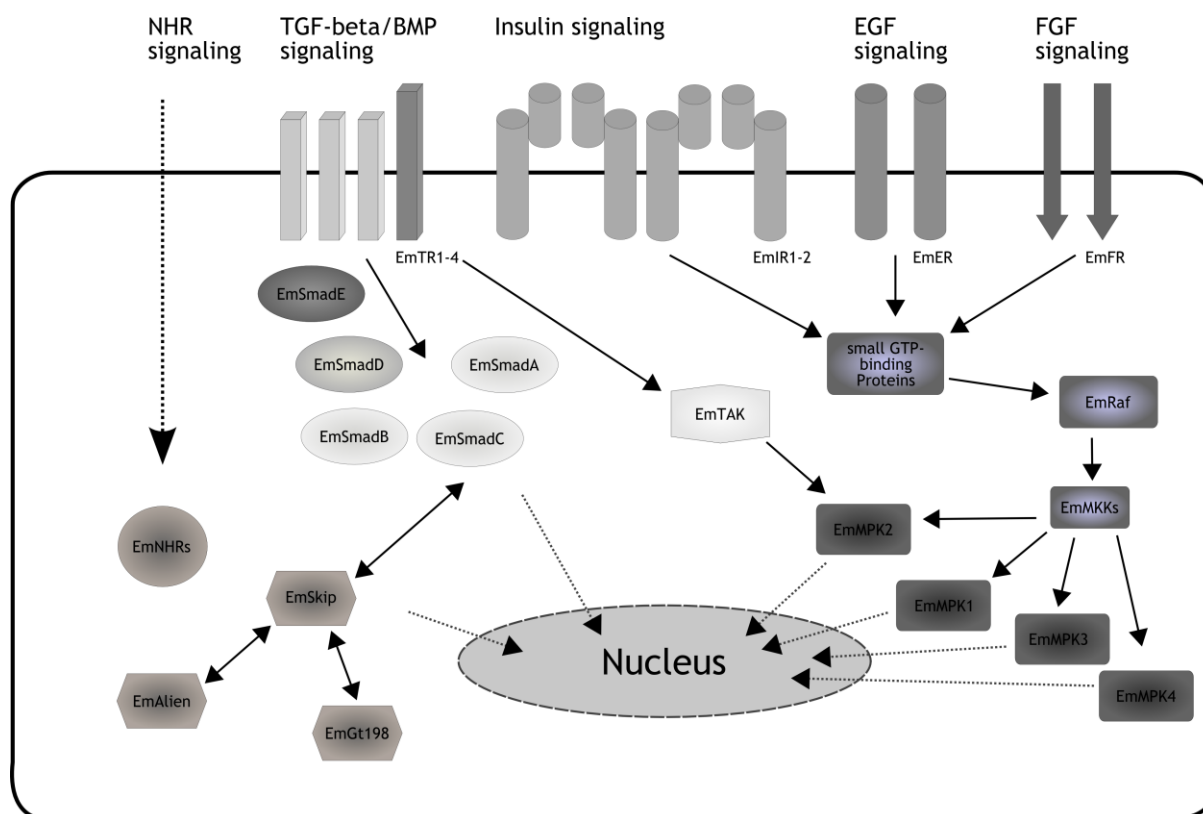


Fig. 4: Conserved signaling systems in *E. multilocularis*. Via EmFR (FGF signaling), EmER (EGF signaling) and EmIR1-2 (Insulin signaling) the MAPK cascade is triggered. Via EmTR1-4 the TGF- β /BMP signaling pathway is activated interacting with different Smad proteins. The presence of NHR signaling is indicated. Unknown ligands might bind to their putative NHRs which are influenced by co-regulators (e.g. EmSkip, EmAlien). EmFR: *Echinococcus multilocularis* FGF Receptor, EmER: *Echinococcus multilocularis* EGF receptor, EmIR1-2: *Echinococcus multilocularis* insulin Receptor 1 and 2, EmTR1-4 *Echinococcus multilocularis* TGF- β /BMP receptors 1 to 4.

3.3. Fibroblast growth factors (FGF) and FGF receptors (FGFRs)

3.3.1. Diversity and function of FGF and FGFRs

FGFs and their specific receptors are highly conserved throughout metazoan evolution [63,64]. They form a complex family of signaling molecules which are widely expressed in embryonic and adult tissue and play an important role in angiogenesis, cellular differentiation and tissue-injury repair [65]. FGFs are polypeptide growth factors interacting with heparin or heparan sulfate proteoglycans which is necessary for FGFs to activate FGFRs effectively [66,67]. The human-mouse FGF family consists of 22 members of which FGF1 (acidic FGF, aFGF) and FGF2 (basic FGF, bFGF) were originally isolated as mitogens for fibroblasts from the brain and pituitary [67].

FGFRs (Fig. 4) are receptor tyrosine kinases (RTK) that contain an extra cellular ligand-binding domain, a transmembrane domain (TM), a juxtamembrane domain (JM) and a split intracellular tyrosine kinase domain (TyrKc). The extra cellular region contains two or three immunoglobulin (Ig)-like domains, and a heparin binding domain [68]. FGFs bind to FGFRs and induce their dimerization and the phosphorylation of specific cytoplasmic tyrosine residues. The fibroblast growth factor receptor substrate 2 (FRS2) is associated with the receptor at the JM domain. The phosphorylation of FGFRs and FRS2 triggers the activation of cytoplasmic signal transduction pathways such as the Ras-MAP kinase pathway which include Erk 1/2, p38 and JNK kinases; the PIP3K/AKT pathway, and the PLC γ pathway [69]. The mentioned pathways are involved in promoting cell cycle progression as the expression of D-type cyclins (e.g. CCND1) is increased and CDK inhibitors such as p27KIP1 are repressed. Moreover, cell survival is affected by the repression of proapoptotic proteins or the increase of the antiapoptotic BCL2-family proteins [70].

Furthermore a fifth FGFR has been described, the fibroblast growth factor receptor like 1 (FGFRL1) [71]. Like the other human FGFR family members, it contains three Ig-like domains. However, the intracellular TyrKc is absent and instead a short histidine-rich motif is present. The gene was not only found in humans, but in all metazoans [72]. FGFs together with heparin also bind to FGFRL1 [73,74] and trigger effects in cell differentiation as well as block cell proliferation [75,76]. Interestingly, FGF1 does not bind to FGFRL1, in contrast to all the other FGFRs [77]. A role in kidney development is suggested because mice with an *Fgfr1* gene deletion have a bilateral kidney agenesis [78]. Moreover, it is believed, that it plays a role in bone formation as human patient with frameshift mutations show craniosynostosis [79]. Most interestingly, FGFRL1 recently attracted attention regarding the fact that the gene shows genomic imprinting [80] and is a key player in stem cell renewal [81]. Considering these facts, the importance of FGFR signaling in developmental processes becomes clear. Still due to its level of complexity a lot of additional functions of the FGF-FGFR signaling pathway have to be understood.

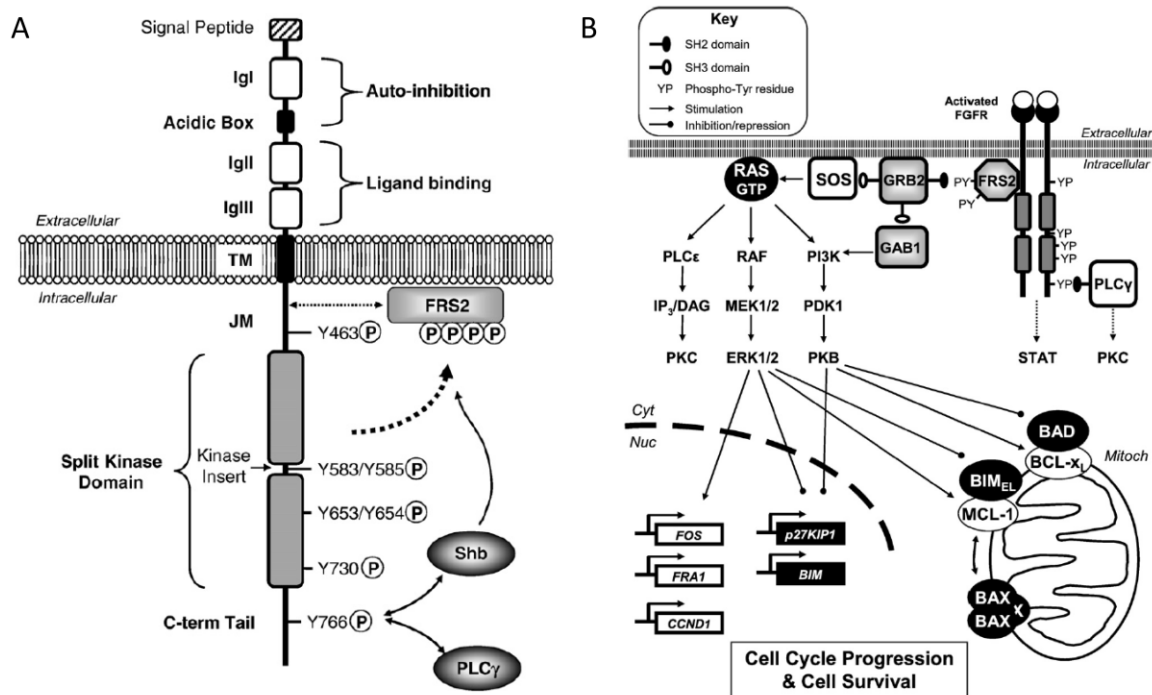


Fig. 5: Schematic representation of the FGFR family (A) and the FGF/FGFR signaling pathway (B) in humans [70]. In this scheme the major tyrosine phosphorylation sites of FGFR1 are depicted. FGFR2, -3 and -4 harbor tyrosine phosphorylation positions which correspond to Y653, Y654, Y730 and T766 in FGFR1. The immunoglobulin-like domain (Ig), acidic box, transmembrane domain (TM), juxtamembrane domain (JM), the split tyrosine kinase domain and the C-terminal cytoplasmatic tail are shown. A trans-phosphorylation takes place upon ligand activation of the FGFR. Subsequently intracellular substrates, like FGFR substrate 2 (FRS2) are recruited and phosphorylated. This allows binding to GRB2, which is associated with the Ras guanine nucleotide exchange factor SOS1/2, and the molecule GAB1, resulting in the activation of the Ras and phosphoinositide-3 kinase (PI3K). Downstream the Raf–MEK1/2–Erk1/2, the PI3K–PKB and the phospholipase C ϵ (PLY ϵ) pathways are activated. Independently of FRS2 also phospholipase C γ (PLC γ) is linked to FGFR signaling. The mentioned pathways are involved in promoting cell cycle progression and cell survival.

3.3.2. FGFRs in platyhelminthes and nematodes

In the platyhelminth *Dugesia japonica* two FGFRs, DjFGFR1 and DjFGFR2, are present [82]. While DjFGFR1 is thought to be responsible for growth, migration and differentiation of undifferentiated and neuronal cells [82], DjFGFR2 plays a role in germ cell development and migration during sexualization [83]. Moreover a gene encoding a fibroblast growth factor receptor (FGFR)-like molecule, nou-darake (NDK), was described by Cebrià et al. [84]. It is specifically expressed in the head region of the planaria and is thought to modulate FGF signaling in stem cells to restrict brain tissues to the head region of planarians.

In the nematode *C. elegans* a single FGFR (EGL-15) with two functionally exclusive isoforms, EGL-15 5A and EGL-15 5B, and two FGFs, LET-756 and EGL-17, have been reported [85,86]. EGL-15 5B plays an important role in viability because null mutations are lethal for the first larval stage of *C. elegans*. This holds also true for LET-756 null mutants [87,88]. A distinct function in the guidance of the migration of sex myoblasts has been described for EGL-15 5A. Null mutations in EGL-15 5A and EGL-17 show specific cell migration and axon maintenance defects [89-93]. Moreover, it was reported that the two different isotypes of EGL-15 are expressed in a tissue specific manner, leading to the assumption that is important in specifying the distinct functions [87,93].

In *E. multilocularis* one FGF-like receptor has been identified EmFR [94]. The deduced amino acid sequence of 562 aa (63kDa) is 41% identical to the FGFR4 of *Rattus norvegicus* and to the FGFR1 of *D. japonica* (data not shown). EmFR shares all common structures of RTKs: a conserved intracellular region TyrKc (sequence alignment, see Fig. 6:), a TM, an extra cellular ligand-binding domain and a signal peptide (Fig. 7). Interestingly, EmFR exhibits only one Ig-like domain, instead of two or three which is accepted knowledge for all other FGFRs.



Fig. 6: Amino acid sequence alignment of tyrosine kinase domains of Fibroblast Growth Factor Receptors. Shown are sequences of *Echinococcus multilocularis* EmFR (residues 288-555), *Dugesia japonica* DjFGFR1 (GI: 20799117; residues 551-818), *D. japonica* DjFGFR2 (GI: 20799119; residues: 558-857), and human HsFGFR3 (GI: 7533125; residues: 360-636). The threshold for identical amino acid residues, which are highlighted in white on black background, is set to 75 %. Similar residues are shaded in grey.

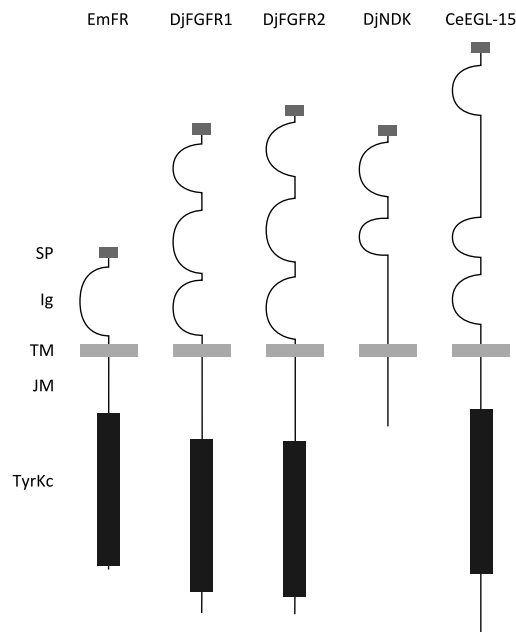


Fig. 7: Schematic drawing of platyhelminth and nematode FGFRs. Domains are indicated as retrieved from the SMART annotation tool [95,96]. Sequences were taken from the original publications: EmFR [94], DjFGFR1 and DjFGFR2 [82], DjNDK [84] and CeEGL-15 [85]. Noteworthy, the membrane proximal Ig-like domain of DjNDK was not indicated by Cebrià et al. SP: Signal peptide, Ig: Immunoglobulin-like domain, TM: transmembrane domain, JM: juxtamembrane domain, TyrKc: Split tyrosine kinase domain.

Expression analysis could show that EmFR is expressed in the metacestode larval stage and in protoscolexes. Furthermore, it was investigated whether human aFGF and bFGF influence the growth and development of metacestodes cysts in vitro. A more pronounced growth stimulating effect of host bFGF over aFGF was observed in a long-term experiment conducted under axenic conditions.

Moreover, after the exogenous addition of host aFGF and bFGF to in vitro cultivated metacestodes a specific phosphorylation of the Erk-like MAP-kinase EmMPK1 was detected. This data hints at the presence of a functional FGF-FGFRs signaling pathway in *E. multilocularis* next to the capability of *E. multilocularis* to sense host FGFs.

Until now, there is no evidence of the existence of other FGFRs or FGFs in either platyhelminthes or parasitic and free-living nematodes.

3.4. Nuclear hormone receptor (NHR) signaling

3.4.1. Function and structure of NHRs

NHRs are DNA-binding transcription factors that are essential in development, differentiation and homeostasis [97]. Apart from their physiological importance these receptors are also involved in tumor genesis, diabetes, or hormone resistance syndromes [98-101].

NHRs form a superfamily of phylogenetically related proteins, encoded by 21 genes in the complete genome of *D. melanogaster*, 48 in humans [102] and, unexpectedly more than 270 genes in the free-living nematode *C. elegans* [103]. In the parasitic trematode *Schistosoma mansoni* 21 members have been identified [104,105].

On the basis of regions of conserved sequence and function NHRs share a universal modular structure that consists of five to six domains, designated A to F, from N-terminus to C-terminus [98]. The N-terminal regulatory domain (region A/B) harbors the activation function 1 (AF1), the activity of which is independent of ligand binding. The DNA-binding domain (DBD, region C) has two zinc finger motifs and is highly conserved among NHRs. The first zinc finger contains the P-box which mediates binding to specific hormone responsive elements (HREs) in the promoter regions of target genes and the second one, known as D-box is involved in receptor dimerization. The so-called variable hinge stretch (region D) follows region C and allows conformational changes in the tertiary structure of the NHR upon ligand binding. It is thought to be responsible for the respective localization of the NHR that is the cytoplasm or the nucleus. The C-terminal ligand-binding domain (LBD, region E) is fairly conserved among NHRs and encloses the activation function 2 (AF2), the activity of which is dependent on the presence of bound ligand [105,106]. Moreover, the LBD is also site of heteromeric interactions with co-regulators, namely co-activators and co-repressors which modulate NHR activities [107]. The mode of action how NHR modulate transcription is quite diverse, involving activation or repression of genes in a ligand-dependent or independent manner [108-111]. It is also described that NHRs can be modified post-translationally [112,113] influencing its functions. In addition, it has been reported that NHR signaling and other signaling pathways, like the TGF- β /BMP pathway cross-communicate. For instance, it was shown that the human Smad3 interacts with the ligand-induced VDR [114].

According to sequence alignments and phylogenetic tree re-construction, human, arthropod and nematode NHRs are divided into six evolutionary groups [115]. The members of the same group share at least 80 – 90 % identity in the DBD and at least 40 – 60% in the LBD. Among the first group the *Homo sapiens* vitamin D3 receptor VDR [116], the pregnane X receptor PXR [117,118] or the constitutive androstane receptor CAR [119] are found. The *C. elegans* DAF-12 receptor and its two paralogs NHR-8 and NHR-48 [120] can be sub-grouped to the ESCKA family of NHRs to which the *H. sapiens* VDR and PXR are the closest vertebrate homologs. Although they are highly related in the DBD, they differ in the DNA recognition helix (P-box) and the LBD. *C. elegans* DAF-12, NHR-8 and NHR 48 also *Pristionchus pacificus* DAF-12 [121] and *Strongyloides stercoralis* DAF-12 [122] (both parasitic nematodes) as well as outside of the flatworms, the *D. melanogaster* DHR96 [123] receptor belong to the ESCKA family. The fact that they share an identical 13 amino acid sequence that comprises the above mentioned DNA recognition helix suggests the recognition of a unique HRE.

The important regulator for hepatocyte differentiation and regulation, the hepatocyte nuclear factor 4 HNF4 [124] belongs to second group of NHRs. Generally, it is a positive transcriptional regulator of multiple hepatocyte genes and involved in the regulation of energy metabolism or bile acid synthesis [125-128]. Interestingly, it binds to the DNA as a homodimer and its ligand are thought to be fatty acyl-CoA thiesters [129]. Its activity is influenced by phosphorylation or acetylation and it was reported that Smad3 and 4 are binding to HNF4, which suggests there is a cross-talk between different signaling pathways [130-132].

3.4.2. NHRs in parasitic helminths

As already mentioned NHRs are present in *S. mansoni*, *P. pacificus* and *S. stercoralis*. Also, for *S. japonicum* NHRs have been reported [133] and it contains roughly the same set of NHRs as *S. mansoni*.

In *S. mansoni*, for instance, members of the nuclear receptor subfamily I, e.g. SmNR1 [134], the retinoid X receptor RXR homologues, SmRXR1 and RXR2 [135-137] and other NHRs, like SmFTZ-F1 α (Fushi tarazu-factor 1 α ; [138] or SmCAR [139] have been described. Moreover, a novel subfamily - 2DBD-NRs - of nuclear receptors containing two DNA-binding domains was reported in 2007 [140,141]. The nuclear receptors of *S. mansoni* interfere with schistosome development as SmRXR1 may have an important role in the regulation of the female-specific p14 genes [137]. Of course other functions are discussed since nuclear receptors regulate homeostasis, differentiation, metamorphosis and reproduction in metazoans. Long before the description of these NHRs in *Schistosoma*, it was recognized that host hormones, including steroids and thyroid hormone, affect parasite growth and metabolism as well as the maturation of larvae in vitro [142]. This indicates a cross-talk of host hormones with parasite receptors.

For *Taenia crassiceps* a regulation of the parasite by host hormones was reported. Hormones such as 17-beta estradiol, progesterone, testosterone or dihydrotestosterone do influence parasite growth and differentiation although only in vitro and at non-physiological concentrations [143,144]. However, no structural evidence for the expression of NHRs in *T. crassiceps* was found so far.

For *E. multilocularis*, it was known that at least three NHRs are present [Brehm, unpublished data], yet these receptors have not been fully characterized. One of them, EmNHR1 [62] contains both a typical DBD and a LBD. It is homolog to the subfamily of NR1 receptors. The EmNHR1 encoding gene, *Emnhr1*, contains 8 exons spanning about 6.5 kb. The cDNA encoding EmNHR1 spans 2.5 kb and the deduced amino acid sequence (651 aa) results in a putative protein of 72 kDa [145]. Furthermore, members of the transcriptional co-regulators have been described in *E. multilocularis*. EmSkip [61] is a member of the SNW/SKIP family and EmNIP1 which is a homolog to the co-repressor Alien [62].

3.5. Objectives

Diseases caused by parasitichelminths result in millions of deaths each year, predominantly in low- and middle-income countries. Among those diseases schistosomiasis, filariasis and cysticercosis are of importance. Also, the zoonotic diseases caused by *Echinococcus* species, especially Cystic Echinococcosis which is due to *E. granulosus* infection, have a significant impact on the global economical situation in the world [146].

With the genome of *E. multilocularis* at hand, and the knowledge that *E. multilocularis* and *E. granulosus* share more than 99 % identity within their genomic sequence, *E. multilocularis* is considered a well-suited model organism to study helminth infections. Especially, with the accessibility of an in vitro cultivations system, *E. multilocularis* is of utter importance to learn about larval cestode development and host-parasite interactions.

Using this system, both early parasite development [50,147], and also late developmental processes [48,49,148,149] can be studied. By these means, it was revealed that parasite development is either influenced by factors secreted by co-cultivated mammalian feeder cells or by substances present in host serum [20,149,150]. Moreover, it is now well established that several evolutionary conserved *Echinococcus* signaling systems for the EGF, the insulin, and the TGF- β /BMP pathways play a role in *E. multilocularis* development [20,150]. Yet, it was described that also a FGFR-FGF signaling pathway [94] as well as a NHR, namely EmNHR1 is present in *E. multilocularis* [145].

However, still a lot of answers regarding FGFR-FGF and NHR signaling have yet to be unraveled. Moreover, there is a constant need to improve the *E. multilocularis* in vitro cultivation system in order tackle even more complex developmental processes in vitro.

Therefore, the following questions were addressed and investigated in this work:

- How many members of the NR family are expressed by *E. multilocularis*?
- What is the role and function of EmNHR1 in particular?
- How do steroids/lipophilic proteins influence the development of the fox-tapeworm?
- In contrast, how do the small FGF molecules influence parasite development?
- Does *E. multilocularis* sense host FGFs, which would suggest parasite-host cross-communication?
- Is the established in vitro cultivation system of *E. multilocularis* adaptable to serum-free conditions applying PanserinTM401?

4. Materials and Methods

4.1. Material

4.1.1. Equipment

Analytical Balance	Sartorius, Göttingen, Germany
Agitation Incubator G25	New Brunswick Scientific, Edison, NJ, USA
Blotting Tanks: Mini Trans-Blot Cell (7.5 x 10 cm blotting area)	BioRad, Munich, Germany
Bruker Autoflex Mass Spectrometer	Bruker Daltonics, Bremen, Germany
Cooling Centrifuges: Sorvall RC-5B	Thermo Scientific, Wilmington, DE, USA
Beckman J2-21	Beckman Coulter GmbH, Krefeld, Germany
Sigma 3K30	Sigma, Munich, Germany
DNA – Gel Electrophoresis Chamber	BioRad, Munich, Germany
Gel-Documentation System MidiDOC	Herolab, Wiesloch, Germany
Heating Block, Dri-Block Heater DB-3	Techne, Cambridge, UK
Incubators: Heraeus B 6200	Thermo Electron GmbH, Karlsruhe, Germany
Autoflow 8500	NuAire Plymouth, MN, USA
Laminar Air Flow Hoods: NU-437-400E / Series 3	NuAire Plymouth, MN, USA
MSC-Advantage (1.2)	Thermo Scientific, Wilmington, DE, USA
Light Optical Microscope, Leica DM IL LED	Leica, Wetzlar, Germany
Magnetic Stirrer, RCT basic IKAMAG	IKA Werke GmbH & Co. KG, Staufen, Germany
Neubauer Counting Chamber (0.1 mm)	Hartenstein Laborversand, Würzburg, Germany
Overhead Agitation Wheel	Renner GmbH, Dannstadt, Germany
pH Meter	WTW GmbH, Weilheim, Germany
Pipettes, Eppendorf Research (10 µl, 100 µl, 1000 µl)	Eppendorf Deutschland, Hamburg, Germany
Power Supplies Power Pack P25 and P24	Biometra, Göttingen, Germany
Protein Separation Chambers: Mini-Protean II	BioRad, Munich, Germany
Sequencer, ABI Prism™ Sequencer 377	Perkin Elmer, Weiterstadt, Germany
Spectrophotometer: NanoDrop™ 1000	Thermo Scientific, Wilmington, DE, USA
U-2000	Hitachi, NY, USA
Multiskan EX	Thermo Scientific, Wilmington, DE, USA
Speed Vac Plus SC110A	Savant, NY, USA
Table Centrifuge Mikro 200	Hettich GmbH & Co. KG, Tuttlingen, Germany
Tabletop Processor, Curix60	Agfa HealthCare GmbH, Cologne, Germany
Thermocycler: Trio-Thermoblock	Biometra, Göttingen, Germany
T-Gradient	Biometra, Göttingen, Germany
Thermomixer 5436	Eppendorf, Hamburg, Germany
Ultrasonication Apparatus: Sonifier®II	Branson, Danbury, CT, USA
Desintegrator Modell 250	
Vortexer: Power Mix	Hartenstein Laborversand, Würzburg, Germany

4.1.2. Consumables

0.5 – 2.0 ml reaction tubes	Sarstedt, Nümbrecht, Germany
15 ml and 50 ml sterile centrifugation tubes	Greiner, Nürtingen, Germany
6-, 12- and 24-well plates for cell culture	Nunc, Roskilde, Denmark
96-well plates ELISA	Nunc, Roskilde, Denmark
400 µm Anchor Plate	Bruker Daltonics, Bremen, Germany
Blotting paper	Schleicher & Schüll, Dassel, Germany
Cell culture flasks from 25 to 175 cm ²	Sarstedt, Nümbrecht, Germany
Cell scraper (25 cm)	Sarstedt, Nümbrecht, Germany
Centrifuge beaker, 15 and 50 ml, Quickseal	Beckman, Munich, Germany
Centriprep YM-10 10kDa and 30kDa	Millipore Billerica, MA, Germany
Pipette tips (10 µl, 100 µl, 1000 µl)	Hartenstein Laborversand, Würzburg, Germany
Positively charged nylon membrane <i>porablot NY plus</i>	Macherey & Nagel, Düren, Germany
Petri dishes (various diameter)	Hartenstein Laborversand, Würzburg, Germany
Sterile filters, 150 ml bottle top filter, 0.45 µm	Nalgene, Rochester, NY, USA
Syringes and needles, sterile (0.45, 0.6, and 0.9 diameter)	Braun Melsungen AG, Melsungen, Germany
X-Ray film hyperfilm MP	Amersham, Braunschweig, Germany

4.1.3. Chemicals, Enzymes and Solutions

Acetonitrile	Sigma-Aldrich GmbH, Steinheim, Germany
Activated Charcoal	Sigma-Aldrich GmbH, Steinheim, Germany
Agarose NEE0	Carl Roth GmbH + Co. KG, Karlsruhe, Germany
Agar-Agar, Bacto-Peptone, Yeast Extract, Glucose, Yeast Nitrogen Base w/o Amino Acids	Difco Laboratories, Augsburg, Germany
Aldosterone	Sigma-Aldrich GmbH, Steinheim, Germany
Alpha-Cyano-4-Hydroxycinnamic Acid	Sigma-Aldrich GmbH, Steinheim, Germany
Ammonium Persulfate (APS)	Sigma-Aldrich GmbH, Steinheim, Germany
Antibiotics (ampicillin, kanamycin, chloramphenicol)	Sigma Chemie GmbH, München, Germany
Benchmark™ Prestained Protein Ladder	Life Technologies GmbH, Invitrogen Division, Darmstadt, Germany
BIBF1120	Selleck Chemicals LLC, Houston, TX, USA
Biotin	Sigma-Aldrich GmbH, Steinheim, Germany
Bile Salts (BS)	Sigma-Aldrich GmbH, Steinheim, Germany
Broad Range Prestained Protein Marker	New England Biolabs GmbH, Frankfurt, Germany
Calf Intestinal Phosphatase (CIP)	New England Biolabs GmbH, Frankfurt, Germany
Chenodesoxy Acid (CDA)	Sigma-Aldrich GmbH, Steinheim, Germany
Cholic Acid (CA)	Sigma-Aldrich GmbH, Steinheim, Germany
Coomassie Brilliant Blue (SimplyBlue SafeStain)	Life Technologies GmbH, Invitrogen Division, Darmstadt, Germany

Desoxycholic Acid (DCA)	Sigma-Aldrich GmbH, Steinheim, Germany
Developer 153, Part A + B	Agfa HealthCare GmbH, Cologne, Germany
Dextran T70	Sigma-Aldrich GmbH, Steinheim, Germany
Diethylpyrocarbonate (DEPC)	Sigma Chemie GmbH, München, Germany
DNase I, Rnase-free	Roche Deutschland Holding GmbH, Grenzach-Wyhlen, Germany
dNTPs, lyophilized	Carl Roth GmbH + Co. KG, Karlsruhe, Germany
Dulbecco's Minimal Essential Medium (DMEM), (4.5 g glucose/L)	Life Technologies GmbH, Invitrogen Division, Darmstadt, Germany
Dulbecco's Phosphate Buffered Saline (PBS) without Ca ²⁺ /Mg ²⁺	Biochrom AG, Berlin, Germany
Fetal Bovine Serum Superior (FBS)	Biochrom AG, Berlin, Germany
Fixer G354	Agfa HealthCare GmbH, Cologne, Germany
FGF (aFGF and bFGF), recombinant human	ImmunoTools, Friesoythe, Germany
Heparin	Sigma-Aldrich GmbH, Steinheim, Germany
Immunoglobulin G, rat	Biomol GmbH, Hamburg, Germany
Insulin solution, human	Sigma-Aldrich GmbH, Steinheim, Germany
Lithocholic Acid (LCA)	Sigma-Aldrich GmbH, Steinheim, Germany
Low Molecular Weight Marker (N3233)	New England Biolabs GmbH, Frankfurt, Germany
ONPG (ortho-nitrophenyl-β-galactoside)	Sigma-Aldrich GmbH, Steinheim, Germany
Panserin 401	PAN Biotech, Aidenbach, Germany
Penicillin / Streptomycin (P/S)	Life Technologies GmbH, Invitrogen Division, Darmstadt, Germany
Polysorbate 20 (TWEEN 20)	Merck KGAA, Darmstadt, Germany
Phusion High-Fidelity DNA Polymerase	New England Biolabs GmbH, Frankfurt, Germany
Pierce ECL Western Blotting Substrate	Pierce Protein, Rockford, IL, USA
ProBond Resin	Life Technologies GmbH, Invitrogen Division, Darmstadt, Germany
Progesterone	Sigma-Aldrich GmbH, Steinheim, Germany
Restriction Enzymes	New England Biolabs GmbH, Frankfurt, Germany
Serotonin (5-Hydroxytryptamine Creatinine Sulfate Complex)	Sigma-Aldrich GmbH, Steinheim, Germany
SMART ladder, molecular weight marker	Eurogentec GmbH, Cologne, Germany
Sodium Taurocholate	Sigma Chemie GmbH, München, Germany
Sterile Water	Fresenius, Bad Homburg, Germany
SU5402	Tocris Biosciences, Bristol, UK
T4 DNA Ligase	New England Biolabs GmbH, Frankfurt, Germany
Tavanic (Levofloxacin)	Sanofi-Aventis GmbH, Frankfurt, Germany
Trifluoroacetic Acid (TFA)	Sigma-Aldrich GmbH, Steinheim, Germany
TRIzol (15596-018)	Life Technologies GmbH, Invitrogen Division, Darmstadt, Germany
Trypan Blue, 0.5 %	Biochrom AG, Berlin, Germany
Trypsin, 0.05% (1X) with EDTA 4Na, liquid	Life Technologies GmbH, Invitrogen Division

Vitamin B12	Sigma-Aldrich GmbH, Steinheim, Germany
X-Gal (5-bromo-4-chloro-3-indolyl- β -D-galactopyranoside)	AppliChem GmbH, Darmstadt, Germany

4.1.4. Commercial Kits

Ambion AM1906 Kit	Life Technologies GmbH, Applied Biosystems Division, Darmstadt, Germany
BCA Protein Assay	Pierce Protein, Rockford, IL, USA
ECL Chemiluminescence Kit	Amersham, Braunschweig, Germany
Matchmaker Two Hybrid System 3	Clontech, Heidelberg, Germany
Montage In-Gel-DigestZP Kit	Millipore Billerica, MA, Germany
NucleoBond® PC 100 Midi Kit	Machery-Nagel GmbH & Co.KG, Düren, Germany
OmniScript RT PCR Kit	Qiagen GmbH, Hilden, Germany
pBAD/Thio expression Kit	Invitrogen, Groningen, Netherlands
QIAEX II Gel Extraction Kit	Qiagen GmbH, Hilden, Germany
QIAGEN Gelextraction Kit	Qiagen GmbH, Hilden, Germany
QIAGEN PCR Cloning Kit	Qiagen GmbH, Hilden, Germany
QIAGEN Plasmid Midi Kit	Qiagen GmbH, Hilden, Germany
QIAprep Spin Miniprep Kit	Qiagen GmbH, Hilden, Germany
QIAquick Nucleotide Removal Kit	Qiagen GmbH, Hilden, Germany
QIAquick PCR Purification Kit	Qiagen GmbH, Hilden, Germany
QIAquick RNEasy Mini Kit	Qiagen GmbH, Hilden, Germany
TOPO-TA Cloning®KIT	Invitrogen, Groningen, Netherlands

All buffers and solutions were prepared with distilled water, autoclaved and sterile filtrated, respectively. For RNA purposes, either DEPC-treated or commercially available RNase-free water was used. For enzymatic reactions, double distilled and autoclaved water was used.

4.2. Oligonucleotides

All oligonucleotides were ordered from Sigma-Aldrich/Sigma-Genosys in lyophilized form and were reconstituted with PCR grade water at a final concentration of 50 μ M.

Vector	Oligonucleotide Name	Oligonucleotide Sequence 5' - 3'
pBAD/Thio-TOPO®	pBAD forward	GCTATGCCATAGCATTTTTATCC
	pBAD reverse	GAATAATTAGACATAGTCCG
	Trx forward	GTCCTCGACGCTAACCTG
	pBAD up 60	CTGATTTAATCTGTATCAGGC
pCR®2.1® TOPO-TA	Topo M13	CAGGAAACAGCTATGACCAT
	Topo T7	TACGACTCACTATAGGGCGA
pDrive	pDrive T7	TAATACGACTCACTATAGGG
	pDrive SP6	ATTTAGGTGACACTATAGAA
pET30c(+)	T7 priming site	AATACGACTCACTATA

	T7 Terminator	CTAGTTATTGCTCAGCGGTGG
pGADT7	Y2H T7 seq	TAATACGACTCACTATAGGGC
	Y2H AD seq	AGATGGTGCACGATGCACAG
pGBTk7	Y2H T7 seq	TAATACGACTCACTATAGGGC
	Y2H BD seq	TTTTCGTTTTAAACCTAAGAGTC
	Y2H BD up	TAAGAGAGTCACACTTTAAATTTGTAT
pGEX-5X	pGEX 5' Sequencing Primer	GGGCTGGCAAGCCACGTTTGGTG
	pGEX 3' Sequencing Primer	CCGGGAGCTGCATGTGTCAGAGG
pJG4-5	JG4-5'	CTTATGATGTGCCAGATTATG
	JG4-5' nest	CTCCGAATTCGGCACGAG
	JG45-3'	TTGGAGACTTGACCAAACCT
	JG45-3' nest	CTGGCGAAGAAGTCC
pQE30	pQE seq dw	CCCGAAAAGTGCCACCTG
	pQE seq up	GTTCTGAGGTCATTAAGTGG
pRSETA	T7 pRSET	AATACGACTCACTATA
	T7 Terminator	CTAGTTATTGCTCAGCGGTGG
pSecHygroA	T7 pSec	TAATACGACTCACTATAGGG
	BGH reverse	TAGAAGGCACAGTCGAG
cDNA	Oligonucleotide Name	Oligonucleotide Sequence 5' - 3'
	CD3	ATCTCTTGAAAGGATCCTGCAGG
	CD3nest	CTCTTGAAAGGATCCTGCAGGACT
	CD3RT	ATCTCTTGAAAGGATCCTGCAGGTTTTTTTTTT TTTTTTTTTTTTTTTTV (T26,V= G+C+A)
gene	Oligonucleotide Name	Oligonucleotide Sequence 5' - 3'
<i>emact</i>	EmAct2 dw	TCAATCCTAAAGCCAATC
	EmAct2up	CGTACAACGACAGCAC
<i>emelp</i>	em10-15	AATAAGGTAATCAGTCGATC
	em10-16	TTGCTGGTAATCAGTCGATC
	siRNA-EmElp	AACCUUUCUAAGACUGGAUAAGA
	siRNA-EmElp-as	UCUUAUCCAGUCUUAGAAAGGUU
<i>emfr</i>	EmFR-exp-dw	GTTTCATCGAGACCTGGCGG
	EmFR-exp-up	CAAAAGACCATATGTCCGATTT
	EmFR-seq-ORF-1212-dw	GCTCGTCAAATCGCCATTGGG
	EmFR-Iso-A-up	CAAAAGACCATATGTCCGATTT
	EmFR-Iso-B-up	CAAAAGACCATCTGAAGGAGTG
	EmFR-Iso-dw	GTTTCATCGAGACCTGGCGG
	EmFR-Iso-up	GTTTGACCTCCTCTCGGAG
	EmFR-Iso2-dw	GTGTTCTCTAAAGTGGATGG
	EmFR-Iso2-up	GATTGGCTGCTGGTGAATCGC
	EmFR-pSecHygroA-BamH1-dw	GCGGATCCGCATCAACACCCTCCACCCTTC

EmFR-pSecHygroA-Not1-up	GAGCGGCCGCACACCCCTGTAAGAACTT
EmFR-TK-mut-dw	GTCGCAAAAATCGCCGATAACGCTCTCAC GCGCAAGGTG
EmFR-TK-mut-up	CACCTTGCGCGTGAGAGCGTTATCGGC GATTTTTGCGAC
siRNA EmFR-74	UUCAGUCUUAACGGGCUCGUCUU
siRNA EmFR-74-as	AAGACGAGCCCGUUAAGACUGAA
EmFRin-pBAD/Thio-dw	CGTCCCCAACGAATGATTTTC
EmFRin-pBAD/Thio-up	AATGTCCTTGAGGCGAGGTAGAC
FRin-BD-BamH1-dw1	ACTGCGGGATCCGTCCCCAACGAATG
FRin-BD-PstI-up	TCAACCTGCAGGTAAGAACTTTGACAGTGT
FRin-AD-XmaI-dw	TGCGCCCCGGTCCCCAACGAATG
FRin-AD-ClaI-up	TCAACATCGATGTAAGAACTTTGACAGTGT
FRex-pET30a(+)-BamH1-dw	TCTGGGATCCCGCATCAACACCCTCCACCC
FRex-pET30a(+)-Sal1-up	GGCGTCGACTACCTGAGAGACACTGTGTCATG
EmFRin_pGEX5X_BamH1_dw	CTGGATCCGTCGTCCCCAACGAATG
EmFRin_pGEX5X_Not1_up	GTGCGGCCGCACAATGTCCTTGA
EmFR-qRT-3-dw	GATGAAGAAGCTTCTCTGG
EmFR-qRT-3-up	TAAGAACTTTGACAGTGTAGC
pQE30-FRin-BamH1-dw	CGGATCCCGTCCCCAACGAATGATTTTC
pQE30-FRin-Sal1-up	GTCGTCGACTCAAATGTCCTTGGAGGCGAG
<i>emfyn</i>	
EmFyn-dw	CCGAGAGAATGCTTTTG
EmFyn-up	GCTTTATTGCATACATATTCC
<i>emhnf4</i>	
c3313-pos-15555-dw	GGACATCTCACACTCTGG
c3313-pos-15704-dw	GTTCGTCACCTTAACGATCTG
c3314-pos-209-up	GCCCAGTAGCACTATCG
c3314-pos-5552-up	GACATGCGTAATCAATGCCG
EmHNF4-fullcDNA-dw	GAGCCTCCAGAGTAGACATG
EmHNF4-fullcDNA-up	ACTTCCGTACATTCTTCATAATG
EmHNF4-ORF-dw	ATGGACCTCTACAATAGCAGCAG
EmHNF4-ORF-up	TCATTGCTTTTCAACGTCCTCTTG
HNF4-put-ORF-dw1	ATGTCATTCTTCTACAACGTCCG
HNF4-put-ORF-dw2	TGAACTCAGAATCAGGAATCG
HNF4-put-ORF-dw3	ATGCTGACAGCTATTGTCAATG
HNF4-put-ORF-dw4	ATGGCCTCTTTTGAAGTCA
HNF4-put-ZnF-up	TGCTGATTTTATCGCGCTCG
HNF4-put-ORF-up1	TCAATCACCTGAAAGTAGTATG
HNF4-put-ORF-up2	GCAGCAGAAGTAGTGGAACG
HNF4-put-5RACE-nes-up1	GATGGATAGAGAGGCAGAACCCGAGG
HNF4-put-5RACE-up1	GACAGTTGGAGATGGATAGAGAGG
HNF4-put-5RACE-nes-up2	GAAGTGTTACGAATTGTTGTG
HNF4-put-5RACE-up2	GAACTCCTCGCCTGAAGTG
HNF4-put-5RACE-nes-up3	GATGCCACCGCTGCTGCTATTGTAGAG

	HNF4-put-5RACE-up3	GTAGAGGTCCATTTCAAAGTTGTGTGG
	HNF4-put-3RACE-dw1	CAAAGGATCTTTCCTCTACTGG
	HNF4-put-3RACE-nest1-dw	CAATTGGGCAAGACAGCTGG
	HNF4-put-3RACE-dw2	GAACTCCTCGCCTGAAGTG
	HNF4-put-3RACE-nest2-dw	GAAGTGTTACGAATTGTTGTG
	HNF-DBD-Pool-mut-dw	CCGTTTTTGCCGGCTGAAAAAGTGCTTCC GGGTGG
	HNF-DBD-Pool-mut-up	CCACCCGGAAGCACTTTTTTCAGCCGGCAA AAACGG
	HNF4-DBD-AD/BD-NdeI-dw	ATCCATATGTGTCTTATTTGTGGAG
	HNF4-DBD-PI-AB/BD-EcoR1up	GCTGAATTCATCGCGCTCGTTTTGG
	HNF4-DBD-Pa-AB/BD-EcoR1up	GGTGAATCCCCCACC GGAAAGCAC
	EmHNF4-LV-4/5-dw	CCGCGCAGCGGTCCAAAAC
	EmHNF4-SV-4/8-dw	CCGCGCAGGTCACCTTAAC
	EmHNF4-e8-up	CCACAAGAAATCCTGAAACCCG
	EmHNF4-qRT-5-dw	CAAGTTGGATGCTATTCTC
	EmHNF4-qRT-5-up	GAGGCAAATAAACTCTGTC
<i>emmpk3</i>	EmMPK3-exp-dw	TGGGTAGTGATGGTAATCTCG
	EmMPK3-exp-up	AGGGCGCGATGAAGTCG
<i>emnhr1</i>	EmNHR-ab-dw	GACTATCACTCACACTCTCTAG
	EmNHR-ab-up	GAGAAGGATATGACCATAGTTGTC
	EmNHR-ab2-NcoI-pRSET-dw	CCGCCATGGCATCAACAGACACCACCTC
	EmNHR-ab2-HindIII-pRSET-up	GTGAAGCTTTTCCAGATAGTGCTTCAACAG
	EmNHR1-NTS-NcoI-fwd	GTACCATGGTGAATACTTCTGGTTTTTTG GTACGG
	EmNHR1-ALT-XmaI-rev	TAGCCCGGGGTCAGAGCCTGTAACCTCG
	EmNHR1-LHQ-NcoI-fwd	TGCCATGGATCTTCATCAGGATCGCTTACC
	EmNHR1-FIE-XmaI-rev	CACCCCGGGCACTCGATAAACATATGTACC
	EmNHR1-SLV-XmaI-rev	CCACCCGGGTTACCAAACACTACTTATAG
	EmNHR1-DNY-NcoI-fwd	CTCCCATGGACAACATATGGTCATATCC
	EmNHR1-LHQ-dw	CTTCATCAGGATCGCTTACCTAC
	EmNHR1-SLV-up	TCACCAAACACTTATAGTAATATTTGAG
	NHR1-H95-ATG-NdeI-dw	AATCCTCATATGACGTCCCAAAGCAAG
	NHR1-H95-TAA-up	TTAGGAGGAATTAGTCATGTTAG
	NHR1-H95-DBD-Y2H-XmaI-up	CCGTGGCCCGGGAGATGCTGAGATCAAAGG
	NHR1-H95-DBD-SHS-up	TTATGAGATGCTGAGATCAAAGG
	NHR1-DBD-RERK-up	TTTCGCTCCCGATTACGCTG
	EmNHR1-qRT-2-dw	TCAATCGGTATCCAATATC
	EmNHR1-qRT-2-dw	ATTAGTCAACACGGCAG
	EmNHR1-ATG-UP1-dw	ATGTCTAGTGTGATTCATGACG
	SL-ATG-dw	CTTACCTTCGAGTTTTGTATG
<i>gfp</i>	siRNA eGFP-658	CAUAGCGUUGGCUACCCGUGAUA
	siRNA eGFP-658-as	UAUCACGGGUAGCCAACGCUAUG

<i>Hstub12</i>	Tub12up	CCCCAAGTGTATGATACTGG
	Tub12ST	CTGGGCAGTGC GGCAACCA

4.3. Determination of nucleic acid concentration and purity

The nucleic acid concentration was photometrically determined at a wavelength of 260 nm using the spectrophotometer NanoDrop 1000. The purity of the nucleic acids was analyzed on the basis of the ratios of 260 nm/280 nm (for protein impurity) and 260 nm/230 nm (for salt impurity). DNA concentration was further estimated by comparing the intensity of ethidium bromide staining between a DNA fragment of unknown concentration with DNA size marker fragments of known concentrations (SmartLadder, Eurogentec).

4.4. RNA applications

4.4.1. Isolation and purification of total RNA from *E. multilocularis*

RNA isolation from in vitro cultivated axenic metacystode vesicles and protoscolecocytes was performed with TRIzol Reagent as described in [52]. Briefly, about 3-4 metacystode vesicles or 20 μ l purified protoscolecocytes were washed three times in pre-warmed 1x PBS. Vesicles were mechanically disrupted by sucking them through a syringe (G20, 0.9 cm diameter). Subsequently the material was subjected to 1 ml of TRIzol Reagent. The following steps were performed according to the manufacturer's protocol. RNA isolation of in vitro axenic primary cells followed the protocol as published by Förster et al. [145].

For purification of the RNA solution either the Ambion AM1906 Kit was used according to the manufacturer's instructions or the RNA was subjected to a DNase digest with 0.2 U/ μ l RNase-free DNase (Roche) for 1 h at 37 °C in the presence of 0.05 M sodium acetate (CH₃COONa) and 0.05 M Magnesium sulfate (MgSO₄). Then the RNA was purified applying the RNEasy Mini Kit (QIAGEN) following the manufacturer's recommendations.

4.4.2. First strand cDNA synthesis

For reverse transcription the Omniscript RT-PCR kit (QIAGEN; Hilden, Germany) was used. However, the manufacturer's protocol was slightly altered. Between 0.5 μ g and 2 μ g total RNA in a volume of 12 μ l were mixed with 1 μ M of the CD3-RT oligonucleotide [44] and incubated for 10 min at 65 °C. Subsequently after letting the solution cool to room temperature, the remaining components (Reverse Transcriptase, RNase Inhibitor, dNTPs and RT buffer) were supplemented. The reaction (20 μ l) was allowed to incubate for 90 min at 37 °C.

4.5. DNA procedures

4.5.1. Isolation and purification of chromosomal DNA from the metacestodes

Metacestode vesicles were washed three times in 1xPBS, disrupted by pipetting with a 1ml tip. After centrifugation (short spin, full speed) the supernatant was removed and lysis buffer (100 mM NaCl, 10 mM Tris-HCl, pH 8.0, 50 mM EDTA, pH 8.0, 0.5 % SDS, 20 µg/ml RNase A; 1.2 ml per 100 mg pellet) supplemented with 0.1 mg/ml Proteinase K was added. To ensure that samples were totally digested an overnight incubation at 50 °C under constant agitation was the method of choice. DNA was extracted by 1 volume of phenol-chloroform-isoamyl (25:24:1) alcohol. After centrifugation (25 min, 2000 g, room temperature) the upper aqueous phase was transferred to a new tube and phenol-chloroform-extraction was repeated. Subsequently the DNA was precipitated with 2 volumes of 96% ethanol in the presence of 0.1 volumes LiCl (5 M stock; pH 4.5) and incubated at -20°C overnight. The DNA was completely precipitated at 20,000 rcf for 30 min at 4 °C. After carefully removing the supernatant, and washing with 70 % ethanol, the DNA pellet was dried at room temperature and resuspended in 1xTE buffer (10 mM Tris, 1 mM EDTA, pH 8.0). The Quality of the DNA was assessed with a photo spectrometer and with agarose gel electrophoresis.

4.5.2. Isolation of plasmid DNA from *E. coli*

The isolation of plasmid DNA from *E. coli* strains was performed with the QIAprep Spin Miniprep Kit (QIAGEN), the Plasmid Midi Kit (QIAGEN) or the NucleoBond® PC 100 Midi Kit (Machery-Nagel) following the exact instructions of the producer.

4.5.3. Gel electrophoresis of DNA

Agarose gels were prepared as 0.7 % - 1.0 % 1xTAE (40 mM Tris, 1 mM EDTA, pH 8.0, 0.11 % glacial acetic acid ad 1 l dH₂O, pH 8.5) for fragments between 0.25 kb and 7 kb or 2 % 1xTBE (89 mM Tris base, 89 mM Boric acid, 2 mM EDTA, pH 8.0) gels for fragments smaller than 0.25 kb. The corresponding amount of agarose was dissolved by heating in 1xTAE or 1xTBE, respectively. Subsequently, the agarose-buffer solution was allowed to cool down to 50 °C – 60 °C and was then poured into a horizontal gel sleigh in which loading wells were left by appropriate combs. The DNA sample to be analysed was mixed with a 6 x agarose buffer containing 0.25 % bromo phenol blue, 0.25 % xylene cyanol, 40 % saccharose and 30 % glycerol. The DNA was allowed to separate on the gel for about 30 – 50 min at room temperature at voltages between 70 V and 100 V until the dyes included in the loading buffer were sufficiently separated. In a 1 % agarose gel, the bromo phenol blue band and the xylene cyanol correspond to a 0.3 kb and 3 kb fragments, respectively. Later the DNA was visualized by incubating the gel in ethidium bromide (2 mg/l ethidium bromide in 1xTAE or 1xTBE, respectively) for about 10 min and exposing the gel to UV light. The SmartLadder (Eurogentec) or the Low Molecular Weight DNA Ladder (NEB, N3233) were used as marker to estimate DNA fragment size.

4.5.4. Purification and DNA precipitation

PCR amplicons and DNA treated with restriction enzymes was purified with the help of the QIAquick PCR Purification Kit or the QIAquick Nucleotide Removal Kit, while DNA in an agarose gel was

extracted either with the QIAEX II Gel Extraction Kit or the QIAgen Gelextraction Kit (all QIAgen) following the instructions of the manufacturer.

DNA from a sample solution was precipitated with 2.5 volumes of 96 % ice-cold ethanol and 0.1 volume of 3 M sodium acetate (pH 5.2). After incubation for up to 24 h at -20 °C the DNA was fully precipitated by centrifugation (30 min, 15,000 rpm, 4 °C). Then the supernatant was removed, the DNA was washed with 70 % ethanol and dried at room temperature. When the pellet resumed a white colour, the DNA was dissolved either in DNase-free water or 1xTE buffer (10 mM Tris, 1 mM EDTA, pH 8.0).

4.5.5. Sequencing of DNA

DNA was sequenced according to Sanger employing an ABI prism 377 DNA sequencer (Perkin-Elmer; Rodgau-Juegesheim, Germany). The DNA sample (300 ng plasmid DNA; 50 ng PCR purified amplicon) was mixed with 1 µl of a 50 µM oligonucleotide, 2 µl of a 5 x sequencing solution to a final volume of 10 µl. The PCR protocol was as follows: 25 cycles of 96 °C for 10 s, 45 °C –60 °C for 5 s and 72 °C for 1 min. The annealing temperature for the sequencing oligonucleotide was calculated with the equation $T_a [^{\circ}\text{C}] = 4x (G+C) + 2x (A+T) - 5$.

4.5.6. Amplification of DNA via PCR

Defined DNA fragments were amplified by utilizing sequence specific oligonucleotides in a polymerase chain reaction (PCR) with either the Trio-Thermoblock or the T-Gradient (both Biometra). Depending on the purpose of PCR either the non-proofreading Taq DNA polymerase (NEB) or the proofreading enzymes PfuTurbo (Stratagene) and Phusion High-Fidelity DNA Polymerase (Finnzymes) were applied.

Following the equation $T_a [^{\circ}\text{C}] = 4x (G+C) + 2x (A+T)$ to calculate the oligonucleotide annealing temperature, usually oligonucleotides with an approximate T_a of 58 °C and a G/C content between 40 – 60 % were designed.

In detail, cycling and reaction conditions were as follows depending on which enzyme was used for the reaction:

- Taq DNA polymerase (NEB): initial denaturation for 30 - 60 seconds (s) at 94 °C, 30 cycles of a denaturation, primer annealing and a elongation step (30 s at 94 °C, 30 s at T_a-5 °C, 60 s/1000 bp at 72 °C) and with a final elongation for 10 to 30 min at 72 °C. The PCR mix comprised 1-5 µl template, 2 µl 10 x buffer, 0.2 µl 10 mM dNTPs, 0.2 µl 50 µM oligonucleotide I, 0.2 µl 50 µM oligonucleotide II, 0.2 µl Taq DNA polymerase (2 U/µl) ad a final volume of 20 µl.
- Phusion High-Fidelity DNA Polymerase (F-531S) and PfuTurbo were used according to the manufacturer's instructions and with the supplied reagents.

4.5.7. Rapid amplification of cDNA ends (RACE)

In order to define the 5' and 3' ends of target genes RACE experiments were conducted. As template an already existing cDNA library was chosen [39]. For the first PCR one specific oligonucleotide of the respective 5' or 3' end of the target gene and one oligonucleotide complementary to the vector backbone were used. For the second PCR - nested PCR - a pair of oligonucleotides was chosen, which binds between the first set of primers.

4.5.8. Semi-quantitative RT PCR

Total RNA was isolated as described earlier (4.4.1) from metacestode vesicles, primary cells and both activated and dormant protoscolecocytes. Equal amounts of RNA were reverse transcribed using the Omniscript RT-PCR Kit (QIAGEN) and the oligonucleotide CD3-RT. Subsequently, equivalent amounts of cDNA were subjected to PCR expression analyses. In detail, ten-fold serial dilutions were analyzed by this mean. Different PCR protocols were used for the genes of interest:

- *Emnhr1*: The oligonucleotides EmNHR1-LHQ-dw (5'-CTT CAT CAG GAT CGC TTA CCT AC-3') and EmNHR1-SLV-up (5'-TCA CCA AAC TAC TTA TAG TAA TAT TTG AG-3) were used. The constitutively expressed gene *Emelp* [44] served as control using the primers Em10-15 (5'-AAT AAG GTC AGG GTG ACT AC-3') and Em10-16 (5'-TTG CTG GTA ATC AGT CGA TC-3') The protocol was chosen as specified: initial denaturation of 1 min at 94 °C, 35 cycles of 30 s at 94 °C, 30 s at 57 °C and 50 s at 72 °C with a final elongation step of 10 min at 72 °C.
- *Emfr*: the primers EmFR-exp-dw (5'-GTT CAT CGA GAC CTG GCG G-3') and EmFR-exp-up (5'-CAA AAG ACC ATA TGT CGG ATT T-3') were utilized. As control *Emact-dw* (5'-TCA ATC CTA AAG CCA ATC-3') and *Emact-up* (5'-CGT ACA ACG ACA GCA C-3') for *Emactin2* [147] employing a protocol of initial denaturation of 1 min at 94 °C, followed by 30 cycles of 30 s at 94 °C, 30 s at 56 °C and 30 s at 72 °C with a final elongation step of 10 min at 72 °C.
- *Emmpk3*: The oligonucleotides EmMPK3-exp-dw (5'-TGG GTA GTG ATG GTA ATC TCG -3') and emMPK3-exp-up (5'-AGG GCG CGA TGA AGT CG -3') were used. Again, the constitutively expressed gene *Emelp* [44] served as control using the primers Em10-15 and Em10-16. The protocol was chosen as specified: initial denaturation of 1 min at 94 °C, 28 cycles of 30 s at 94 °C, 30 s at 56 °C and 30 s at 72 °C with a final elongation step of 10 min at 72 °C.

4.5.9. PCR based mutagenesis

In a PCR based mutagenesis approach specific mutations to a particular DNA sequence were introduced using oligonucleotides which harbor the desired mutation. The procedure first involved the amplification of the entire plasmid vector, in which the mutation was introduced. Then, the mixture of original and mutated vector was digested with the dam-methylation sensitive restriction enzyme *DpnI*. Thus, the original plasmids were digested, but not the newly amplified plasmids because methylations of plasmids are only introduced when plasmids are expanded in bacteria. After the *DpnI* digest bacteria were transformed with this DNA mixture. Single colony bacteria were harvested after overnight incubation, plasmid DNA was isolated and subjected to sequencing to verify the introduced mutations.

- Design of oligonucleotides: The length was between 25–45 nucleotides and the mutation site was situated in the middle of the sequence. The average GC content numbered 40 %.
- Annealing temperature for PCR: To calculate T_a the following equation was used: $T_a = 81.5 \times 0.41 (\% GC) - 675/N - \% \text{ mismatch}$ was used; (% GC : number of G and C nucleotides of the primer; % mismatch: percentage of non-binding nucleotides; N : total number of nucleotides of the primer)
- PCR reaction mix: The PCR was conducted in total volume of 50 μl with 10 ng of the respective plasmid as template, 0.2 mM dNTPs and 125 ng each of the respective oligonucleotides. All other ingredients were added according to the manufacturer's protocol (Phusion High-Fidelity DNA-Polymerase, NEB)

- PCR protocol: initial denaturation of 1 min at 98 °C, 18 cycles of 30 s at 98 °C, 30 s at T_a+3 °C and 5 min at 72 °C with a final elongation step of 10 min at 72 °C
- *DpnI* digest: 0.5 µl (10 U/µl) directly added to the PCR mix after PCR reaction; incubation for 3 h at 37 °C.
- Transformation: 2 µl and 5 µl of the reaction mixture following the transformation protocol (see section 4.7.3)
- DNA plasmid preparation (see section 4.5.2) and sequencing (see section 4.5.5).

4.5.10. TA cloning

When amplifying DNA with Taq DNA Polymerase (NEB) the resulting amplicons possess an additional 3' A. This overhang was used for cloning into the pCR[®]2.1[®]TOPO-TA vector or the pBAD/Thio-TOPO[®] vector (both Invitrogen) which both harbor a complementary 5'T overhang. Successful ligation of the insert into the vector results in white colonies on the agar plate, while blue colonies represent bacteria with religated vectors. Purified DNA fragments which lack a 3' A overhang from PCR reactions with Phusion High-Fidelity DNA Polymerase were incubated with Taq DNA polymerase and dATP for 1 h at 72 °C to add a 3' A, thus allowing TA cloning.

4.5.11. Colony-PCR

To check whether the DNA insert integrated into the multiple cloning site (MCS) of the respective plasmid backbone, bacterial clones were analyzed in a colony PCR. Single bacterial colonies were picked with a sterile tip from the agar plate and resuspended in 20 µl sterile water. The suspension was incubated on a shaker for 10 – 20 min at room temperature. For PCR analysis 2 µl of the suspension was used as template with Taq DNA polymerase (NEB; see section 4.5.6).

4.5.12. Restriction digest of DNA

DNA restriction digests were conducted using NEB restriction enzymes following the manufacturer's instructions. The reaction volume was 20 µl. Simultaneous double digests of DNA inserts were the method of choice when needed for directional cloning only if enzymes met the same temperature and buffer specificities. After a single restriction digest, the DNA fragment was dephosphorylated at the 5' end using Antarctic Phosphatase (NEB) or CIP as recommended by the producer before the subsequent ligation step.

4.5.13. Ligation of DNA fragments

DNA fragments were ligated using the T4 DNA ligase (NEB). In detail, the reaction was carried out in total volume of 20 µl at 16 °C over night. The vector-insert ratio was 1:3 with usually 50–100 ng of plasmid vector.

4.6. Protein analysis

4.6.1. Determination of protein concentration

The BCA Protein Assay Kit (Pierce Biotechnology) was used to determine the protein concentration of samples late used for SDS-PAGE (see section 4.6.2). The working solution was obtained by mixing Reagent A and B in a ration 50:1. As protein standard bovine serum albumin (BSA) was chosen in the following concentrations ($\mu\text{g/ml}$): 50, 100, 200, 400, 600, 800, 1000 und 1200. From each concentration and from the samples of unknown concentration 50 μl were taken and mixed with 1 ml working solution. Then the mixture was incubated for 30 min at 37 °C. Subsequently the absorption at 562 nm was measured in the ELISA reader Multiscan Ex Primary EIA V.2.1-0 (Thermo).

4.6.2. SDS-PAGE

The sodium dodecyl sulfate-polyacrylamide gel electrophoresis (SDS-PAGE) was conducted in the Mini-Protean separation chambers by BioRad. The following working solutions were used:

- PAA: 30 % acrylamide / 0.8 % bis-acrylamide (Roth)
- 4x Lower-Tris: 1.5 M: Tris-HCl, pH 8.8, 0.4 % SDS
- 4x Upper-Tris: 0.5 M Tris-HCl, pH 6.8, 0.4 % SDS
- TEMED: *N,N,N',N'*-tetramethylethane-1,2-diamine (Merck)
- APS: 16 % ammonium persulfate dissolved in H₂O
- Running buffer: 192 mM glycine, 25 mM Tris base; 1 % SDS
- 2x stop mix: 2 ml 0.5 M Tris-HCl pH 6.8
1.6 ml glycerol
1.6 ml 20 % SDS
1.4 ml dH₂O
0.4 ml 0.05 % (w/v) bromophenol blue
7 μl β -mercaptoethanol / 100 μl
- 5x sample buffer: 25 % v/v 250 mM Tris pH 6.8
50 % v/v glycerin
10 % w/v SDS
25 % v/v β -mercaptoethanol)
- Resolving gel composition:

	5 %	7.5 %	10 %	12 %	15 %	17.5 %
PAA	4 ml	6 ml	8 ml	10 m	12 ml	14 ml
4x Lower Tris	6 ml	6 ml	6 ml	6 ml	6 ml	6 ml
dH ₂ O	14 ml	12 ml	10 ml	8 ml	6 ml	4 ml

- Stacking gel composition: 1.5 ml PAA; 2.5 ml 4x Upper-Tris, 6.5 ml dH₂O

The polymerization of the acrylamide of either the resolving or the stacking gel was initiated by the addition of 40 μ l TEMED and 120 μ l APS or 40 μ l TEMED and 70 μ l APS, respectively. The polymerization took approximately 25–30 min at room temperature. For the stacking gel combs with either 10 or 15 wells were applied. The volumes mentioned above for the stacking and the running gel are sufficient for six Mini gels (100 mm x 75 mm x 1 mm). Before loading the samples onto the gel, they were mixed with 2x stop mix, heated at 100 °C for 5–10 min and subsequently centrifuged (short spin, full speed at room temperature). Separation was allowed at 150 V for about 30–90 min depending on the resolution needed. To determine the protein size of the separated samples the broad range prestained protein marker (NEB) was loaded in one lane of the gel.

After discarding the stacking gel, the resolving gel was either subjected to Coomassie staining, silver staining or Western blot analysis.

4.6.3. Coomassie staining of protein gels

Coomassie staining of the PAA gels was conducted for approximately 30 min at room temperature with Coomassie staining solution (0.25 % Coomassie R250, 50 % methanol, 10 % glacial acetic acid). For destaining of unspecific stained areas and visualization of protein bands the Coomassie destaining solution (45 % methanol, 45 % H₂O, 10 % glacial acetic acid) was used. The destaining solution was renewed several times, until the optimal result was obtained.

When needed for mass spectrometry analysis PAA gels were stained according to Bente et al. [151]. Briefly, gels were colloidal Coomassie brilliant blue stained overnight in 1.6% ortho phosphoric acid (Fluka), 8 % ammonium sulfate (Fluka), 0.12 % Coomassie blue G 250 (Merck), and 20 % methanol (Merck) and destained in 25 % methanol.

4.6.4. Silver staining of protein gels

Silver staining of PAA gels was conducted according to a previously described protocol published by Rabilloud [152]. First, the gel was fixed in fixing solution (50 % ethanol, 12 % acetic acid, 38 % dH₂O) for 1 h at room temperature. After washing for 20 min in 30 % ethanol, the gel was sensitized in sensitizing solution (66 μ l 37 % formaldehyde, 25 μ l 43 % Na₂S₂O₃ in dH₂O, ad 100 ml dH₂O) for 1 min. Subsequently the gel was washed three times in dH₂O for 1 min each and then impregnated with silver staining solution (66 μ l 37 % formaldehyde, 0.2 g AgNO₃, ad 100 ml dH₂O) for 30 min at room temperature. Again, the gel was washed two times for exact 30 s. Finally, the gel was incubated in developer (50 μ l 37 % formaldehyde, 1.8 μ l 43 % Na₂S₂O₃, 6 g Na₂CO₃, ad 100 ml dH₂O) until the gel was optimally developed. The Reaction was stopped with freshly prepared EDTA-solution (13.7 g/l).

4.6.5. Western blotting

For transferring the resolved proteins onto nitrocellulose membranes the Mini Trans-Blot Cell (BioRad) was used. The transfer was conducted for 1 h at 350 mA. Subsequently to blotting, the nitrocellulose membrane was blocked with blocking solution and then incubated with the desired antibody overnight at 4 °C. Then, the membrane was washed three times for 10 min with washing buffer before being incubated with secondary antibody solved in blocking buffer for 1 h at room temperature on a seesaw. The washing steps were repeated and the proteins were visualized by chemiluminescence (ECL, Pierce) and exposing to X-ray films. The films were developed with a Curix 60 automated developer (Agfa).

The following buffers and setups were applied for Western blotting:

- Western blot buffer: 25 mM Tris-HCl
192 mM Glycin
20 % Methanol
- Western blot setup: Sponge, Whatman paper, PAA-gel, nitrocellulose, Whatman paper
Sponge
- Cooling block: mounted in the transfer chamber for blotting
- Blocking buffer: 5 % skim milk (SM) or 5 % BSA dissolved in 1x TBST (20 mM Tris, 150 mM NaCl, pH 7.5, 0.1 % Tween20)
- Washing buffer: 1x TBS / 0.1 % Tween20 (TBST)

Primary Antibody	Dilution	Buffer	Company	Source
anti- β -actin	1:1000	5 % BSA-TBST	Cell Signaling	rabbit
anti-Erk1/2	1:1000	5 % SM-TBST	Stressgen	rabbit
anti- Erk (pT _p Y 185/187)	1:1000	5 % SM-TBST	Invitrogen	rabbit
anti-elp	1:1000	5 % SM-TBST	mAb2810 [153]	mouse
anti-HA	1:1000	5 % SM-TBST	Santa Cruz Biotechnologies	rabbit
anti-IGF-I clone Sm1.2	1:500	5 % SM-TBST	Millipore	mouse
anti-insulin	1:500	5 % SM-TBST	Sigma	mouse
anti-myc	1:1000	5 % SM-TBST	Santa Cruz Biotechnologies	mouse
anti-phospho-Akt	1:1000	5 % BSA-TBST	Cell Signaling (#9275)	rabbit
anti-phospho-FGFR (Tyr653/654)	1:500	5 % BSA-TBST	Cell Signaling	rabbit
anti-V5	1:5000	5 % SM-TBST	Invitrogen	mouse
anti-His	1:1000	5 % SM-TBST	Cell signaling	mouse

Secondary Antibody

anti- mouse IgG – HRP	1:10,000	blocking buffer	Jackson ImmunoResearch	
anti-rabbit IgG – HRP	1:5000	blocking buffer	Jackson ImmunoResearch	
anti-rat IgG - HRP	1:1000	5 % SM-TBST	BioLegend	goat

4.6.6. Mass spectrometry

Matrix-assisted laser desorption/ionisation time-of-flight mass spectrometry (MALDI-TOF-MS) of protein spots was conducted essentially as described [154]. The desired protein spots were cut from the Coomassie brilliant blue stained gel with a wide-bore pipet tip. Then the gel pieces were placed into single wells of a ZipPlate (Montage In-Gel-DigestZP Kit, Millipore) and according to the manufacturer's instructions the proteins in the gel plugs were destained, digested with trypsin (Promega), extracted, purified on a C18 reverse phase matrix, and eluted in 8 μ l of 60 % acetonitrile, 0.1 % trifluoroacetic acid (TFA).

Then, 2.5 μ l of the eluted peptides were spotted onto a 378-well, 400 μ m Anchor Plate (Bruker Daltonics). Shortly before the solvent was completely evaporated, 1 μ l of matrix solution (saturated α -cyano-4-hydroxy-cinnamic acid (Sigma) solution in 50 % acetonitrile, 0.1 % TFA) was added. After

the plate was air-dried, MALDI-TOF-MS was conducted on a Bruker Autoflex Mass Spectrometer (Bruker Daltonics, Bremen). The experiments were run in the reflection mode applying the following settings: Ion source 1 voltage: 19 kV; ion source 2 voltage: 16.5 kV; reflector voltage 20 kV; lens voltage 8 kV; 40 ns pulse time, 120 ns pulse extraction time, matrix suppression <500 Da. For internal calibration a mix of peptides (Nr. A9525 Angiotensin II MolMass 1046.5; Nr. A9650 Angiotensin I Mol. Mass 1296; Nr. A109 ACTH clip 1-10 Mol. Mass 1299; Nr. A2407 ACTH clip 1-17 Mol. Mass 2093; Sigma) was used. Analysis of obtained spectra was conducted by means of Mascot (www.matrixscience.com; Peptide Mass Fingerprint; MSDB 20060831).

4.7. Working with bacteria

4.7.1. Bacteria strains and media

Bacteria Strains	Company	Genotype
<i>E. coli</i> DH5 α	Invitrogen	F Φ 80 <i>dlacZ</i> Δ M15 Δ (<i>lacZY-argF</i>) U169 <i>recA1 endA1 hsdR17</i> (rk-,mk-) <i>phoA supE44 thi-1</i> λ <i>gyrA96 relA1 tonA</i>
<i>E. coli</i> TOP10	Invitrogen	F Φ <i>mcrA</i> Δ (<i>mrr-hsdRMS-mcrBC</i>) Φ 80 <i>lacZ</i> Δ M15 Δ <i>lacX74 recA1 araD139</i> Δ (<i>ara-leu</i>)7697 <i>galU galK rpsL</i>
<i>E. coli</i> BL21	Amersham	F Φ , <i>ompT, hsdS_b</i> (r _B \bar{m} _B $\bar{}$), <i>gal, dcm</i>
<i>E. coli</i> BL21(DE3) pLysS	Novagen	F Φ <i>ompT hsdS_b</i> (r _B \bar{m} _B $\bar{}$) <i>gal dcm</i> (DE3) pLysS (cam ^R)
Media		
Luria-Broth (LB)	Invitrogen	
LB agar plates		LB medium with 1.5% Bacto-Agar
SOC	Invitrogen	

Bacteria cultures were grown at 37 °C either in LB liquid medium under constant shaking (225 rpm) or on LB agar plates. The appropriate selective antibiotic was supplemented depending on the propagated plasmid (100 μ g/ml ampicillin, 50 μ g/ml kanamycin or 100 μ g/ml chloramphenicol).

4.7.2. Chemically competent *E. coli*

Chemically competent bacteria were produced using the CaCl₂ method. Briefly, 50 ml LB medium were inoculated with 1 ml overnight culture of the respective *E. coli* strain. The bacteria were then incubated approximately 2–3 h at 37 °C at 225 rpm until an OD_{600nm} of 0.5–0.7 was reached. In the next step, the culture was separated into 2 aliquots, centrifuged at 4000 rpm for 10 min at 4 °C. After decanting the supernatant the pellet directly placed on ice. Each pellet was carefully resuspended in 12 ml ice cold 100 mM CaCl₂ and the centrifugation step was immediately repeated. Then the resulting pellet was dissolved in 1 ml fresh CaCl₂ by gently resuspending. After incubating the bacteria for 30 min up to 60 min on ice, glycerol was added to a final concentration of 20 %. The bacteria were immediately stored at -80 °C in 50 μ l aliquots.

4.7.3. *E. coli* transformation

For each transformation 25 μ l competent cells were incubated with the respective plasmid or ligation mixture for 30 min on ice. Subsequently, heat shock at 42 °C for 1 min followed. After addition of 125 μ l SOC medium, the bacteria were incubated between 30 min and 60 min at 37 °C under constant shaking (225 rpm). Then the bacteria were transferred on LB agar plates supplemented with the corresponding antibiotic (100 μ g/ml ampicillin, 50 μ g/ml kanamycin or 100 μ g/ml chloramphenicol) and incubated at 37 °C overnight.

4.7.4. Heterologous expression in *E. coli* and purification of the recombinant proteins

pBAD/Thio-TOPO® vector system

In this work, recombinant EmNHR1-ab and EmFRin were expressed in DH5 α *E. coli* using the pBAD/Thio expression Kit (Invitrogen). The vector was designed to express fusion proteins under the control of an inducible araBAD promoter with an N-terminal thioredoxin tag which can be cleaved at the enterokinase site. Moreover, a V5 epitope tag is fused to the C-terminus followed by a His₍₆₎-tag. The former was used to detect fusion proteins by means of Western Blot (anti-V5-antibody) and the latter was used for native affinity chromatography. As stated by the manufacturer, the V5 epitope tag and the His₍₆₎-tag contribute 16 kDa to the size of the fusion protein. After ligation of the vector and the respective PCR amplicon (EmNHR-ab: EmNHR-ab-dw and EmNHR-ab-up; EmFRin: EmFRin-pBAD/Thio-dw and EmFRin-pBAD/Thio-up) the construct was introduced in *E. coli*, selected under ampicillin pressure and checked for correct insertion by means of sequencing. Positive clones were used for pilot expression studies according to the manufacturer's specifications.

For large scale recombinant expression, an overnight culture (LB medium, 100 μ g/ml ampicillin) of the respective clones was used as inoculum (1:200). The culture was propagated until the bacteria reached an OD_{600nm} of 0.5. Then the induction of protein expression was started by adding 0.2 % L-arabinose and the culture was incubated for 6 h at 37 °C under constant shaking (225 rpm). Subsequently, the bacteria were harvested by centrifugation (4 °C, 6000 g, 20 min) and the pellet was resuspended in native lysis buffer (300 mM NaCl, 50 mM sodium phosphate-buffer pH 8.0, 10 mM imidazol) supplemented with 5 mg/ml lysozyme and incubated on ice for 30 min. Then suspension was stored at -20 °C until protein purification. Upon thawing the lysed pellet was treated with sonification for a least three times for 30 s (continuous output of 4-5, duty-cycle of 40-50 %) until the mixture was viscous. Subsequently an RNase (5 μ g/ml) – Dnase (5 μ g/ml) treatment followed for 15 min at 30 °C before centrifugation at 4 °C and 6000 g for 20 min. Then the supernatant was transferred to FastPrep® Lysing Matrix B tubes (Qbiogene, Bio 101 Systems, Heidelberg, Germany) and transferred to a FastPrep® for 45 s at speed 6.5. After centrifugation for 15 min at 4 °C (maximum speed) the supernatant was pooled and 4 ml Nickel beads (ProBond Resin, Invitrogen) which had earlier been equilibrated with lysis buffer were added. This mixture was incubated at 4 °C overnight under constant but slow rotation. After washing three times in 300 ml native washing buffer (300 mM NaCl, 50 mM sodium phosphate-buffer pH 8.0, 20 mM imidazol) the beads were put on a PD-10 column (GE Healthcare) and the protein was eluted in a first step with 6 ml elution buffer I (300 mM NaCl, 50 mM sodium phosphate-buffer pH 8.0, 250 mM imidazol) and in a second

step with 6 ml elution buffer II (300 mM NaCl, 50 mM sodium phosphate-buffer pH 8.0, 500 mM imidazol). The eluted fractions were analysed by Western blot or Coomassie staining of the PAA-gel run in an SDS-PAGE. Fractions which harbored the desired protein were collected, pooled and dialysed overnight in 5 l 1xPBS at 4 °C.

pGEX-5X Vector System

The pGEX-5X system (Amersham) was used to express recombinant EmFRin. Recombinantly expressed fusion proteins have an N-terminally fused glutathione-s-transferase (GST) of *S. japonicum* which is about 26 kDa in size. The fusion protein expression is under the control of an IPTG (isopropyl- β -D-thiogalactopyranoside) inducible promoter. For cloning EmFRin the following oligonucleotides were used: EmFRin_pGEX5X_BamH1_dw and EmFRin_pGEX5X_Not1_up and positive clones were verified by sequencing.

Protein expression was conducted as follows: LB-medium containing 100 μ g/ml ampicillin was inoculated 1:50 with *E. coli* BL21 from an overnight culture. The suspension was incubated at 37 °C and constant shaking (225 rpm) until an OD_{600nm} of 0.5. Subsequently the protein expression was induced by the addition of 1 mM IPTG and allowed to for 2 h. Then the bacteria were centrifuged at 4 °C at 6000 g for 20 min. After resuspension in 10 ml pre-chilled 1xTBS containing 5 mg/ml lysozyme the suspension was frozen at -20 °C overnight. Upon thawing the lysed pellet was treated with sonification for a least three times for 30 s (continuous output of 4-5, duty-cycle of 40-50 %) until the mixture was viscous. Next an RNase (5 μ g/ml) and DNase (5 μ g/ml) treatment followed for 15 min at 30 °C before 1 % Triton-X—100 was added. After an incubation period of 1 h at 4°C, the cell debris was pelleted by centrifugation (4 °C, 6000 g for 20 min). The supernatant was transferred to a new reaction tube and mixed with glutathione sepharose beads that had been previously equilibrated with 1x PBS 1 % Triton X-100. After 4 h constant agitation at 4 °C, the beads were washed three time with 1x TBS, 1 % Triton-X-100 and then the protein was eluted in several fractions by using the elution buffer I (25 mM glutathione in 1x TBS) and II (50 mM glutathione in 1x TBS), each three times. The eluted fractions were analysed by Western blot or Coomassie staining of the PAA-gel run in an SDS-PAGE. Fractions which harbored the desired protein were collected, pooled and dialysed overnight in 5 l 1xPBS at 4 °C.

pET30c system

The pET30 vector (Novagen) was used to express recombinant EmFRex. For cloning EmFRex the following oligonucleotides were used: FRex-pET30a(+)-BamH1-dw and FRex-pET30a(+)-Sal1-up and positive clones were verified by sequencing. Protein expression was conducted in *E. coli* BL21(DE3) pLysS cell und ampicillin and chloramphenicol selection according to the manufacturers specifications.

pRSET-A

The pRSET-A vector (Invitrogen) was used to express recombinant EmNHR-ab. For cloning EmNHR-ab the following oligonucleotides were used: EmNHR-ab2-NcoI-pRSET-dw and EmNHR-ab2-HindIII-pRSET-up and positive clones were verified by sequencing. Protein expression was conducted *E. coli*

host strain BL21(DE3)pLysS under ampicillin and chloramphenicol selection and IPTG induction according to the manufacturer's instruction. Protein purification was done as described for pBAD/Thio-TOPO[®] fusion His₍₆₎-tag proteins.

pQE30

The pQE30 vector (QIAexpressionist, QIAGEN) was used to express recombinant EmFRin. For cloning EmFRin the following oligonucleotides were used: pQE30-FRin-BamH1-dw and pQE30-FRin-Sal1-up and positive clones were verified by sequencing. Protein expression was conducted *E. coli* host strain M15[pREP4] under ampicillin selection and IPTG induction according to the manufacturers specifications. Protein purification was done as described for pBAD/Thio-TOPO[®] fusion His₍₆₎-tag proteins.

4.8. Working with yeast

4.8.1. Yeast strains and media

Yeast strains

AH109	BD Biosciences Clontech	<i>MATα</i> , <i>trp1-901</i> , <i>leu2-3, 112</i> , <i>ura3-52</i> , <i>his3- 200</i> , <i>gal4Δ</i> , <i>gal80Δ</i> , <i>LYS2::GAL1UASGAL1TATA- HIS3</i> , <i>GAL2UAS GAL2TATA-ADE2</i> , <i>URA3::MEL1UAS-</i> , <i>MEL1TATA-lacZ</i>
Y187	BD Biosciences Clontech	<i>MATα</i> , <i>ura3-52</i> , <i>his3-200</i> , <i>ade2-101</i> , <i>trp1-901</i> , <i>leu2-3, 112</i> , <i>gal4Δ</i> , <i>met -</i> , <i>gal80Δ</i> , <i>URA3::GAL1UAS-GAL1TATA-lacZ</i> , <i>MEL1</i>

Media

YPDA	20 g/l Difco peptone 10 g/l Yeast extract 20 g/l Bacto agar (for plates) dH ₂ O ad 950 ml pH 6.5 adjusted by adding 25 % HCl After autoclaving 50 ml of 40 % glucose and 15 ml of 0.2% adenine hemisulfate solution were added. Both solutions were filter sterilized.
SD	6,7 g Difco™ Yeast Nitrogen Base w/o Amino Acids 20 g Difco™ Bacto Agar x g of the corresponding drop out supplement (DOS) (Clontech) dH ₂ O ad 930 ml or 950 ml pH 6.5 adjusted by adding 25 % HCl After autoclaving 50 ml of 40 % glucose were supplemented.

SD - Trp	+ 0.64 g/l -Leu/- Trp DOS + 20 ml 50x Leu (5 mg/ml)
SD - Leu	+ 0.64 g/l -Leu/- Trp DOS + 20 ml 50x Trp (1 mg/ml)
SD - Leu/- Trp	+ 0.64 g/l -Leu/- Trp DOS
SD - Leu/-Trp/ -His	+ 0.6 g/l -Ade/- His/- Leu/-Trp DOS + 0.003 % (v/v) adenine hemisulfate
SD - Leu/- Trp/ -His/-Ade	+ 0.6 g/l Ade/ - His/ - Leu/ - Trp DOS

4.8.2. Yeast-two hybrid analysis

In a yeast-two-hybrid approach protein-protein interactions were analysed. For that, the MATCHMAKER™-system (Clontech) was used and the experiments were performed as previously described [60]. Briefly, translational fusions of the proteins or protein domains of interest with the Gal4 DNA-binding domain (pGBKT7; BD) or the Gal4-activation domain (pGADT7; AD) were generated. These fusion constructs were co-transformed into the yeast strain AH109. For transformation YPDA medium was inoculated with AH109 and cultured at 30 °C overnight and 200 rpm. Then the culture was collected and centrifuged (700 g, 5 min, 4 °C) and subsequently the pellet was resuspended in freshly prepared transformation buffer (40 % PEG 3350, 200 mM lithium acetate, 100 mM DTT; 100 µl for 1 ml yeast culture). 100 µl aliquots of the yeast-transformation-buffer solution were subjected to reaction tubes and 200 ng DNA of each plasmid construct were added. The suspension was incubated for 30 min at 45 °C before being transferred on leucine/tryptophan-deficient selective plates. Selection was allowed for 4 d at 30 °C. Then the proper expression of the fusion proteins was verified by Western blot analyses utilizing antibodies against the Gal4-AD (anti-HA; SantaCruz Technologies) and Gal4-BD (anti-cmyc; SantaCruz Technologies). Interaction trap analysis of the double-transformants was conducted according to the MATCHMAKER™ instruction specifications using selective agar plates lacking leucine, tryptophan (as plasmid selection markers) and either histidine in the presence of 7.5 mM 3-amino-triazole (3-AT) for medium stringency or histidine plus adenine for high stringency selection. Colony formation was assessed after 3 days of incubation at 30 °C.

The AD and BD constructs for the full-length EmNHR1 coding sequence, the DBD, the complete and the truncated forms of the LBD have been obtained by directional cloning. First, the full-length *Emnhr1* was cloned into the pDrive (Qiagen PCR cloning kit) plasmid amplified from H95 metacestode cDNA using the primers NHR1_H95_ATG_NdeI_dw and NHR1_H95_TAA_up. Second, the respective fragments were PCR amplified from the pDrive plasmid. The DBD was amplified using NHR1_H95_ATG_NdeI_dw and NHR1_H95_DBD_Y2H_XmaI_up and for the constructs of the LBD the following primers were chosen: EmNHR1-LHQ-NcoI-fwd/EmNHR1-FIE-XmaI-rev; EmNHR1-LHQ-NcoI-fwd/EmNHR1-ALT-XmaI-rev; EmNHR1-NTS-NcoI-fwd/EmNHR1-FIE-XmaI-rev; EmNHR1-LHQ-NcoI-fwd/EmNHR1-SLV-XmaI-rev; EmNHR1-NTS-NcoI-fwd/EmNHR1-ALT-XmaI-rev; EmNHR1-DNY-NcoI-fwd/EmNHR1-FIE-XmaI-rev. EmNHR1-FL was introduced to pGADT7 via *NdeI/SacI* and to pGBKT7 via *NdeI/SalI* restriction digest. To introduce EmNHR1-DBD into pGADT7 and pGBKT7 an *NdeI/XmaI*

restriction digest was applied. All LBD constructs were introduced to pGBKT7 by *NcoI/XmaI* restriction digest. For the respective LBD AD clones the LBD inserts were cut from the positive BD clone with the following enzymes: *NdeI* for and *NdeI/XmaI* and inserted into pGADT7, cut with the same restriction enzymes, respectively.

The ORF for EmFR was amplified from cDNA with the primers EmFR-pSecHygroA-*BamHI*-dw and EmFR-pSecHygroA-*NotI*-up. Then the intracellular domain (EmFRin) was PCR amplified using the following oligonucleotides: FRin-AD-*XmaI*-dw/FRin-AD-*Clal*-up and FRin-BD-*BamHI*-dw1/FRin-BD-*PstI*-up, respectively. The inserts were cloned via the restriction sites *XmaI/Clal* and *BamHI/PstI* into the AD and BD yeast vectors, respectively. Using the oligonucleotides HNF4-DBD-AD/BD-*NdeI*-dw and HNF4-DBD-PI-AB/BD-*EcoRI*-up or HNF4-DBD-Pa-AB/BD-*EcoRI*-up, the different EmHNF4 DBD isoformes were amplified from the respective pDrive clones, which had resulted from amplifying EmHNF4 (EmHNF4-ORF-dw/EmHNF4-ORF-up) from cDNA Pools and activated protoscoleces DNA. EmHNF4 DBD isoformes were amplified and cloned via *NdeI* and *EcoRI* into the expression vectors. All the clones were fully sequenced to ensure that no unwanted mutations had been introduced due to incorrect PCR amplification. Yeast-two hybrid fusion plasmids for EmSmadA, EmSmadB, EmSmadC, EmSmadD, EmSkip, EmAlien, EmGt198, EmElpN, EmElpC, EmPDZ have been previously described [37,58,60-62].

4.8.3. Liquid culture β -galactosidase assay

The liquid culture β -galactosidase assay was performed as described by Förster et al. [145]. For that, the plasmid constructs (see section 0) were co-transformed into the yeast strain Y187. The assay was conducted according to the MATCHMAKERTM specifications. Briefly, co-transformants were grown in leucine/tryptophan deficient medium over night, diluted and let grown again for 5 h. The cultivation was conducted either in the presence or absence of certain substances which were analysed for their impact on protein-protein interactions. The optical density at OD_{600nm} was measured before harvesting the yeast cells and washing them in Z buffer (16.1 g/L Na₂HPO₄•7H₂O; 5.50 g/L NaH₂PO₄•H₂O; 0.75 g/L KCl; 0.246 g/L MgSO₄•7H₂O; pH 7.0). After three freeze-and-thaw cycles with liquid nitrogen, first Z buffer/0.27% v/v β -mercaptoethanol and then 0.67 mg/ml o-nitrophenyl β -D-galactopyranoside were added. The reaction was stopped immediately after the yellow colour had developed with 1 M Na₂CO₃.

Analysed substances have been: 5 % FBS, 10 % FBS, 20 % FBS, 20 % heat inactivated FBS, 5 % human serum, 10 % human serum, 20 % *E. multilocularis* hydatid fluid, 20% FBS treated with dextran coated charcoal, 10 % FBS <10 kDa, 10 % FBS >10 kDa, FBS <30 kDa, 10 % FBS >30 kDa (Centriprep YM-10 10 kDa and 30 kDa), 0.013 mg/l Biotin, 0.013 mg/l Vitamin B12, 10 % DMEM with/without FBS, 10 % Panserin or conditioned Panserin, 10 % Panserin without lipids, 10 % Panserin without lipids/cholesterol, 10 % Panserin without lipids/cholesterol/vitamins, 10 % conditioned A4 medium and 400 μ g/ml Proteinase K treated FBS.

4.9. Working with mammalian cell lines

4.9.1. Cell lines and media

Cell lines	Acronym	ATCC no.	Media
Rat Reuber hepatoma cells	RH-	CRL-1600	Dulbecco's minimal essential medium (DMEM; GIBCO BRL); Panserin™ 401
Human embryonic kidney cells	HEK293	CRL-1573	DMEM; GIBCO BRL

4.9.2. Cultivation of RH- cells under serum-free conditions: Panserin™ 401

RH- cells were gradually adapted to serum-free conditions according to the manufactures suggestions. Briefly, RH- cells cultivated in DMEM supplemented with 10 % FBS were taken from the logarithmic growth phase and seeded in Panserin™ 401 enriched with 5 % FBS. After two passages the amount of serum was reduced to 1 %. Subsequently, the step was repeated and the concentration of FBS was lowered to 0.5 % and finally to 0 % FBS. Passaging regime was conducted in parallel with RH- growing in DMEM/10 % FBS.

4.9.3. Transfection of HEK293 cells

HEK293 cells were cultured in DMEM containing 10 % fetal bovine serum (FBS), 1 % penicillin and 1 % streptomycin (1 % P/S) at 37 °C with 5 % CO₂. HEK293 cells were transfected with constructs of the vector pSecHygroA encoding wild-type EmFR and mutant EmFR TkD-, a dead box kinase in which the amino acid motif DFG was mutated to DNA. As mock control the empty vector was used.

One day prior to the transfection, the medium from the HEK293 cells was removed and the cells were detached by trypsin/ETDA treatment for 5 min at 37 °C. 8×10^4 cells were seeded per well into a 6-well plate containing 5 ml DMEM, 10 % FBS, 1 % P/S and incubated overnight at 37 °C and 5 % CO₂. Then, the medium was replaced by 4 ml fresh medium and the transfection solution (DNA-salt-complex) was added drop wise. The transfection solution consisted of 7.5 µg of plasmid DNA mixed with 62 µl 2 M CaCl₂ and was supplemented to a final volume of 500 µl with dH₂O. After mixing, 500 µl 2x HBS buffer (50 mM HEPES, 1.5 mM Na₂HPO₄, 280 mM NaCl, 10 mM KCl, 12 mM α-D-glucose, pH 7.1) were added. Then, the suspension was inverted for 2-4 times and incubated for 30 min at room temperature. After 7 h, the medium was carefully replaced with fresh medium and the incubation was continued for 24 h. Yet, another medium change was performed, letting the cells grow again for 24 h before harvesting. For CIP treatment (NEB) the cells were harvested, and adjusted to 100 µl with NEB Buffer 3. 20 U (2 µl) of CIP were added and the suspension was incubated for 45 min at 37 °C. Then 5x western blot sample buffer was added in a 1:5 dilution. Also, 1 mM Na₃VO₄, 10 mM NaF and 1x phosphatase inhibitors (PhosSTOP, Roche Applied Science, Mannheim, Germany) were included. Other samples for the analysis of protein expression by western blotting were treated as follows. The medium was removed and the cells were adjusted to 150 µl 1xPBS with a final concentration of 1 mM Na₃VO₄, 10 mM NaF and 1x phosphatase inhibitors and mixed 40 µl 5x western blot sample buffer. All samples were heated to 100 °C for 10 min, shortly

spun down to pellet the debris and the supernatant was subjected to SDS-PAGE and Western blot analysis. The remaining supernatant was frozen at -20 °C for further analysis.

4.10. Transfection and treatment of *Xenopus laevis* oocytes

All experiments with *Xenopus laevis* oocytes were part of a joint project and have been conducted by E. Browaeys-Poly and K. Cailliau at the Laboratoire de Régulation des Signaux de Division, University Lille 1 Sciences and Technology, Villeneuve d'Ascq Cedex, France as a joint project.

Briefly, capped messenger RNA (cRNA) encoding the full-length sequence of EmFR was synthesized in vitro utilizing the T7 mMessage mMachin Kit (Ambion, Austin, TX, USA). Stage VI oocytes were used for microinjection [155] of EmFR cRNA (60 ng in 60 µl) 48 h before the addition of 1, 5 or 10 nM human aFGF or bFGF (R&D systems, Abingdon, UK) to the medium. As a positive control cRNA of pleurodeles FGFR1 which was identified as homologous to human receptor [156] (gift of Shi D.L. CNRS UMR 722, Paris VI) was microinjected. Additionally, BIBF1120 (stock solution 10 mM in DMSO) was added (0.1 to 20 µM final concentration) 1 h before ligand stimulation (10 nM aFGF or bFGF) on EmFR and FGFR1 expressing oocytes. Subsequently, 15 h after FGF stimulation the oocytes, either treated or untreated with inhibitor, were analyzed for their state of progression in the cell cycle. G2/M transition or Germinal Vesicle Breakdown (GVBD) is visible by the detection of a white spot at the animal pole of the oocytes. Non-injected oocytes treated or untreated with 10 µM progesterone served as positive and negative controls of GVBD, respectively. In each assay, 20-30 oocytes which were taken from three animals have been used.

For Western blot analysis the oocytes were handled as follows: The oocytes were subjected to lysis buffer (50 mM HEPES pH 7.4, 500 mM NaCl, 0.05 % SDS, 5 mM MgCl₂, 1 mg/ml BSA, 10 µg/ml leupeptin, 10 µg/ml aprotinin, 10 µg/ml soybean trypsin inhibitor, 10 µg/ml benzamidine, 1 mM PMSF, 1 mM Na₃VO₄). Then the lysates were centrifuged for 15 min at 10,000 g and 4°C. Subsequently, the membrane pellets were resuspended in lysis buffer supplemented with 1 % Triton X-100, were incubated for 15 min at 4 °C and again centrifuged as before. Finally, the supernatants were subjected to SDS-PAGE analysis. Proteins were transferred to a Hybond ECL membrane (Amersham Biosciences, Orsay Cedex, France). For detection, the membranes were treated with anti-c-myc (1/50 000, Invitrogen, Cergy Pontoise Cedex, France) or anti-p-tyr (1/8000, BD Biosciences, France) antibodies. An HRP-coupled anti-mouse IgG antibody (1/50 000, Biorad, Marnes-la-Coquette, France) served as secondary antibody. Signals were detected with the use of ECL advance Western blotting detection kit (Amersham Biosciences, Orsay Cedex, France).

4.11. Working with *E. multilocularis*

4.11.1. *E. multilocularis* isolates

Isolate	Source	Use
H95	primary infection of <i>M. unguiculatus</i> by oncosphere uptake	metacestode cultivation in vitro isolation and cultivation of primary cells
GH09	Java monkey as intermediate host, secondary infection of <i>M. unguiculatus</i>	metacestode cultivation in vitro isolation and cultivation of primary cells protoscoleces isolation and cultivation
J31	Java monkey as intermediate host, secondary infection of <i>M. unguiculatus</i>	protoscoleces isolation and cultivation

4.11.2. In vivo cultivation of metacestode larvae and isolation from Mongolian jirds

Maintenance of *E. multilocularis* metacestodes strictly requires constant passages in Mongolian jirds (*Meriones unguiculatus*). For that, the animals were infected with homogenized larval material by means of intraperitoneal injection. The jirds developed a secondary alveolar echinococcosis within 2–3 months and were then sacrificed with CO₂. The larval material was isolated under sterile conditions and the sterile instruments were repeatedly substituted while also avoiding injuring the digestive tract of the animals or touching the animals' fur hair. Subsequently the parasite material was cut into small tissue blocks and subjected onto a metallic tea strainer for sieving. The ground material was washed at least three times with 1xPBS in order to get rid of host cells. Next, the material was subjected to different actions depending on the needs for the following experiment. For the isolation of protoscoleces (see section 4.11.3). For other purposes, the suspension was incubated overnight at 4 °C in the presence of Tavanic (1 mg/ml). After washing out the antibiotic with 1xPBS, the suspension was used for injection of a new laboratory animals (0.3 – 0.9 µl inoculums) or the material was taken to start a new in vitro culture of metacestode larvae [49,50,54].

4.11.3. Isolation and activation of protoscoleces

Protoscoleces were isolated from *in vivo* cultivated parasite material according to a previously established protocol [44]. For that, one volume of freshly isolated and ground parasite material (see section 4.11.2) was diluted with three volumes of 1xPBS. Then the suspension was vigorously shaken for approximately 10 min in order to release the protoscoleces from the metacestode larvae material. Subsequently the suspension was sieved through polyester gauze (150 µm pore size) and the flow-thru was taken to be sieved through a second polyester gauze (30 µm pore size). The protoscoleces do not pass the 30 µm gauze and thus were collected from the gauze by resuspension with 1xPBS. The material was transferred to a petridish (diameter: 10 cm). By horizontal rotation of the petridish, the protoscoleces concentrate in the middle and were transferred with a 1000 µl pipette into a fresh reaction tube for further applications.

The freshly isolated protoscoleces were activated by pepsin/low pH treatment as described by [52]. In detail, 0.5 -1 ml protoscoleces were transferred to 25 ml 0.05 % pepsin in DMEM without FBS at pH 2 to mimic the gastrointestinal passage. After 30 min at 37 °C under constant shaking (125 rpm)

the material was allowed to precipitate by gravity. After three washing steps with 1xPBS, the protoscoleces were resuspended in 0.2 % sodium taurocholate (solved in DMEM without FBS, pH 7.4) and an incubation period of 3 h at 37 °C and 125 rpm followed. Finally, after three washing steps, the protoscoleces were either subjected to RNA isolation (see section 4.4.1) or in vitro cultivation with and without treatment (see section 4.11.5).

4.11.4. In vitro cultivation of metacestode larvae

Metacestode larvae were cultured in vitro in the absence or presence of host cell as described [48,148]. For that, the homogenized material which was freshly isolated from animals (see section 4.11.2) was used.

In the co-cultivation system 1 ml of ground parasite material was incubated in 50 ml standard culture medium (see table below) in a 75 cm² flask together with 1x10⁷ trypsinized RH- feeder cells. The suspension was cultivated at 37 °C and 5 % CO₂ for approximately ten days. Then the parasite material was poured into 50 ml tubes and was allowed to precipitate by gravity. The supernatant was decanted and replaced by fresh standard medium. Over the next weeks of incubation (up to three months) the medium was replaced weekly by precipitation. Each time the medium was changed, fresh feeder cells were supplemented while using the same flask several fold. Once the metacestode vesicles reached a diameter of 3–5 mm, the vesicles were taken for experiments.

Axenic cultivation: Metacestode vesicles (3–4 mm in diameter) from co-culture were transferred to A4 or B2 medium supplemented with reducing agents for axenic cultivation [48]. To eliminate transferred host cells, the vesicles were washed three times with 1xPBS. The medium was renewed every 48 h to 72 h and the vesicles were incubated at 37 °C under nitrogen atmosphere. During the first week of axenic culture the vesicles were washed once in 1xPBS. For the following passages only the medium was renewed. After two or three weeks, the vesicles were subjected to experiments.

Media	Medium / FBS content	antibiotics
normal culture medium	DMEM, 10 % FBS	1 % P/S
starvation medium	DMEM, 0.2 % FBS or 0 % FBS	1 % P/S
pre-conditioned medium (cDMEM-1 = A4)	filter sterilized supernatant of RH- culture (1x10 ⁶ RH- in 50 ml DMEM, 10 % FBS; for seven days in a 75 cm ² flask)	1 % P/S
pre-conditioned medium (cDMEM-2 = B2)	filter sterilized supernatant of RH- culture (2x10 ⁷ RH- in 50 ml DMEM, 10 % FBS, for three days in a 75 cm ² flask)	1 % P/S
axenic culture medium (nitrogen atmosphere)	A4 or B2, 1 µl/ml β-mercaptoethanol, 1 µl/ml bathocuproine disulfonic acid (BAT), 1 µl/ml L-cysteine (L-Cys)	1 % P/S
Panserin TM 401 (Pan)	0 % FBS	1 % P/S
Conditioned Panserin TM 401 (cPan)	filter sterilized supernatant of Panserin TM 401 RH- culture (1x10 ⁶ RH-/50 ml Panserin, for seven days in a 75 cm ² flask)	1 % P/S

4.11.5. **In vitro cultivation and treatment of activated protoscolec**

Activated protoscolec (20 µl) were transferred to A4 or DMEM (10 % FBS, 1% P/S) medium supplemented with reducing agents for axenic cultivation. The medium (1 ml) in the 24-well plate was renewed every 48 h to 72 h. The protoscolec were incubated at 37 °C under nitrogen atmosphere with the substances in different concentrations or in the presence of the respective solvent (DMSO or water) at identical concentration. In all experiments the viability of the protoscolec which is indicated by active movement was repeatedly analyzed by means of light microscopy. The experiments were conducted in duplicates and repeated three times.

4.11.6. **Treatment of the metacystode vesicles**

In order to analyze the effect of drugs or growth factors axenic metacystode (3–4 mm in diameter) were manually picked and washed one time in 1xPBS. In all experiments the viability of the cysts which is indicated by an intact cyst wall was repeatedly analyzed by means of light microscopy.

Assessment of multiple metacystode vesicles in 12-well culture plates

Vesicles were cultured in groups of five to eight per well in a final volume of 2 ml. As medium either DMEM (10 % FBS, 1% P/S) or A4 supplemented with reducing agents and the respective drugs was chosen. In order to examine the effect of growth factors, metacystode vesicle were incubated under starving condition (DMEM 0.2 % FBS 1 % P/S) for 4 days prior to the stimulation. The vesicles were incubated at 37 °C under nitrogen atmosphere with the substances in various concentrations or as a control in the presence of the respective concentration of the solvent (DMSO, ethanol, methanol, chloroform, HCl or water). The experiments were conducted in duplicates repeated three times.

Assessment of single metacystode vesicles in 15 ml centrifugation tubes:

The metacystode vesicles were singled out in 15 ml tubes and either DMEM (10 % FBS, 1% P/S), B2, A4, Panserin™401, or conditioned Panserin™401 supplemented with reducing agents and the respective drugs were used. As a control the metacystode vesicles were cultured either in untreated medium or medium supplemented with the respective solvent: water, ethanol, methanol and chloroform. Medium was replaced every 48 h to 72 h and the tubes were incubated at 37 °C under nitrogen atmosphere. For each group 5 to 10 replicates were prepared.

4.11.7. **Isolation and cultivation of *E. multilocularis* primary cells**

E. multilocularis primary cells were isolated from axenic two to three months cultivated metacystode vesicles according to a previously published protocol [49] with slight alterations. Metacystode vesicles (30 ml volume) were washed three times with 1x PBS before being disrupted by sucking them into a 10 ml pipette and carefully resuspending. Then the vesicles were pelleted for 5 min at 800 g, the supernatant was discarded, and still intact vesicles were disrupted using a 1 ml tip. Subsequent to a washing step with 1x PBS, the cells were subjected to centrifugation for 3 min at 600 g. Then the pellet was resuspended in 8 volumes of pre-warmed trypsin/EDTA solution and incubated for 15 min at 37 °C. Every 2 minutes the solution was thoroughly mixed until it became turbid. The cells from the germinal layer were obtained and separated from debris by shaking intensively for two min before placing the solution on top of a 150 µm gaze. The flowthrough was run over a 30 µm gaze. Subsequently the second flow through was centrifuged for 1 min at 80 g in order

to pellet the calcium bodies leaving the isolated germinal cells in the supernatant. Consequently the supernatant was poured into a new tube and was now centrifuged for 10 min at 400 g and 5 min at 600 g. The resulting cell suspension was taken up in 1x PBS to a total volume of 0.75 ml. Cells were seeded on 12-well plates at a concentration of 60 μ l suspension in 2 ml culture medium per well. A4, B2 or conditioned PanserinTM401 supplemented with reducing agents served as medium. The plates were incubated at 37 °C under a nitrogen atmosphere for three weeks with medium change every 48 h to 72 h. For the cells were allowed to settle for about 10 min before carefully sucking up half the medium and replacing it with 1 ml fresh medium supplemented with reducing agents calculated to the total volume of 2 ml.

4.11.8. Treatment of *E. multilocularis* primary cells

For the drug treatment experiments, the primary cells were seeded as into A4 or conditioned PanserinTM401. Also, for the stimulation with growth factors, the primary cells were incubated in A4 or conditioned PanserinTM401. The respective drug or growth factor was added for short periods of time (seconds up to 24 h) before subjecting the samples to SDS-PAGE and Western Blot. Long-term observation studies took place for three weeks with replacing the medium and supplementing with the substance of interest as described for metacystode vesicles or protoscoleces. Control samples with the respective concentration of solvent were also analyzed. The experiments were conducted in duplicates and repeated three times.

4.11.9. Verification of purity of *Echinococcus* material

In order to exclude, that DNA/cDNA had been isolated from feeder cells, the synthesized echinococcal cDNA was analyzed in a PCR using oligonucleotides specific for host tubulin cDNA: Tub12up (5' CCC CAA GTG TAT GAT ACT GG-3') and Tub12ST (5' CTG GGC AGT GCG GCA ACC A-3').

4.11.10. BrdU-Proliferation Assay

Proliferation of *E. multilocularis* metacystode vesicles and primary cells was assessed in a bromodesoxyuridine (BrdU)-based method. For that, axenic metacystode vesicles (2-4 mm in diameter) were manually picked and starved for 2 days in 12-well plates with 8 vesicles per well (Greiner BioOne, Kremsmünster, Germany) in 2 ml DMEM (Invitrogen; Karlsruhe, Germany) under 5 % CO₂ atmosphere. Freshly isolated primary cells from metacystode vesicles were plated on 12-well plates and grown for 2 days under axenic conditions in 2 ml Ax-cDMEM-A [49]. Then in both cases the medium was changed by removing 1 ml volume and replacing it with 1 ml DMEM or 1 ml Ax-cDMEM-A for vesicles and primary cells, respectively. BrdU (SigmaAldrich, Taufkirchen, Germany), recombinant human aFGF and bFGF (Immunotools, Friesoythe, Germany) were supplemented at 1 mM, 100 nM and 100 nM final concentrations, respectively. The cultures were incubated for 48 hours at 37 °C under 5 % CO₂ for metacystode vesicles or under nitrogen atmosphere in the case of primary cell culture. Samples were prepared in duplicates in three independent experiments. As control, the metacystodes and primary cells were incubated in either DMEM or Ax-cDMEM-A with 1 mM BrdU, without the addition of FGFs.

Then cells were harvested for the isolation of genomic DNA. In detail, the metacystode vesicles and primary cells were washed with 1x PBS. The vesicles were disrupted by pipetting and both vesicles and primary cells were subsequently pelleted and transferred to lysis buffer (100 mM NaCl, 10 mM

Tris-HCl, pH 8.0, 50 mM EDTA, pH 8.0, 0.5 % SDS) supplemented with 20 µg/ml RNase A and 0.1 mg/ml Proteinase K. For total digestion of *Echinococcus* cells, the samples were incubated for 4 h at 50 °C under constant shaking. The DNA was extracted by two rounds of phenol chloroform extraction (1 volume of phenol-chloroform-isoamyl-alcohol 25:24:1). Subsequently, the DNA was precipitated with 2 volumes of 96 % ethanol and 0.1 volumes 5 M LiCl pH 4.5 over night at -20 °C. The following day, the DNA was completely precipitated at 20,000 rcf for 30 min at 4 °C. After washing with 1 volume 70 % ethanol, the pellet was air-dried for 15 min and was resuspended in 1x TE buffer (10 mM Tris, 1 mM EDTA pH 8.0)

Then the DNA was prepared for coating onto a 96-well plate (96 Well Optical Bottom Plates, Nunc, Langensfeld, Germany). For that, 1 volume of DNA (at 1-5 µg) were combined with 1 volume of Reacti-Bind DNA Coating solution (Pierce Biotechnology, Rockford, IL, USA) and mixed for 10 min. The DNA mixture was added to the microplate in duplicates and incubated overnight at room temperature with gentle agitation. The TE/Reacti-Bind DNA Coating Solution mix served as negative control. Unbound DNA was removed by washing three times with 1xPBS. After blocking with 5 % nonfat dry milk in 1xPBS for 1 h at room temperature and an extensive washing step with 1xPBS, 100 µl of anti-BrdU-POD (Cell Proliferation ELISA, BrdU; Roche Applied Science, Mannheim, Germany) was added and incubated for 90 min at room temperature. After the incubation period, microplates were washed three times with 1xPBS buffer and 100 µl substrate solution (Cell Proliferation ELISA, BrdU; Roche Applied Science, Mannheim, Germany) was added and incubated for 30-60 min. Stop solution was added (25 µl of 1 M H₂SO₄) and absorbance of the samples was measured using ELISA reader at 450 nm.

4.11.11. **siRNA knock-down of EmFR**

Preliminary siRNA knock-down experiments were performed as described [147] with some alterations. 30 ml of axenic metacystode vesicles were washed one time with 200 ml 1x PBS. Then vesicles were disrupted by slowly passing them once through a 10 ml plastic pipette. Subsequently, the broken vesicles were transferred into a 50 ml tube and centrifuged for 5 min at 400xg. After decanting the supernatant and the residual, still intact vesicles the broken vesicles were washed one time by filling the tube with 1x PBS, loosening the pellet by gentle agitation, incubating for 5 min at room temperature and centrifugating 5 min at 400xg before decanting the supernatant. Then eight volumes of pre-warmed 0.05 % Trypsin-EDTA were added and a careful agitation followed to loosen the vesicle pellet. After incubation at 37 °C for 20 min and careful agitation every 3 min the primary cells were detached from the laminated layer. Careful shaking was performed until the liquid became turbid. Subsequently, the cells were filtered through a 30 µm gaze sieve using a self-made sieving device (30 µm polyester filters, A. Hartenstein, Germany, PES5). The calcium bodies were removed by centrifugation for 1 min at 100 g. The supernatant which contained the primary cells was centrifuged at 300xg for 15 min. Then the still turbid supernatant was discarded by decanting and resuspending the cells very carefully in the residual fluid using a 1 ml tip. Now, the cells were seeded drop-wise into 3 wells of a 6-well plate (1 well per 10 ml starting material) each containing 4 ml cDMEM-1 supplemented with BAT only. Then the cells were resuspended by slowly pipetting up and down. After waiting 3 min the clumpy cell aggregates were removed. Then the cells were incubated over night at 37 °C, 5 % CO₂. After checking microscopically for mini-aggregate formation these mini-aggregates were carefully collected with a pipette, transferred into a 15 ml tube and filled up to 14 ml with DMEM / 10 % FBS. Under constant shaking (100 rpm) the cells were allowed to settle for

20 min at room temperature. After decanting the supernatant the step was repeated. The still turbid supernatant was entirely removed by pipetting and the pellet was carefully resuspended in electroporation buffer (siPort™ siRNA electroporation buffer, Ambion) by pipetting very slowly up and down. 50 µl electroporation buffer for 1 ml vesicle starting material was used. Then 50 µl of mini-aggregate/ electroporation buffer suspension was added to 50 µl of electroporation buffer containing 3 µg of double stranded 23 bp siRNA (for either EmFR, EmElp, control RNA: QIAGEN 1022564 or no siRNA). Subsequently, the mixture was filled into a 1 mm gap electroporation cuvette and electroporated at 200 V, 25 µF, 13 Ohm using a saw-wave electroporator. Then the electroporated cells were incubated for 10 min at 37°C, 5% CO₂ and transferred to 1 ml of DMEM/10 % FBS with BAT with 1x 10⁴ freshly trypsinized RH- feeder cells. 50% of the medium was changed every 3-4 days and monitored light-microscopically.

4.12. Computer analyses and statistics

For amino acid sequence comparisons the basic local alignment search tool (BLAST) [157,158] on the nr-aa database collection (<http://blast.genome.jp>) was used. CLUSTAL W alignments were generated with the help of the BioEdit Sequence Alignment Editor (version 7.0.0) applying the BLOSUM62 matrix. MUSCLE alignments were generated using the following platform: <http://www.ebi.ac.uk/Tools/msa/muscle/>. Domain predictions were implemented by using the simple modular architecture research tool (SMART) [96,159] available under <http://smart.emblheidelberg.de>. Predictions for protein localization in cells were done with PSORT II (<http://psort.hgc.jp/form2.html>). For the analyses of genomic and gene loci as well as BLAST searches against the latest assembly version of the *E. multilocularis* whole genome the respective resources of the Sanger Institute (Hinxton, UK) available under <http://www.sanger.ac.uk/cgi-bin/blast/submitblast/Echinococcus> were used. From this resource also transcriptome data has been made public and was taken for gene loci analyses, screening for transcription units.

Two-tailed, unpaired student's T-tests were performed for statistical analyses (GraphPad Prism, version 4). Error bars represent standard error of the mean. Differences were considered significant for p-values below 0.05 (indicated by *)

4.12.1. Iterative BLAST for the identification of putative *E. multilocularis* NHRs

The identification of putative *E. multilocularis* NHRs was carried out as described [145]. Briefly, an iterative tBLASTN was performed against the *E. multilocularis* genome assembly using the deduced amino acid sequence of EmNHR1 DBD [145] applying the WinBlast software, version 0.2.0. With this procedure a certain set of putative DBD sequences was retrieved. To ensure a comprehensive identification of *E. multilocularis* NHRs also *S. mansoni* NHRs [105] along with the identified set of NHRs from the iterative tBLASTN were taken for further BLAST searches. Subsequently, the zinc-finger structures of the identified DBDs were evaluated and a BLASTX analysis using boundaries of 2 kb downstream and 5 kb upstream of the respective sequences was run for all identified genes (<http://blast.ncbi.nlm.nih.gov/Blast.cgi>).

For phylogenetic tree reconstruction, respective sequences that were previously aligned with the help of CLUSTAL W, were allocated to MEGA 4.0. The Neighbour-Joining complete deletion method with a bootstrap value of 1000 was used.

4.13. Ethics Statement

All experiments were carried out in accordance with the European and German regulations on the protection of animals (Tierschutzgesetz, Section 6). Ethical approval of the study was obtained by the local ethics committee of the government of Lower Franconia (621-2531.01-2/05).

5. Results

5.1. FGFR signaling - EmFR

In this work the role and function of EmFR, originally described by Schäfer [94], was analyzed in detail. Thus far, EmFR (562 amino acids, 63 kDa) was described as a single FGFR in the parasitic helminth *E. multilocularis*. EmFR harbors the typical structure common for FGFRs: a characteristic tyrosinekinase domain (sequence alignment; see 3.3.2), a transmembrane domain, an extracellular LBD and a signal peptide (for domain structure, see 3.3.2). Interestingly and conversely to all other known FGFRs, the LBD of *E. multilocularis* is composed of one single IG-domain instead of normally two or three IG-domains. This characteristic was meanwhile confirmed by the available genome data. Furthermore, it was found that after exogenous addition of either aFGF or bFGF to in vitro cultivated metacestode vesicles, a specific phosphorylation of the Erk-like MAP-kinase EmMPK1 occurred [94]. Here, the expression pattern of EmFR was analyzed in different larval stages of *E. multilocularis*. The effect of host FGFs, heparin and specific FGFR inhibitors was analyzed in vitro (including metacestode vesicles, primary cells, dormant, and activated protoscoleces) in more detail and also on molecular level (proliferation studies, and signaling analysis).

5.1.1. EmFR expression analysis in *Echinococcus* larval stages

FGFRs are highly conserved throughout metazoan evolution [64]. They form a complex family of signaling molecules which are widely expressed in embryonic and adult tissue. Moreover, FGFRs play an important role in cellular differentiation and tissue-injury. First the expression of *Emfr* in *Echinococcus* larval stages was investigated by semi-quantitative RT-PCR.

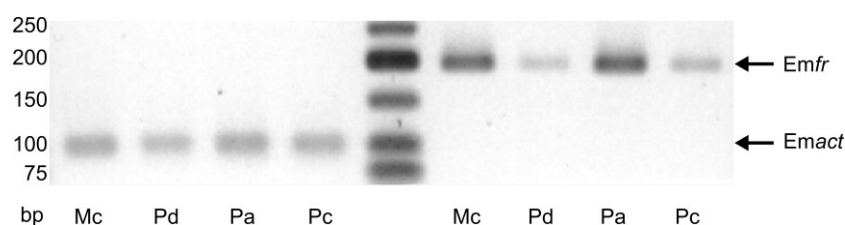


Fig. 8: Expression profile of *Emfr* in *E. multilocularis* larval stages. Total RNA was isolated from in vitro cultivated metacestode vesicles (Mc), dormant (Pd), low-pH/pepsin activated protoscoleces (Pa), and in vitro cultivated primary cells (Pc). Total RNA was reverse transcribed and the resulting cDNA was then used as a template for semi-quantitative PCR using primers specific for *Emfr* and the constitutively expressed control gene *Emact* [160]. PCR products were run on a 2 % agarose gel and stained with ethidium bromide. The sizes of the marker bands (middle lane) are indicated left.

Emfr transcripts were clearly detected in regenerating primary cells, in metacestode vesicles and in protoscoleces prior to (dormant) and after (activated) treatment with pepsin/low pH, although higher expression was observed in the metacestode and the activated protoscolex (Fig. 8). In parallel to genome sequencing, next generation transcriptome profiling is currently carried out at the Sanger Institute on all the larval stages mentioned above. Analyses of the respective dataset show expression of *Emfr* in all larval stages with about two to three times higher expression in metacestode vesicles and activated protoscoleces (data not shown). Thus the results obtained by

semi-quantitative RT-PCR were confirmed. Hence, *Emfr* is expressed in all larval stages that are involved in the infection of the intermediate host.

5.1.2. Protein-protein-interactions studies of the intracellular domain of EmFR

FGFs bind to FGFRs and induce their dimerization and the phosphorylation of specific cytoplasmic tyrosine residues. FRS2 is associated with the receptor and the phosphorylation of FGFRs and FRS2 triggers the activation of cytoplasmic signal transduction pathways such as the Ras-MAP kinase pathway [69]. Therefore I tested whether the intracellular domain of EmFR (EmFRin) possibly interacts with the already described components of the *E. multilocularis* MAPK cascade.

	Fusion with Gal4-DNA binding domain	
	pGBKT7	EmFRin
Fusion with Gal4-activation domain	pGADT7	-
	EmElpN	-
	EmElpC	-
	EmPDZ	-
	EmRas	-
	EmRal	-
	EmRap1	-
	EmRap2	-
	Em14-3-3	-
	EmMKKA	-
	EmMKKB	-
	EmRaf	-
	EmFRin	-

Fig. 9.: Protein-protein-interaction of EmFRin. Translation fusions were generated for the Gal4-DNA binding domain (BD; vector pGBKT7) and the Gal4-activation domain (AD; vector pGADT7) with the intracellular domain of EmFR (EmFRin). These were transformed into yeast strain AH109 together with empty vectors (pGADT7, pGBKT7) or with different fusions for EmRas, EmRal, EmRap1, EmRap2, Em14-3-3, EmMKK1, EmMKK1, EmRaf [52,54,55,57,161] and EmElpN, EmElpC, EmPDZ [37,153]. Positive control (pGADT7-T x pGBK-53) and negative control (pGADT7-T x pGBK-Lam) were performed as described in the MATCHMAKER-manual (Clontech). Growth of colonies was assessed according to the MATCHMAKER-manual (Clontech). No growth could be detected (indicated by “-”) All experiments were repeated three to five times independently.

First a translational fusion of EmFRin in pGADT7 and pGBKT7 was constructed. Then in a yeast-two hybrid approach these constructs were tested for interaction with EmRas, EmRal, EmRap1, EmRap2, Em14-3-3, EmMKKA, EmMKKB, and EmRaf [52,54,55,57,161]. Moreover, the interaction of EmElpN, EmElpC, and EmPDZ [37,153] with EmFRin was assessed (Fig. 9). EmElp, is an Ezrin-Radixin-Moesin-like protein and most likely involved in cell-cell adhesion which is described for its mammalian counterparts [162,163]. EmPDZ interacts with EmElp and might represent an orthologue of mammalian ERM interaction partner EBP50 [37]. It is also known that bFGF signaling depends on heparan sulfate syndecan-4 to transduce an intracellular signal through its receptors (FGFRs). Interestingly the PDZ domain containing protein syntenin binds the C2 domain of the syndecans

[164,165]. Syntenin functions as a rate limiting factor for syndecan plasma membrane recycling and most likely for the recycling of heparin sulfate associated cargo like FGF/FGFR [166]. In the experiment, no interaction between EmFRin and any of the tested proteins (Fig. 9) was observed. Thus, neither components of the *E. multilocularis* MAPK cascade nor proteins related to FGF-FGFR-recycling did interact with EmFRin.

5.1.3. Host derived FGFs stimulate *de novo* DNA Synthesis in *Echinococcus* larvae in vitro

Incorporation of bromodeoxyuridine (BrdU) into DNA as a measurement of cell proliferation has previously been used to demonstrate that FGFs stimulate the proliferation of various cell types, for example bone marrow derived stem cells [167]. In this experiment, metacystode vesicles and primary cells from the *E. multilocularis* isolate H95 were treated with either 10 nM and 100 nM aFGF or 10 nM and 100 nM bFGF in the presence of 1 mM BrdU for 48 h. *De novo* DNA synthesis as detectable by BrdU-incorporation was analysed in an ELISA using equal amounts of isolated chromosomal DNA. For detection of incorporated BrdU an anti-BrDU peroxidase-coupled antibody was used.

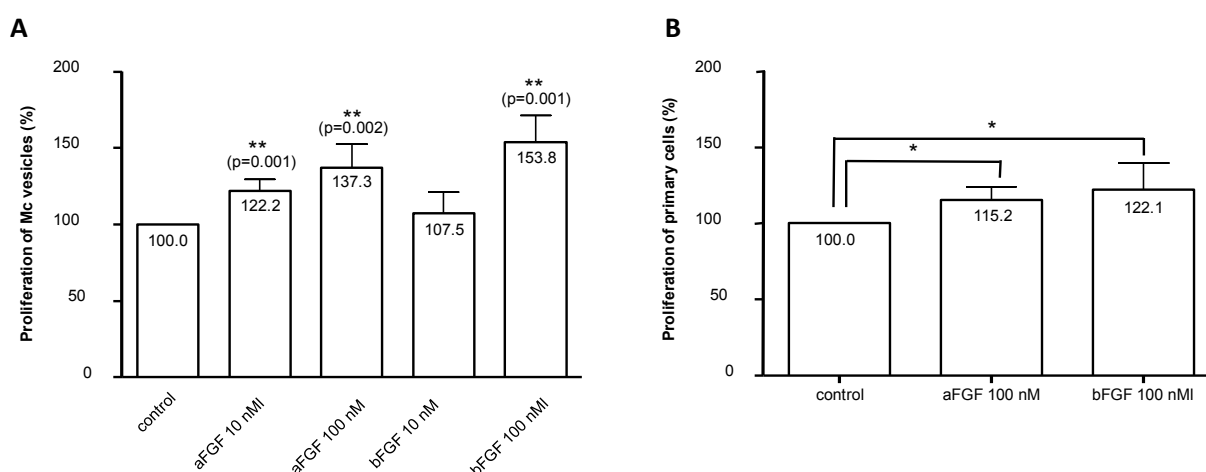


Fig. 10: Effect of FGFs on the proliferation of metacystode vesicles and primary cells of *E. multilocularis*. (A) Axenic metacystode vesicles (eight per well; H95) were starved for 48 h in 2 ml DMEM and (B) freshly isolated primary cells (H95) were grown for 48 h in 2 ml cDMEM-1. Then BrdU (1 mM) and FGFs (aFGF and bFGF: 10 or 100 nM) were supplemented and cells were incubated for another 48 h. Cells were harvested, washed with PBS before lysis and DNA isolation. *De novo* DNA synthesis as detectable by BrdU-incorporation was analysed in an ELISA. For that, equal amounts of DNA (1 - 5 µg) were coated over night on a 96-well plate. Detection of incorporated BrdU was performed with an anti-BrDU peroxidase-coupled antibody using the substrate TMB. Colorimetric analysis was performed after 30 - 60 min with a spectrometer at 450 nm after stopping the reaction with 200 mM sulfuric acid. The bars represent the percentage of BrdU incorporation with the cDMEM-1 control set to 100 %. The statistical evaluation of four independent experiments (n=4) which were conducted in duplicates is shown (error bars are indicated). Student's t-test (two-tailed): *p < 0.05.

Both, aFGF (at 10 nM: 122.2 % and at 100 nM: 137.3 %) and 100 nM bFGF (154 %) significantly stimulated the proliferation of metacystode vesicles when compared to the untreated control which was set to 100 % (Fig. 10 A). The same significant effect was detectable for primary cells of *E. multilocularis*: 100 nM aFGF (115 %) and 100nM bFGF (122.1) significantly stimulated the

proliferation compared to the control sample (100 %) (Fig. 10 B). Thus, it is evident that both, aFGF and bFGF stimulated the proliferation of metacystode vesicles and primary cells of *E. multilocularis*.

5.1.4. Growth and development of *E. multilocularis* is stimulated by host FGFs in vitro – primary cells

FGFs have diverse biological activities including roles in mitogenesis and cellular differentiation [64]. In the above mentioned study by Schäfer [94] it was demonstrated that axenic metacystode vesicles cultured in cDMEM-1 in the presence of 100 nM aFGF or 10 nM bFGF grew twice the volume (0.28 ml) compared to the untreated control (0.14 ml) (Fig. 11 A). Also, after 4 weeks of incubation the effect was clearly visible. The FGF stimulated vesicles had approximately a 2.2 times larger volume (aFGF treated vesicles: 4.1 ml and bFGF treated vesicles: 4.3 ml) than the unstimulated control vesicles (1.9 ml) (Fig. 11 A; adapted from [94]).

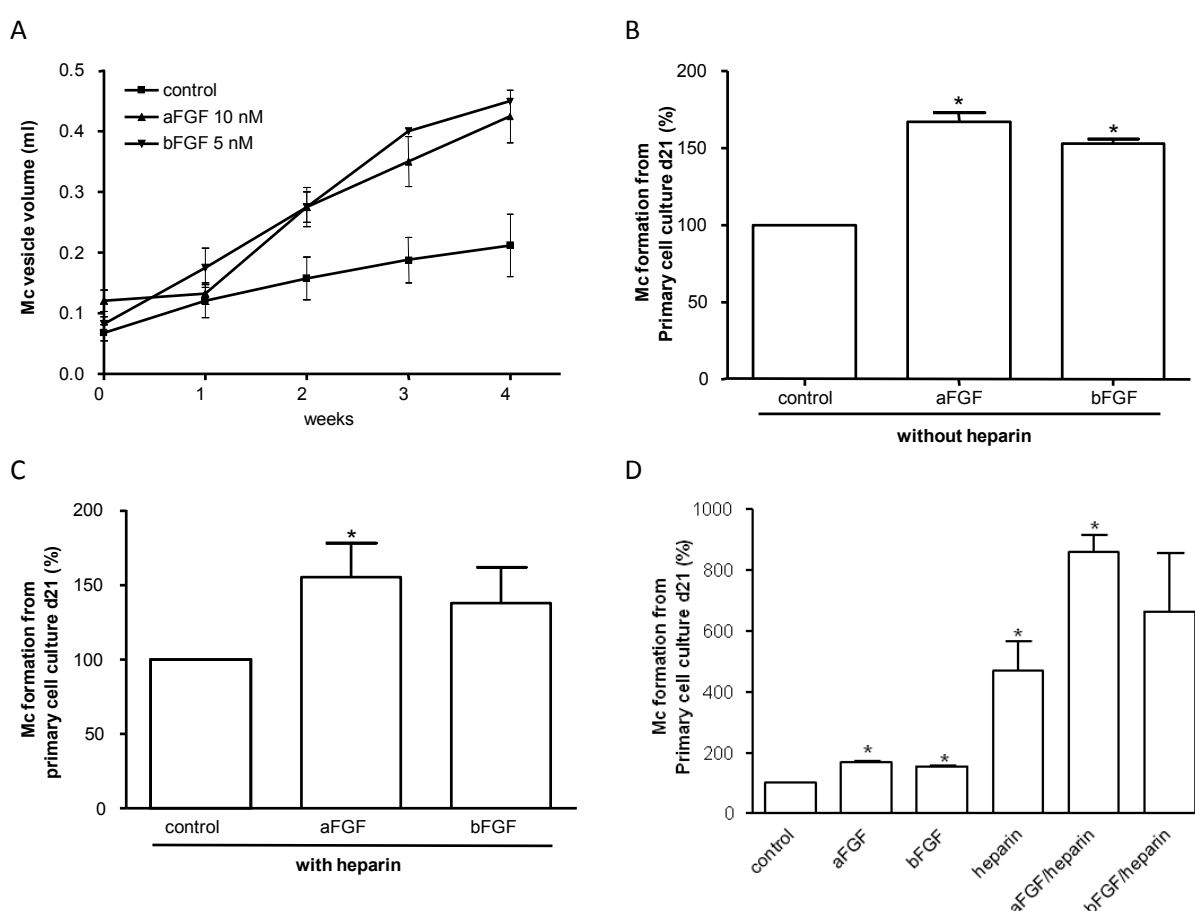


Fig. 11: Effect of FGFs on *E. multilocularis* metacystode vesicles and primary cells. (A) Single axenic metacystode vesicles of the isolate H95 were in vitro cultivated in cDMEM-1 for four weeks in the presence of 10 nM acidic and 5 nM basic FGF. The complete medium (1 ml) was changed every other day as well as the growth factors were supplemented. Control vesicles were kept in cDMEM-1. Growth (in ml) of vesicles was monitored. In each of the three independent experiments (n=3) four vesicles were examined for every single condition. The mean was calculated and the standard error of the mean (SEM) is indicated. (B-D) The regeneration process of axenically cultivated H95 primary cells was monitored for 21 days. Cells were cultured in cDMEM-1 (control), with the addition of 100 nM aFGF or 100 nM bFGF in either the presence or absence of 10 µg/ml heparin. Half of the medium volume was renewed every other day and growth factors were

supplemented at concentrations calculated to the entire cultured volume. The number of newly formed metacystode vesicles at day 21 was analyzed. The bars represent the percentage of formed vesicles compared to the cDMEM-1 control without heparin (**B**) and (**D**) or with heparin (**C**). The statistical evaluation of three independent experiments (n=3) which were conducted in duplicates is shown (error bars are indicated). Student's t-test (two-tailed): *p < 0.05.

Since FGFs are key players in differentiation processes, the regeneration of axenically cultivated H95 primary cells was also monitored for 21 days. Cells were cultured in cDMEM-1, with the addition of 100 nM aFGF or 100 nM bFGF in either the presence or absence of 10 µg/ml heparin. After 21 days the formation of newly built metacystode vesicles was assessed as a measure of parasite development. When primary cells were stimulated with either aFGF or bFGF (Fig. 11 B) clearly more vesicles formed after 21 days compared to the untreated control. In the presence of aFGF and bFGF about 167 % and 153% more vesicles were formed, respectively. Interestingly, when heparin was introduced to the system, generally more vesicles appeared after 21 days, also in the non-FGF treated samples (Fig. 11 C). When taking the heparin stimulated cells as control, compared with the simultaneously treated aFGF/heparin or bFGF/heparin cells, the FGF effect is still clearly detectable and significant. Whereas the vesicles regenerating from heparin treated primary cells were set to 100%, 155% and 138% vesicles were counted in the aFGF and bFGF treated samples, respectively. Moreover, the effect of heparin on the system of regeneration metacystode vesicles from primary cells was also examined (Fig. 11 D). The normal untreated control was set to 100 %. It is obvious, that in the presence of heparin approximately five times the amount of vesicles was formed after 21 days (470 %; Fig. 11D). If FGFs were added to the system even more vesicles were countable after the incubation period; 862 % for aFGF and 663 % for bFGF (Fig. 11D). Taken together, it becomes clear, that not only aFGF and bFGF stimulate the regeneration process of developing primary cells, but also heparin positively influences the process while still the FGFs can elicit their potential.

5.1.5. Targeting the FGF signaling pathway of *E. multilocularis*: BIBF1120- effects on metacystode vesicles and primary cells

BIBF1120 [Vargatef; (Z)-methyl3-(((4-(N-methyl-2-(4-methylpiperazin-1-yl)acetamido)phenyl) amino) (phenyl)methylene)-2-oxoindoline-6-carboxylate] is triple-tyrosine kinase inhibitor. It inhibits human VEGFR-1, -2, and -3, FGFR-1, -2, and -3, and PDGFR α and β by binding to the ATP-binding site in the cleft of the kinase hinge region. It shows also activity against members of the Src family of kinases but displays a lower efficiency with a two- to three-fold higher IC₅₀ compared to the above mentioned targets [21]. Since *E. multilocularis* only harbors one FGFR homologue but none for PDGF or VEGF the inhibitor might mainly block FGF-EmFR signaling. Therefore, BIBF1120 was chosen in this study.

To test the effect of the FGFR inhibitor BIBF1120 on the viability and differentiation process in *E. multilocularis* in vitro, axenically cultivated metacystode vesicles and freshly isolated primary cells were incubated with DMSO (0.1%) or BIBF1120 at different concentrations (1 µM, 5 µM and 10µM) for several weeks (Fig. 12A). A dose-dependent effect was observed in both *E. multilocularis* cultures. Metacystode vesicles lost integrity over time (Fig. 12A-C). Whereas more than 90 % of the vesicles which were treated with DMSO survived after 18 days, only 8.75 % of the 1 µM, 2.5 % of the 5 µM and none of the 10 µM BIBF1120 treated vesicles survived. The first effect of the inhibitor was detectable after three days of incubation with 5 µM and 10 µM BIBF1120 causing about 7.5 % and 19.6 % vesicle destruction, respectively. Statistically, 50 % of the vesicles were dead after 8, 10 and

13 days when treated with 1 μ M, 5 μ M or 10 μ M of BIBF1120, respectively. As expected, the inhibitor also caused changes in the regeneration process of primary cells (Fig. 12D). After one day the samples did not show any differences, the primary cells started to form small aggregates. However, in the presence of 5 μ M and 10 μ M the primary cells failed to develop further; After 21 days, only 1.8 % and 0 % newly formed vesicles were detected, respectively. Despite the tremendous effect of 5 μ M and 10 μ M, the treatment with 1 μ M BIBF1120 did not cause any morphological changes (Fig. 12D-F) or alterations in regeneration. After 21 days control cultures and 1 μ M BIBF1120 treated cells, reached the same numbers of newly formed vesicles.

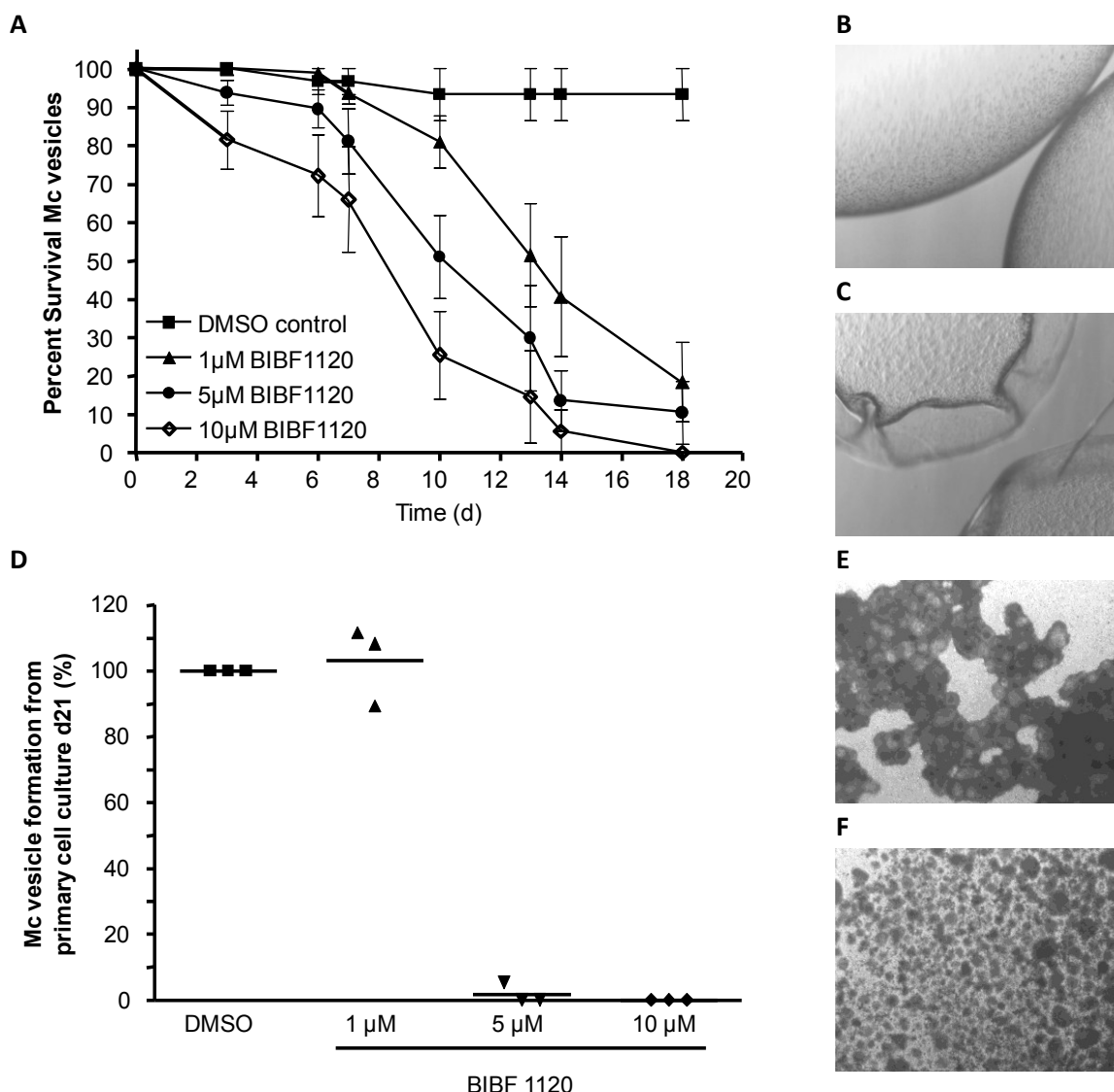


Fig. 12: Treatment of *E. multilocularis* metacystode vesicles and primary cells with BIBF1120. (A) Axenically cultivated metacystode vesicles and freshly isolated primary cells of the isolate H95 were incubated with DMSO (0.1 %) and BIBF1120 at different concentrations (1 μ M, 5 μ M and 10 μ M) for several weeks. Metacystode vesicles were cultured in cDMEM-1 on a 12-well plate in 2 ml volume with 6- 8 vesicles per well. The survival of vesicles is depicted in percentages as the mean value and error bars indicate the SEM. The experiment was repeated three times in duplicates. (B) Intact, viable metacystode vesicle from in vitro culture treated with DMSO (0.1 %). (C) Metacystode vesicle after treatment with BIBF1120 for seven days. (D) Primary cells were cultured in cDMEM-1 on a 12-well plate in 2 ml volume supplemented with (E) DMSO control (0.1 %) and BIBF1120 at different concentrations 1 μ M, 5 μ M and (F) 10 μ M. Magnification 25x. After 21 days the numbers of newly formed metacystode vesicles were counted. The DMSO control for each of the three experiments was set to 100 %. The horizontal line marks the mean value of all experiments.

In another experiment metacestode vesicles were either treated with DMSO or 5 μ M BIBF1120 for five days. In both conditions, more than 90 % of all metacestode vesicles survived. Subsequently, primary cells were isolated according to the established protocol [49] and seeded on 12-well plates. Then, the cells were cultivated in the presence of DMSO (Fig. 13 A) and under various conditions: 1 μ M BIBF1120, 10 μ g/ml heparin or a mixture of heparin (10 μ g/ml) together with aFGF and bFGF (each 100 nM) with DMSO as solvent at 0.1 % (Fig. 13 A-C).

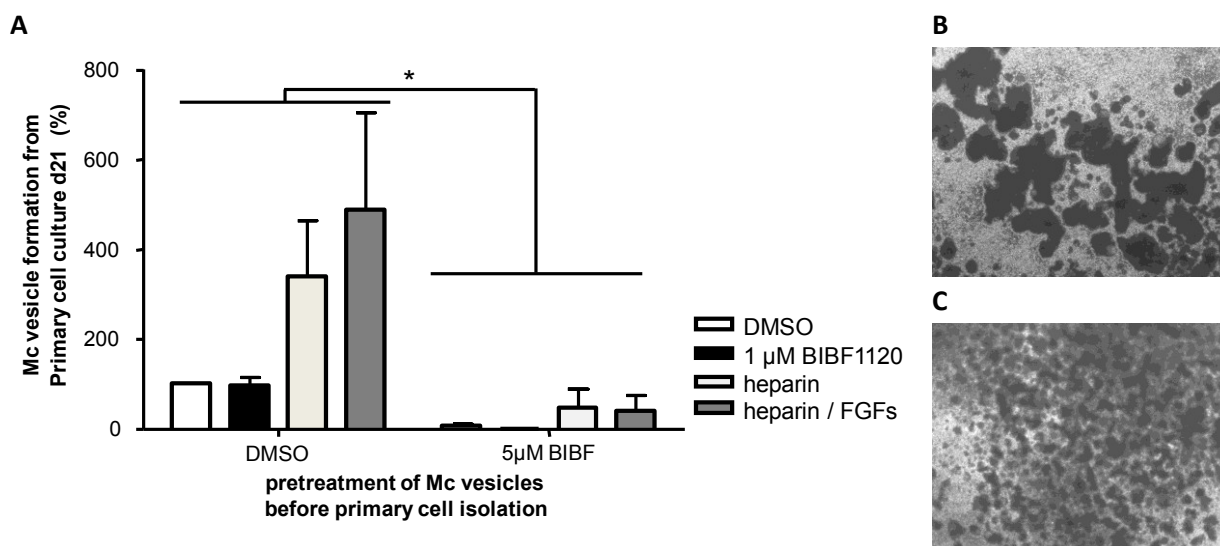


Fig. 13: The effect on the regeneration of primary cells isolated from metacestode vesicle pre-treated with BIBF1120. (A) Axenically cultivated metacestode vesicles were incubated in the presence of 0.1 % DMSO with or without 5 μ M BIBF1120 for five days, after which more than 90 % of the vesicles survived in all conditions. Subsequent to isolation, primary cells from treated vesicles were seeded in 12-well plates as duplicates and were all cultivated in the presence of DMSO (DMSO control, open box) and under various conditions: 1 μ M BIBF1120 (black box), 10 μ g/ml heparin (large pixel box) and heparin (10 μ g/ml) together with aFGF and bFGF (each 100 nM; small pixel box). The bars represent the calculated percentage of formed metacestode vesicles compared to the total number of vesicles in the DMSO control. (B) Microscopic pictures from heparin-treated primary cells, isolated from (B) DMSO or (C) 5 μ M BIBF1120 pre-treated metacestode vesicles (day 21). Magnification 25x. In all cases, the error bars indicate the SEM from the five independent measurements which were performed in duplicates. Student's t-test (two-tailed): * $p < 0.05$.

Although more than 90 % of the 5 μ M BIBF1120 treated vesicles did not show any sign of disintegrity after five days, primary cells from these vesicles only marginally regenerated after 21 days (Fig. 13 A); 7 % (DMSO post-treatment) and 0 % (1 μ M BIBF1120 post-treatment). Only when stimuli like heparin or heparin with the addition of aFGF and bFGF were supplemented a nominal development of new vesicles was detected; 46.5 % and 38.5 % respectively setting the DMSO pre-treated, DMSO post-treated culture as 100 %. Thus, it can clearly be stated, that although the integrity of metacestode vesicles might not be affected, BIBF1120 had a clear effect on the cells within the metacestode vesicles, preventing the formation of new vesicles when used for the isolation of primary cells. Taken together, the above experiments demonstrated that BIBF1120 effectively inactivated in vitro cultivated metacestode vesicles and prevented regeneration of primary cells at 5 μ M and 10 μ M.

5.1.6. The effect of host FGFs and BIBF1120 on in vitro cultivated protoscolexes

In addition to metacestode vesicles and primary cells of *E. multilocularis*, also protoscolexes as the infective larval stage of the final host were under investigation. Therefore, FGFs were applied to in vitro cultivated, activated protoscolexes from the isolate GH09. In detail, the protoscolexes were cultivated in cDMEM-1 for 21 days in the presence of either aFGF, bFGF (both 100 nM) or heparin (10 µg/ml). The medium was routinely exchanged every second or third day. In parallel the culture was monitored by light microscopy. After 21 days the culture was assessed for different phenotypes of protoscolex structures (Fig. 14 A and Fig. 15).

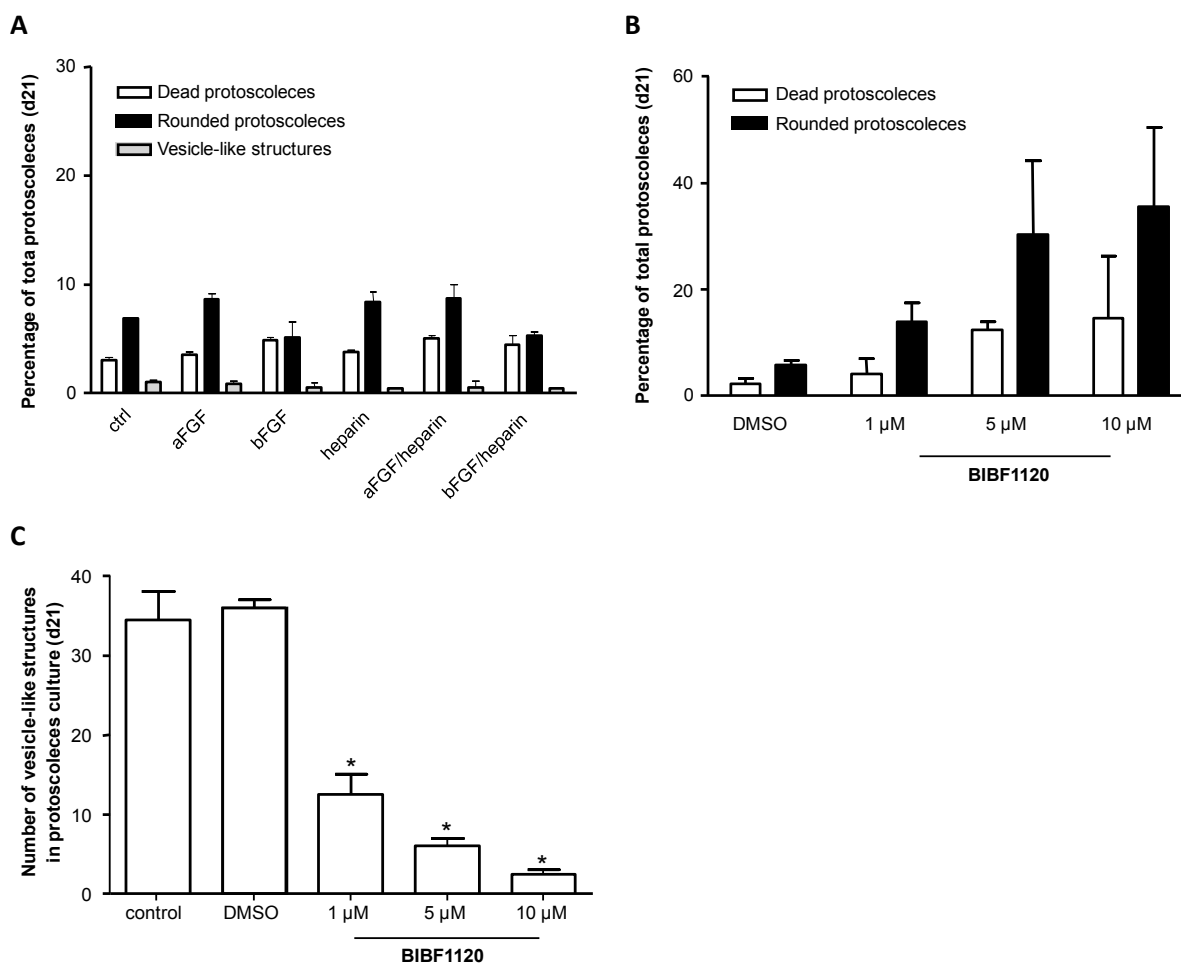


Fig. 14: Effect of FGFs and BIBF1120 on *E. multilocularis* in vitro activated protoscolexes. (A) In vitro activated protoscolexes of the isolate GH09 were in vitro cultivated in cDMEM-1 for 21 days in the presence of either FGFs (aFGF, bFGF: 100 nM), heparin (10 µg/ml) alone or in combination. (B and C) In vitro activated protoscolexes of the isolate GH09 were in vitro cultivated in cDMEM-1 for 21 days in the presence of either DMSO (0.1 %) or BIBF1120 (1 µM, 5 µM or 10 µM). Half the medium (1 ml) was changed every second or third day as well as the supplements calculated to the total volume of 2 ml. Control protoscolexes were kept in cDMEM-1. In each of the two independent experiments (n=2) duplicates of approximately 100-200 protoscolexes were examined. The mean was calculated and the standard error of the mean is indicated. Student's t-test (two-tailed): *p < 0.05.

At the beginning of the experiment, all protoscolexes appeared evaginated and were motile (Fig. 15A-C). In the course of treatment with host FGFs or heparin, there was no difference in the

phenotypic development of the *in vitro* cultivated and by low-pH pepsin treatment activated protoscolecetes (Fig. 15 D - I). After three weeks of incubation most of protoscolecetes presented the strobilar form, but yet changes in morphology occurred: Non-moving, also in shape and structure degraded protoscolecetes were accounted as “dead”. Also fully globular structures which were floating in the media were observed, and were considered as “vesicle like structures”. In contrast, a small proportion of the protoscolecetes rounded up over time, resulting in vesicle-like structures, but the suckers still were clearly detectable. Thus these structures were called “rounded protoscolecetes”. After 21 days, the number of apparently dead protoscolecetes was below 10 % in all cultures. The same holds true when analyzing the percentage of globular “rounded” protoscolecetes (Fig. 14 A).

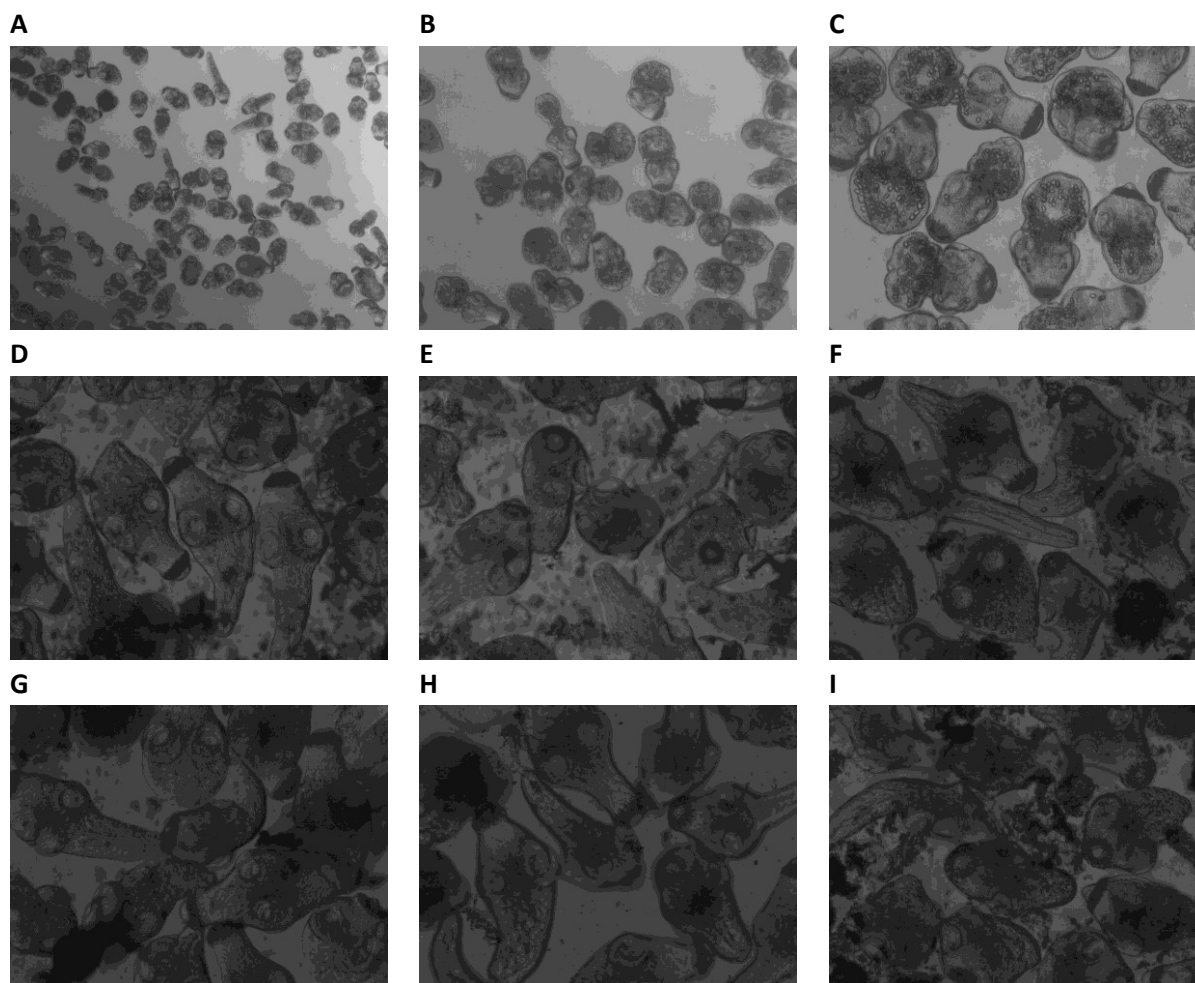
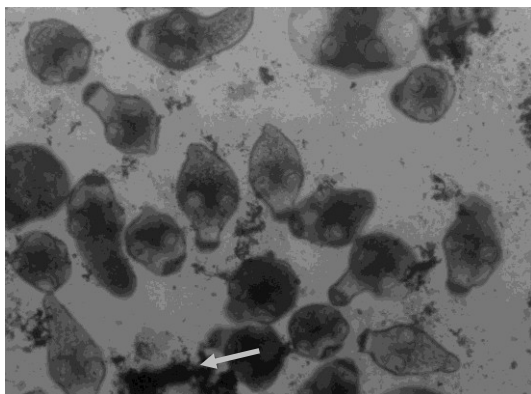
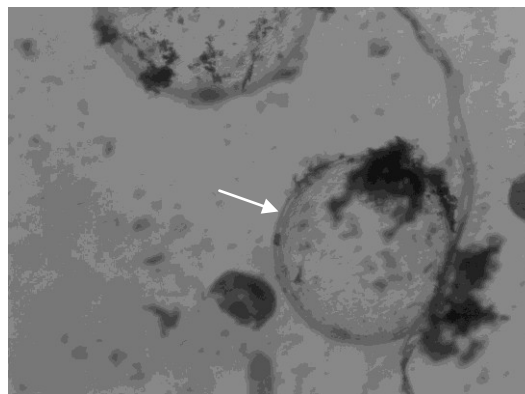
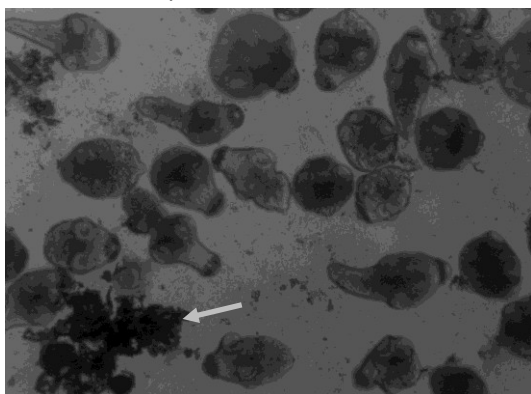
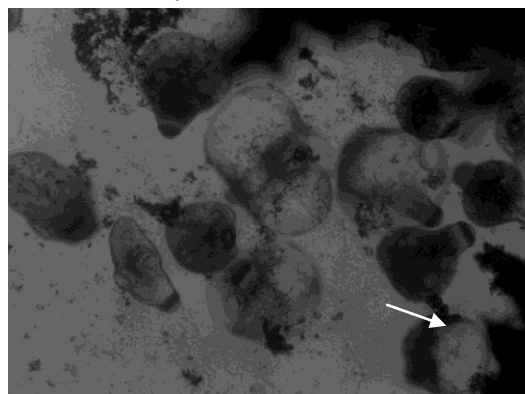


Fig. 15: Effect of host FGFs on *in vitro* cultivated, activated protoscolecetes. *In vitro* activated protoscolecetes of the isolate GH09 were *in vitro* cultivated in cDMEM-1 for 21 days in the presence of either FGFs (aFGF, bFGF: 100 nM), heparin (10 μ g/ml) alone or in combination. Micrograph of control (A) 25x (B) 50x and (C) 100 x magnification on day of isolation and activation by low pH-pepsin treatment. Micrograph of control (D), aFGF (E), bFGF (F), heparin (G), aFGF/heparin (H) and bFGF/heparin (I) treated protoscolecetes on day 14 at 100x magnification. Half the medium (1 ml) was changed every second or third day as well as the supplements calculated to the total volume of 2 ml. Control vesicles were kept in cDMEM-1. In each of the 2 independent experiments (n=2) duplicates of approximately 100 - 200 protoscolecetes were examined.

In another experiment the effect of BIBF1120 on *in vitro* cultivated and by low pH / pepsin treatment activated protoscolecetes was assessed. For that, *in vitro* activated protoscolecetes of the isolate GH09 were further *in vitro* cultivated in cDMEM-1 for 21 days in the presence of either DMSO (0.1 %) or

BIBF1120 (1 μ M, 5 μ M, or 10 μ M). Half the medium (1 ml) was changed every second or third day as well as the supplements calculated to the total volume of 2 ml. Control protoscolecids were kept in cDMEM-1. Again, the culture was analyzed in respect to different phenotypes (Fig. 14 B, C and Fig. 16). At the beginning of the experiment, all protoscolecids appeared evaginated and were motile (Fig. 16 A). After three weeks of incubation most of control and DMSO-treated protoscolecids kept the strobilar form, were still moving and less than 10 % seemed dead or rounded (Fig. 14 B). Yet, the body form with tegument and structures like rostellum and suckers were clearly defined throughout incubation. However, when incubated with BIBF1120 in various concentrations, changes in morphology and viability occurred (Fig. 14 B, C and Fig. 16). A clear tendency was recognized, that in a concentration dependent manner, more protoscolecids appeared dead. In DMSO treated control cultures 2.1 % protoscolecids were dead compared to 4 %, 12.4 % and 14.6 % in 1 μ M, 5 μ M, and 10 μ M BIBF1120 treated samples, respectively. In respect to the normal strobilar morphology, again a dose-dependent effect was present. The more inhibitor was present in the system the more globular and round the protoscolecids appeared. In DMSO treated control cultures 5.8 % protoscolecids were rounded to 13.9 %, 30.2 % and 35.5 % in 1 μ M, 5 μ M, and 10 μ M BIBF1120 treated samples, respectively (Fig. 14 B). The well-defined structure was lost and the neck was not identifiable anymore. Also, the appearance was lighter and less granular than in the DMSO control group. With respect to the appearance of vesicle-like structures not harboring any indications of structures like suckers it was obvious that the number of these structures decreased with increasing concentrations of BIBF1120 (Fig. 14 C). These experiments suggest that in regard to morphology and agility host FGFs do not alter the protoscolecids in in vitro culture. However, BIBF1120 seems to affect the morphology of in vitro cultivated protoscolecids resulting in globular structures and a higher percentage of dead protoscolecids over time.

A DMSO control**B DMSO control****C BIBF1120 1 μ M****D BIBF1120 1 μ M**

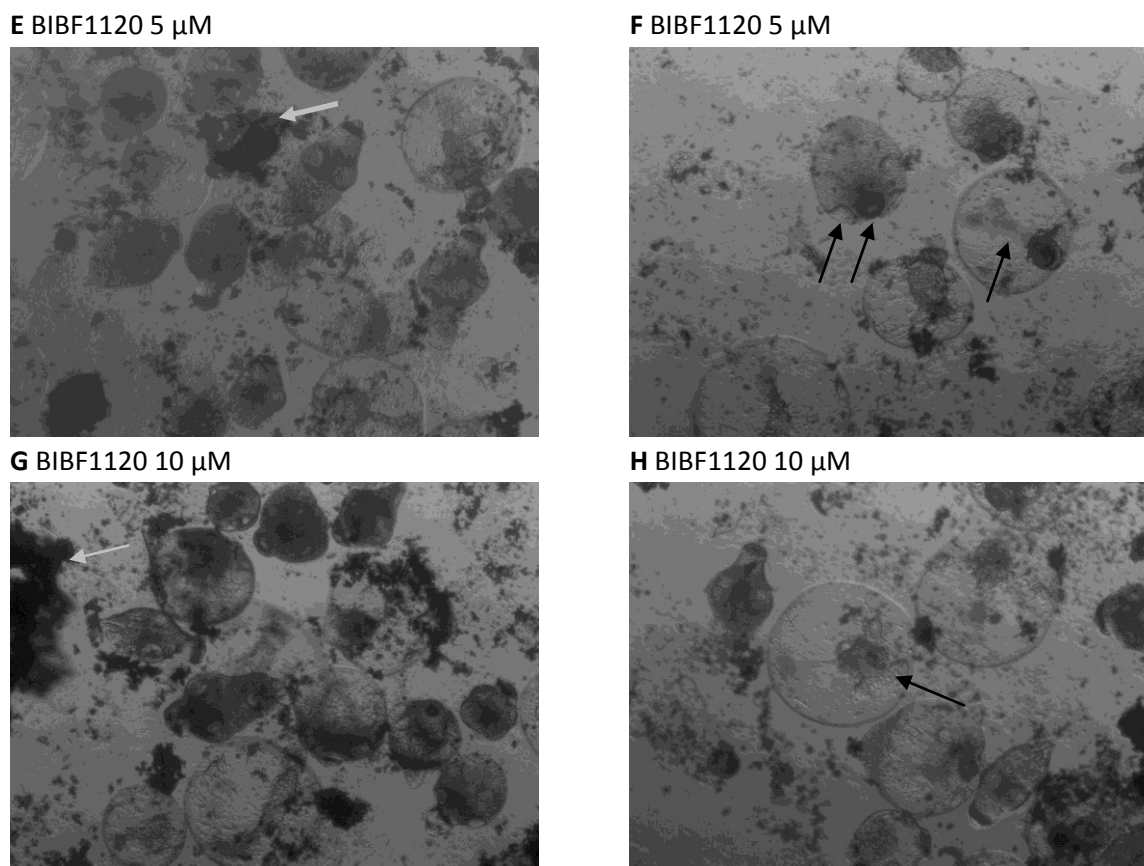


Fig. 16: Effect of BIBF1120 on in vitro cultivated, activated protoscolecocytes. In vitro activated protoscolecocytes of the isolate GH09 were in vitro cultivated in cDMEM-1 for 21 days in the presence of either DMSO (0.1 %) or BIBF1120 (1 µM, 5 µM, or 10 µM). Half the medium (1 ml) was changed every second or third day as well as the supplements calculated to the total volume of 2 ml. In each of the two independent experiments (n=2) duplicates of approximately 100-200 protoscolecocytes were examined. **A, B** Micrograph of control samples **C, D** Micrograph of 1 µM BIBF1120 **E,F** Micrograph of 5 µM BIBF1120 and **G,H** Micrograph of 10 µM BIBF1120 treated protoscolecocytes after 21 days of culture. Black arrows indicate defined structures as rostellum and suckers. White arrows indicate vesicle-like structures and grey arrows indicate at debris or dead protoscolecocytes.

5.1.7. Targeting the FGF signaling pathway of *E. multilocularis*: SU5042– effects on metacestode vesicles and primary cells

A second inhibitor, SU5042 (3-[(3-(2-carboxyethyl)-4-methylpyrrol-2-yl)methylene]-2-indolinone), which was described to specifically block FGFR kinase activity and also possibly VEGFR activity, was used for in vitro experiments. The inhibitor is like BIBF1120 part of the indolinone family. Its inhibitory effect is due to direct interactions of the inhibitor with the catalytic domain of human FGFR1. Both inhibitors binds to FGFR1 in the ATP binding cleft [28]. Binding of BIBF1120 to the human VEGFR-2 is mediated by binding to Cys919 and Glu917 [21]. However, the interacting residues of human FGFR1 with BIBF1120 have not been described so far. For SU5042 it is known that the hydrogen bond between the side chain amide of FGFR Asn568 in the hinge region and the carboxyethyl group of SU5042 confers to the specificity of the inhibitor. The respective Asn is conserved between FGFR1 and EmFR (Asn458).

To test the effect of the FGFR inhibitor SU5042 on the viability and differentiation process in *E. multilocularis* in vitro, axenically cultivated metacestode vesicles and freshly isolated primary cells

were incubated with DMSO (0.1 %) or SU5042 at different concentrations (100 nM, 500 nM, 1 μ M, 5 μ M, 10 μ M, and 50 μ M) (Fig. 17). When metacestode vesicles were treated with the inhibitor no change in viability or morphology was observed in comparison to the DMSO control samples. The highest concentration tested was 10 μ M and did not harm the metacestode vesicles (Fig. 17 C). The growth of these differently treated vesicles has not been analysed in this study. Interestingly, when SU5042 was applied to regenerating primary cells, a dose-dependent effect was observed. The more inhibitor was present, the more vesicles developed after 18 days. In Fig. 17 A – C it becomes clear, that in the presence of SU5042 more vesicles regenerated, indicated by the white arrows. However, in these two independent experiments the total numbers of newly formed vesicles was not determined.

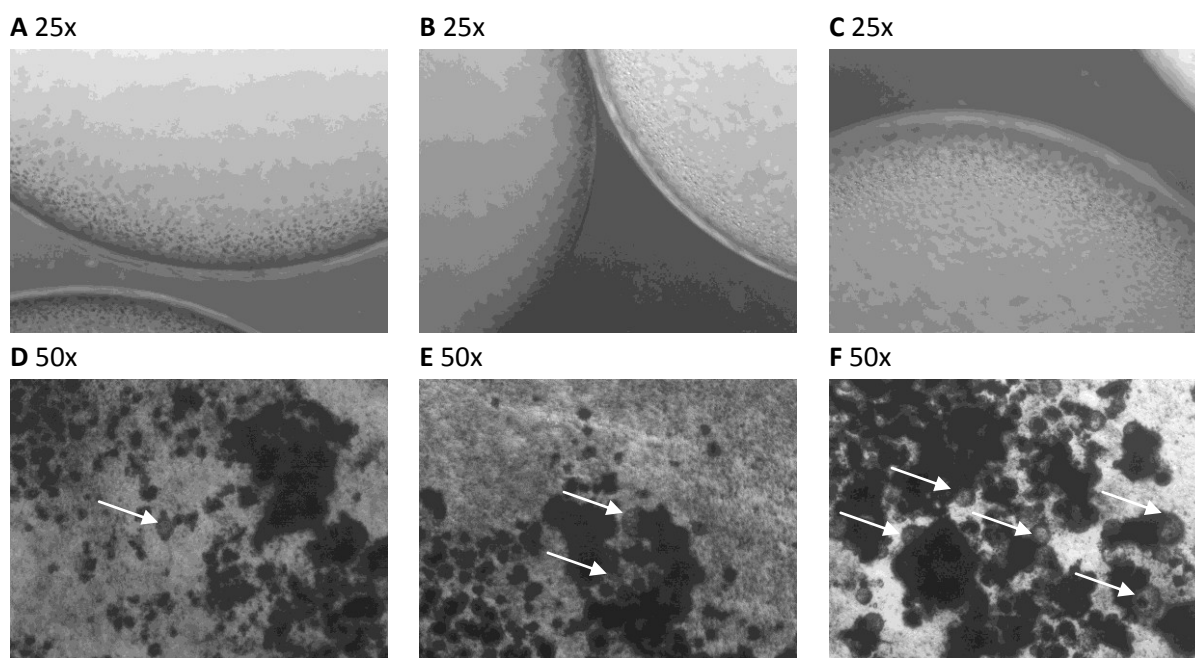


Fig. 17: Treatment of *E. multilocularis* metacestode vesicles and primary cells with SU5042. (A-C) Axenically cultivated metacestode vesicles and freshly isolated primary cells of the isolate H95 were incubated with 0.1% DMSO (A) and SU5042 at 5 μ M (B) and 10 μ M (C) for two weeks. Metacestode vesicles were cultured in DMEM / 10 % FBS on a 24-well plate in 1 ml volume with 5 vesicles per well. The experiment was conducted in duplicates. (D-F) Primary cells were isolated from axenic metacestode vesicles (isolate H95) and cultured in cDMEM-1 on a 12-well plate in 2 ml volume supplemented with (D) DMSO control (0,1%) and SU5402 at different concentrations (E) 5 μ M and (F) 10 μ M for three weeks. Light microscopic pictures were taken on day 18. The experiment was conducted twice in duplicates Magnification as indicated. White arrows indicate regenerating vesicle-like structures.

In another experiment metacestode vesicles were either treated with 0.1 % DMSO or 10 μ M SU5042 for five days. Under both conditions, more than 95 % of all metacestode vesicles survived. Subsequently, primary cells were isolated according to the established protocol [49] and seeded on 12-well plates. Then, the cells were cultivated in the presence of 0.1% DMSO (Fig. 18 A, D), 10 μ M SU5042 (Fig. 18 B, E) or with host aFGF/bFGF (each 100 nM) (Fig. 18 C, F) for two weeks. It seemed that the pre-incubation of metacestode vesicles with 10 μ M SU5042 might have a positive effect on regeneration. When comparing the DMSO control samples of either DMSO pre-treated or 10 μ M SU5042 pre-treated vesicles, the regenerating vesicles from primary cells seemed more packed. Also, it seemed that more vesicles had developed after two weeks (Fig. 18 A, D).

Interestingly, SU5402 did not cause the same effect as BIBF1120 on *E. multilocularis* larval stages. There are several reasons to explain the observed effects of SU5402. First, although the respective Asn residue is conserved between FGFR1 and EmFR additional residues of the hinge region differ between FGFR1 (Tyr-Ala-Ser-Lys-Gly-Asn) and EmFR (Tyr-Arg-Met-Lys-Gly-Asn). This might cause conformational differences resulting that SU5402 is not able to bind to the specific site and therefore is not able to block EmFR signaling. One could address this question with the help of the *Xenopus* oocytes model system. If SU5402 does not block EmFR signaling induced by aFGF or bFGF, GVBD will still be observed. Second, due to above speculated conformational differences SU5402 might be able to activate EmFR which again could be addressed in GVBD assays. An activation of EmFR could explain why metacystode vesicles withstand SU5402 treatment (the influence on growth was not assessed in the study) and why primary cells regenerated comparable as if they had been stimulated with FGFs.

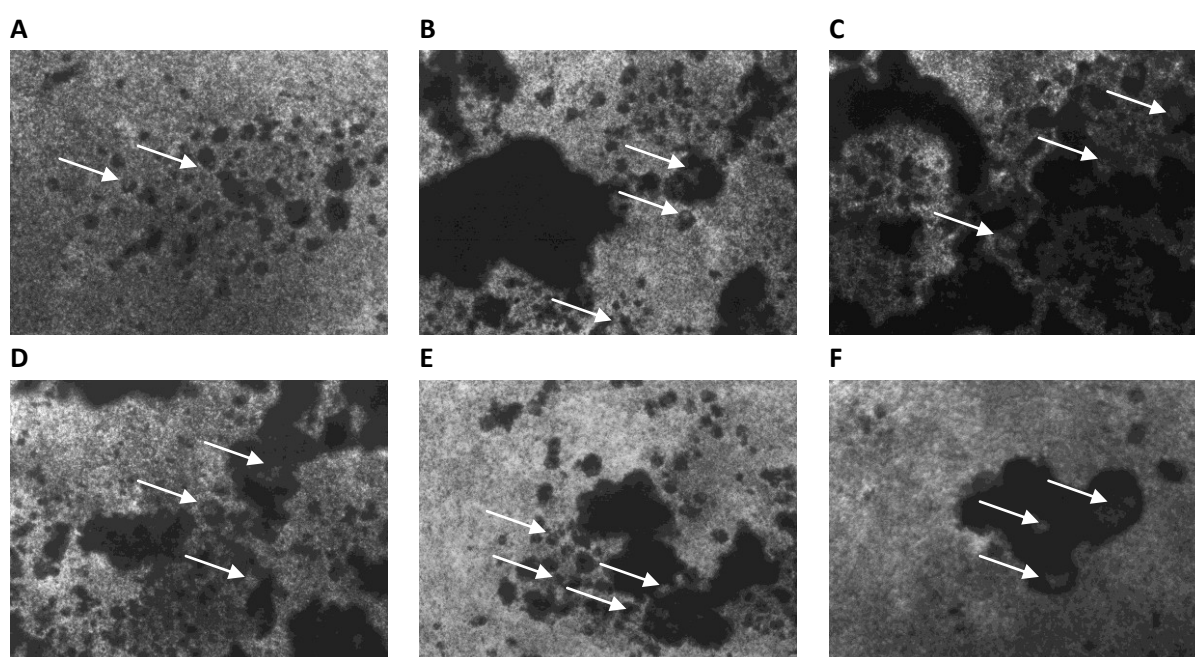


Fig. 18: The effect on the regeneration of primary cells isolated from metacystode vesicle pre-treated with SU5402. Axenically cultivated metacystode vesicles were incubated in the presence of 0.1 % DMSO (A–C) or in the presence of 10 μ M SU5402 (D–F) for 5 days, after which more than 95% of the vesicles survived in all conditions. Subsequent to isolation, primary cells from treated vesicles were seeded in 12-well plates as duplicates and were all cultivated in the presence of 0.1 % DMSO (A, D), 10 μ M SU5402 (B, E), or with host aFGF/bFGF (each 100 nM) (C, F). Microscopic pictures were taken after two weeks. Magnification 50 x. The experiment was in duplicates. White arrows indicate regenerating vesicle-like structures.

The effect was even more pronounced when primary cells from either DMSO or 10 μ M SU5402 pre-treated vesicles were incubated in the presence of 10 μ M SU5402 (Fig. 18 B, E). Compared to the respective control, the regenerating primary cells appeared more condensed and seemed to produce more vesicle-like structures, as indicated with the white arrows in the micrographs. The addition of host FGFs seemed to have a similar effect as the treatment with 10 μ M SU5402 (Fig. 18 C, F).

In summary, SU5402 did not result in morphological changes of metacystode vesicles over a period of two weeks, whereas primary cells tended to regenerate better under increasing concentrations of the inhibitor. When metacystode vesicles were pre-treated with inhibitor prior to primary cell isolation, this seemed also to positively affect the regeneration process. In future experiments, the

effect of SU5042 in combination with host FGFs should be analysed to validate the data obtained in this study.

5.1.8. siRNA knock-down of EmFR – preliminary data

To unravel the function of EmFR in more detail a first experiment was conducted in order to knock-down EmFR with the use of a siRNA technique. It was published that *E. multilocularis* primary cells have been successfully exploited in siRNA knock-down experiments with promising results in achieving a knock-down on mRNA and protein level for EmE1p and Em14-3-3 [147].

Therefore, an experiment according to the published protocol has been performed. Subsequent to isolation, primary cells were seeded in a 6-well plate, allowed to form mini-aggregates and were afterward subjected to electroporation with electroporation buffer, control siRNA Mm/Hs_MAPK1, EmE1p siRNA and EmFR siRNA. The cells were seeded in fresh DMEM / 10 % FBS medium supplemented with BAT in the presence of RH- feeder cells. Half the medium was changed every 3 -4 days and development of the cells was analysed light microscopically. The experiment was performed in quadruplicates in order to collect RNA and protein samples at two different time points. However, RNA and protein isolation failed in this experiment. Thus only light microscopic morphological assessment of the experiment could be performed. After six days, in all samples some aggregates had developed with an orange inclusion in the middle which is indicated by black arrows (Fig. 19). It seemed that in the siRNA-EmFR sample slightly more aggregates had appeared. In a second approach the primary cells were cultured in cDMEM-1 after electroporation. Compared to control siRNA (GFP siRNA) the primary cells treated with EmFR siRNA appeared not as dense and compact. However, both experiments were stopped after two weeks because apparently too much material was lost while media was changed. Until now, the effect of siRNA knock-down of EmFR is still elusive and further experimentation is needed.

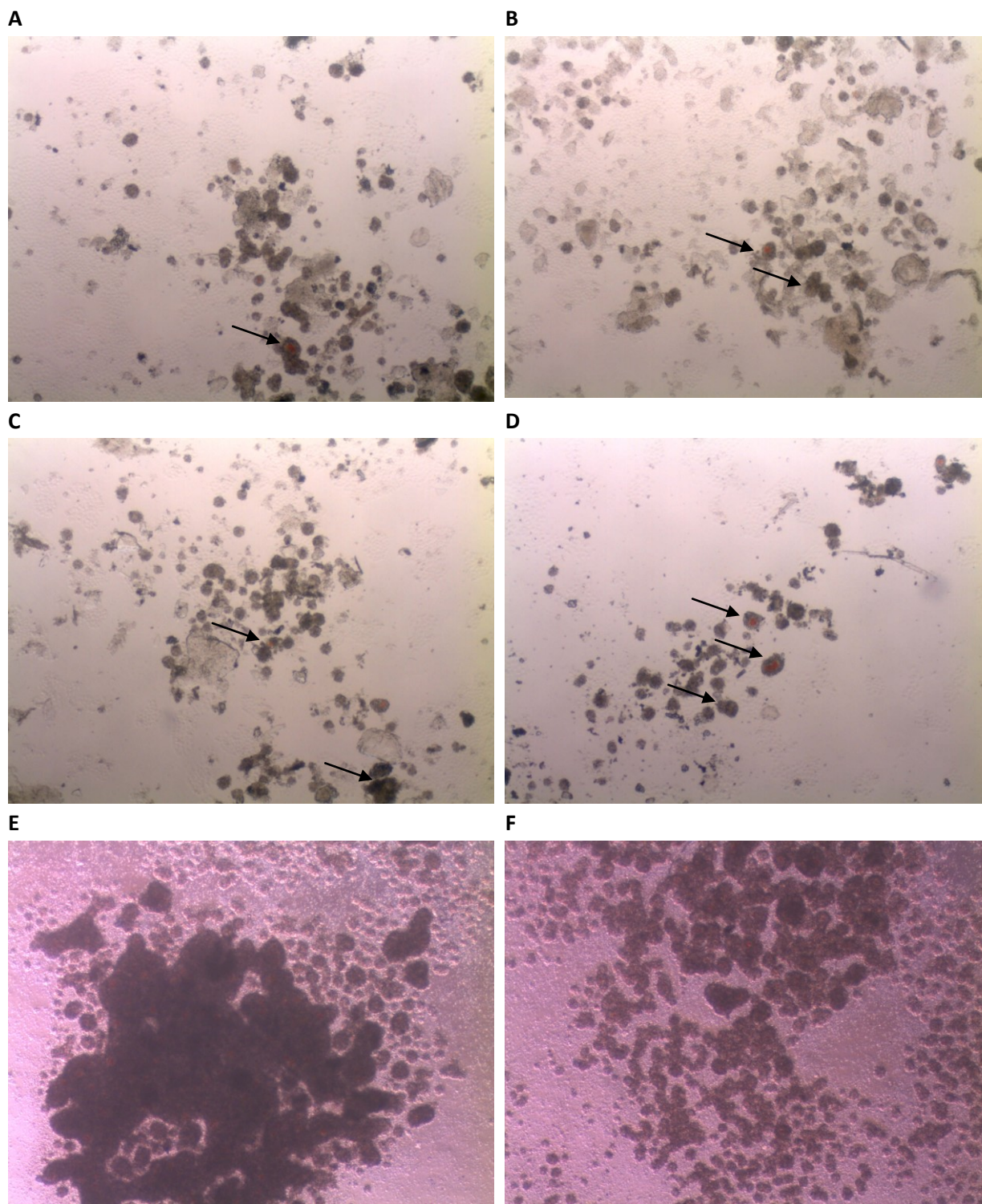
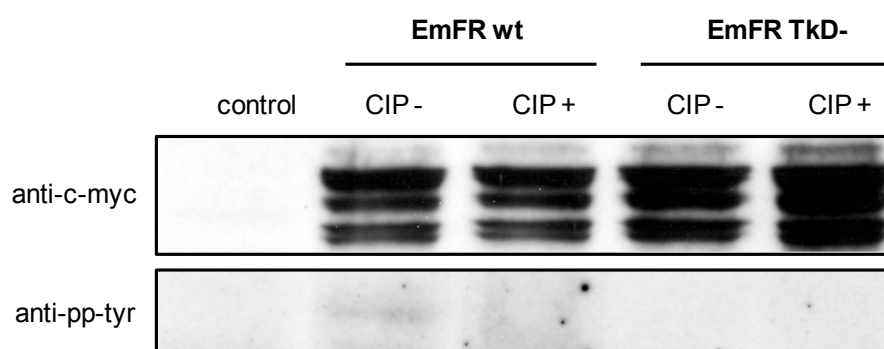


Fig. 19: siRNA knock-down of EmFR in *Echinococcus* primary cells – preliminary data. Subsequent to isolation according to [147], primary cells were seeded in a 6-well plate, allowed to form mini-aggregates and were subsequently subjected to electroporation with (A) electroporation buffer (B) control Mm/Hs_MAPK1 siRNA (C) EmElp siRNA and (D) EmFR siRNA. (E) In a second approach GFP-siRNA was used as control in comparison to (F) EmFR siRNA. Half the medium was changed every 3 -4 days. Microscopic pictures were taken after 6 days (A-D) and after three days (E, F). Magnification 25 x. Black arrows indicate regenerating aggregate structures

5.1.9. EmFR is activated by aFGF and bFGF, leading to MAP-kinase signaling in *Xenopus laevis* oocytes

In order to analyse the functional activity of EmFR, EmFR and the mutant EmFR TkD- were first expressed in HEK293T cells (Fig. 20). FGFRs are activated by FGFs as can be measured by phosphorylation which triggers the activation of cytoplasmic signal transduction pathways [64]. Interestingly, EmFR was phosphorylated without stimulation through FGF in this system (Fig. 20 A). The phosphorylation of EmFR was effectively blocked by calf intestinal phosphatase (CIP) treatment. Also, the dead-box kinase EmFR TkD- did not show any phosphorylation activity, neither in the absence nor in the presence of FGFs. For detection of transfection efficiency an anti-c-myc antibody was used. Phosphorylation was analysed with an anti-phospho-FGF receptor (Tyr653/654; anti-pp-tyr) antibody. Nevertheless, the heterologous expression of EmFR in HEK293T cells was not appropriate to analyse the effect of FGFs on EmFR because the receptor itself apparently was constitutively active in the system, also in the absence of the FGF stimuli.

A



B

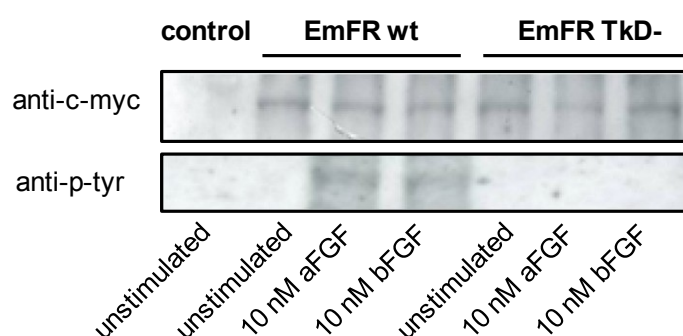


Fig. 20: Western blot analyses of heterologously expressed EmFR and EmFR TkD- in HEK293T cells and *Xenopus* oocytes. Depicted are Western blot experiments of HEK293T cell lysates and *Xenopus* oocytes expressing EmFR and EmFR TkD- using the anti-c-myc and either the anti-phospho-FGF receptor (Tyr653/654; anti-pp-tyr) or an anti-phospho tyrosine (anti-p-tyr) antibodies detecting the overall amount of EmFR and EmFR-TkD- and the phosphorylated EmFR, respectively. (A) HEK293T cells were transfected using the standard procedure and prior to lysis parts of the sample was subjected to 30 min treatment with calf intestinal phosphatase (CIP). Cells were transfected with empty vector psecHygroA for control. (B) *Xenopus* oocytes were allowed to express EmFR or EmFR TkD- for 48 h, then 10 nM aFGF or bFGF were added and cells were submitted to lysis after 24 h. As control a mock injection was chosen.

Therefore, EmFR and the mutant dead box kinase EmFR TkD- were expressed in stage VI *Xenopus* oocytes and checked on the one hand the phosphorylation (Fig. 20 B) status and on the other hand for germinal vesicle breakdown (GVBD) in the presence and absence of aFGF or bFGF (Fig. 21). Functional analyses of receptor tyrosine kinases using heterologous protein expression in stage VI *Xenopus* oocytes has been reported before [156,168,169] and in the case of pleurodele FGFR1 it was demonstrated that after stimulation with aFGF, GVBD of *Xenopus* oocytes as a measure of receptor activity and active signaling occurs [156]. EmFR did not induce GVBD in the absence of the FGF stimuli (Fig. 21 A). However, upon the addition of either aFGF or bFGF a dose dependent induction of GVBD was observed (Fig. 21 A) with aFGF being more potent than bFGF.

Then the *Xenopus* oocyte membrane fractions were analysed in western blot analyses using an anti-c-myc and an anti-phospho tyrosine antibodies detecting the overall amount of EmFR and EmFR-TkD- and the phosphorylated EmFR, respectively. Without the addition of FGFs the wild type EmFR does not show any phosphorylation, suggesting that in this system EmFR is not constitutively active. With the stimulation of either aFGF or bFGF a clear receptor phosphorylation was detected (Fig. 20 B). In the case of the dead-box kinase EmFR TkD- phosphorylation of the receptor was not detect at any condition. This lead to the assumption that also for EmFR the DFG motif is essential for tyrosine kinase activity.

In addition to the experiments outlined above, BIBF1120 was tested in the *Xenopus* system (Fig. 21 B). BIBF1120 can efficiently block the effect of aFGF and bFGF on EmFR at 10 μ M and 20 μ M, whereas with 1 μ M still 90 % GVBD with aFGF and 50 % GVBD with bFGF were observed. GVBD induced by pleurodele FGFR1 stimulated with 10 nM aFGF [156] was also successfully blocked. The inhibition was even more pronounced because 1 μ M BIBF1120 led to less GVBD (30 %) suggesting that BIBF1120 more effectively binds to FGFR1. Moreover, as expected BIBF1120 treatment did not alter the outcome of samples which expressed EmFR TkD-. EmFR TkD- is a dead box kinase unable of signal transduction and never led to GVBD in the presence of stimuli.

In summary, with the use of the *Xenopus* expression system, it was demonstrated that EmFR is an active tyrosine kinase when activated by either aFGF or bFGF and thus causing GVBD. The effect was reversed when BIBF1120 was applied which successfully blocked EmFR signaling.

A		aFGF			PG	
		none	1 nM	5 nM	10 nM	10 μ M
Oocytes expressing						
EmFR		0%	0%	90%	100%	100%
Pleurodele amphibian FGFR		0%	n.d.	100%	n.d.	100%
		bFGF				
Oocytes expressing		none	1 nM	5 nM	10 nM	
EmFR		0%	0%	0%	90%	
Pleurodele amphibian FGFR		0%	n.d.	90%	n.d.	

B	Oocytes expressing	BIBF1120			
		none	1 μ M	10 μ M	20 μ M
	EmFR	0%	0%	0%	0%
	EmFR + aFGF [10 nM]	100%	90%	0%	0%
	EmFR + bFGF [10 nM]	90%	50%	0%	0%
	EmFR TkD-	0%	0%	0%	0%
	EmFR TkD- + aFGF [10 nM]	0%	0%	0%	0%
	EmFR TkD- + bFGF [10 nM]	0%	0%	0%	0%
	HsFGFR1	0%	0%	0%	0%
	HsFGFR1 + aFGF [10 nM]	100%	40%	0%	0%

Fig. 21: The induction of GVBD in *Xenopus* oocytes expressing EmFR and EmFR TkD-. (A) Oocytes were allowed to express EmFR or pleurodele FGFR1 for 48 h, and then aFGF or bFGF ligands were added with different concentrations (1 nM, 5 nM, and 10 nM). (B) Wild type EmFR, mutant EmFR TkD- and pleurodele FGFR1 were expressed in *Xenopus* oocytes for 48 h, and then 10 nM aFGF or bFGF were added in the presence or absence of various concentrations of BIBF1120 (1 nM, 10 nM and 20 μ M). Native oocytes treated with or without progesterone (10 μ M) served as positive and negative controls, respectively. In all experiments GVBD was observed after 24 h of stimulation. Percentages of GVBD as indication for receptor activity in each group are shown. Each experiment was performed using a set of 20-30 oocytes and was repeated two times.

5.1.10. Phosphorylation status of EmMPK1 in metacestodes and primary cells

Since FGFs displayed a clear growth-stimulating and proliferative effect on *E. multilocularis* metacestode vesicles and primary cells, the underlying molecular signaling mechanisms of these phenomena were analysed. In mammalian systems, it is known that FGFs signal via FGFRs and induce an activation of the MAP-kinase cascade. Interestingly, EmMPK1 was simulated in *E. multilocularis* metacestode vesicles upon exogenous addition of aFGF or bFGF [94] This was detected by means of Western blots using the anti-Erk1/2 and the anti-phospho-Erk antibodies to measure the overall EmMPK1 and phosphorylated EmMPK1, respectively [55]. However, it was not clear, whether host FGFs can induce the phosphorylation of EmMPK1 in *Echinococcus* primary cells. In a previous preliminary study [170] in which 1 nM of either aFGF or bFGF were used for stimulation of primary cells there was no change in phosphorylation of EmMPK1 compared to control samples. However, in this study, primary cells were incubated for two days in DMEM with 0.2% FBS and were subsequently stimulated with 10 nM or 100 nM aFGF or bFGF for two days. Using these conditions with elevated FGF concentrations an increase of phosphorylation of EmMPK1 was detected in the stimulated samples. Most clearly when 10 nM aFGF and 100 nM bFGF were applied (Fig. 22).

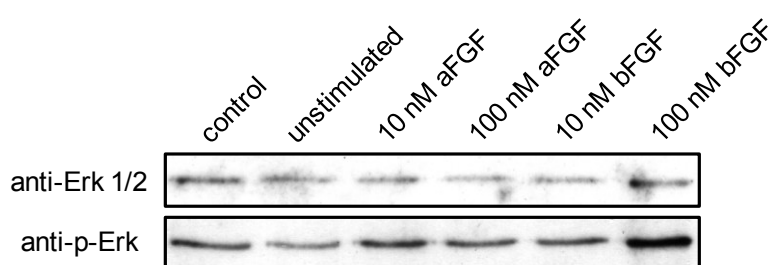


Fig. 22: The effect of FGFs on the EmMPK1 of primary cells. Depicted are Western blot experiments of primary cell lysates using the anti-Erk1/2 and the anti-phospho-Erk antibodies detecting the overall EmMPK1 and phosphorylated EmMPK1, respectively after separation on a 12% PAA gel. Intact primary cells were kept in cDMEM-1 (control), starved in DMEM with 0.2% FBS for two days (unstimulated) or after starvation have been treated with 10 nM or 100 nM aFGF or bFGF for two days.

Moreover, this study investigated the effect of BIBF1120 on the phosphorylation of EmMPK1. As the inhibitor caused a dose-dependent damage of the metacystode vesicles, a block in regeneration of primary cells and is known to act on FGFRs, one could speculate that the MAP-kinase cascade is blocked. For that, axenic metacystode vesicles were starved in DMEM without FBS for 4 days and then treated with either 5 μ M or 10 μ M BIBF1120 for 30 min. Indeed a slight reduction of the phosphorylated EmMPK1 was detectable (Fig. 23 A). The effect was more pronounced for 10 μ M BIBF1120. Experiments, in which BIBF1120 was applied to primary cells, gave similar results. In detail, freshly isolated primary cells were directly subjected to cDMEM-1 supplemented with either 5 μ M or 10 μ M BIBF1120 for 4 h. Control samples were treated with 0.1 % DMSO. With both inhibitor concentrations tested, the phosphorylation of EmMPK1 was diminished compared to control DMSO treated primary cells (Fig. 23 B).

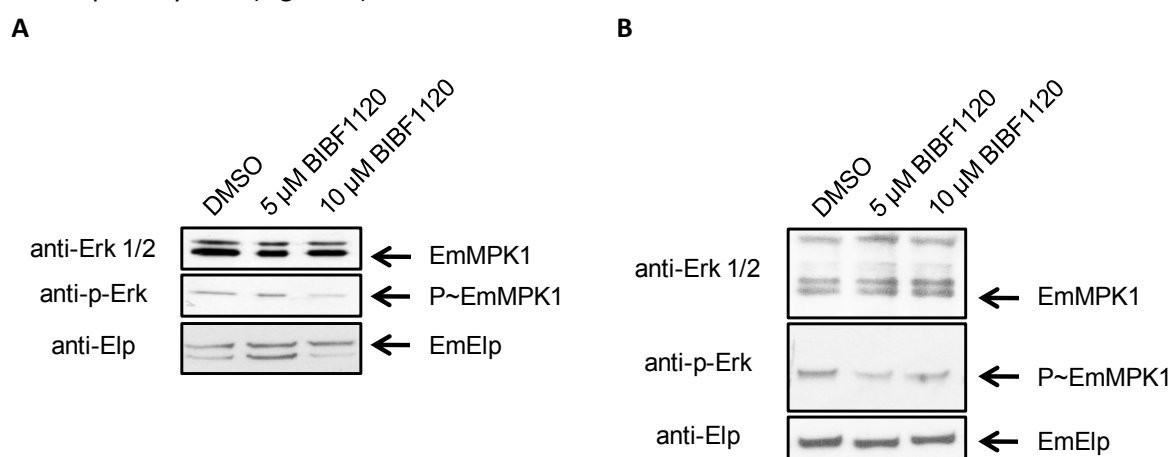


Fig. 23: The effect of BIBF1120 on the EmMPK1 phosphorylation of metacystode vesicles and primary cells. Depicted are Western blot experiments of (A) metacystode vesicle lysates and (B) primary cell lysates using the anti-Erk1/2 and the anti-phospho-Erk antibodies detecting the overall EmMPK1 and phosphorylated EmMPK1, respectively after separation on a 12% PAA gel. Axenic metacystode vesicles were starved in DMEM without FBS for 4 days and then treated with either 5 μ M or 10 μ M BIBF1120 for 30 min. Freshly isolated primary cells were directly subjected to cDMEM-1 supplemented with either 5 μ M or 10 μ M BIBF1120 for 4 h. Control samples were treated with 0.1 % DMSO. Subsequently to treatment protein lysates were prepared immediately. Internal control for protein content of the lysates, the constitutively expressed protein EmElp was detected with an anti-EmElp antibody.

All together, these data demonstrate that aFGF and bFGF stimulate EmMPK1 phosphorylation in metacestode vesicles and primary cells. Furthermore, BIBF1120 caused a dephosphorylation of EmMPK1 in metacestode vesicles and primary cells suggesting that FGF-FGFR signaling in *E. multilocularis* involves the MAP-kinase signaling cascade.

5.1.11. Phosphorylation status of EmAkt in metacestode vesicles and primary cells

It is known that FGFs signal via FGFRs and induce an activation of the MAP-kinase cascade. Moreover, in mammals the PI3 kinase/AKT pathway is activated and implicated in cell survival and cell fate determination [171,172]. EmAkt has been identified in a previous study [173]. Therefore, the effect of host FGFs and BIBF1120 on EmAkt signaling was investigated and the phosphorylation of EmAkt was analysed using anti-phospho-Akt antibody in protein lysates of primary cells.

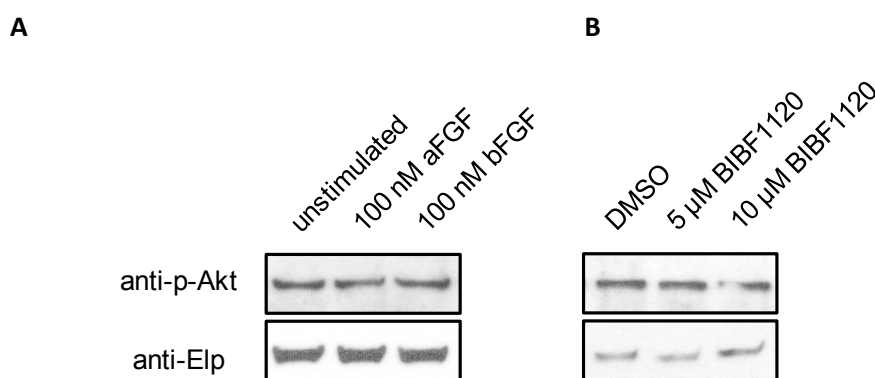


Fig. 24: The effect FGFs on the EmAkt phosphorylation of primary cells Depicted are Western blot experiments of primary cell lysates using the anti-phospho-Akt and the anti-EmElp antibodies after separation on a 12% PAA gel. **(A)** Freshly isolated primary cells were starved in DMEM 0.2 %FBS for two days and then treated with either 100 nM aFGF or 100 nM bFGF for 3 h. **(B)** Freshly isolated primary cells were directly subjected to cDMEM-1 supplemented with either 5 μM or 10 μM BIBIF1120 for 4 h. Control samples were treated with 0.1 % DMSO. Subsequently to treatment protein lysates were prepared immediately.

In detail, freshly isolated primary cells were starved in DMEM 0.2 %FBS for two days and then treated with either 100 nM aFGF or 100 nM bFGF for 3 h. Compared to untreated primary cells, there was no difference in phosphorylation of EmAkt in the aFGF or bFGF treated samples (Fig. 24A). Moreover, the influence of BIBF1120 was investigated. For that, freshly isolated primary cells were directly subjected to cDMEM-1 supplemented with either 5 μM or 10 μM BIBIF1120 for 4 h. Control samples were treated with 0.1 % DMSO. In untreated and BIBF1120 treated samples a clear phosphorylation was detected (Fig. 24B). However, there was no difference in intensity between DMSO control cells and BIBF1120 treated cells. Thus far, the phosphorylation of EmAkt has not been analysed in metacestode vesicles or protoscoleces. Altogether, in primary cells, the activation of EmAkt is not influenced by FGFs or BIBF1120. In treated and untreated samples a comparable, but clear phosphorylation was present.

5.1.12. The *E. multilocularis* genome does not encode for own canonical FGFs

A variety of at least 23 FGFs have been identified in several organisms ranging from nematode and *Drosophila* to humans. Although, FGFs vary in size they usually share a conserved core region of 120 amino acids [67]. FGFs act in concert with heparin or heparan sulfate proteoglycan to activate FGFRs and to induce the pleiotropic responses which lead to the range of cellular responses. Thus, one could assume if *E. multilocularis* encodes a FGFR, also FGFs might be present in this particular cestode organism. However, when searching with either human or *C. elegans* *egl-17* and *let-756* FGFs against the *E. multilocularis* genome and transcriptome data, no significant BLAST hit was obtained, suggesting that no canonical FGF is present in the *E. multilocularis*. In detail, it is reported that FGFs are sometimes linked to certain genes on the genome of for example humans. For instance, *FGF1* is located on chromosome 5q in proximity to *FGFR4* [63,64]. When analysing the genomic surrounding of *Emfr* on contig 1713 (Fig. 25) with BLAST searches based on transcriptome data, downstream within 10 kb just a homolog to the *integrator complex subunit 7* and upstream within 10 kb a homolog to *sideroflexin* was identified. There was no evidence for any FGF homologue. Then, the surrounding of the putative *E. multilocularis* nou-darake (*Emndk*; sequence see supplementary material) was analysed. Nou-darake was first described in *Dugesia japonica* and is involved in planarian brain development [84]. It is a putative actor of the FGF signaling pathway present in all major metazoan phyla [72]. EmNDK exhibits a high homology to the planarian NDK including the extracellular domain consisting of three IG domains, a transmembrane domain and as expected the intracellular Tkd typically for FGFRs is absent. In humans, the homologous gene is described as FGFR-like 1 (FGFRL1), but in this case it was named the *E. multilocularis* gene *Emndk*, as the homology to the planarian gene is more pronounced. In the literature, it is reported, that nou-darake and some FGFs are co-expressed. Conversely, no FGF homologue could be identified in the genome data, in the proximity to *Emndk* situated on contig 3410 of the latest genome assembly. Upstream within 30 kb of *Emndk*, a ribose-phosphate pyrophosphokinase 1,2 homolog and a GTP-binding Ras-like homolog was identified. Downstream within a range of 50 kb of *Emndk*, two transcriptional units were identified. However, in a BLAST search either no significant (n.s.) hit was retrieved, suggesting the presence an *E. multilocularis* specific transcript or just a hypothetical non characterized (n.c) protein was identified. Thus, with the *in silico* data analyses conducted in this study, it is most likely that *E. multilocularis* does not possess any canonical FGFs.

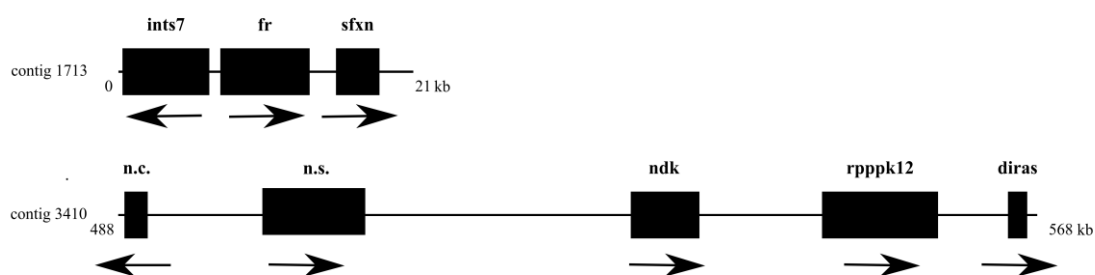


Fig. 25: Gene locus maps for *Emfr* and *Emndk* genes on assembled *E. multilocularis* genome contigs. Schematically displayed are the *Emfr* and *Emndk* loci present on contigs 1713 and 3410, respectively, of the latest *E. multilocularis* genome assembly version as well as the 5' and 3' flanking reading frames. Black arrows indicate the reading direction of the respective open reading frame. *diras*: GTP-binding Ras-like; *fr*: fibroblast growth factor receptor; *ints*: integrator complex subunit 7; *n.c.*: no characterized, but hypothetical protein in BLAST analysis; *ndk*: nou-darake; *n.s.*: no significant hit in the BLAST analysis; *rppk12*: ribose-phosphate pyrophosphokinase 1,2; *sfxn*: sideroflexin.

5.2. NHR signaling – EmNHR1

5.2.1. Expression analysis of *Emnhr1* in *Echinococcus* larval stages

The expression of *Emnhr1* (sequence see 7.1) in larval stages was analyzed by semi-quantitative RT-PCR [145]. *Emnhr1* transcripts are present in all analysed stages: metacystode vesicles, in protoscoleces before (dormant protoscoleces) and after activation through pepsin/low-pH treatment protoscoleces (activated protoscoleces) as well as in in vitro cultivated primary cells (Fig. 26). It seems, that *Emnhr1* is to some extent higher expressed in the dormant protoscolex and is least expressed in activated protoscoleces. Data from the transcriptome profile (kindly provided by the Sanger Institute, Hinxton, UK) of *Emnhr1* support these findings, with the relative expression level of *Emnhr1* highest in dormant protoscoleces which was set to 100 % (Fig. 26B). Least expression was detected in in vitro cultivated metacystode vesicles (28.9 %) and activated protoscoleces (35.2 %)

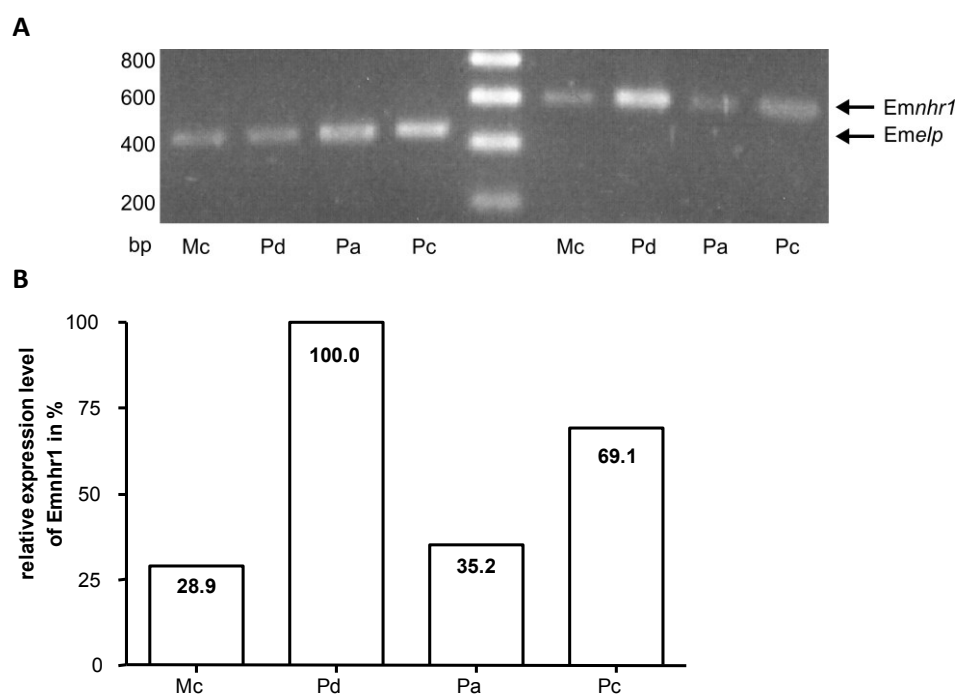


Fig. 26: Expression analysis of *Emnhr1*. (A) After isolation of total RNA from in vitro cultivated metacystode vesicles (Mc), dormant (Pd) and activated protoscoleces (Pa) as well as in vitro cultivated primary cells (Pc) the RNA was reverse transcribed. Subsequently, the cDNA was subjected to PCR with oligonucleotides specific for *Emnhr1*. As control the constitutively expressed gene *Emelp* [44] was used. The resulting PCR amplicons were separated on a 1 % agarose gel and stained with ethidium bromide. DNA size marker bands are indicated to the left. Figure taken from [145] (B) Expression of *Emnhr1* from transcriptome profiling analysis. Normalized relative gene expression is given, with the highest expression set to 100 %.

Taken together, these data indicate that *Emnhr1* is constitutively expressed in important larval stages of the parasite's lifecycle, namely of the intermediate host and on its way to the system of the definitive host.

5.2.2. Recombinantly expressed EmNHR1 – an attempt to raise a specific antibody

For the analysis of protein expression levels of EmNHR1 in different *E. multilocularis* larval stages a specific antibody for detection is a useful tool. Therefore, the deduced amino acid of EmNHR1 was subjected to *in silico* analysis using a tool for predicting antigenic peptides within a protein sequence (<http://immunax.dfci.harvard.edu/Tools/antigenic.html>). Hence, a partial sequence of EmNHR1 (EmNHR1-ab, residue 170 – 408) was chosen and cloned into the pBAD/Thio-® vector for recombinant expression in *E. coli*. After the induction with 0.2% arabinose for 4 h in *E. coli* BL21, the fusion protein EmNHR1-ab was purified under native conditions via the 6xHis – tag. The quality of the protein purifications was validated by both Coomassie staining and Western blotting (Fig. 27) with anti-V5 antibody. Apparently, the recombinant protein was expressed as detected by Western blot (Fig. 27 B), but the purity of the recombinant protein was not very high. Another attempt to express EmNHR1 in the vector pRSET and to purify the respective fusion protein failed. For the production of a polyclonal antibody against EmNHR1 rabbits were intravenously immunized at immunoGlobe® Antikörpertechnik GmbH. The recombinantly expressed EmNHR1 was used for this and was dialysed against 1xPBS before immunization. Rabbits were boosted three times before the final bleeding. However, with each final serum, the EmNHR1-ab fusion protein which had been used to immunize the rabbit could not be detected in Western blot assays (data not shown). Thus, the attempt to generate a polyclonal antibody specific against EmNHR1 was not successful.

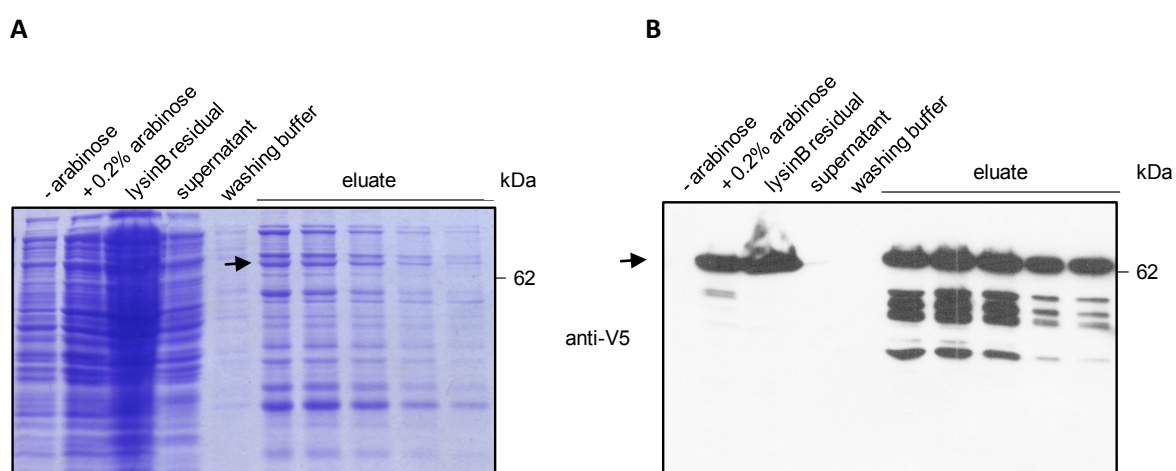


Fig. 27: Recombinant expression of EmNHR-ab in *E. coli* using the pBAD-thio vector. The expression of the fusion protein EmNHR1ab/Thio was induced with 0.2 % arabinose for 4 h in *E. coli* BL21 using the pBAD/Thio-Topo® vector (Invitrogen) and was subsequently purified via the 6xHis-tag under denaturing conditions as described. The induction and purification was analyzed on a 12 % PAA –gel followed by Coomassie staining and Western blotting with anti-V5 antibody (Invitrogen) according to the manufacturer’s recommendations. The samples separated on the PAA-gel were: *E. coli* lysate prior (- arabinose) and after (+ 0.2 % arabinose) induction; the lysisB residual, the protein fraction, which did not bind to the Ni²⁺ column (supernatant) and the washed out unspecific bound proteins (washing buffer); the eluted protein fractions. The arrow marks the corresponding fusion protein, while the smaller fragments detected with the anti – V5 antibody were most likely degradation products.

5.2.3. Protein-protein interaction studies of EmNHR1 and its domains: LBD and DBD

It has been repeatedly reported that NHR receptors are modulated by NHR co-regulators, namely coactivators or corepressors, also through direct protein-protein interaction [174,175].

	Fusion with Gal4-DNA binding domain			
	pGBKT7	EmNHR1-FL	EmNHR1-DBD	EmNHR1-LBD
pGADT7	-	-	-	-
EmNHR1-FL	-	(+)-	n.d.	n.d.
EmNHR1-DBD	-	n.d.	(+)-	n.d.
EmNHR1-LBD	-	n.d.	n.d.	(+)-
EmSkip	-	-	-	-
EmSmadA	-	-	-	-
EmSmadB	-	-	-	-
EmSmadC	-	+	++	-
EmSmadD	-	-	-	-
EmSmadE	-	-	-	-
EmSmadE*	-	-	-	-
EmSmadA*	-	-	-	-
EmSmadB*	-	-	-	-
EmSmadC*	-	+	++	-
EmAlien	-	-	-	-
EmGt198	-	-	-	-

A

	Fusion with Gal4-activation domain			
	pGADT7-TY**	EmNHR1-FL	EmNHR1-DBD	EmNHR1-LBD
pGBKT7-EmJab1	(+)-	-	+	+

B

Fig. 28: EmNHR1 protein interaction studies with *E. multilocularis* NHR co-regulators, EmSmads and EmJab1. (A) Translation fusions were generated for the Gal4-DNA binding domain (BD; vector pGBKT7) and (B) the Gal4-activation domain (AD; vector pGADT7) with the full-length EmNHR1 (EmNHR1-FL), EmNHR1-LBD and EmNHR1-DBD. These were transformed into yeast strain AH109 together with empty vectors (pGADT7, pGBKT7) or with different fusions for EmSkip [61] and EmSmadA, EmSmadB [60] as well as EmSmadC, EmSmadD [58]. An asterisk marks the constitutively active forms of EmSmadA, EmSmadB, EmSmadC [58,60] and EmSmadE [176]. Positive control (pGADT7-T x pGBK-53) and negative control (pGADT7-T x pGBK-Lam) were performed as described in the MATCHMAKER-manual (Clontech). Growth of colonies was assessed according to the MATCHMAKER-manual (Clontech). The characters “-”, “+”, and “++” indicate no growth or growth under medium and high stringency conditions. Slight growth under medium stringency conditions, which is blocked under 7.5 mM 3-AT treatment is indicated by “(+)-”. Instead of empty pGADT7 control, pGADT7-TY was used as described [177] and indicated by “**”. Not defined (n.d.) shows that no double-transformants for this plasmid combination were generated. Figure and legends adapted from [145]. Several independent experiments (n= 3-5) were performed.

In a yeast-two hybrid approach it was therefore tested, whether EmNHR1 interacts with EmSkip [61], EmAlien [62], or EmGt198 [178]. To this end a translational fusion of full length EmNHR1-FL, EmNHR1-DBD and EmNHR1-LBD in pGADT7 and pGBKT7 was constructed. In the experiments, no

interaction between any of the EmNHR1 domains and EmSkip, EmAlien or EmGt198 (Fig. 28 A) was observed, suggesting that other parasite specific co-regulators of NHR could be present. Moreover, the interaction of EmJab1 with EmNHR1-FL and EmNHR1-DBD was assessed (Fig. 28 B). EmJab1 is a homolog to the *H. sapiens* Jab1 which is part of the signalosome complex and involved in hormone-dependent activation of steroid-hormone-receptors [179]. Jab1 also acts as a modulator of intracellular signaling (reviewed in [180,181]). It was described earlier [177], that EmNHR1-LBD (construct by [62]) positively interacts with EmJab1. In this study, a positive interaction between EmJab1 and EmNHR1-LBD, EmNHR1-LBDtrunc and EmNHR1-DBD was detected, whereas no interaction was observed with EmNHR1-FL (Fig. 28). In addition it has been reported that members of the Smad family, intra-cellular transcription factors of the TGF β /BMP-signaling pathway interact with NHR [114,182]. Noteworthy, it was found that the translational fusion of EmSmadC and its constitutively activated form EmSmadC* expressed in the pGBK positively interact with the empty pGADT7 [58]. Therefore both, the translational fusions of all EmNHR1 constructs in pGADT7 and pGBKT7 were tested in order to exclude false positive results. Whereas EmSmad A, constitutively activated EmSmadA (EmSmadA*), EmSmadB, constitutively EmSmadB (EmSmadB*) [60], EmSmadD [58], EmSmadE and constitutively activated EmSmadE (EmSmadE*) [176] did not interact with either EmNHR1-FL, EmNHR-DBD or EmNHR-LBD, a clear protein-protein interaction was detected between EmSmadC and EmNHR1-FL and EmNHR1-DBD. Also, EmSmadC* interacted with EmNHR1 and EmNHR1-DBD (Fig. 28A). Hence, EmNHR1 might act in concert with TGF- β /BMP-signaling in the parasite.

5.2.4. EmNHR1-LBD dimerization studies

NHR like VDR usually form homo- or heterodimers upon ligand binding [183]. Therefore, it was investigated if the EmNHR1-LBD and its C-terminally truncated form (EmNHR1-truncLBD) can form homodimers (Fig. 29 A). As method of choice a modified yeast-two-hybrid was used in which the LBD of NHRs is fused to the Gal4-DBD or to the Gal4-LBD and double transformants are incubated in the presence of potential ligands [145]. In the presence of non-cognate compounds, no interaction is detected, whereas in the presence of cognate ligand, the NHR LBDs form dimers that result in positive readout [1,17-20].

Translational fusions of EmNHR1-LBD (cloned with oligonucleotides: EmNHR1-LHQ-NcoI-fwd, EmNHR1-FIE-XmaI-rev) as well as EmNHR1-truncLBD (cloned with oligonucleotides: EmNHR1-LHQ-NcoI-fwd, EmNHR1-ALT-XmaI-rev) in pGBKT7 and EmNHR1-LBD in pGADT7 were transformed into Y187 yeast strain and grown in selective medium. First, no homodimerization was detected when the yeast was grown in selective unsupplemented medium (Fig. 29 A). Once 5 % human or bovine serum was added to the yeast cultures a clear positive signal in the liquid β -galactosidase assay was seen as a measure of homodimerization of EmNHR1-LBD. The effect was also detectable with 10 % (data not shown) and 20 % (Fig. 29 B) serum. A dimerization of EmNHR1-LBD has also been detected when transformed yeast were grown in the presence of 20 % *E. multilocularis* hydatid fluid (Fig. 29 A; HF). However, no dimerization was observed, when BD-EmNHR-truncLBD was tested with AD-EmNHR-LBD. Thus, the ability of EmNHR1-LBD to form homodimers is dependent on the C-terminus of the LBD. In Fig. 29 B the reaction of EmNHR1 LBD to fractionated FBS is depicted. Briefly, a putative ligand is present in FBS fractions between 10–30 kDa of molecular mass, because a positive signal was detected in the FBS fraction smaller than 30 kDa (FBS < 30 kDa) but larger than 10 kDa (FBS > 10 kDa).

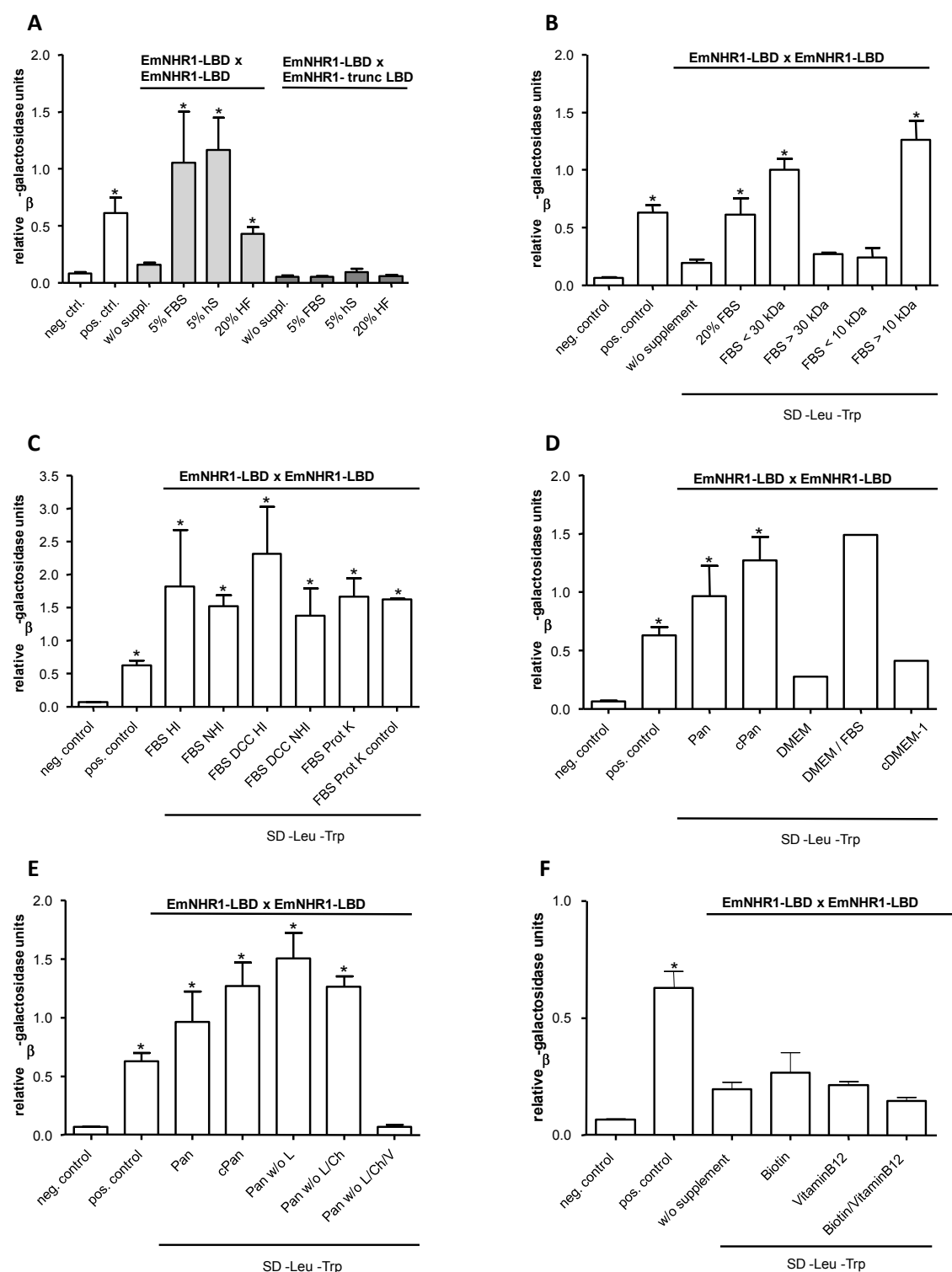


Fig. 29: Comparative β -Galactosidase liquid assays to determine EmNHR1-LBD dimerization. Yeast cells (strain Y187) were transformed with the pGADT7-EmNHR1-LBD and pGBKT7-EmNHR1-LBD or a C-terminal truncated pGBKT7-EmNHR1-LBD. (A) The cells were then cultured over night in selective SD-Leu/-Trp medium either without supplement (w/o suppl.) or in the presence of 5 % FBS, 5 % human serum (5 % hS) or 20 % *E. multilocularis* hydatid fluid (20 % HF). Figure adapted from [145]. (B-E) The assay was performed with pGADT7-EmNHR1-LBD and pGBKT7-EmNHR1-LBD transformed yeast. Selective SD-Leu/-Trp medium was supplemented with: 20 % FBS, FBS < 30 kDa, FBS > 30 kDa, FBS < 10 kDa, FBS > 10 kDa, heat inactivated FBS (FBS HI), non heat inactivated FBS (FBS NHI), NHI or HI dextran-coated charcoal treated FBS (FBS DCC NHI or HI), Panserin (Pan), conditioned Panserin (cPan), Panserin devoid of either lipids (Pan w/o L),

Lipids/Cholesterol (w/o L/Ch) or Lipids/Cholesterol/Vitamins (w/o L/Ch/V), DMEM, DMEM/FBS or cDMEM-1. pGAD-ElpN/pGBK-ElpC as positive control [37] (pos. control) and pGADT7-T/pGBK-Lam as negative control (neg. control). The statistical evaluation of 3-5 independent measurements of β -Galactosidase activity is shown including the standard error of the mean (SEM), * $p < 0.05$.

Moreover, the signal resulting from the FBS could not be eliminated by treatment with either 400 $\mu\text{g/ml}$ Proteinase K for 90 min at 56 °C or dextran-coated charcoal regardless whether it has been heat inactivated twice for 45 min at 56 °C (Fig. 29 C).

In additional experiments different culture media for *E. multilocularis* cultivation were subjected to the modified Y2H assay (Fig. 29 D). PanserinTM401 (Pan) and conditioned PanserinTM401 (cPan) both lead to a positive signal, indicating that the putative ligand for EmNHR1 is present in these media. DMEM without FBS on the other hand did not result in a positive signal supporting the idea that the ligand is present in the FBS. Conditioned DMEM (cDMEM-1) resulted in a slight positive reaction which might be due to the fact that some components of the FBS are used by the RH- cells. In an additional experiment PanserinTM401 either without lipids, without lipids/cholesterol or without lipids/cholesterol/vitamins was analysed. These components are usually supplemented in the medium. Interestingly, in the absence of the vitamins no homodimerization of EmNHR1-LBD could be detected whereas the absence of lipids or cholesterol did not alter homodimerization. However, no specific vitamin could be identified in this study. Vitamin B12 (0.013 mg/l) and Biotin (0.013 mg/l) were tested alone and in combination, but neither could induce a homodimerization of EmNHR1-LBD (Fig. 29 F). Taken together, these results indicated that host serum contains at least one ligand that can be recognized by EmNHR1. When a truncated version of the EmNHR1 LBD was used (lacking parts of the C-terminal LBD region), no elevated β -Galactosidase units were measured, indicating that the complete LBD was necessary for ligand-dependent dimerization of EmNHR1 [145].

5.2.5. Effect of bile salts and conjugated bile salts on axenically cultivated metacestode vesicles

To examine the effect of bile salts and related substances (conjugated bile salts) as well as progesterone and aldosterone H95 metacestode vesicles from 3 months in vitro co-culture were transferred to axenic conditions in the presence of these substances. The growth was monitored over a time period of 6 weeks. Substances to be tested were applied at physiological concentrations present in the portal vein blood of humans as indicated (Fig. 30 A and B). Control vesicles were cultured with the respective solvent: water, ethanol, methanol or chloroform. The medium (cDMEM-1; 2 ml) of each 15 ml tube was replaced every second or third days in every 15 ml tube and incubated at 37 °C under nitrogen atmosphere. For each group ten replicates were prepared.

Compared to the respective control metacestode vesicles, those that were grown in the presence of bile salts (BS), cholic acid (CA), desoxycholic acid (DCA) as well as lithocholic acid (LCA) were significantly bigger after six weeks (Fig. 30 A and B). The influence of 2 μM LCA (Fig. 30 A) seemed to be more pronounced (3.1 fold increase in diameter), than the positive effect of 0.02 μM LCA (2.6 fold increase in diameter) and 0.02 μM DCA (2.5 fold increase in diameter). Upon stimulation with 0.02 μM BS a 1.7 fold increase in vesicle diameter was observed. Also the presence of CA resulted in a 1.9 fold increase in diameter. Moreover, chenodesoxy acid (CDA) resulted in a better growth of the vesicles: 1.8 fold and 2.3 fold at 2 μM and 0.02 μM CDA, respectively (Fig. 30 A). However the effect was not statistically significant. Furthermore, the influence of progesterone and aldosterone as

members of the steroid hormone family was tested. Both substances did not alter the growth rate of the vesicles over time. The metacestode vesicles reached a diameter between 7 mm and 13 mm, comparable to the control vesicles (7 – 11 mm). The effect of all mentioned substances has not been tested on *E. multilocularis* primary cells yet.

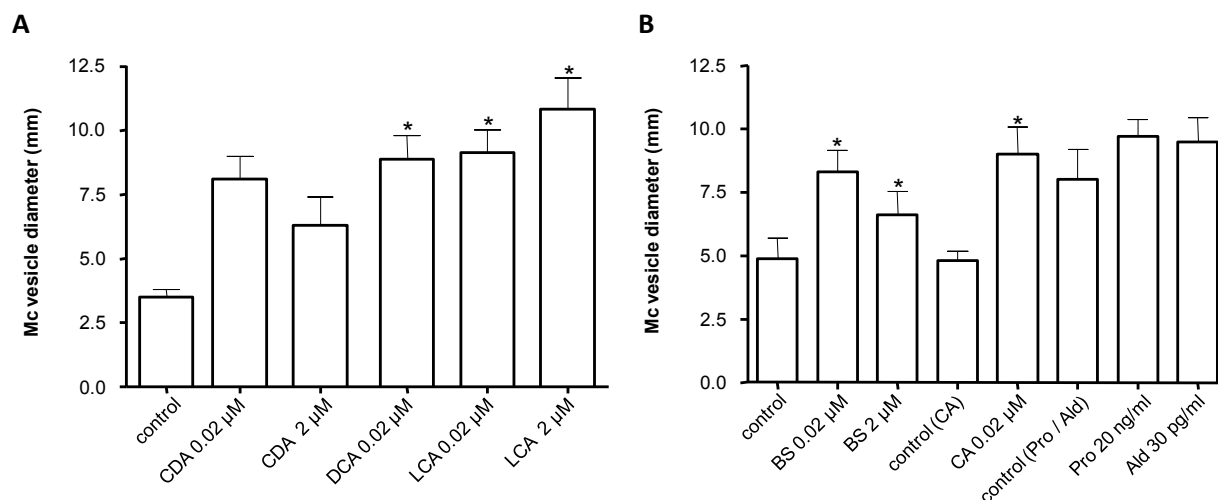


Fig. 30: Influence of bile salts, conjugated-bile salts, progesterone and aldosterone on axenic metacestode vesicles. Metacestode vesicles were grown in 15 ml tubes over a time period of six weeks. Medium was changed every 2-3 days supplemented with (A) chenodesoxy acid (CDA), desoxycholic acid (DCA) and lithocholic acid (LCA) at indicated concentrations or (B) bile salts (BS), cholic acid (CA), progesterone (Pro) and aldosterone (Ald) at indicated concentrations. Control vesicles were cultured with the respective solvent: water, ethanol, methanol or chloroform. For each group ten replicates were prepared. The mean was calculated and the standard error of the mean (SEM) is indicated, respectively. For estimation of significance a Student's t-test (two-tailed) was performed with a significance level of $*p < 0.05$.

Taken together the presence of various bile salts and conjugated bile salts resulted in an increase of metacestode vesicles over time compared to the respective controls. The stimulation with either progesterone or aldosterone did not result in a better growth.

5.3. NHR signaling – other putative EmNHRs

5.3.1. *In silico* analysis and identification of putative *E. multilocularis* NHRs

With the *E. multilocularis* genome at hand the question whether additional putative NHR are present in the parasite genome was addressed by *in silico* analysis. To this end various BLAST analyses on the available genome information were carried out. First, the EmNHR1 Znf-C4 zinc finger motif as well as the respective motifs from *S. mansoni* NHRs [105] were used for the identification of related sequences in the *E. multilocularis* genome. To identify the entire set of NHRs that is present in *E. multilocularis* an iterative TBLASTN search was conducted using as query the deduced amino acid sequence of EmNHR1 DBD (contig 3395) [145]. All together, 17 additional sequences which showed similarities to the respective DBD domains were identified. The subsequent SMART analysis detected in 16 out of these 18 sequences ZnF_C4 motifs (Table 1). An alignment of the EmNHR1 DBD (contig 3395) and the other putative NHR-DBD of *E. multilocularis* indicates a high conservation of the DBDs harbouring the ZnF_C4 motif including conserved cysteine residues (Fig. 31 A). Furthermore a phylogenetic tree in which the DBDs of the *E. multilocularis* NHRs are compared to those of *S. mansoni* was reconstructed (Fig. 31 B) and shows that most of the *Echinococcus* NHRs do have close orthologs in the trematode [145]. In the next step all 18 sequences including 2 kb down-stream and 5 kb up-stream of the putative DBD coding sequence were submitted to BLASTX analyses (against database nr) and scanned for homologies (Table 1, [145]). The best hit judged by the lowest E-value and the homologues found in the trematode *S. mansoni* were listed (Table 1). The sequence of contig 1756 did not produce a significant hit suggesting either a false positive prediction or a possible species specific NHR. Among the other sequences it is obvious that the putative NHR of *E. multilocularis* show homologies to *S. mansoni* NHRs: SmTR4 (contig 1644), SmTRb (contig 1680), SmHNF4 (contig 1702), SmE78 (contig 2122), SmHR96a (contig 3309), SmNR4A5 (contig 3425), and SmFTZ-F1a (contig 3442) (Table 1; nomenclature of the schistosome NHRs, [105]). Moreover, the structural unusual NHR containing two DBDs have been identified (contig 1779, 1872, and 2681; Fig. 31), homologous to nuclear receptor 2DBD- γ and 2DBD- α , respectively [140,141]. Furthermore, for the putative *Echinococcus* NHR, encoded on contig 1798, clear homologies to SmTLL were observed in the DBD but not in the LBD (Table 1).

The NHR, encoded on contig 3440, exhibited homologies within the LBD to SmRXR2 but is characterized by an untypical P-box (CDSCRA; Fig. 31) which cannot be found in any of the schistosome receptors. Although the NHR encoded on contig 2878 displayed homology to SmRAR-like in the DBD, no other true orthologs for both schistosome RXR receptors as well as SmDSF, SmPNR or SmRAR-like were not found in the *E. multilocularis* genome [145]. However, unlike *S. mansoni*, the genome of *E. multilocularis* contained an additional member of the CESCKA family, EmNHR1, besides the *Echinococcus* ortholog encoded on contig 3309 (Fig. 31; Table 1). Moreover, similar sequence analyses were performed on the *E. granulosus* genome [145]. The same set of NHRs was identified as in *E. multilocularis* (data not shown). This demonstrates, that cestodes of the genus *Echinococcus* contain less NHRs than schistosomes. The main difference between the NHR subsets of the analysed cestodes compared to the trematode is the absence of true RXR orthologs and the presence of only one member of group 2E NHRs which, in schistosomes, is made up of the receptors SmTLL, SmPNR and SmDSF [105]. Conversely, *Echinococcus* has more receptors with DBD and LBD similarities to the HR-96 group, including EmNHR1.

Table 1: *In silico* identification of 17 members of the NHR family in *E. multilocularis*

Contig # ^a	TBLASTN Position ZnF_C4 ^b	SMART E-value	BLASTX Position ^b	E-value	Best hit - homologues ^c	Homology to <i>S. mansoni</i>
1644	481637 - 481467	2.63E-30	483637 - 476467	3.00E-29	>ref XP_002581285.1 Tr4/Tr2 (homologue) [<i>Schistosoma mansoni</i>] emb CAZ37524.1 Tr4/Tr2 (homologue) [<i>Schistosoma mansoni</i>]	SmTR4
1680	186953 - 187156	2.88E-27	184956 - 192156	2.00E-46	>ref XP_002573733.1 thyroid hormone receptor [<i>Schistosoma mansoni</i>] emb CAZ29965.1 thyroid hormone receptor, putative [<i>Schistosoma mansoni</i>]	SmTRb
1702	102326 - 102150	2.67E-31	104329 - 97150	1.00E-35	>gb ACD77184.1 putative hepatocyte nuclear factor 4 nuclear hormone receptor [<i>Callosobruchus maculatus</i>]	SmHNF4
1756 ^d	6913 - 8633	n.d.	8913 - 1833	> 0.1	n.d. - No NHR -	-
1779	88954 - 86636 85722 - 83572	1.65E-22 2.4E-29	90954 - 81636	2.00E-17	>ref XP_002573082.1 nuclear hormone receptor [<i>Schistosoma mansoni</i>] emb CAZ29314.1 nuclear hormone receptor, putative [<i>Schistosoma mansoni</i>]	Sm2DBDy
1798	6287 - 6364	6.09E-26	4287 - 11364	4.00E-14	>gb ADG26734.1 tailless protein [<i>Platynereis dumerilii</i>]	SmTLL (DBD)
1872	361173 - 366071 365772 - 366071	1.24E-26 1.4E-29	359176 - 371071	5.00E-32	>ref XP_002582074.1 nuclear receptor 2DBD-gamma [<i>Schistosoma mansoni</i>] emb CAZ39174.1 nuclear receptor 2DBD-gamma [<i>Schistosoma mansoni</i>]	Sm2DBDy
2122	200727 - 203164	6.67E-32	198730 - 208164	1.00E-28	>ref XP_002410392.1 nuclear receptor, putative [<i>Ixodes scapularis</i>] gb EEC12905.1 nuclear receptor, putative [<i>Ixodes scapularis</i>]	SmE78
2681	142976 - 143859 144838 - 145255	7.8E-10 5.9E-33	140985 - 150258	5.00E-13	>ref XP_002578901.1 nuclear hormone receptor [<i>Schistosoma mansoni</i>] emb CAZ35139.1 nuclear hormone receptor, putative [<i>Schistosoma mansoni</i>]	Sm2DBDβ
2822	79036 - 79239	2.31E-26	77036 - 84239	6.00E-30	>ref XP_001994574.1 GH17319 [<i>Drosophila grimshawi</i>] gb EDV91203.1 GH17319 [<i>Drosophila grimshawi</i>]	-
2878	337761 - 335686	8.03E-26	339761 - 330692	4.00E-08	>ref XP_002575396.1 RAR-like nuclear receptor [<i>Schistosoma</i>	SmRAR-like

					<i>mansoni</i>] emb CAZ31629.1 RAR like nuclear receptor [<i>Schistosoma mansoni</i>]	NR (DBD)
2891 ^d	140405 - 144600	n.d.	138405 - 145485	3.00E-13	>ref XP_002575730.1 nuclear hormone receptor [<i>Schistosoma mansoni</i>] emb CAZ31964.1 nuclear hormone receptor, putative [<i>Schistosoma mansoni</i>]	-
3309	400163 - 399395	2.63E-21	402163 - 395080	3.00E-19	>ref XP_002575014.1 nuclear receptor nhr-48 [<i>Schistosoma mansoni</i>] gb AAV80235.1 CAR [<i>Schistosoma mansoni</i>] emb CAZ31247.1 nuclear receptor nhr-48, putative [<i>Schistosoma mansoni</i>]	SmHR96 α
3395	9827 - 9726	1.91E-18	11830 - 4726	9.00E-31	>emb CBM40944.1 nuclear hormone receptor 1 [<i>Echinococcus multilocularis</i>]	SmHR96 α
3400	259948 259748	1.29E-24	261948 - 254751	3.00E-29	>ref XP_002572951.1 steroid hormone receptor ad4bp [<i>Schistosoma mansoni</i>] emb CAZ29183.1 steroidogenic factor 1 (stf-1) (sf-1) (adrenal 4 binding protein) (steroid hormone receptor ad4bp) (fushi tarazu factor homolog 1), putative [<i>Schistosoma mansoni</i>]	SmFTZ-F1- α
3425	163477 - 164189	5.95E-29	161477 - 169189	3.00E-16	>ref XP_002569614.1 nuclear hormone receptor nor-1/nor-2 [<i>Schistosoma mansoni</i>]	SmNR4A5
3440	155860 - 156036	6.11E-08	153866 - 161036	3.00E-08	>ref XP_001660403.1 Nuclear hormone receptor (HR78) [<i>Aedes aegypti</i>] gb EAT47063.1 Nuclear hormone receptor (HR78) [<i>Aedes aegypti</i>]	SmRXR2 (LBD)
3442	72501 - 72713	4.51E-20	70504 - 77713	1.00E-79	>emb CAX73127.1 nuclear receptor subfamily 5, group A, member 2 [<i>Schistosoma mansoni</i>]	SmFTZ-F1

a,b: Position of the DBD and the 2 kb down-stream- 5 kb up-stream sequence of the putative DBD on the respective contig. In 2DBD members, both ZnF_C4 motifs are indicated.

c: Highest LBD homologies (% identical/% similar residues) to NHRs of *S. mansoni* (above) or to proteins present in the nr-aa database (<http://www.genome.jp>).

d: No LBD could be identified.

Table adapted from [145]

5.3.2. Expression of other EmNHRs in *Echinococcus* larval stages

The expression profile of all identified *E. multilocularis* NHR was analyzed using the transcriptome dataset provided by the Sanger Institute (Hinxton, GB) for *E. multilocularis* larval stages. The majority of the identified NHR is expressed constitutively in the different larval stages: metacestode vesicles, dormant and activated protoscoleces and primary cells (Table 2; [145]). Interestingly, a clear differential expression pattern was observed for NHRs encoded on contigs 2822 (only expressed in metacestode), 2878 (absent in metacestode vesicles) and 3425 (only expressed in protoscoleces) [145]. No or very weak expression was detected in the larval stages for the NHR encoded on contigs 1680 and 1798. Taken together, at least 17 different NHR are present in the *E. multilocularis* genome and are most likely transcribed throughout the various *E. multilocularis* developmental stages with the exception of the NHR encoded on contigs 1680 and 1798.

Table 2: Expression data of *E. multilocularis* putative NHR derived from direct transcriptome sequencing on rRNA-depleted total RNA^a.

Contig	metacestode vesicle	dormant protoscoleces	activated protoscoleces	primary cells
1644	+ ^b	+	+	+
1680	-	-	-	-
1702	+/-	+/-	+/-	+/-
1779	+	+	+	+
1798	-	+/-	-	-
1872	+	+	+	+
2122	+/-	+	+/-	+
2681	+	+	+	+
2822	+	-	-	-
2878	-	+	+	+
3309	+/-	+	+	+/-
3395	+	+	+	+
3400	-	+/-	+/-	+/-
3425	-	+	+	-
3440	+/-	+	+	+
3442	+	+	+	+

a: <http://www.sanger.ac.uk/resources/downloads/helminths/echinococcusmultilocularis.html>.

b: "+" indicates clear expression, "+/-" weak expression and "-" no detectable expression.

5.4. NHR signaling – EmHNF4

5.4.1. Isolation and characterization of the *Emhnf4* cDNA and the genomic locus

As described before the *in silico* analysis of the *E. multilocularis* genome identified 17 putative NHR (5.3.1), among them a hepatocyte nuclear factor 4-like receptor (EmHNF4). Human HNF4 plays an important role in liver development and is a key player in metabolic pathways [128,184]. Since *E. multilocularis* primarily manifests its growth in the human liver, EmHNF4 was characterized in more detail.

Two different transcripts for this gene were identified by RACE experiments: *Emhnf4a* and *Emhnf4b*. More specifically, the full cDNA sequence of *Emhnf4a* was amplified from a cDNA library [185] and *Emhnf4b* from cDNA of *E. multilocularis* J31 activated protoscoleces (see supplement). The full length cDNA measured 2299 bp and 1711 bp for *Emhnf4a* and *Emhnf4b*, respectively, with the identical 5'UTR of 39 bp, the identical 3'UTR of 181 bp and an alternate putative polyadenylation signal (TATGAA, [186]) 15 bp upstream of the polyA tail. For both isoforms two putative start codons were identified (position 19 and 40 of the cDNA sequence). The second start codon displayed a good quality Kozak sequence (GxxATGG; [187,188]). Thus the putative coding sequence was selected from the second ATG. The resulting open reading frame was 2079 bp for *emhnf4a* and 1491 bp for *Emhnf4b* which encoded for putative proteins of 692 aa and 496 aa with a theoretical molecular mass of 76 kDa and 55 kDa, respectively. Due to limitations in time no further studies have been conducted if other putative isoforms of *Emhnf4* are present. However, there were first hints, that other putative isoforms could be present in metacestode vesicles and primary cells.

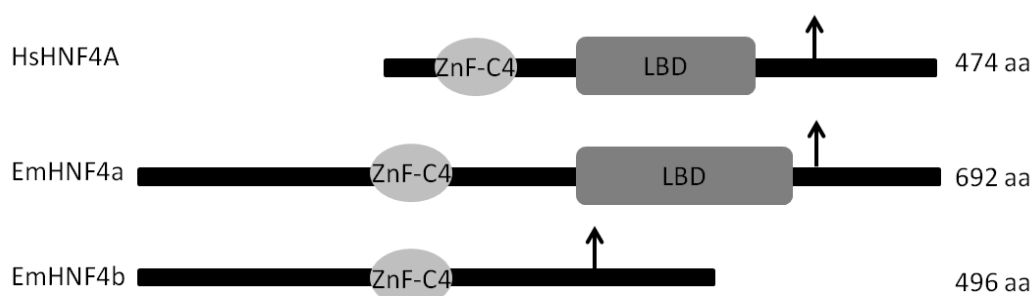


Fig. 32: Domain structure of EmHNF4a, EmHNF4b and the human HNF4A protein. The *in silico* analysis using SMART predicted a DNA binding domain containing a Zn-finger (ZnF_C4) for all analyzed protein sequences. For HsHNF4A (P41235.3) and EmHNF4a also a LBD which is typical for NHR was present. In all three sequences an activation motif 2 AF-2 (black arrow) was identified. Lengths of the proteins are indicated on the right.

Domain analysis using SMART (<http://smart.embl-heidelberg.de/>; [95,96]) displayed the following results for the two isoforms EmHNF4a and EmHNF4b (Fig. 32). Both putative proteins reveal the presence of a typical C4 zinc finger (ZnF_C4) DBD between residues 221 and 292 which is typical for NHRs. However, only EmHNF4a displayed a hormone receptor LBD between residues 355 and 542 whereas EmHNF4b harbors a truncated LBD, below threshold. Therefore, it was not detectable in SMART. This is explained by the fact that the LBD is encoded by exons V – VIII, of which exons VI-VIII are absent in EmHNF4b. Moreover, an AF-2 motif (LLGDILL) was identified between residues 585 and 590 for EmHNF4a and between residues 389 and 394 for EmHNF4b. This AF-2 motif follows the rule

ΦΦΧαΦΦα/L [189]. However, instead of the acidic glutamic acid it contains the acidic aspartic acid at the fourth position within the AF-2 motif, when comparing the *E. multilocularis* HNF4 isoforms with the human HNF4A or sequences from *D. melanogaster* HNF4 or *C. elegans* NHR64.

Several homolog proteins from various species have been identified when the nucleotide sequence was subjected to BLASTX [157,158] search against SWISSPROT. The overall identity of EmHNF4a and EmHNF4b was 23%/16% to the human HNF4A and, 19%/13% to *D. melanogaster* HNF4 and 17%/11% to *C. elegans* NHR64 (Table 3), respectively. When analysing the DBD of both *E. multilocularis* HNF4 isoforms and the other HNF4 proteins the identity was remarkably high. For example, EmHNF4a and EmHNF4b DBD displayed 76.9%/62.8% identity to the DBD of HsHNF4A (Table 3). The identities within the LBD are overall lower between 9.2% (LBD EmHNF4b/LBD CeNHR64) and 28.2% (LBD EmHNF4a/LBD HsHNF4A; Table 3). The multiple alignment of the DBD and the LBD region of the above analyzed proteins is depicted in Fig. 33 and was obtained from MUSCLE for the alignment. In an additional analysis using PSORTII two nuclear localisation signals pat4 (RRKH at position 253) and pat7 (PRSRCRR at position 171) have been identified for both *E. multilocularis* HNF4 isoforms. However, no bipartite motif was identified. Furthermore, there were no hints for RNA-binding motifs, N-myristoylation patterns, or prenylation motifs.

Table 3: Identity matrix of the two putative EmHNF4 isoforms and other HNF4 proteins^a.

Full coding sequence					
	EmHNF4a	EmHNF4b	CeNHR64	HsHNF4A	DmHNF4
EmHNF4a	ID				
EmHNF4b	70.6	ID			
CeNHR64	17.0	10.8	ID		
HsHNF4A	23.3	15.9	31.1	ID	
DmHNF4	19.2	12.9	20.9	37.0	ID
DBD^b					
	EmHNF4a	EmHNF4b	CeNHR64	HsHNF4A	DmHNF4
EmHNF4a	ID				
EmHNF4b	80.7	ID			
CeNHR64	64.1	51.2	ID		
HsHNF4A	76.9	62.8	71.7	ID	
DmHNF4	73.0	60.2	70.5	92.3	ID
LBD^c					
	EmHNF4a	EmHNF4b	CeNHR64	HsHNF4A	DmHNF4
EmHNF4a	ID				
EmHNF4b	30.2	ID			
CeNHR64	21.7	9.3	ID		
HsHNF4A	28.2	14.7	34.8	ID	
DmHNF4	24.6	10.3	32.7	65.6	ID

a: full length sequence of the different HNF4 proteins (*C. elegans* NHR64: CeNHR64, O44960.2; *D. melanogaster* HNF4: DmHNF4, P49866.2 and human HNF4A: HsHNF4A, P41235.3);

b: DNA binding domain of the different HNF4 proteins;

c: Ligand binding domain of the different HNF4 proteins

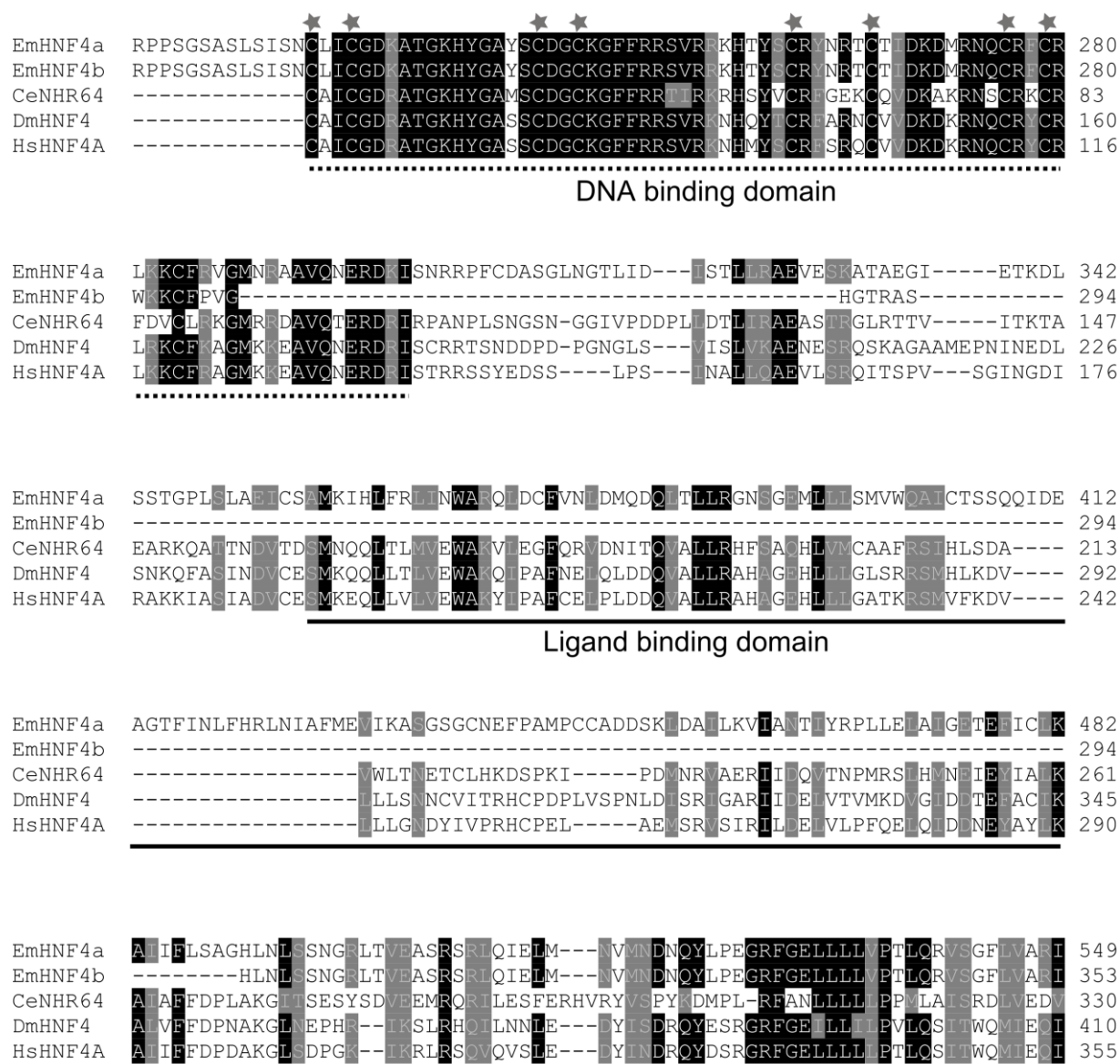
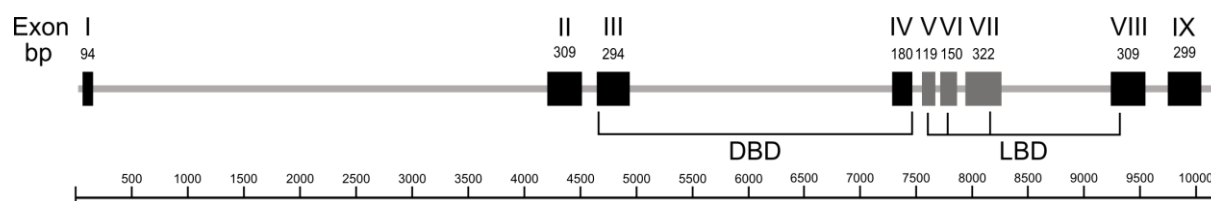


Fig. 33: Amino acid sequence alignment of EmHNF4a/EmHNF4b DBD and other HNF4 proteins. Shown are sequences of EmHNF4a (residues 210 – 549), EmHNF4b (residues 210 – 353), *C. elegans* NHR64 (CeNHR64; O44960.2; residues: 27 - 330), *D. melanogaster* HNF4 (DmHNF4; P49866.2; residues: 104 - 410), and human HNF4A (HsHNF4A, P41235.3; residues: 60 - 355). The threshold for identical amino acid residues, which are highlighted in white on black background, is set to 75 %. Similar residues are shaded in grey. The DNA binding domain and the LBD domain are indicated by a dotted and black line below the alignment, respectively. The conserved C residues of the ZnF-C4 motif are marked by stars.

The genomic *Emhnf4* locus was analyzed by pairwise alignment of the *E. multilocularis* genome (*E_multilocularis_contigs_070110.fa*) and the *Emhnf4a* transcript. The locus spans a region of 10.5 kb. Within the coding region, 8 introns (length between 43 bp and 4049 bp) with canonical gt-ag splice sites were identified and separated 9 exons between 94 bp to 322 bp. Exons VI, VII and VIII are absent in transcript *Emhnf4b*. The gene *emhnf4* is localized on contig 1702 of the *E. multilocularis* genome assembly (*E_multilocularis_contigs_070110.fa*). In an earlier assembly (*M_multilocularis_contigs_230108*) the gene was situated on contigs 3313 and 3314.

A



B

Exon	length (bp)	splice donor	splice acceptor	intron length (bp)	amino acid
				5'UTR (39)	
I	94	ACGgtgagt	aagACT	4049	D32
II	309	AGAgtaagca	cagAGA	140	K135
III	294	CGGgtgggtt	tagGCA	2337	G233
IV	180	CAGgtgag	tagCGG	86	A293
V*	119	GCGgtagatt	tagACA	43	A332
VI*	150	CAGgtattgt	tagCTG	75	Q382
VII*	322	CGGgtaatttt	aagGTC	1064	G490
VIII	309	CAGgtgatt	cagGTC	209	G593
IX	299			3'UTR (181)	

Fig. 34: Chromosomal organisation of the *E. multilocularis* *hnf4* locus. **A)** The chromosomal region as determined in this study is depicted as a grey line. Exons (I–IX) are shown as black boxes with the size of each exon (in bp) given above. The dark grey shaded exons are absent in the *Emhnf4b* transcript. The locations of coding regions for DBD and the LBD are indicated by black lines. The bar below represents the scale bar in bp. **B)** Gene structure of *Emhnf4*. The gene *Emhnf4* is localized on contig 1702 of the genome assembly file *E_multilocularis_contigs_070110.fa*. All exon/intron boundaries display canonical gt-ag motifs. Asterisks indicate that exons V, VI and VII are alternatively spliced in the *Emhnf4b* isoform, whereas *Emhnf4a* contains all IX exons.

Taken together, these analyses showed that EmHNF4a is a typical NHR and related to the NR2A1 family [115]. In mammals HNF4 controls embryogenesis and has a central role in hepatocyte differentiation and function [128,190]. The role and function of the *E. multilocularis* HNF4 proteins has to be analyzed in additional studies especially in regard to the AF-2 motif.

5.4.2. Expression analysis *Emhnf4a* and *Emhnf4b* in *Echinococcus* larval stages

The expression of *Emhnf4a* and *Emhnf4b* in larval stages was analyzed by semi-quantitative RT-PCR [145]. Fig. 35 A demonstrates, that *Emhnf4a* and *Emhnf4b* transcripts are present in all analysed stages: metacystode vesicles, in protoscoleces before (dormant protoscoleces) and after activation through pepsin/low-pH treatment protoscoleces (activated protoscoleces) as well as in in vitro cultivated primary cells. *Emhnf4a* is to some extent higher expressed in metacystode vesicles and *Emhnf4a* is least expressed in dormant protoscoleces. Data from the transcriptome profile of *Emhnf4* support these findings, being expressed in all analyzed stages.

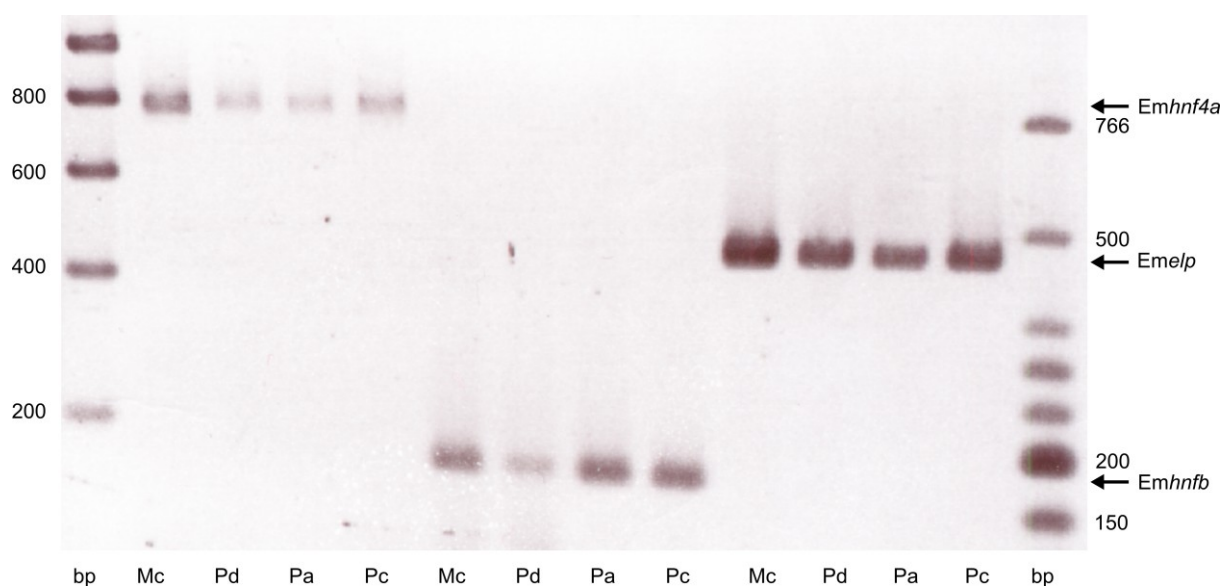


Fig. 35: Expression analysis of *Emhnf4a* and *Emhnf4b*. After isolation of total RNA from in vitro cultivated metacystode vesicles (Mc), dormant (Pd) and activated protoscoleces (Pa) as well as in vitro cultivated primary cells (Pc) the mRNA was reverse transcribed. Subsequently, the cDNA was subjected to semi-quantitative PCR with oligonucleotides specific for *Emhnf4a* and *Emhnf4b*. As control the constitutively expressed gene *Emelp* [44] was used. The resulting PCR amplicons were separated on a 1 % agarose gel and stained with ethidium bromide. DNA size marker bands are indicated to the left and the right.

5.4.3. Protein-protein interaction studies of EmHNF4

NHR receptors are modulated by NHR coactivators or corepressors and also through direct protein-protein interaction [174,175]. In a first experiment I it was tested whether the DBD of either EmHNF4a (EmHNF4a-DBD) or EmHNF4b (EmHNF4b-DBD) interact with EmSkip [61] and EmAlien [62]. For that translational fusions of EmHNF4a-DBD and EmHNF4b-DBD (Fig. 36) in pGADT7 and pGBKT7 were constructed.

```
EmHNF4a-DBD CLICGDKATGKHYGAYSCDGCKGFFRRSVRRKHTYSCRYNRTCTIDKDMRNQCRFCRLKKCFRVGMNRAAVQNERD
EmHNF4b-DBD CLICGDKATGKHYGAYSCDGCKGFFRRSVRRKHTYSCRYNRTCTIDKDMRNQCRFCRWKKCFVVG-----
```

Fig. 36: Amino acid comparison of EmHNF4a-DBD and EmHNF4b-DBD. Identical amino acid residues are highlighted in white on black background. Variant residues are in black on white background. Amino acid residues are given in 1-letter code.

In the experiments, no interactions between EmHNF4a-DBD and EmHNF4b-DBD with EmSkip (Fig. 37) were observed. Whereas EmHNF4a-DBD did not interact with EmAlien, there was an intermediate interaction between EmHNF4b-DBD and EmAlien. Yet other parasite specific co-regulators of NHR could be present and need to be identified.

Moreover, it has been described that members of the Smad family interact with NHR [114,182]. Since the translational fusion of EmSmadC and its constitutively activated form EmSmadC* expressed in the pGBK positively interact with the empty pGADT7 [58] the translational fusions of all EmHNFa/b-DBD-constructs in pGADT7 and pGBKT7 were tested in order to exclude false positive results. EmHNFa-DBD did not interact with any of the EmSmad proteins (Fig. 37). EmSmadA, EmSmadA*, EmSmadB, EmSmadB* [60], EmSmadC [58] and EmSmadC* [58] did not interact with EmHNF4b-DBD (Fig. 37). An intermediate protein-protein interaction was detected between EmHNF4b-DBD and EmSmadD as well as EmSmadE [176] and also constitutively activated EmSmadE (EmSmadE*) [176] (Fig. 37). Again, an *E. multilocularis* NHR might act together with TGF- β /BMP-signaling in the parasite.

		Fusion with Gal4-DNA binding domain		
		pGBKT7	EmHNF4b-DBD	EmHNF4a-DBD
Fusion with Gal4-activation domain	pGADT7	-	-	-
	EmHNF4a-DBD	-	-	-
	EmHNF4b-DBD	-	-	-
	EmNHR1-FL	-	-	-
	EmNHR1-DBD	-	-	-
	EmNHR1-LBD	-	-	-
	EmSkip	-	-	-
	EmAlien	-	+	-
	EmSmadA	-	-	-
	EmSmadB	-	-	-
	EmSmadC	-	-	-
	EmSmadD	-	+	-
	EmSmadE	-	+	-
	EmSmadA*	-	-	-
	EmSmadB*	-	-	-
	EmSmadC*	-	-	-
	EmSmadE*	-	+	-

Fig. 37: EmHNF4a-DBD and EmHNF4b-DBD protein interaction studies with *E. multilocularis* NHR co-regulators and EmSmads. Translation fusions were generated for the Gal4-DNA binding domain (BD; vector pGBKT7) and the Gal4-activation domain (AD; vector pGADT7) with the EmHNF4a-DBD and EmHNF4b-DBD. These were transformed into yeast strain AH109 together with empty vectors (pGADT7, pGBKT7) or with different fusions for EmSkip [61], EmAlien [62], EmSmadA, EmSmadB [60] as well as EmSmadC, EmSmadD [58] and EmSmadE [176]. An asterisk marks the constitutively active forms of EmSmadA, EmSmadB, EmSmadC [58,60] and EmSmadE [176]. Positive control (pGADT7-T x pGBK-53) and negative control (pGADT7-T x pGBK-Lam) were performed as described in the MATCHMAKER-manual (Clontech). Growth of colonies was assessed according to the MATCHMAKER-manual (Clontech). - and + indicate no growth or growth under medium stringency. Several independent experiments (n= 3) were performed.

5.5. Serum-free cultivation of *E. multilocularis*

The standard in vitro cultivation system for *E. multilocularis* uses hepatoma cell lines as feeder cells because these cells secrete host factors which help the parasite to proliferate and to differentiate in vitro [47,161]. To exclude direct effects of the feeder cells an axenic cultivation system devoid of these feeder cells was established [48]. Noteworthy, the vesicles were grown in medium which was preconditioned by RH- and allowed growth for several months. Yet, in this system one cannot study the exclusive effect of hormones or other substances and notably serum is still absolutely necessary to support larval growth. Therefore, I aimed to develop a defined minimal, serum-free medium for the cultivation of *E. multilocularis* in vitro either in the presence or absence of RH- feeder cells.

5.5.1. Adaptation of RH- to serum free conditions

PanserinTM401 is a commercially available serum-free medium and was chosen in these experiments in order to establish a defined minimal, serum-free cultivation system for *E. multilocularis*. First, the growth of RH- in PanserinTM401 was analysed. Direct transfer from normal culture medium containing 10 % FBS to PanserinTM401 was not satisfying because RH- cells did not attach as firmly to the cell culture flask's bottom as cells which were kept under serum conditions (Fig. 38A-E). Also, the formation of cell aggregates ("clumps") was observed (Fig. 38D, E). Therefore, a second approach was chosen: RH- cells were slowly adapted to grow under serum-free conditions with continuously reducing the amount of FBS every passage (Fig. 38F-M). In detail, cells from normal medium (DMEM 10 % FBS) were transferred to PanserinTM401 supplemented with 10 % FBS at 1×10^6 cells in 50 ml volume. After one week cells were transferred to PanserinTM401 containing 5 % FBS (Fig. 38F). Subsequently the concentration of FBS was reduced to 1 % followed by 0.5 %. RH- cells grew comparable to control cells which were kept in DMEM/10 % FBS (Fig. 38G, H). When FBS was omitted (Fig. 38I) RH- still firmly attached on the flask bottom, but grew slower as the control cells (Fig. 38B). However, morphology and adherence to the plastic surface were comparable to the control cells. After successive passages, RH- cells adapted to the serum-free medium (Fig. 38L) and resumed normal growth rate at approximately passage ten (Fig. 38M).

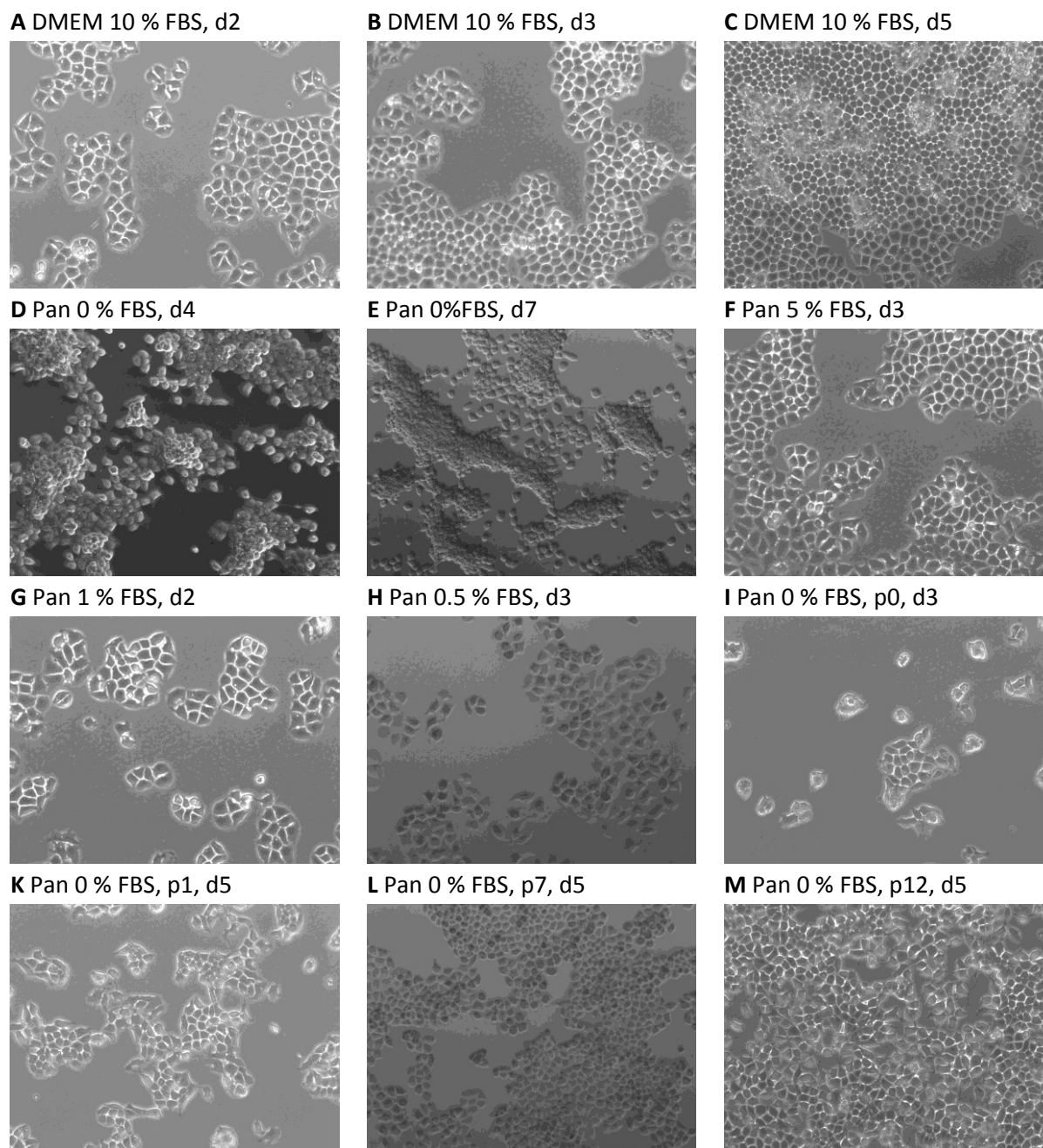


Fig. 38: Adaption of RH- cell line to serum-free Panserin™401. (A-C) RH- cells were cultured in DMEM/10 % FBS as control. (D-E) Direct transfer of 1×10^6 RH- cells from normal medium to 50 ml serum-free Panserin™401 at day four (D) and day seven (E). (F-M) Successive decrease of serum concentration from 5 % FBS (F), 1 % FBS (G), 0.5 % FBS (H) to Panserin™401 without supplemented serum (I). (L, M) Cells were continuously kept in serum-free Panserin™401. (L) RH- cells adapted to Panserin™401 after seven weeks (passage seven) and after 12 weeks (I). d: day, p: passage, Pan: Panserin™401. Magnification 10x.

5.5.2. Co-cultivation of *E. multilocularis* under serum-free conditions and in vivo passage

With RH- adapted to serum-free Panserin™401 I tested whether the usual co-cultivation system for *E. multilocularis* metacestode vesicles [47,161] was to be directly transferred to a new serum-free co-cultivation system with Panserin™401 (passage p1). For that, *E. multilocularis* H95 material was isolated from a jird and subjected to in vitro co-cultivation under serum-free conditions. In detail, Panserin™401 and RH- cells which have previously been adapted to serum-free Panserin™401 have been applied with the same parameters as the regular serum-supplemented cell culture (1 ml parasite material in 50 ml Panserin™401 with 1×10^6 RH- cells). As control the material was grown in DMEM/10 % FBS with RH- cells from standard culture (Fig. 39A). Over time, both culture conditions successfully proved to support the formation of metacestode vesicles (Fig. 39A-K). However, it was obvious that under serum-free conditions the quantity of developing metacestode vesicles was reduced and also the volume of these vesicles was smaller (Fig. 39 B, F) compared to the standard co-cultivation procedure (Fig. 39A, E, I). Nonetheless, material from both cultivation systems has been successfully cultured up three months. After this time period still less metacestode vesicles were obtained from the serum-free co-culture system. In order to overcome this phenomenon metacestode vesicle from serum-free culture were subjected to axenic conditions (see section: Axenic cultivation of metacestode vesicles and cultivation of primary cells under serum-free conditions) and thereafter were injected into the peritoneum of jirds. Subsequently, after two months the animals were sacrificed, *E. multilocularis* material was isolated and subjected to serum-free Panserin™401 RH- co-culture. The developing metacestode vesicles (passage p2; Fig. 39C, G) presumably adapted to Panserin™401 and grew better than the material from the first experiment (Fig. 39B). The volume and the quantity of the metacestode vesicles were higher, still less as the control co-culture supplemented with serum (Fig. 39A, E). Again, the procedure was repeated and a second and third *in vivo* passage was conducted. Metacestode vesicles from the third (passage p3; Fig. 39H) and fourth round (passage p4; Fig. 39K) of co-cultivation in Panserin™401 reached the same volume but never reached the same quantity of vesicles. Nevertheless, a noticeable adaptation to serum-free co-culture was reached by the means of intercalating multiple *in vivo* passages.

Noteworthy is the fact that *E. multilocularis* material was also grown in Panserin™401 without any feeder cells. However, no formation of metacestode vesicles has been observed (data not shown). Moreover, the introduction of insulin (860 nM) to the system did not alter the outcome. This suggests that Panserin™401 does not contain all necessary growth or differentiation factors needed for proliferation and differentiation of *E. multilocularis* metacestodes vesicles and insulin cannot compensate the situation.

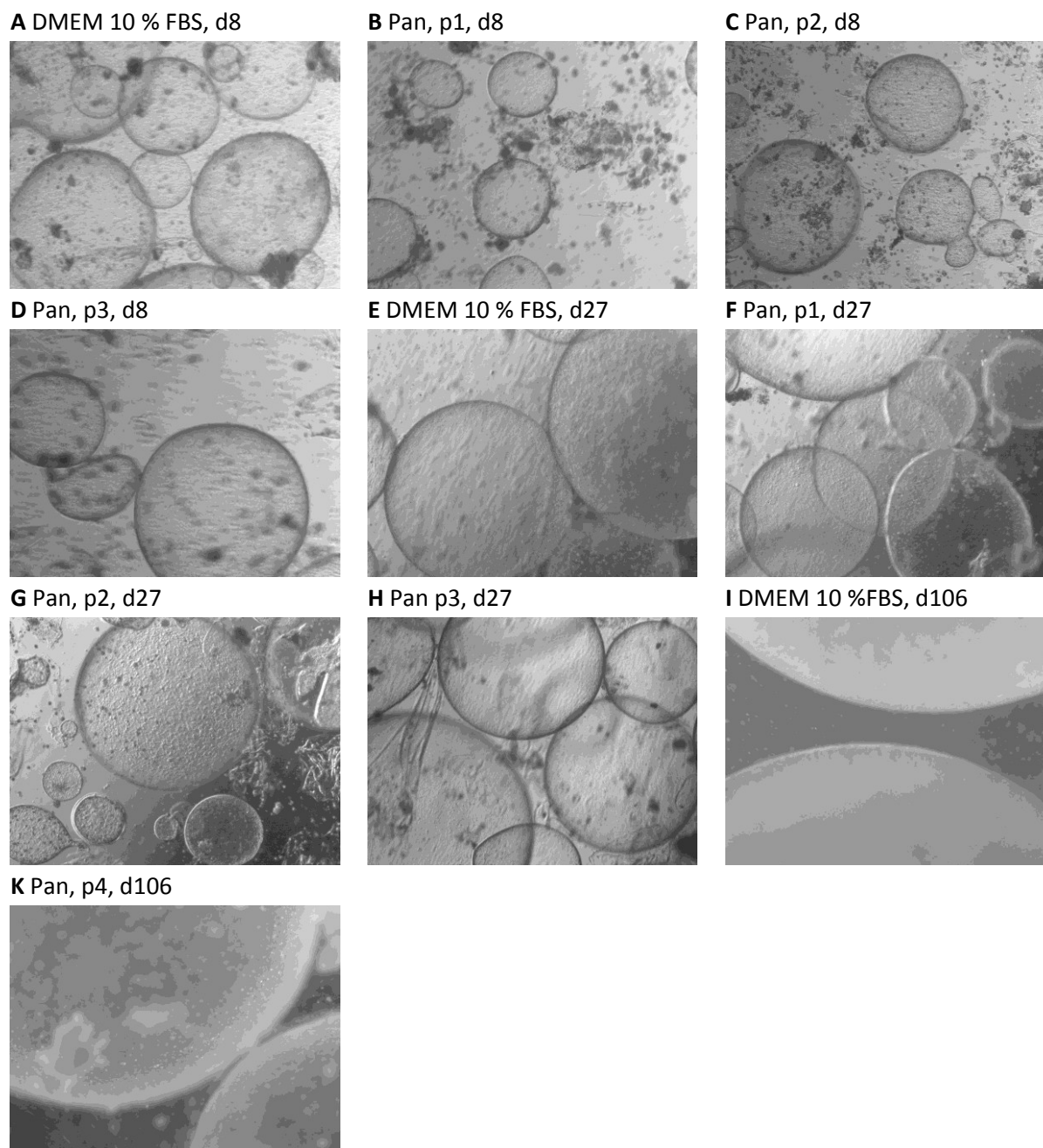


Fig. 39: Co-cultivation of *E. multilocularis* metacystode vesicles with RH- cells under serum-free conditions. *E. multilocularis* material isolated from a jird was either cultured in DMEM/10 % FBS in the presence of feeder cells (**A, E, I**) or in serum-free Panserin™ 401 in the presence of RH- cells (**B, F**). Images were taken after eight days (**A, B**), 27 days (**E, F**) and 106 days (**I**) of cultivation. Following axenic cultivation, the material was subjected to in vivo passage. Thereafter, the *E. multilocularis* material was isolated from a jird and either cultured in DMEM/10 % FBS in the presence of feeder cells (**A, E**) or in serum-free Panserin™ 401 in the presence of RH- cells (**C, G**). This procedure was repeated twice (**D, H, K**). d: day, p: passage of co-cultivation, Pan: Panserin™ 401. Magnification 2.5x

5.5.3. Axenic cultivation of metacestode vesicles and cultivation of primary cells under serum-free conditions

After the serum-free co-culture system had been developed the next step was to establish an axenic serum-free cultivation system for *E. multilocularis*. For that conditioned PanserinTM401 (cPan) was produced by RH- seeded at 1×10^6 cells in 50 ml PanserinTM401 and cultivated for seven days. Axenic cultivation was performed as described for the standard method [49]. The pre-conditioned medium was supplemented with the reducing agents (BAT, β -mercaptoethanol, L-Cys) under nitrogen atmosphere and was replaced with new medium every other day. Two observations which differ from the standard axenic culture have been made in this experimental setup. First, residual RH-seemed to stick on the metacestode surface. Therefore, it took a longer cultivation period to eliminate the feeder cells. The best time point was not determined. Second, the metacestode vesicles appeared less turbid and were less robust compared to the standard axenic metacestode vesicles (data not shown). These two facts made it difficult to obtain enough material for the isolation of primary cells.

Consequently, the first three attempts to regenerate metacestode vesicles from isolated primary cells from axenic, serum-free metacestode vesicles failed (data not shown). The isolated primary cells were either cultured in conditioned PanserinTM401 or hydatid fluid from axenic serum-free metacestode vesicles under reducing conditions in nitrogen atmosphere. Also the cultivation of the primary cells together with RH- feeder cells using PanserinTM401 as medium applying a trans-well system did not result in regenerating metacestode vesicles. In a final experiment the double amount of axenic metacestode vesicles had been used for primary cell isolation compared to the volume of the standard isolation procedure. Subsequent to isolation the primary cells were cultured in conditioned PanserinTM401 in the presence or absence of a cocktail of growth factors: 100 nM insulin, 100 nM aFGF, 10 nM bFGF and 10 μ g/ml heparin. The experiment was performed under reducing conditions in a nitrogen atmosphere. Half the medium was replaced every other day and new growth factors were supplemented. After three weeks of incubation metacestode vesicle-like structures had developed under both conditions. There was no difference in the number of formed metacestode vesicle-like structures (Fig. 40A, C). Compared to the regeneration of metacestode vesicles from primary cells kept under serum-conditions it was obvious that the cells in this experiment also attached to the bottom of the plate and formed mini-aggregates (Fig. 40C, D). This effect was more visible when the growth factors had been present (Fig. 40D).

In summary, this is the first time where metacestode vesicle-like structures have formed under serum-free conditions. However, improvement of the experimental setup is needed to routinely obtain regenerating vesicles under serum-free conditions.

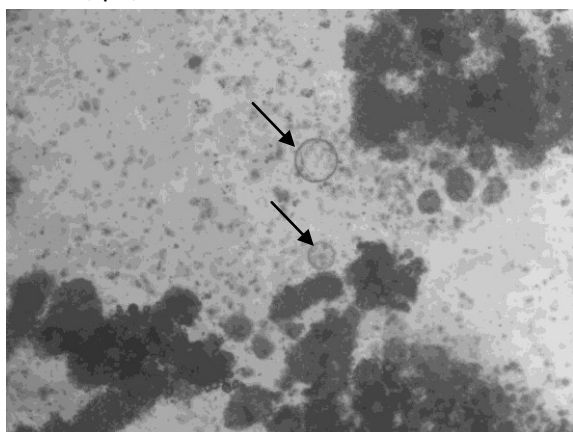
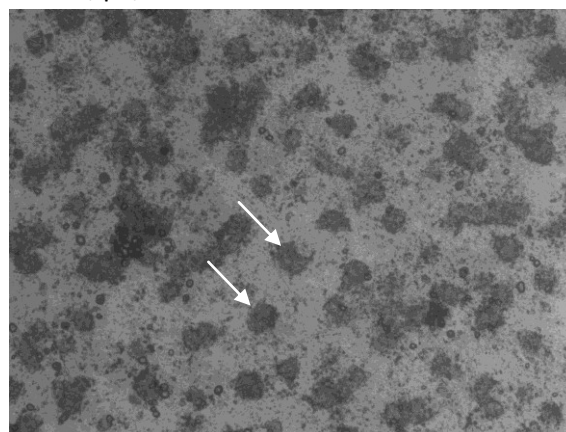
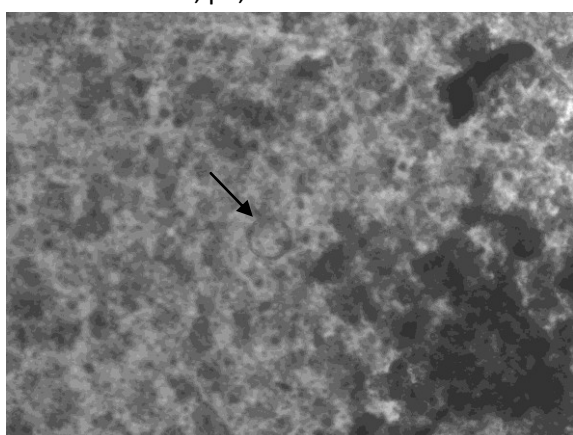
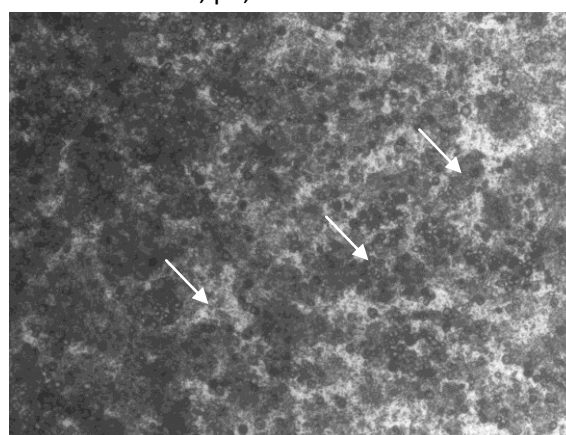
A cPan, p1, d21**B** cPan, p1, d21**C** cPan + stimuli, p1, d21**D** cPan + stimuli, p1, d21

Fig. 40: Cultivation of *E. multilocularis* primary cells under serum-free conditions. Axenic metacystode vesicles from serum-free culture were used for primary cell isolation. Subsequent to isolation the primary cells were cultured in conditioned Panserin™401 in the absence (A, B) or presence (C, D) of the growth factors: 100 nM insulin, 100 nM aFGF, 10 nM bFGF and 10 µg/ml heparin for 21 days. White arrows indicate newly formed metacystode vesicle-like structures. Black arrows indicate mini-aggregate formation attached to the bottom of the plate. Images were taken after three weeks of incubation. cPan: pre-conditioned Panserin™401, d: day, p: serum-free passage. Magnification 5x

5.5.4. Influence of insulin and serotonin on axenic metacystode vesicles cultured in Panserin™401

Although a serum-free co-cultivation and an axenic cultivation system was established it was still not possible to investigate potential direct effects of selected substances on the growth, proliferation and differentiation of *E. multilocularis* larval stages. In the co-cultivation system the feeder cells directly or indirectly influence these processes by the secretion of substances or by cell-cell contact. With the usage of the axenic model the secreted host factors from RH- cells possibly change the development of *E. multilocularis* and might alter the response to selected substances. Therefore, another set of experiments was performed. Briefly, *E. multilocularis* material was isolated from infected jirds and subjected to standard co-cultivation using DMEM/10 % FBS with RH- feeder cells. Once the metacystode vesicles had developed to a diameter of 2-3 mm, the vesicles were transferred to axenic conditions in order to eliminate host feeder cells. Subsequently single axenic

metacestode vesicles were incubated in a nitrogen atmosphere in 15 ml tubes under various conditions. Most importantly PanserinTM401 was chosen for cultivation in comparison to pre-conditioned PanserinTM401. With this setting I was able to investigate whether host factors from RH-cells possibly change the response to selected substances for the first time without the influence of serum.

Initially, the effect of insulin on metacestode growth was analysed. It was described that insulin (86 nM) promotes the growth of H95 metacestode vesicles cultured in DMEM/10 % FBS [161,191]. However, when grown in cDMEM-1 medium this positive effect was not observed. The volume of the metacestode vesicles was less (0.8 ml) than the control metacestode vesicles (1.05 ml) which were kept in cDMEM-1 medium [161]. These results have been reproduced in this study (Fig. 41A, B). Here, GH09 metacestode vesicles cultured in DMEM/10 % FBS reached a diameter of 4 mm whereas vesicles stimulated with insulin (100 nM) had an average diameter of 5 mm after an incubation period of five weeks. When the metacestode vesicles were subjected to cDMEM-1 medium in the presence or absence of insulin, the positive effect was absent. Under both conditions the vesicles had a diameter of 7 mm after five weeks of incubation (Fig. 41A, B). A similar observation was made using PanserinTM401 and pre-conditioned PanserinTM401 for cultivation (Fig. 41C-E). On the one hand a dose dependent insulin effect on metacestode vesicles cultured in PanserinTM401 was detected. The presence of 100 nM insulin (isolate H95) caused only a slight increase in diameter after five weeks of incubation (Fig. 41C). However, the presence of 860 nM insulin (isolate GH09) lead to a clear increase of vesicle diameter from 6 mm to 8 mm compared to the respective control (Fig. 41D). On the other hand, the study revealed that insulin exhibits the opposite effect when the metacestode vesicles were grown in pre-conditioned PanserinTM401 (Fig. 41E). As mentioned above the same holds true when pre-conditioned cDMEM-1 medium was applied (Fig. 41B, F). Interestingly, both PanserinTM401 and pre-conditioned PanserinTM401 lead to a comparable growth; after five weeks of incubations the vesicles had a diameter of about 6 mm. In contrast, vesicles cultured in DMEM/10 % FBS did not reach the same diameter compared to cDMEM-1; after five weeks of incubations the vesicles had a diameter of about 4 mm and 7 mm, respectively.

Moreover the survival rate of the analysed metacestode vesicles after five weeks of incubation reached between 90–100 % when cultured either in pre-conditioned cDMEM-1 (100 %, 100 %) or PanserinTM401 (100 %, 90 %) media in the presence or absence of insulin, respectively. In contrast, survival rates of metacestode vesicles were reduced (50–80 %) under the regimen of DMEM/10 %FBS (50 %; 80 %) or PanserinTM401 (80 %, 70 %) in the presence or absence of insulin, respectively. These data are in concordance with previous observations [161].

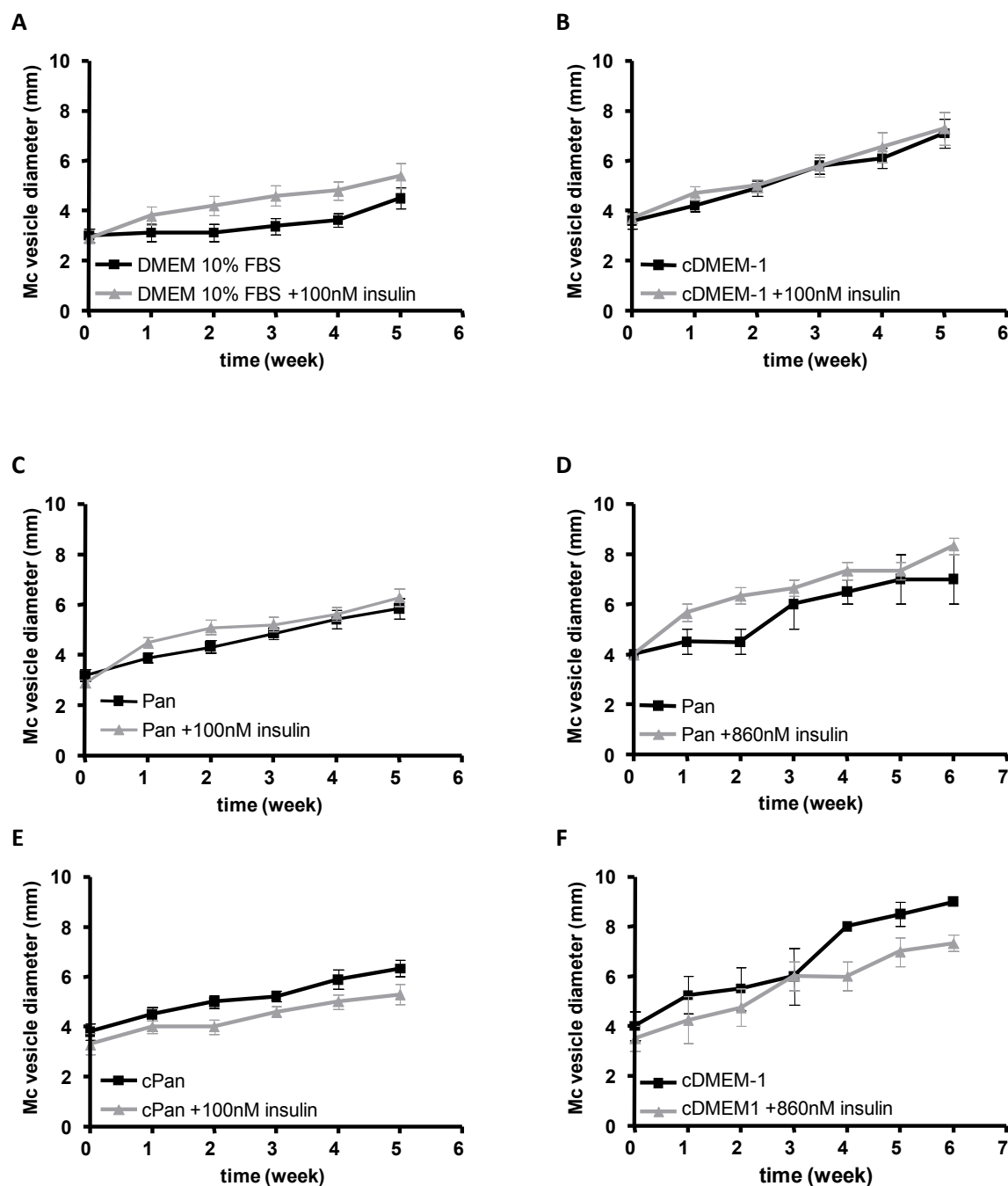


Fig. 41: Influence of insulin on axenic metacystode vesicles cultured in different media. Single axenic metacystode vesicles of the isolate GH09 (A – D) or H95 (E, F) were in vitro cultivated in different media for six weeks in the presence of 100 nM (A–C, E) or 860 nM (D, F) insulin. The complete medium (1 ml) was changed every other day as well as the growth factors were supplemented. Control vesicles were kept the respective medium without insulin. Increase of vesicles diameter was monitored over time. In this experiments (n=1) 10 vesicles were examined for every particular condition. The mean was calculated and the standard error of the mean is indicated.

Furthermore the process of brood capsule formation as an important differentiation step towards the protoscolex larval stage was examined in this study (Fig. 42). There was a striking difference in the percentage of brood capsule formation when comparing none pre-conditioned media (DMEM/10 % FBS or Panserin™401) to pre-conditioned media (cDMEM-1 or cPan). After five weeks of incubation 25 % percent of the vesicles which were kept in DMEM/10 %FBS developed brood capsules compared to 90 % of the vesicles cultured in cDMEM-1. The difference between Panserin™401 and cPan was even more pronounced: 14.4 % to 90 % (Fig. 42). The presence of insulin did not change the outcome. After five weeks of incubation 90 or 100 % of all metacestode vesicles developed brood capsules when cultured in cDMEM-1 or cPan, respectively. However, only 40 % or none of the metacestode vesicles had developed brood capsules after cultivation in DMEM/ 10 %FBS or Panserin™401, respectively. Interestingly, it seems that the process of building up brood capsule is faster in cDMEM-1 conditions compared to cPan irrespective of insulin (Fig. 42 B). Whereas 90 % of the metacestode vesicles cultured in cDMEM-1 developed brood capsules only 10 % of the vesicles cultured in cPan built up brood capsules after two weeks.

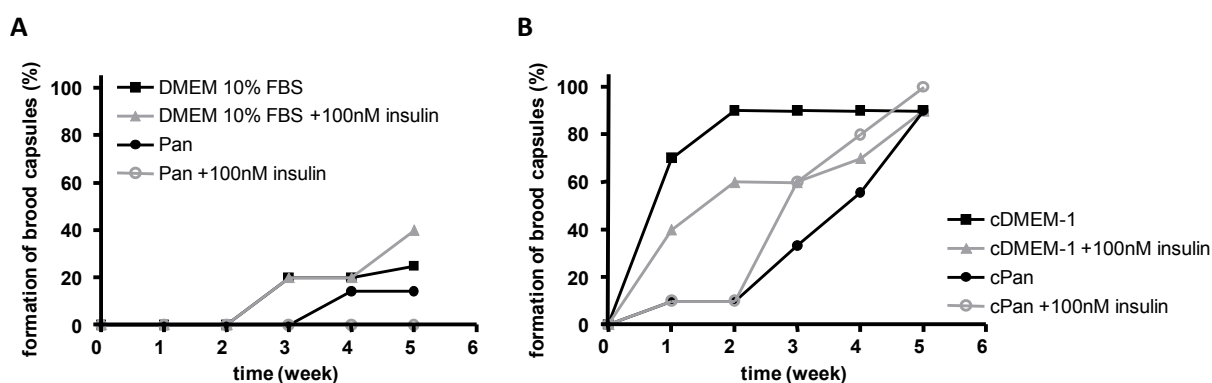


Fig. 42: The influence of insulin on the formation of brood capsules in different culture media. Single axenic metacestode vesicles of the isolate GH09 were in vitro cultivated in the presence of 100 nM insulin using different media for six weeks. In (A) none pre-cultured media: DMEM/ 10 % FBS and Panserin™401 (Pan) were examined whereas in (B) pre-conditioned media cDMEM-1 and Panserin™401 (cPan) were analyzed. The complete medium (1 ml) was changed every other day as well as the growth factors were supplemented. Control vesicles were kept the respective medium without insulin. The formation of brood capsules was monitored over time. In this experiments (n=1) ten vesicles were examined for every particular condition and the percentage of vesicles showing brood capsules is plotted.

The influence of serotonin on the growth of metacestode vesicles was also analysed (Fig. 43). Serotonin might play a role in liver regeneration and liver cirrhosis [192-194]. In this experiment serotonin negatively influenced the growth of metacestode vesicles under all conditions tested. Metacestode vesicles were cultured either in cDMEM-1 or Panserin™401 in the presence or absence of 50 ng/ml serotonin. After six week of incubation control vesicles reached a diameter of 7 mm in Panserin™401 or 9 mm in cDMEM-1 compared to 7 mm and 4 mm under serotonin treatment, respectively.

Unfortunately, the experiment could not be performed with DMEM/10 % FBS or conditioned Panserin™401 due to limited sources of metacestode vesicles.

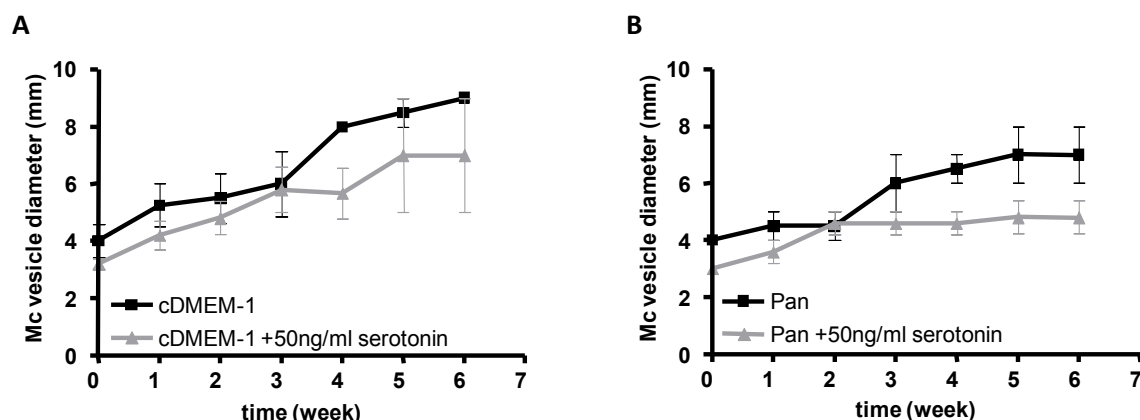
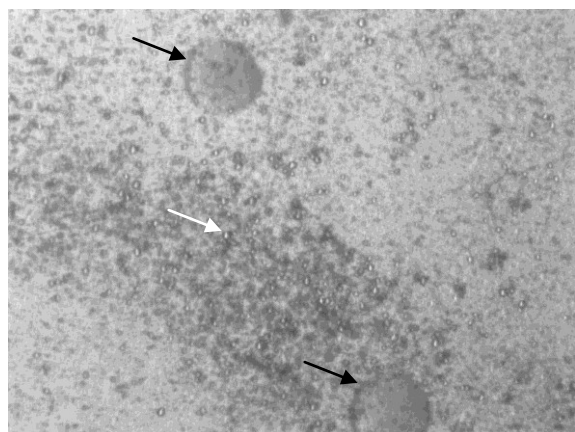


Fig. 43: Influence of serotonin on axenic metacestode vesicle growth cultured in different media. Single axenic metacestode vesicles of the isolate H95 were in vitro cultivated in cDMEM-1 (A) or PanserinTM401 (B) for six weeks in the presence of 50 ng/ml serotonin. The complete medium (1 ml) was changed every other day as well as the growth factors were supplemented. Control vesicles were kept the respective medium without serotonin. Increase of vesicles diameter was monitored over time. In this experiments (n=1) Ten vesicles were examined for every particular condition. The mean was calculated and the standard error of the mean is indicated.

5.5.5. Cultivation of primary cells in serum-free PanserinTM401

A Pan



B Pan + 100 nM insulin

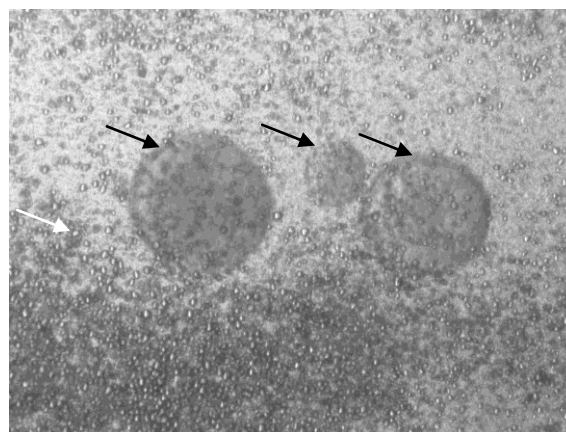


Fig. 44: Serum-free cultivation of primary cells derived from metacestode vesicles cultured in cDMEM-1. The regeneration process of axenically cultivated H95 primary cells was monitored for 21 days. Primary cells were isolated from metacestode vesicles kept in cDMEM-1. After isolation cells were cultured in PanserinTM401 (A) (Pan) or with the addition of 100 nM insulin (B). Half of the medium volume was renewed every other day and growth factors were supplemented at concentrations calculated to the entire cultured volume. Developing metacestode-like structures are indicated by black arrows. White arrow point at calcium bodies.

As mentioned in the last section, there is a need to analyze the effects of substances on the growth and differentiation of *E. multilocularis* larval stages without the influence of either host cells or serum, as both conditions might influence the outcome of the development and differentiation.

Therefore, I tested if PanserinTM401 alone supports growth of freshly isolated primary cells derived from standard axenic culture in serum and host factor-containing cDMEM-1. In detail, freshly isolated primary cells of the isolate H95 were incubated for three weeks in PanserinTM401 in the absence or presence of 100 nM insulin (Fig. 44) under reducing atmosphere. Compared to the standard protocol

for the cultivation of axenic primary cells using cDMEM-1, it was obvious, that the morphology of the vesicle-like structures that developed after three weeks was very different. No clear laminar layer was formed and it seemed that these structures were rather “dense aggregates” of primary cells, than a vesicle composed of an outer laminated and an inner germinal layer with hydatid fluid within (Fig. 44). There was no difference in outcome between none stimulated samples (Fig. 44A) compared to insulin stimulated samples (Fig. 44B). In this experiment the influence of aFGF, bFGF and serotonin was also examined. No clear result was obtained for these substances. There was the impression that aFGF and bFGF promoted the development of vesicle-like structures (data not shown). Serotonin seemed to have no influence on the regeneration when compared to the control. However, the numbers of regenerating vesicle-like structure was not quantified in this experiment. Yet it remains unclear if these aggregates were true metacystode vesicles. Because of the atypical morphology this experimental setup was not followed up. Noteworthy, due to time constraints the experiments in which pre-conditioned PanserinTM401 was used for cultivation of primary cells derived from axenic cDMEM-1 metacystode vesicles have not been conducted.

5.5.6. Mass spectrometry and Western blot analyses of pre-conditioned Panserin™401

In a previous study it was reported that RH- cells secrete insulin during in vitro cultivation into the medium [195]. The insulin transcript was detected by RT-PCR of isolated mRNA from RH-. With the development of the serum-free axenic cultivation system for *E. multilocularis* the question whether RH- secrete certain substances into the medium was re-addressed. In this study I decided to detect potentially secreted substances on protein level by means of SDS-PAGE/Western blot analyses. According to the manufacturer Panserin™401 does not contain any insulin. I analysed Panserin™401 medium in comparison to pre-conditioned Panserin™401. First, equal amount of the two different media were subjected to SDS-PAGE and proteins were visualized by silver staining (Fig. 45). Interestingly a protein band of approximately 55 kDa was present in pre-conditioned Panserin™401 but was absent in the Panserin™401 medium. This protein band was most clearly observed in the sample of pre-conditioned Panserin™401 which was diluted in water (1:10) before. Moreover, a protein band of approximately 12 kDa was detected in pre-conditioned Panserin™401 only. As control also DMEM/10 % FBS and cDMEM-1 were analyzed. There was no obvious difference in the protein pattern between these two media (Fig. 45). Very prominent in all samples appeared a protein band of approximately 60–65 kDa, which supposedly was albumin.

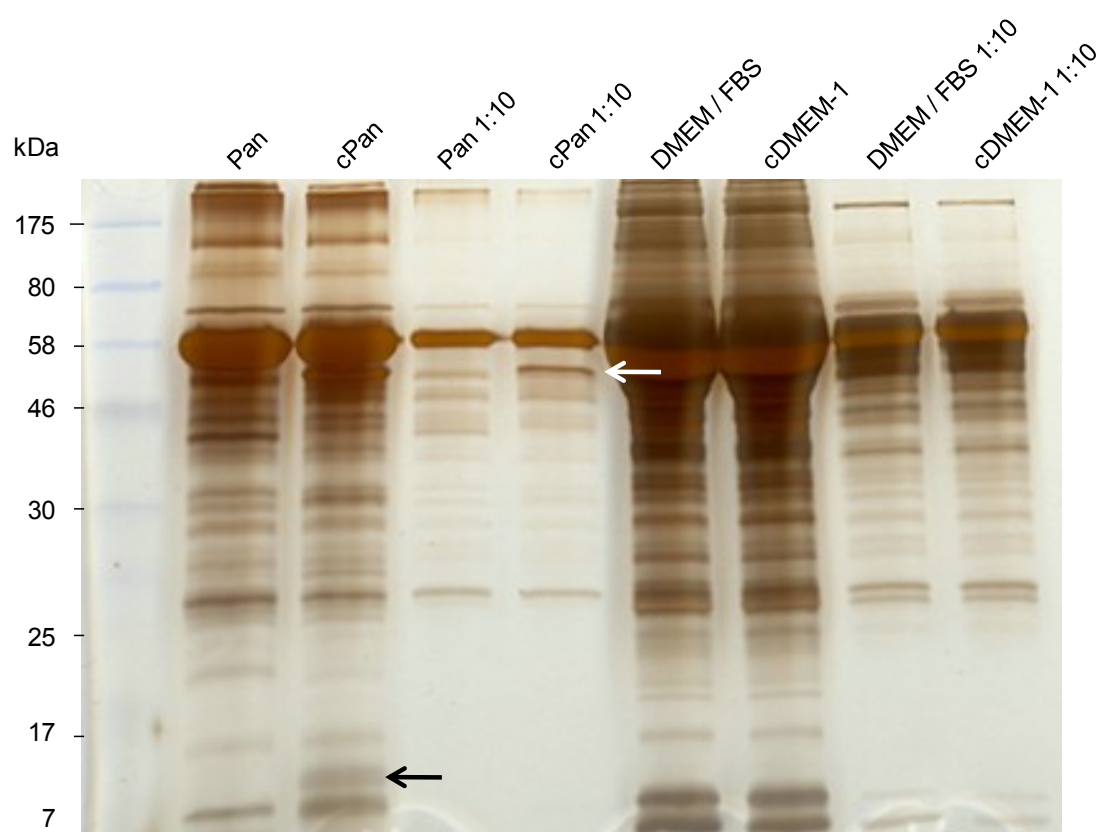


Fig. 45: Silver-stained PAA-gel of different media used for the culture of *E. multilocularis*. Equal amounts of none diluted or a 1:10 dilution of Panserin™401 (Pan), pre-conditioned Panserin™401 (cPan), DMEM/10 % FBS (DMEM/FBS) or pre-conditioned DMEM/10% FBS (cDMEM-1) were applied onto a 12 % PAA-gel. The samples were separated by SDS-PAGE followed by silver staining. The white and black arrow mark protein bands of approximately 55 kDa and 12 kDa which are present in cPan, respectively.

In order to identify the two protein bands a mass spectrometry analyses was conducted in cooperation with J. Clos (Bernard-Nocht-Institute). However, the protein of 12 kDa could not be excised from the PAA-gel. Thus it could not be analyzed by mass spectrometry. The analyses of the 55 kDa protein band resulted in one significant hit when the identified peptides were subjected to the Mascot platform. The protein of interest was identified as *Bos taurus* albumin which is according to the manufacturer present in Panserin™401 medium.

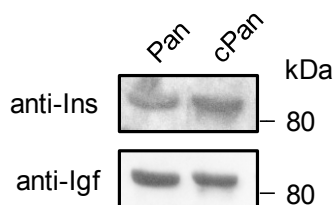


Fig. 46: Western blot analyses of Panserin™401 medium and RH- conditioned Panserin™401. Equal amounts a 1:10 dilution of Panserin™401 (Pan) and pre-conditioned Panserin™401 (cPan) were applied onto a 12 % PAA-gel. The samples were separated by SDS-PAGE followed by western blot analyses using the anti-insulin and the anti-Igf antibodies after separation.

Moreover, a western blot analyses was conducted. For that equal volumes of Panserin™401 and pre-conditioned Panserin™401 were separated by SDS-PAGE and blotted onto a nitrocellulose membrane. I was interested whether insulin or insulin-like growth factor (Igf) were detectable in these two different media. Insulin promotes growth of *E. multilocularis*. Also insulin-like growth factor (Igf) was chosen for analyses. Igf is closely related, but did not promote growth and survival of *E. multilocularis* metacystode vesicles under axenic conditions in vitro [161].

All proteins of interest, insulin and Igf were detected by specific antibodies in this analysis in pre-conditioned Panserin™401, but unexpectedly also in Panserin™401. However, these proteins were not detected at the expected molecular weight of insulin 12 kDa and Igf 6 kDa. Instead both proteins were detected as proteins of approximately 82 kDa molecular weight. This hints that the proteins are in complex with albumin. Interestingly, insulin was detected at a higher level in pre-conditioned Panserin™401, suggesting that in vitro cultivated RH- indeed secrete insulin into the medium.

5.6. EmMPK3 – a serum-responsive MAPK

5.6.1. Phosphorylation of EmMPK3 is not induced by serum in metacystode vesicles, dormant and activated protoscoleces

EmMPK3 has been recently described as a third MAPK of *E. multilocularis* [196]. EmMPK3 is a homologue to the Erk7/Erk8 protein family. It was reported that EmMPK3 is serum-responsive [170]. This observation was made when freshly isolated primary cells of *E. multilocularis* were cultured in the absence of serum for one day and thereafter stimulated with 10 % serum for 3 h (Fig. 47A; taken from [170]). In Western blot analyses a band of approximately 70 kDa was unexpectedly detected with a phospho-specific antibody for Erk MAPK. This antibody recognizes the pT-E-pY motif [197], which is not only present in EmMPK1, but also in EmMPK3. With this information at hand, I performed three other sets of experiments, testing whether EmMPK3 is also serum responsive in metacystode vesicles, dormant and activated protoscoleces.

In detail, axenic metacystode vesicles of H95 were kept in DMEM without serum for four days before being treated with 10 % FBS for three hours. Protoscoleces of J31 were isolated and either non-activated or pepsin/low-pH activated according to the standard procedure in the presence or absence of 10 % serum. Western blot analyses of these samples were performed after separating equal amounts of total protein on acrylamid gel using the anti-Erk1/2 and the anti-phospho- Erk antibodies (Fig. 47B). In this experimental setting no signal representing a protein of approximately 70 kDa was detectable upon stimulation with serum using the phospho-specific antibody for Erk MAPK. This suggests that EmMPK3 is not serum-responsive in these analyzed larval stages in contrast to the finding that EmMPK3 was serum-responsive in *E. multilocularis* primary cells [170]. About the activation of EmMPK1 it is known that EmMPK1 is phosphorylated in standard in vitro cultured metacystode vesicles as well as in dormant and pepsin/low-pH activated protoscoleces [161]. Standard in vitro culture medium contains serum. In this study a clear activation of EmMPK1 after serum stimulation was detectable with the phospho-specific antibody Erk (Fig. 47B). The activation of EmMPK1 under serum stimulation in activated protoscoleces was not as pronounced as in metacystode vesicles or dormant protoscoleces (Fig. 47B). This might be explained by the fact that the overall protein amount of EmMPK1 is less in activated protoscoles compared to metacystode vesicles or dormant protoscoleces [161]. Nonetheless a faint protein band using the phospho-specific antibody was detectable in the samples of activated protoscoleces (Fig. 47B). Most importantly, with this study I demonstrated that EmMPK1 is activated by serum stimulation in metacystode vesicles, dormant and activated protoscoleces whereas this observation has not been made in primary cells ([170];Fig. 47A).

Taken together, EmMPK3 is serum-responsive in primary cells, but not in metacystode vesicles or dormant and activated protoscoleces. However, EmMPK1 activation seems to have to the inverse pattern compared to EmMPK3 activation.

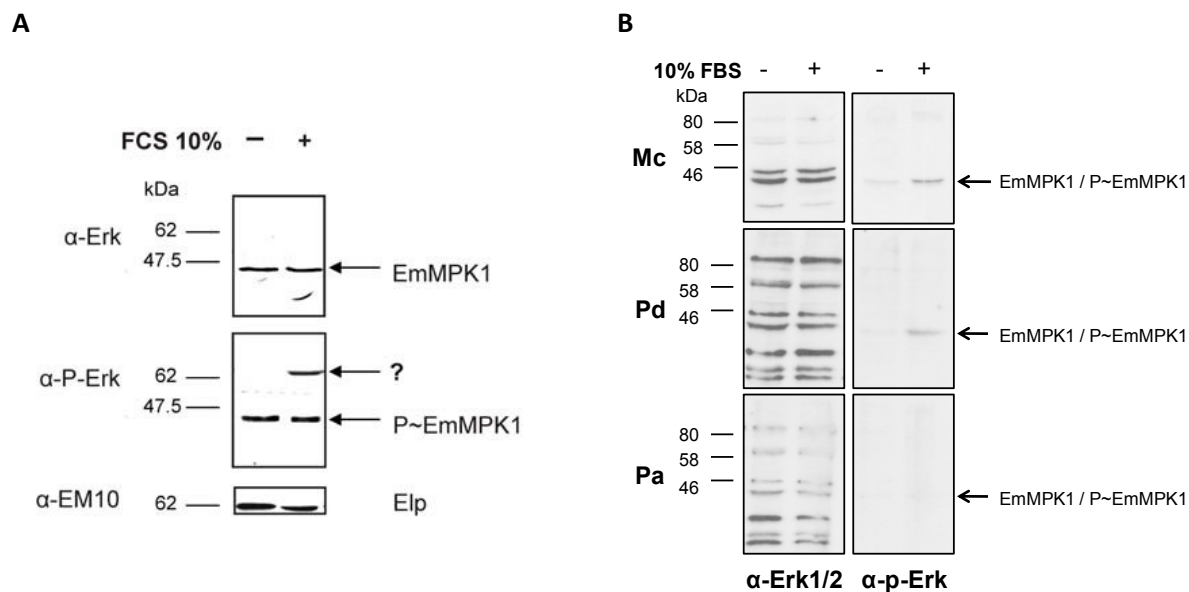


Fig. 47: Stimulation of *Echinococcus* primary cells, metacystode vesicles, dormant and activated protoscoleces with serum. (A) Freshly isolated primary cells were incubated in medium without serum for 24 h and afterwards stimulated with 10 % FBS for 3 h. A Western blot analysis of these cells was realized after sample separation on acrylamid gel using the anti-Erk1/2, anti-phospho-Erk and the anti-Em10 antibodies as indicated to the left. Figure and figure legends are taken from [170]. (B) Metacystode vesicles (Mc) of H95 were kept in DMEM without serum for four days before being treated with 10 % FBS. Protoscoleces of J31 were isolated and either non-activated (Pd) or pepsin/low-pH activated (Pa) following the standard procedure in the presence or absence of serum. A Western blot analysis of these samples was performed after separating equal amounts of total protein on acrylamid gel using the anti-Erk1/2 and the anti-phospho-Erk antibodies as indicated on the bottom.

5.6.2. Expression analysis of *Emmpk3*

The expression of *Emmpk3* in larval stages with and without serum stimulation was analyzed by semi-quantitative RT-PCR [145] (Fig. 48A). *Emmpk3* is higher expressed in the activated protoscoleces and least expressed in dormant protoscoleces and metacystode vesicles under both conditions. When comparing serum-treated and non-treated samples, the expression of *Emmpk3* is clearly enhanced in primary cells in the presence of serum. Metacystode vesicles and activated protoscoleces do not show differences in expression level compared to the non-stimulated samples. But it seems that the expression is slightly down-regulated when dormant protoscoleces are serum-treated. Data from the transcriptome profile of *Emmpk3* showed that the relative expression level of *Emmpk3* was the highest in activated protoscoleces which was set to 100 % (Fig. 48B) followed by primary cells with 90 % expression. Least expression was detected in in vitro cultivated metacystode vesicles (4.7 %). The dataset was generated from material kept under serum conditions. Thus, one must compare transcriptome analysis with the expression of *Emmpk3* under serum stimulation. Yet, the material was not treated exactly alike, as the samples of the semi-quantitative RT-PCR analysis have been starved before serum stimulation and samples from the transcriptome analysis have not. Nevertheless, expression of *Emmpk3* in serum-treated samples was the highest in activated protoscoleces and primary cells. This is in accordance with the transcriptome dataset.

In summary, *Emmpk3* is highest expressed in activated protoscoleces, but expression of *Emmpk3* is up-regulated in primary cells upon serum-stimulation.

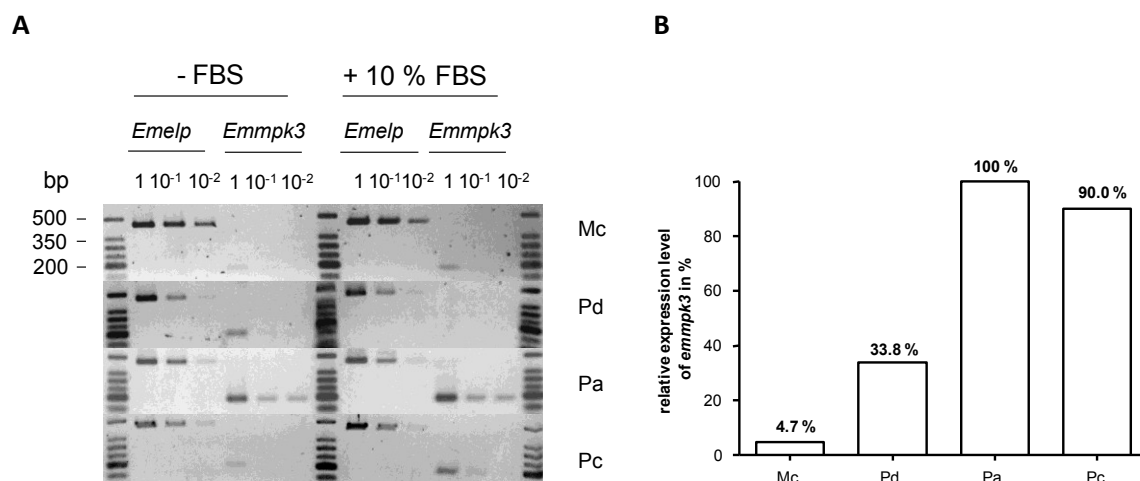


Fig. 48: Expression analysis of *Emmpk3* in the presence and absence of 10 % serum in *Echinococcus*. (A) Axenic metacystode vesicles were cultured in DMEM without FBS for four days and then stimulated with 10 % FBS for 3 h. Protoscoleces were isolated with the standard method in the presence and absence of 10 % FBS in the medium. Dormant protoscoleces were activated (by low pH/pepsin treatment) either in the presence or absence of 10 % serum. Freshly isolated primary cells were subjected to DMEM without FBS for 24 h and thereafter stimulated with 10 % FBS for 3 h. Subsequently, RNA was isolated and reverse transcribed. Serial dilutions of cDNA were subjected to PCR with oligonucleotides specific for *Emmpk3*. As control the constitutively expressed gene *Emelp* [44] was used. The resulting PCR amplicons were separated on a 1 % agarose gel and stained with ethidium bromide. DNA size marker bands are indicated to the left. (B) Expression of *Emmpk3* from transcriptome profiling analysis. Normalized relative gene expression is given, with the highest expression set to 100 %. Mc: metacystode vesicles, Pd: dormant protoscoleces, Pa: activated protoscoleces, Pc: primary cells.

6. Discussion

Parasitic helminths share a large degree of common genetic heritage with their various vertebrate or non-vertebrate hosts. This includes basic cellular functions, proteins and also conserved cell-cell-communication mechanisms which involve small peptide cytokines and lipophilic/steroid hormones. In vitro studies have proven that serum as a supplement is crucial for the development of *E. multilocularis* larvae, most probably because it contains signals that are essential for the development and the survival of the parasite [20,46,47]. In the present work the role of FGF signaling via the transmembrane receptor EmFR and the function of lipophilic/steroid hormones signaling via EmNHRs for the development of *E. multilocularis* were the major points of interest. Understanding these conserved signaling mechanisms is important to develop new strategies in order to combat helminth diseases. Such studies might also be facilitated if a serum-free in vitro cultivation system for *E. multilocularis* was available to exclude effects from substances present in the serum. Therefore, I also investigated the feasibility of a defined minimal medium for *E. multilocularis*.

6.1. FGFR signaling - EmFR

In metazoans, signaling via transmembrane receptor kinases is an evolutionary conserved mechanism. For *E. multilocularis* interactions between parasite receptor kinases and corresponding host cytokines have been identified for various pathways. For example, molecular mechanisms involved include the EGF, the insulin, and the TGF- β /BMP pathways [20,55,56,170,176,195]. In the present work, I studied the FGF-FGFR pathway of *E. multilocularis* and whether this pathway is important for the development of the parasite. FGFs and their specific receptors build up a complex family of signaling molecules and contribute to angiogenesis, cellular differentiation and tissue-injury repair [65]. Previous work on *E. multilocularis* larvae indicated that the FGF signaling pathway might be involved in proliferative processes since host FGF stimulated metacystode growth when exogenously added to in vitro cultivated vesicles. Furthermore, an *E. multilocularis* FGFR ortholog, EmFR, was characterized at the molecular genetic level and was shown to encode a tyrosine kinase with a single extracellular Ig-like domain, instead of two or three Ig domains as it is usually the case for vertebrate and invertebrate FGFRs. This particular domain is critical for sensing and binding the specific FGF ligands [63,64].

Due to the availability of the first draft of the *E. multilocularis* genome sequencing project [198,199], the situation of FGF signaling in this parasite could, in this work, be approached from a genomic perspective. These analyses first confirmed the unusual structure of the *E. multilocularis* FGFR since upstream of the so far characterized, single Ig-domain (determined according to cDNA 5' RACE data, [94]), no further Ig-domain encoding sequences were found. Furthermore, apart from EmFR no other FGFR-like tyrosine kinase is encoded by the *E. multilocularis* genome. Hence, despite its biochemically unusual structure in the extracellular domain, EmFR was indeed the likeliest candidate to mediate effects of host FGF on the parasite and thus chosen for further analyses.

Next, I was interested whether EmFR, despite the unusual extracellular structure, is principally able to sense host FGFs. To this end, EmFR was first functionally expressed in HEK293T cells. However, in this system the receptor was constitutively active, indicated by phosphorylation of the double tyrosine motif corresponding to the human FGFR1 pYpY653/654 residues, even in the absence of exogenously added FGF. HEK293 cells might express and secrete intrinsic FGFs [200] which could

activate the cestode receptor causing the phosphorylation. Thus, additional functional analyses were carried out using the model system of *Xenopus* oocytes in which EmFR and the dead-box kinase, EmFR TkD-, were expressed. In this system GVBD is used as read out and it only occurs if active signaling via the MAPK cascade takes place mediated by heterologously expressed kinase receptors [201]. In these experiments, both exogenously added human aFGF and bFGF induced GVBD in a dose-dependent manner when wild-type EmFR was heterologously expressed, but no GVBD was observed upon expression of a kinase-dead EmFR mutant. Furthermore, EmFR, but not the dead-box kinase mutant, was phosphorylated at a conserved motif in the presence of human FGFs. These results clearly indicated that EmFR, despite its unusual extracellular domain, is capable of sensing human FGFs and that it undergoes autophosphorylation in a manner typical for FGFRs. Furthermore, these results also indicated that at least in this heterologous system, activated EmFR is able to transmit signals to the Erk-like MAPK cascade module since GVBD in *Xenopus* oocytes strongly depends on the activation of this module [156,169].

Having had established that EmFR is a functional kinase capable of sensing human aFGF and bFGF, the study was extended to in vitro analyses using different *E. multilocularis* larval stages. I wanted to examine the effect of human FGFs on *E. multilocularis* parasites in vitro mainly focusing on growth and differentiation processes. First, *E. multilocularis* metacystode vesicles and primary cells were cultured in the presence of BrdU and stimulated with either aFGF or bFGF. By measuring BrdU incorporation into the DNA it was demonstrated that the host cytokines, aFGF and bFGF, promoted proliferation. A higher de novo DNA synthesis rate was detected for metacystode vesicles as well as for regenerating primary cells upon FGF stimulation. These findings support earlier observations that stimulation with either aFGF or bFGF result in increased metacystode vesicle volume over time [94]. Another line of evidence supporting the proliferative effect of FGFs comes from experiments in which regenerating primary cells were cultured with FGFs. Compared to control samples significantly higher numbers of metacystode vesicles developing from primary cells have been detected in the presence of aFGF and bFGF. This finding was even more pronounced when heparin was introduced to the system. It is known that heparin or heparan sulfate proteoglycans interact with FGFs and are needed to activate FGFRs effectively [69,202]. Taken together, these data clearly indicated that host-derived FGFs are able to promote parasite proliferation and development in vitro.

The only cell type of free-living and parasitic flatworms that is able to undergo mitosis are neoblasts (totipotent stem cells that are also called germinal cells or germinative cells; [150]) and previous investigations already showed that *Echinococcus* primary cell cultures are strongly enriched in this type of cells [49]. Since exogenously added FGFs significantly induced BrdU incorporation in primary cell cultures (as well as metacystode vesicles) it is reasonable to assume that this is due to a direct stimulation of neoblast proliferation by host cytokines. Interestingly, previous investigations on the regeneration capacity of planarians already indicated that in these organisms the FGFRs are expressed in neoblasts and control stem cell differentiation and growth [82]. Hence, similar to the situation in the free-living ancestors of cestodes, EmFR might be expressed in the *Echinococcus* stem cell population and activate the parasite's Erk-like MAPK cascade module, leading to enhanced proliferation and subsequent differentiation. This hypothesis is further supported by findings of this and a previous study [94] which indicate that the *Echinococcus* Erk-like MAPK module is stimulated in metacystode vesicles upon exogenous addition of host FGF, leading to phosphorylation and thereby activation of the Erk-like MAPK EmMPK1 [55]. This study now could show that the same holds true for primary cells. Upon stimulation with exogenous host FGF the Erk-like MAPK EmMPK1 is activated.

This process is very likely mediated through EmFR, because EmNDK, the other FGFR-like molecule identified in this study, does not possess a tyrosine kinase domain. It is also unclear whether NDK-like proteins bind canonical FGFs. Therefore, EmNDK most likely will not be able to transduce signals to downstream MAPK modules.

To further investigate the role of EmFR in *Echinococcus* development and to assess whether FGF signaling pathways might be promising for the development of novel chemotherapeutics against AE, studies using the tyrosine kinase inhibitor BIBF 1120 (VargatefTM) were performed. BIBF 1120 is a small molecule compound originally designed to bind to human FGFRs [203]. It has been shown to effectively inhibit human FGFR1-3 as well as the FGFR-related receptors VEGFR1-3 and PDGFR α and β by binding to the ATP-binding site in the cleft of the kinase hinge region [204]. It shows also activity against members of the Src family of kinases but displays a lower efficiency with a two- to three-fold higher IC₅₀ compared to the above mentioned targets [204]. The compound is well tolerated by human cancer patients and shows low cross-reactivity in the human kinome [203,204]. Since the *E. multilocularis* genome only harbors the gene for one FGFR homologue, EmFR, but no genes for PDGF- or VEGF-like receptors the inhibitor might mainly block FGF-EmFR signaling. Therefore, BIBF1120 was chosen in this study.

In a first set of experiments, the effect of BIBF 1120 on the activity of EmFR in the *Xenopus* GVBD assay system was studied. Although slightly less active than against the human FGFR, BIBF 1120 could effectively inhibit GVBD in EmFR-transgene oocytes upon stimulation with aFGF and bFGF. Hence, BIBF 1120 should not only be of use to study the role of EmFR in *Echinococcus* development, but can also act as a lead substance for the identification of drugs that display higher activity against EmFR and lower affinities against human FGFRs and related kinases. When tested in in vitro cultivation systems for *Echinococcus* larvae, BIBF1120 displayed remarkable activity against metacystode vesicles and effectively inhibited the regeneration process of primary cells. These results sustain the assumption that FGF-EmFR signaling contributes to *E. multilocularis* development as the block of the signaling cascade has significant impact on these two larval stages.

Especially stem cells of the parasite seem to be influenced by these signaling mechanisms because the regeneration processes was also blocked when primary cells were taken from *E. multilocularis* metacystode vesicles pre-treated with sub-lethal dosages of BIBF1120. Mechanistically BIBF1120 first seems to affect proliferating stem cells, probably killing them, before the complex structure of the metacystode vesicle breaks down. Primary cells isolated from such vesicles might contain lower numbers of functional stem cells, leading to a significantly reduced regeneration capacity. Interestingly, FGFs or heparin significantly increased numbers of vesicles developed from these pre-treated cells. This implies that by triggering the FGF-EmFR signaling pathway, residual stem cells are stimulated to proliferate and subsequently differentiate toward metacystode vesicles.

Next, I wanted to assess whether the negative effect of BIBF1120 on metacystode vesicles and primary cells can be correlated with a block of phosphorylation of EmMPK1 upon FGF stimulation. This would suggest that the inhibitor indeed interferes with the Erk-MAP-kinase module of the parasite. Indeed, in metacystode vesicles and primary cells, the activation of EmMPK1 was clearly blocked although the phosphorylation of EmMPK1 was not completely abolished. This might be due to several other stimuli present in the serum which might lead to the activation of this particular signaling pathway [55].

In humans FGF-FGFR signaling triggers not only the RAS-MAP kinase pathway, but also the PIP3K/AKT pathway is induced. For example, FGF-2 signaling via FGFR2 activates the AKT pathway protecting

human embryonic stem cells from stress-induced cell death [205]. Therefore, I investigated, if the putative PIP3K/AKT-like pathway of *E. multilocularis* might be affected by BIBF1120 treatment. However, there was no difference in AKT phosphorylation between BIBF1120 treated and un-treated primary cells. Also, host FGFs failed to induce AKT activation in primary cells of *E. multilocularis*. This suggests that in contrast to the human system, FGF-FGFR signaling in *E. multilocularis* primary cells occurs mainly through the MAPK cascade module, but not via PIP3K/AKT signaling.

Until now, the role of FGF-EmFR signaling was only examined in metacystode vesicles and primary cells because these stages are relevant for the human cause of disease. Primary cells mimic the early phase of infection whereas metacystode vesicles represent later stages of infection [150]. To broaden the picture of potential functions of this particular signaling pathway I examined whether FGFs and also BIBF1120 might influence the maintenance of activated *E. multilocularis* protoscoleces, particularly.

Protoscoleces of *E. granulosus* show the unique capacity of being able to mature into strobilar adult stages when ingested by a definitive canid host, but also of 'dedifferentiating' into fully developed cysts when released into the intermediate host body cavity upon cyst rupture [206]. This capacity appears to be also shared by protoscoleces of *E. multilocularis* [13], which could also routinely be observed in in vitro systems where *E. multilocularis* protoscoleces were incubated with hepatocyte-conditioned media for longer periods of time (my own observations). In the presence of FGFs there was no obvious alteration in morphology compared to un-stimulated control protoscoleces. The polarized body with suckers and hooks was clearly visible. However, although FGFs did not change the morphology and agility of activated protoscoleces, BIBF1120 did indeed have an impact on this larval stage. Under BIBF1120 treatment the distinct polarized body changed over time resulting in globular structures. Also, a higher percentage of dead or dying protoscoleces was detected. Thus the inhibitor interferes with developmental processes leading to a dedifferentiation. Hence, FGF-FGFR signaling possibly contributes to the maintenance of the protoscolex structure. This would support the result that FGFs did not change protoscolex morphology over time, but maintain its structural integrity. Of course, one can speculate that EmFR was not accessible for the FGFs but for the inhibitor. Thus, FGFs did not alter protoscolex morphology in contrast to the inhibitor, which affected this larval stage. However, FGFRs can also bind non-canonical ligands like cadherins or other cell adhesion molecules which control for example vascular integrity in humans, mesoderm layer formation in *D. melanogaster* or axon maintenance in *C. elegans* [207-209]. This would also explain why FGFs did not induce effects in in vitro cultivated protoscoleces. However BIBF1120 did affect protoscoleces as it blocks the signaling via the EmFR receptor regardless of which ligand induces the signaling process. The potential importance of FGF-EmFR signaling to maintain and stabilize the protoscolex larval structure, is further supported by the finding that the gene *Emfr* showed highest expression in activated protoscoleces, although the transcript is detectable in all intermediate larval stages that participate in the infection of the intermediate host.

Taken together, BIBF1120 was shown to effectively kill metacystode vesicle, to prevent formation of vesicles from primary cells and led to the depolarization of protoscoleces. These findings are promising and make BIBF1120 and its derivatives interesting drugs on the way to improve AE treatment options. BIBF1120 is an indolinone derivative which is thought to bind to the ATP binding site in the kinase domain of the receptor, resulting in interference with receptor dimerization and

blockage of signaling [203,204]. Structural analysis of the catalytic domain of EmFR and comparison with human homologues could be helpful in order to identify EmFR-specific inhibitors.

To complement the *in vitro* experiments I conducted bioinformatic analyses to identify further potential components of the FGF-EmFR signaling cascade of *E. multilocularis*. The Ras-Raf-MAPK pathway is well characterized in *E. multilocularis* [161]. However, molecules homolog to the fibroblast growth factor receptor substrate 2 (FRS2) which is usually associated with the human receptors and triggering the activation to the cytoplasmic signal transduction pathway could not be identified by means of these computational approaches. This might be due to the fact that putative *Echinococcus* FRS2 is not well conserved and therefore not detectable by homology searches. FRS adaptor proteins usually link vertebrate FGFRs to Grb2 and subsequently via SOS to Ras [70]. However, *C. elegans* FGFR signaling can also occur independently of the multi-substrate adaptor FRS2 [210]. That is why I investigated whether EmFR possibly interacts directly with the down-stream MAPK cascade components, for example EmRas or EmRaf. However, no such direct interactions between EmFR and the ERK-MAPK components have been identified in the yeast-two hybrid experiments. Thus future studies are needed to examine the exact molecular mechanism of FGF-EmFR signaling and its respective signaling components.

Another highly interesting question in this context is whether *E. multilocularis* does not only express factors for the detection of host-derived FGF-ligands, but also FGF-like molecules itself. Along with FGFRs, such ligands are expressed by organisms of all major metazoan lineages from chordates to insects, nematodes and even cnidarians [64,211,212]. Sequence conservation between these factors, e.g. human FGF and FGF-ligands of cnidarians, are usually high enough to identify respective molecules by BLAST searches. When I used human, insect, nematode and cnidarians FGF-ligand sequences in searches on the *Echinococcus* genome sequence, however, no significant match was found. In contrast to the co-evolution of FGF-FGFRs which has led to an increased ligand-receptor specificity in vertebrates [64] this might not apply to the parasite's FGF-FGFR signaling system. One might speculate that *Echinococcus* and other flatworms (like Planarians) have lost their FGF encoding genes over time. But FGFRs might have been under positive selection because signaling via integrin or cadherin receptors occurred [207-209]. To this end the complex structure of the multiple Ig-domains was no longer needed and lost. However, when *Echinococcus* and other flatworms encountered their mammalian hosts, FGFs ligands of host origin came in contact with the parasite's FGFR molecules which were then capable to sense these peptides. For *Echinococcus* it is likely that host FGFs are available, especially in the early phase of infection. *Echinococcus* induces liver damage [213] and FGFs counteract this damage by orchestrating liver regeneration processes. [214,215]. Thus, the parasite might sense signals of the host which could regulate parasite development. This hypothesis could also apply to parasitic trematodes because the FGFR-like molecule of schistosomes also depicts a similar domain structure compared to the *Echinococcus* EmFR, and canonical FGF-like ligands have not been identified either (Brehm, personal communication).

In conclusion, the presented data demonstrate that host-parasite hormonal cross-communication in the case of FGF-FGFR signaling take places and is an important mechanism for the development of the parasite. Thereby host FGFs influence proliferation and differentiation of the parasite *in vitro*. The parasite expresses one FGFR which is able to sense these host peptides. Stimulation with host FGFs activates the parasite's Erk-like MAPK, very likely mediated by EmFR. *In vivo*, host and parasite

are in close contact, as metacystode tissue grows infiltratively inside the liver of the host and induces liver damage [213]. Thereby host FGFs are secreted to induce liver regeneration and therefore should also be able to bind to the surface of the parasite's FGFR. Thus, FGF-EmFR signaling should occur and most likely is important for the early phase of metacystode establishment, for the proliferation and maintenance of metacystode vesicles as well as for the survival of protoscolexes at a later time point of infection. Nevertheless, future studies are needed to identify all components of the FGF-EmFR signaling pathway. This together with additional siRNA screens [147] could help to understand the various functions of the pathway for *E. multilocularis* development. Moreover, this study clearly indicates that EmFR can be considered an interesting drug target since intervention with the small molecule inhibitor BIBF1120 caused parasite death. In the future EmFR-specific inhibitors should be developed to minimize side effects in individuals who are treated against AE.

6.2. NHR signaling – EmNHR1, EmHNF4 and other putative EmNHRs

Serum is essential for the development of *E. multilocularis* because it contains peptide hormones like insulin, EGF, or TGF- β . These substances provide essential signals for the development and the survival of the parasite [20,46,47]. Also lipophilic/steroid hormones are present in serum and fulfill important functions for differentiation and homeostasis [98,216,217]. Lipophilic/steroid hormones are usually sensed by NHRs which form a superfamily of phylogenetically related proteins. They are essential in development, differentiation and homeostasis [97]. While in the parasitic trematode *S. mansoni* 21 members of NHRs have been identified [104,105], little was known about the presence of NHRs and their potential role in developmental processes for the cestode *E. multilocularis* [62,178]. In theory, the *E. multilocularis* should also be capable to react to lipophilic host hormones and therefore I assessed the role of NHRs in parasite development.

In a bioinformatic analysis based on the genome and the transcriptome data available for *E. multilocularis* I was able to identify a set of 17 *E. multilocularis* NHRs. These putative receptors partly cover the set of trematode *S. mansoni* and *S. japonicum* NHRs. For 11 *Echinococcus* NHRs high similarities within the DBD and the LBD to the respective orthologous factors in schistosomes were found. This indicates similar structure and function relationships of these receptors between the species. For the *Echinococcus* NHR which is encoded on contig 2891, no prediction of a LBD was possible. However, neither a LBD was predicted for the longest available EST sequence of the closest *S. mansoni* ortholog, SmHR96b, again indicating similar structure and function of NHRs. Yet prominent differences have been detected between the sets of NHRs of *E. multilocularis* and schistosomes. No clear SmRXR ortholog was predicted in the *E. multilocularis* genome. Instead, one *Echinococcus* gene with homologies to the SmRXR2 in the LBD but not in the DBD was identified. Whether this NHR is capable to undergo heterodimer-formation with other *Echinococcus* NHRs, as typical for this type of receptors, remains to be established. In addition only one ortholog in *Echinococcus* was identified to the closely related SmTLL, SmDSF and SmPNR receptors as well as for the SmTRa, SmTRb and SmRAR-like receptors, indicating again differences in NHR signaling between cestodes and trematodes. This is emphasized by the fact that *E. multilocularis* has at least two receptors showing no homology to the NHR set of schistosomes (contigs 2878 and 3395). One of them is EmNHR1 (contig 3395) the sequence of which has been identified previously by the analysis of a cDNA library of trans-spliced *Echinococcus* genes [62]. With the dataset of the putative NHRs at hand, the expression of the genes was investigated based on the transcriptome dataset. It seems

that most of the receptors are constitutively expressed in the larval stages which were included in the dataset. However, one receptor shows preferential expression in the protoscolex whereas another lacks expression in metacystode vesicles. Noteworthy, for two predicted receptors no significant expression was observed in the analyzed larval stages. This either could mean that these putative receptors are pseudogenes or they might be expressed in adult worms, for which no transcriptional data was available. Thus, on the one hand validation of the transcriptome data is needed either by my means of microarrays or quantitative real-time PCR and on the other hand there is strong need to obtain transcriptome data from all *E. multilocularis* developmental stages, like the adult worm or the oncosphere.

Noteworthy, the identification of 'estrogen receptors' (a and b isoforms) and an 'androgen receptor', which are all members of the NHR family, in the cestode *T. crassiceps* has been claimed [143]. Recently, the same group also reported on the presence of a 'progesterone receptor' in *T. solium* that apparently displayed high homologies to vertebrate members of the progesterone receptor subfamily of NRs [218]. However, none of these studies presented the actual sequences of the cestode NHRs. Instead, primers specifically designed against the DBDs of murine estrogen, androgen and progesterone receptors were employed in PCR amplification from *Taenia* parasite material, and a positive amplicon was taken as evidence that the respective receptors also exist in these cestodes [143,218]. My study of the *E. multilocularis* genome did not discover the presence of such receptors [145], nor are NHRs with high homology to vertebrate steroid receptors present in the genomes of schistosomes [105] or planarians (Brehm, personal communication). There are two possible explanations for these discrepancies. On the one hand, cestodes of the genus *Taenia* could significantly differ from all other flatworms in their set of NHR encoding genes, being equipped with additional members that display considerable homologies to vertebrate sex steroid receptors (possibly acquired by horizontal gene transfer) [145]. On the other hand, the amplified PCR products could have resulted from host contamination that was present in the *Taenia* parasite material, which was directly taken out of mammalian hosts [143,218]. I consider the second explanation likelier, which does, of course, not exclude that mammalian sex steroids might interact with one of the 'flatworm-typical' NHRs that were identified in *E. multilocularis* [145].

As already mentioned above, I identified at least two *Echinococcus* NHRs which do not show homologies to the NHRs of schistosomes, one of them EmNHR1. In this study a detailed structural analyses of EmNHR1 was conducted because on the one hand the receptor shows high homologies to the DAF-12/HR-96 subfamily of NHRs. This family is considered to be an evolutionarily conserved receptor group regulating cholesterol homeostasis and longevity in diverse metazoans [216,219,220]. Both *C. elegans* DAF-12 and *D. melanogaster* HR-96 operate as sentinels for low cholesterol concentration [219,220]. *E. multilocularis*, like all cestodes, is unable to synthesize de novo most of their own membrane lipids, including cholesterol, and has to take them up from the host during an infection [221,222]. Thus, EmNHR1 might play a role to sense cholesterol concentration thereby regulating the cholesterol uptake of *E. multilocularis* from the host. On the other hand, EmNHR1 is a very interesting study object as it is trans-spliced which indicates that the receptor might be involved in cell cycle control or growth of the parasite (Brehm, personal communication).

Cognate ligands of DAF-12 are $\Delta 4$ and $\Delta 7$ dafachronic acids ($\Delta 4$ and $\Delta 7$ DA). DAF-12 binds these ligands and shifts from its ligand-bound form to a ligand-free form and controls the formation of the dauer larval stage once environmental conditions are unfavorable [223,224]. Under harsh environmental conditions, the biosynthesis of these ligands is drastically reduced and subsequent

signaling pathways lead to the formation of the dauer larval stage [225]. Likewise, HR-96 is described to bind cholesterol derivatives sensing cholesterol concentrations. HR-96 is activated when cellular cholesterol concentrations drop below a critical threshold in order to protect cells from severe cholesterol deprivation [219,226]. In mammals, the Liver X receptors LXR α and LXR β are the NHRs with highest homologies to the DAF-12/HR-96 family and ligands are oxidized cholesterol molecules, so called oxysterols which serve as intermediary substrates in steroid hormone and bile-acid synthesis [216]. Based on the homologies of the EmNHR1 LBD to the LBDs of those NHRs, it is possible that the EmNHR1 ligand is also a cholesterol derivative. First hints of the cognate ligand of EmNHR1 come from yeast-two hybrid experiments in which human and bovine serum as well as the serum-free medium PanserinTM401, which contains defined lipid components like cholesterol, caused EmNHR1 LBD dimers, which NHRs in their active state typically form [109]. The cognate ligand of EmNHR1 might either be an *Echinococcus*-internal ligand that arises from cholesterol metabolism, or the actual ligand for this NHR could also be provided by the host. The latter is supported by the fact that sera led to the dimerisation of the EmNHR1-LBD. The fact that hydatid fluid also caused EmNHR1 dimerisation in this yeast-two hybrid approach does not contradict the hypothesis of a host-derived ligand for EmNHR1 because the hydatid fluid contains a large number of host serum components that are transported into the hydatid fluid by still uncharacterized mechanisms [221,227]. Therefore, EmNHR1 could function as a sensor of cholesterol or cholesterol-like substances and thereby could regulate gene that are involved in the uptake of such compounds. Nevertheless, the cognate ligand of EmNHR1 was not elucidated in this study. Therefore, future are necessary and one could use highly sensitive, luciferase-based cellular assays or direct in vitro binding assays on the purified LBD of EmNHR1 to identify the cognate ligand of EmNHR1. Substances, like cholesterol, oxysterols, bile acids or other cholesterol-derived compounds should be considered as potential ligands and therefore should be analyzed. The yeast-two hybrid system applied in this studies has never been used to detect similar interactions for complex cholesterol derivatives and probably was not the optimal method [145]. Thus, whether EmNHR1 indeed fulfils a similar role in *E. multilocularis* as DAF-12 in *C. elegans* or HR-96 in *D. melanogaster* still requires further experimentation [145]. Especially, with respect to the finding, that *E. multilocularis* genome also encodes two additional NHRs of which the LBDs display homologies to DAF-12/HR-96 and LXRs. The one receptor encoded on contig 2681 is a member of the invertebrate-specific 2DBD-NHR family. The other receptor is encoded on contig 3309 and harbors homology to the LBD of HR-96, and also, like EmNHR1, shares the CESCKA motif in the DBD, which is important for DNA-binding [103]. These two putative NHRs have clear homologs in *S. mansoni*, namely Sm2DBDba and SmHR96a. This highlights that EmNHR1 compared to *S. mansoni* is unique to the cestode *E. multilocularis*. Nevertheless, based on the homologies in the DBD and the LBD, EmNHR1 is a homolog of the DAF-12/HR-96 family. The receptor might have evolved by gene duplication, and might therefore fulfill distinct function in *E. multilocularis*, e.g. sensing host-derived ligand to sense environmental stress instead of intrinsic ligands from the parasite.

Concerning the role of EmNHR1 for *Echinococcus* development, one might speculate about downstream target genes. Since EmNHR1 harbors a similar P-box within the DNA recognition helix compared to *C. elegans* DAF-12 and *D. melanogaster* HR-96 this could imply that the receptor may recognize identical DNA binding half sites, most likely hexameric DR5 direct repeats separated by 5 bp as it has been described for *C. elegans* DAF-12 and *D. melanogaster* HR-96 [123,228,229]. A preliminary bioinformatic approach identified similar DR5-like repeats in the promoter region of

genes that are encoding a Fyn-like kinase, a pou-domain-like transcription factor as well as for the ortholog of the Niemann-Pick disease Type C1 gene (data not shown). The latter is required for sterol absorption in the midgut epithelium under control of HR-96 [230]. This points towards the hypothesis that like in *Drosophila* the *Echinococcus* NPC1 could possibly be regulated by EmNHR1.

Furthermore, also important for possible down-stream signaling mechanisms of EmNHR1 is the fact that this study showed a direct interaction between EmNHR1 DBD and the AR-Smad EmSmadC, which is part of the parasite's TGF- β signaling pathway [58]. Until now no direct interactions between DAF-12 and components of the TGF- β signaling pathway have been demonstrated in *C. elegans*. However, it is well established that DAF-12 operates on the convergence of the insulin-like and TGF- β -like signaling pathways in *C. elegans*. Particularly DAF-12 acts down-stream of the two respective pathways and shifts from its ligand-bound form to a ligand-free form and controls the formation of the dauer larval stage once environmental conditions are unfavorable [223,224]. Nevertheless, in mammals it has been described that NHRs like the vitamin-D-receptor (VDR) as well as the LXR form complexes with AR-Smads (Smad 2/3), however, using the NHR co-activator RAP250 as linking protein [231]. Thus cross-communication between NHRs and TGF- β signaling pathways might be another conserved mechanism. Although further investigations are needed to unravel the molecular details and differences because TGF- β signaling either induces the production of cognate NHR ligands or downstream Smad transcription factors, either directly or indirectly, interact with the NHR components [145]. Yet the finding that NHRs and TGF- β signaling possibly cross-communicate in *E. multilocularis* is sustained by the fact that the *E. multilocularis* co-repressor EmSkip also physically interacts with EmSmadA and EmSmadB [58,61]. In the human system, SKIP interacts in a ligand-dependent manner with the heterodimer formed by the VDR and the retinoid-X-receptor (RXR) [232]. In my hands I did not find an interaction of EmNHR1 with EmSkip. In fact EmNHR1 is not a homolog of either VDR or RXR. Therefore, other co-regulators, not yet identified in *E. multilocularis* are potential candidates which might interact with EmNHR1.

Among the 17 putative NHRs also a HNF4-like receptor was identified. Human HNF4 plays an important role in liver development and is a key player in metabolic pathways [128,184]. Endogenous bile acids, which are present in liver tissue, are thought to be the cognate ligands for human HNF4 [233,234]. Also, in *Drosophila* the HNF4 homolog DmHNF4 possibly binds fatty acids and is activated, inducing enzymes that drive fatty acid oxidation for energy production [235]. *Echinococcus* is incapable of synthesizing most of its lipids de novo and fatty acids are known to be important for *Echinococcus* development [221,236]. EmHNF4 was characterized in more detail because it might fulfill similar functions as its human homolog. The cognate ligand should be available for the parasite because it manifests its growth in the liver of the host.

In this study two isoforms of EmHNF4, EmHNF4a and EmHNF4b, have been identified which possibly fulfill distinct functions in *E. multilocularis*. EmHNF4a shows remarkable homologies to the DBD and the LBD of other HNF4 proteins. Therefore, one might speculate that fatty acids might be the cognate ligands for EmHNF4a. This hypothesis is supported by the finding that the Arg 226 of the human HNF4 alpha which binds the carboxylic acid head group of the fatty acid ion is conserved in EmHNF4a (Arg 387) [233]. EmHNF4a is expressed throughout the larval stages which participate during the infection of the intermediate host. On the other hand, EmHNF4b does not harbor a complete LBD. Yet the DBD is highly conserved between all HNF4 homologs. Due to the structural difference in the LBD, one might speculate, that EmHNF4b cannot bind bile acids. EmHNF4b is expressed in all

analyzed larval stages, but upregulated in activated protoscolexes. Thus it might influence developmental processes of the protoscolex. Moreover, the two isoforms seem to differ in respect to their ability to interact with components of the TGF- β /BMP pathway. EmHNF4a does not interact with EmSmads, but EmHNF4b interacts with co-smad EmSmadD and the BR-smad EmSmadE. In the human cell line HepG2, HNF4 alpha expression is repressed by TGF- β [237]. The exact mechanism is not yet clear. There are indications that signaling is mediated via Smads, at least in the murine model. The repression of HNF4 by TGF- β was interfered by dominant negative Smad3 [238]. One can only speculate whether the same holds true for *E. multilocularis* or whether this mechanism might be one aspect of parasite-host-interaction mediated by host TGF- β triggering EmHNF4 responses. This could be analyzed in further studies by stimulating metacystode vesicles with TGF- β and thereafter checking the expression levels of the EmHNF4 isoforms. In conclusion, it appears that there are specific regulatory mechanisms on the convergence of NHR signaling and TGF- β /BMP signaling pathways in *E. multilocularis*. On the one hand, EmNHR1 directly interacts with EmSmadC and on the other hand EmHNF4b interacts with EmSmadD and EmSmadE. The putative functions of the different EmHNF4 isoforms and also the role of NHR-TGF- β /BMP signaling cross-communication must be addressed in further studies. Once for example siRNA screens are established a stage dependent analysis could facilitate to unravel these aspects [147].

Taken together, the data obtained in this study indicate that EmHNF4a might act as classical HNF4 homolog and thereby sensing bile acids, whereas EmHNF4b might regulate different functions mediated by other potential ligands which bind to other distinct parts of the receptor since the typical LBD is absent. At least for *Xenopus* it has been described that a yet unknown protein is able to bind to XHNF4 independently of the LBD. This protein is present in *Xenopus* embryos and inhibits HNF4 binding to the DNA [239]. Moreover, one should examine whether the EmHNF isoforms are involved in the regulation of lipid or cholesterol metabolism, as human HNF4 binds to a hormone-response element in the proximal apolipoprotein M promoter and positively regulates the *apoM* gene expression adjacent to the HNF-1alpha-binding site [240]. Such a process could be highly relevant for parasite development and survival because it recruits host cholesterol via EmABP [221] and thus EmHNF4 could be crucial for the regulation.

To conclude, this is the first comprehensive study on NHR signaling in any cestode. *E. multilocularis* expresses a set of 17 diverse NHRs which partly cover the NHRs of the trematodes *S. mansoni* and *S. japonicum*. However, the cestode also contains several NHRs encoding genes that are unique to the parasite suggesting distinct differences in regulatory mechanisms between the species. There is no evidence for an expansion of NHRs which is for example the case in the nematode *C. elegans* [241]. Among the set of *Echinococcus* NHRs, EmNHR1 is a member of the DAF-12/HR-96 family and might be involved in sensing cholesterol. The cognate ligand was present in host serum and induced LBD dimerisation. This indicates a putative parasite-host cross-communication mechanism, by which at least the parasite senses host hormones. Thereby its development is influenced by the host. Moreover, a HNF4 homolog was identified. EmHNF4a might bind fatty acids because the DBD and the LBD are highly conserved in comparison to the human homolog. Furthermore, EmNHR1 and EmHNF4b both interacted with components of the TGF- β /BMP signaling pathway suggesting a cross-communication between the two different pathways within the parasite. Based on these findings investigations regarding the role of NHR signaling for *E. multilocularis* development will be greatly facilitated.

6.3. Serum-free cultivation of *E. multilocularis*

In vitro cultivation systems for *E. multilocularis* larval stages have been developed and constantly improved over the past years [49,147-149,161]. Now, it is feasible to culture metacestode vesicles, protoscolecocytes and primary cells either in co-culture with feeder-cells or under axenic conditions in the absence of these feeder cells. Yet, for available cultivation systems it is essential to add serum which supports growth and survival of the parasite [150,191]. However, a serum-free cultivation system using a defined-minimal medium for *E. multilocularis* might contribute to unravel mechanisms of parasite development. It might facilitate studies on how either small peptide cytokines or lipophilic/steroid hormones influence the parasite development without side-effect caused by the various substances present in serum.

In this study, a serum-free cultivation method using commercially available serum-free Panserin™401 as medium has been developed. During the experimental procedures it was obvious that Panserin™401 medium supported the development of the parasite but the resulting metacestode vesicles were rather fragile and small. The same was observed under serum-free axenic conditions. Obviously, sub-optimal growth conditions affect the proper formation of the inner cellular layer and the outer laminated layer of the vesicles causing alterations in the development of these vesicles. Interestingly, after in vivo passage of metacestode vesicles from Panserin™401 co-culture with subsequent axenic adaption, the appearance of metacestode vesicles changed. After several in vivo passages the material isolated from the jirds developed into metacestode vesicles which reached the same volume and turbidity as material from standard procedures. This noticeable adaption to serum-free co-culture suggests that possible mechanisms of selection are occurring. In detail, *Echinococcus* stem cells could be responsible for this observation. When jirds are infected with larval metacestode vesicles by intraperitoneal injection, it is believed that stem cells from the metacestode vesicles are causing the infection in the animal and subsequently developing into metacestode tissue. This mechanism is comparable when the intermediate host ingests infective eggs harboring the oncosphere and in this case the oncosphere's stem cells are the only cells that contribute to the formation of the metacestode tissue [20]. Thus, I propose that by in vivo passage stem cells from vesicles, which in vitro grew better under serum-free conditions, were selected and expanded, which lead to an ameliorated generation and growth of metacestode vesicles in the subsequent in vitro passages. This hypothesis is supported by the finding that parasite material which was isolated from the liver of a jird and subjected to in vitro cultivation shows enhanced growth in the liver of a jird after intraperitoneal injection, compared to material that was isolated from the peritoneum of a jird (Hemer, personal communication). The underlying mechanisms such as potential genomic or proteomic adaptations still need to be identified in future experiments.

Because of the difficulties of the above described serum-free cultivation of *E. multilocularis*, the serum-free cultivation system was modified as follows. Prior to the cultivation in Panserin™401 the metacestode vesicles were cultured by means of the established co-culture and axenic culture. Thereafter, these vesicles were directly transferred to serum-free medium. This system allows analyzing substances that potentially influence the parasite's development in a serum-free environment over a sufficient period of time. First, I investigated whether the mitogenic effect of insulin was detectable in this system. Insulin-signaling plays an important role in *Echinococcus* development and host-insulin serves as a mitogenic stimulus inducing proliferation [161,173,195]. Insulin exerted a growth promoting effect on metacestode vesicles which however was abolished

when the vesicles were kept in conditioned Panserin™401. Thereby this study confirmed previously findings [161] when vesicles were cultured in DMEM supplemented with serum. From that I conclude that the effect of insulin is not altered by the presence or absence of serum. However, it is influenced by factors secreted from the feeder cells into the medium. One of these factors is insulin itself as indicated by Western blot analyses. Insulin, presumably bound to albumin, was detected in non-conditioned Panserin™401 but higher amounts of insulin were present in conditioned Panserin™401. This is in contrast to the manufacturer's statement that Panserin™401 does not contain insulin. However, upon inquiry the company stated that the albumin which is supplemented to Panserin™401 is not tested for purity and therefore could be a source of contamination. Thus, I think that insulin is present in Panserin™401 and albumin serves as carrier for these substances. This carrier function of albumin is well known and is even used for therapeutic and diagnostic agents, primarily for diagnosing and treating diabetes, cancer and rheumatoid arthritis [242,243]. In contrast, to the growth promoting effect of insulin, which was not dependent on serum, the formation of brood capsules was strictly dependent on serum and independently of insulin. Thus, serum might influence the outcome of differentiation and possibly proliferation processes of *E. multilocularis*. I therefore, suggest implementing this newly developed axenic serum-free cultivation of metacystode vesicles as the method of choice, when investigating the role of specific substances for the development of *E. multilocularis* metacystode vesicles.

6.4. EmMPK3 – a serum-responsive MAPK

EmMPK3 is a homolog of the Erk7/Erk8 family which in humans plays a role in regulating stress responses [244-247]. It was previously shown that EmMPK3 is activated by serum in primary cells of *E. multilocularis* [196]. Since serum is a critical component for the in vitro cultivation of *E. multilocularis*, this study extended experiments to other *E. multilocularis* larval stages to address the question whether EmMPK3 is activated by serum in the larval stages that contribute to the infection of the intermediate host.

To this end metacystode vesicles and protoscoleces, either non-activated or activated, were cultured in the presence or absence of serum. There was no evidence that serum induced the phosphorylation, hence the activation of EmMPK3 in metacystode vesicles or protoscoleces. Thus, the activation of EmMPK3 mediated through serum is confined to *Echinococcus* primary cells. This finding is supported by the *Emmpk3* gene expression profile. Although the gene *Emmpk3* is expressed throughout the different larval stages an upregulation upon stimulation with serum was only detected in primary cells. Thus, both on transcriptional as well as on translational levels EmMPK3 is induced under serum-conditions. Until now, it remains unclear which component of the serum is leading to the observed effects. Nevertheless, these findings indicate that EmMPK3 might be important for metabolic processes within regenerating primary cells. In the human system Erk8 is activated by serum and has been shown to be associated with Src-kinase activity [245], which is another pathway not yet characterized in *E. multilocularis*. Bioinformatic analysis suggests that homologs of Src-kinases are present in the parasite. Therefore, future studies should address the specific function of EmMPK3 in primary cells. Moreover, I was able to show that EmMPK1 activation by serum seems to be negatively correlated with EmMPK3 activation. There was no change in phosphorylation upon serum stimulation in primary cells, but in metacystode vesicles and protoscoleces, either dormant or activated. EmMPK1 is associated to support cell growth [170].

These differences in MAPK signaling must be further investigated to clearly understand larval development and growth of *E. multilocularis*. Yet other pathways might influence these processes as it has been suggested that also the PIP3K/AKT-like pathway might contribute to the growth of primary cells [170]. Overall, these findings show that EmMPK1 and EmMPK3 fulfill distinct functions in regard to *E. multilocularis* development in a stage-dependent manner.

7. Supplement

7.1. Full length cDNA sequence of *Emnhr1* (isolate H95)

>*Emnhr1*

caccg^uttaatcgg^tccttaccttg^cag^tttt^tgtatg^gATTCCTGGTTCATCAATCCTTGA**ATG**ACGTCa
 CAAAAGCAAGCGCTTCATGCTCAGATGTCTAGTGTGATTCATGACGACCGGCAATGTTTCATGATTCC
 ATCAAGTATTGATTGCAGCAGTTGTCCTCCTGGCAGAGTGCACGAAGAAGAGATGAAAAGAAATGTG
 CTGTCTGTGGAGATCATGCTGTGGGCTTTAACTTTGGGGCCATTGCCTGCGAGTCATGCAAGGCGTTC
 TTCCGTCGTAATGCACTCCGAGCCACCATGCCCCCATGCCTATTCAACGGTAGTTGCTTGATTCAAGT
 GAAAACGCGCCGGTCTGTTTCGCTTGTTCGCTTTTCCAAGTGTGTTGCTGTGGGAATGCGCAAGTCTT
 GCATCATGGATGAAAAGCAAAACGAGAACGAAGGAGAAGATTTCAGCGTAATCGGGAGCGAAAAGTT
 GCCTCAGGTCAAATGCGCGCTCTGGTGGGGCAATTGCGCGCTCGAATTCCCCTCCACGGTGTTATCA
 AGGCAACTCCTCTCCAATCCCGACTATCACTCACACTCTCTAGCCCCAGATCCCTCGGCACCTCCGC
 ACCATCATCAACAGACACCACCCTCCTACTATCCTTTGATCTCAGCATCTCACCTGCCACGGCGACT
 GAGGCGCTGCCCTCCACTGGCTGTCACAATGCTGTCAACGAGGATTCTGGAATGCGGAGTACTTGGA
 GATGCCTCAAATCTTCATCAGGATCGTTACCTACGGTCGAGAGTTCGATACATGCTTATTCTTCCC
 ATCATCTACACCAGTCCCATTTGATGACTCCTCCGTCTCTCCGGGCCTCATCCACCATCCTCGTTT
 GGAGGCATGGAGTCTTATTTCCACCCAGCGCAGTCACTTCCCTGAGGTACAAGGCGCCTCTGAGGCAAc
 ACCCAATGAGGCTGGTTACAATGGTGACCTCGTCGAAGGCACTCGAGGAGAATCCACCACACTAC
 CCTATTTTGTAAAGAAGCCAGCAAAGACAGCTCTCACCACCTCTTCGAAATATCCACCCTCTCACGCG
 AATGAAGACTCTAAGTCCGGTGTAATAATGTCCTTGATGGTCACGTTTGGACACTGGAACCGGAGGA
 TCCATCAAACAAGGAGTGTATAGCGCTGTGTCCAGACTTTTTTAAAATCGGGAATGGCCCGCTCCTCT
 CGAAGCATCAGTGGACGGCGCTGAACGACCTTCGCAGTGCCTACGAGACGTCCTTTCTCGATTGTGCC
 TCCGATCACGCGCCGGAGAGCAGCTCAAATATTACTATAAGTAGTTTGGTGAATACTTCTGGTTTTTT
 GGTACGGAAGTTTATAAAATTTTCGCAAAGAAGTTGGCCGACTTCTCCGTCTCGGTCAAGAGGGTCAAA
 TTTGTCTACTCAAGGGGGTGTCTTAAATGCCCTTTTTTATCCGCTCCGCCAGTCATTATGATGTTATC
 AAGGATGTGTGGGTCACTCCAAAGGGTGAATAACCACCAGTATACTTAAAATTGCTACAGGAATGCA
 AAATCTCTATGAGGAGCACGCCAAGTACTGCAGGAACCTTGTCTGATGTTGTTAAAAGGGACTCCCATT
 TGGTGGCTCTGATGCAGGTGTTGTGTCTCTTCGCTCCAGATCGTCCTCGCCTTCCGATCGTCAATCG
 GTATCCAATATCTACGACCGTTACATTCTACTGTTGAAGCACTATCTGGAAGCCCGCCACGGTTTCAC
 TCGAGGTCGAACTTTATTGGCTGCCGTGTTGACTAATCTGGCGGAGTTACAGGCTCTGACCGACAAC
 ATGGTCATATCCTTCTCCACGTCGATCCAAGCAAGGTGGATCCCCTGATCCTTGAAGTGTCAATCTT
 CCGGATCGTAAGAAGGCTAATAAGGATGTGGTGGAGGTGGGATCAGATTCAAGtCCTTTAATTACGGT
 TGAGGCAAACACCTCCAATTCTAACATGACTAATTCCTCC**TAA**ACCAGAGATTTCAAAGATGGCACAC
 TTGAGAATGATACTCAGACGCACACATCCAACAATCCACAGAGAATGAGACTATGTCCCAATTTTCC
 AGCATAAATATGGTACATATGTTTATCGAGTGATGTCAGTGTCTATATCTTGCCGATTGTAAATAATC
 GCTCCACATTTTTGTGTGTGTGTGCTTCAGTATTGCTGCGTGTGTCAACTCGCGTTTTGNGTCATC
 ACTCACCACACATCCCCCTTCCCCTCCTCGCTTTTTTAAATCACTGACTTTTGTCTTCTTTTTTGAG
 GTGATTTTCTGTAAAGAATTGTGATATGTGTGACTATTCTTTCCTCCTCCTACCCTGCTGCTTCT
 AGGTTTACCTCCCGGCCCTCCCCTTCCCCTTCCCCTTTATTTTTCTGTTCACTCTGACGTCTACG
 CATATTTTGCATTTTAAAGTTGAAGTAGATGTTTCGCTATGA**AATAAA**ATTTTTTGGTCTCTGAAAA
 AAAAAAAAAAAAAA

^u: Spliced Leader; **ATG/TAA**: start codon/stop codon; _t: polyadenylation site

7.2. Full length cDNA sequences of *Emhnf4a* and *Emhnf4b*

>*Emhnf4a*

TGAGCCTCCAGAGTAGAC**ATGA**ATCCACACAACCTTTGAA**ATG**GACCTCTACAATAGCAGCAGCGGTGG
CATCACCCAACACGGCAACATGCACAACAATTCGTGAACACTTCAGGCGAGGAGTTCGAGGACGACT
CCTCCCTCCTCTTGCCAAGTCTCGTCGATACAAATTTTGTGGAGAGTGTTCCCTGGAACCGCCTCCTAC
TACAATGGAACCTCCCGCAACCAATCAGAATGGTGCATGGCTCACACCCCTCCCAACTTCATGTTCCAT
TGAACCGATACATTCAACCGACGTCTATAGACCCTATCTCCCAGATCAAACGCAGCTGCGATGGGAGA
CTCAGGTTGATCCAAATGTGCCTACTATGCACCCGTTCTAGAGCCGATTGGATTACCTGTGCGGAA
ACGTTAATTACCAACCACGAGGAGTATCGAAAGAAGATGAACTCAGAATCAGGAATCGCTGAAGGTGA
GATGCTGACAGCTATTGTCAATGGTGACACCACAGCCAGTGGGTACTCTCAAACCCCTGAGGTGACCT
CTACTCCAAGGTGCGGTTGCCGTCGGGGTTCACAGAATGCCGTAAAGGGAGAGGCCAGCCTGGGGGGA
AGGAATCCCCATCAGGAGGATTCCCTGATGGCCTCTTTTGAAGTCAAATCGACGACCGACCTCCCTC
GGGTTCTGCCTCTCTATCCATCTCCAAGTGTCTTATTTGTGGAGACAAAGCAACGGGCAAACACTACG
GCGCATATTCATGTGACGGGTGTAAGGGATTTTCCGACGTTCTGTGCGTCGAAAACACACCTACAGT
TGTCGGTACaATCGAACTTGACAATTGACAAAGACATGCGTAATCAATGCCGTTTTTGGCgGCTGAa
AAAGTGCTTCCGGGTGGGCATGAACCGCGCAGCGGTCCAAAACGAGcGCGATAAAATCAGCaATCGAA
gGCCGTTTTGCGACGCGTCGGgACTGaaTgGCACTctaATCGATATCAGCACTCTACTTAGAGCCGAG
GTTGAATCCAAGGCGACAGCCGAAGGGATTGAGACAAAGGATCTTTCCTCTACTGGACCACTAAGTCT
AGCTGAAATTTGTTTCAGCCATGAAAATTCATCTTTTTCGTTTAAATCAATTGGGCAAGACAGCTGGATT
GCTTTGTTAATCTGGATATGCAAGATCAGCTGACTTTGCTACGTGGGAACTCGGGGGAAATGCTCCTT
CTAAGCATGGTTTTGGCAGGCCATTTGCACGTCATCTCAACAAATCGATGAGGCTGGGACATTTATCAA
CCTCTTTCATCGGTTAAATATCGCGTTTATGGAAGTAATCAAGGCCAGTGGCAGTGGTTGCAATGAAT
TTCCAGCCATGCCTTGTGCGCTGATGACAGCAAGTTGGATGCTATTCTCAAAGTCATTGCCAATACC
ATTTATCGACCACTGCTGGAGTTGGCGATTGGAGAGACAGAGTTTATTTGCCTCAAGGCAATTATTTT
CTTGAGTGCGGGTCACCTAACCTATCATCCAATGGTGCCTCACCGTAGAAGCCTCACGGAGtcGGC
TTCAAATCGAACTAATGAACGTCATGAATGACAACCAATACCTCCAGAGGGTTCGATTCTGGGGAGCTG
CTTCTTTTGGTGCCGACACTGCAACGGGTTTCAGGATTTCTTGTGGCCAGGATTGGAAGCGTTGCCAC
TACTTCTGCTGCTGCCGCCGCTGTTGCTGCAGCCAATAGCTCAGCCACGGCAGAGTCAGACGAGACTA
TCAATTCACTTAGACTGGATGATCTCCTGGGGGACATACTACTTTCAGGTCCAATGACCATGTTTCGAT
GACCCCAGGTAGAACTAATGGCACTGTAGCTGTTCCTTTCGCCTATCTGCCATTCAGTCACAACAG
TCGATACAATGGGAACGGTGATACGATGTCTTGGCAACCGGAAGGACCTGCAAACAGGGAATAACCA
TGGCTTTCCATCTCCAACCGTTGGCTACTACGTCTACATGTTACTCGCAGCAACAGCAACAAGGACAA
CAGCTCCAGGTTGCTCAAGAATCCATAAATTTCTTTGATAATGCATTACCTATCAAGAGGACGTTGA
AAAGCAAT**TGA**AGGAGAGCCTACTGATGCTTCGACTCCTTCGTGCATTCAATTGGTTCGATTTGAAGGTC
AAATTTGCTGCTCCTTTGGATGTGGGGGAGAATTCTTCCCTGCTCAATCACTAAATTATGACAAATGA
CAATGTCTTATGTATTGATTTTAAGTACCTGCATTATGAAGAATGTACGGAAGTA

>*Emhnf4b*

TGAGCCTCCAGAGTAGAC**ATGA**ATCCACACAACCTTTGAA**ATG**GACCTCTACAATAGCAGCAGCGGTGG
CATCACCCAACACGGCAACATGCACAACAATTCGTGAACACTTCAGGCGAGGAGTTCGAGGACGACT
CCTCCCTCCTCTTGCCAAGTCTCGTCGATACAAATTTTGTGGAGAGTGTTCCCTGGAACCGCCTCCTAC
TACAATGGAACCTCCCGCAACCAATCAGAATGGTGCATGGCTCACACCCCTCCCAACTTCATGTTCCAT
TGAACCGATACATTCAACCGACGTCTATAGACCCTATCTCCCAGATCAAACGCAGCTGCGATGGGAGA
CTCAGGTTGATCCAAATGTGCCTACTATGCACCCGTTCTAGAGCCGATTGGATTACCTGTGCGGAA
ACGTTAATTACCAACCACGAGGAGTATCGAAAGAAGATGAACTCAGAATCAGGAATCGCTGAAGGTGA

GATGCTGACAGCTATTGTCAATGGTGACACCACAGCCAGTGGGTACTCTCAAACCCCTGAGGTGACCT
CTACTCCAAGGTTCGCGTTGCCGTCGGGGTTTCACAGAATGCCGTAAAGGGAGAGGCCaGCCTGGGGGGA
AGGAATCCCCATCAGGAGGATTCCCTGATGGCCTCTTTTGAAGTCAAATCGACGACCGACCTCCCTC
GGGTTCTGCCTCTCTATCCATCTCCAACGTCTTATTTGTGGAGACAAAGCAACGGGCAAACACTACG
GCGCATATTCATGTGACGGGTGTAAGGGGTTTTTCCGACGTTCTGTGCGTCGAAAACACACCTACAGT
TGTCGGTACAATCGAACTTGCACAATTGACAAAGACATGCGTAATCAATGCCGTTTTTTGCCGCTGGAA
AAAGTGCTTTCCGGTGGGGCATGGAACCCGCGCAAGTACCTTAACCTATCATCCAATGGTCGCCTCA
CCGTaGAAGCCTCACGGAGTCGGCTTCAAATCGAACTAATGAACGTCATGAATGACAACCAATACCTC
CCAGAGGGTCGATTCGGGGAGCTGCTTCTTTTGGTGCCGACACTGCAACGGGTTTCAGGATTTCTTGT
GGCCAGGATTGGAAGCGTTGCCACTACTTCTGCTGCTGCCGCCGCTGTTGCTGCAGCCAATAGCTCAG
CCACGGCAGAGTCAGACGAGACTATCAATTCACTTAGACTGGATGATCTCCTGGGGGACATACTACTT
TCAGGTCCAATGACCATGTTTCGATGACCCCCAGGTAGAACTAATGGCACTGTAGCTGTTCTTTTCGC
CTATCTGCCATTTCAGTCACAACAGTCGATACAATGGGAACGGTGATACGATGTCTTGGCAACGCGAAG
GACCTGCAAACAGGGAATAACCATGGCTTTCCATCTCCAACCGTTGGCTACTACGTCTACATGTTAC
TCGCAGCAACAGCAACAAGGACAACAGCTCCAGGTTGCTCAAGAATCCATAAATTTCTTTGATAATGC
ATTCACCTATCAAGAGGACGTTGAAAAGCAA**TGA**AGGAGAGCCTACTGATGCTTCGACTCCTTCGTGC
ATTCAATTGGTCGATTTGAAGGTCAAATTTGCTGCTCCTTTGGATGTGGGGGAGAATTCTTCCTGCT
CAATCACTAAATTATGACAAATGACAATGTCTTATGTATTGATTTTAAGTACCTGCATTATGAAGAAT
GTACGGAAGTA

ATG/TGA: start codon/stop codon;

_: polyadenylation site

7.3. LBD sequences of *E. multilocularis* NHRs from *in silico* analysis

Table 4: LBD sequences of *E. multilocularis* NHRs

Contig	Amino acid sequence of LBD
1644	EMASRVLLVTVDWLKRCPDLQPSDLQNELIALSWVDLDFMLGLCQMFGRRLLGNLRMAFFGSN QDDGCGVDAHPMKSDFNSIVSGFSRAEVTPEEYTYLRYMALFNSGGVRTNDATGLNRVREIEQKV QVEFAGFLSESESQKVNDGDNQRPFEVQTASRGLQLMGLVCGLRRVT
1680	NVIKSRILDVLSFAKFVPGFLLLSVRDQTRLLQSSLLDILTLRAVEALSRRKMARSTINREEDDSESDNQ SVTASKAYAFIARSADGNSKAIRDLARKVLLWKLDVTELALVASILLTSGNDVSDPGAVVAIETLLTN VLVSHVMKGNMDGVKLRRLFSMFSEIHSIT
1702	SAMKIHLFRLINWARQLDCFVNLDMQDQLTLRGNSEMLLLSMVWQAICTSSQQIDEAGTFINL FHRLNIAFMEVIKASGSGCNEFPAMPCCADDSKLDAILKVIANTYRPLLELAIGETEFICLKAIIFLSAG HLNLSSNGRLTVEASRSRLQIELMNVMMNDNQYLPEGRFGELLLVPTLQRVS
1779	NHFHLHSQQVVQFAKLIPGFNQMSLSARGHLVRasLYSEVLLMLSRDYDAAEDRYNFLDFSPTERD IVLRHFPIYNRVVEHLRISGRFFQQLNLTHTEFVYVCAIGILRYYYILANPAYTDARKLLLLARHSLLAT MRSQNESQELVDHKWSRLEAMSEMLSSMSREY
1798	RQLLRTFLQPTTHSSTFQLTPREIARLMSTSWPRVFILEAIEVFLKGQDSKKLISFLAKLCSNGDATDF DATERIESLTCALHLPSTEEFSLKTLCLFSLGSESASQAEFEHLSSLCDLLHQNLVYIQACFPTNM EQKEGLLRCTAIKSPDEMTCIRRRAFLKVFGCSEMIENIDRMIERM
1872	QRFEAHAHQIIRFARAIPGFCDLPRADTKFLLQASMYPIVLVQLSREALPGGDFNFYNFSPHERRHL LAEFPQINPMVDHFYELTGFLGPLNLDNTEAALLCSIIFLRGSNQKLEAEKIYEIYNHAASALQQYIT VRYSSDERFTQLIKLLPSLSSMN
2122	PAISLHIQSVVEFAKAIPNFVSLAQPDQLALLKAAFPEVWVWQAARTISYPEQTIMLCNGHIICRTEL DFIYTPQLTCAMFEFAAEFCALNLSDEIGLFSAILLTKPSRHGLSDSAKVAVMQERFQAALSYQLAE KHESVSDIMNKLALASSRLAQLSESM
2681	QFVSHTRMVVDFSKLIAGFNRLGINDRRQLIRAAMYPIMLIELSRDFQNNSSLSYNYDFPEREKEVI IQRFPPLAKMISHLVQSGKVLRRRLKDDIESTIICIQELLRHKNELEDPASCEHLFLLSMQALVNHEHQ KSKSDAASERLTAFTQLLPILNQLN
2822	FTSTAAIATHYVRWAKQLPFFNNIHKVDQMALLNDALCDIILLTSLQRLNYGIDLLKLHQHNDGEN VKLNLRKLYENINQLTTLNLFVEACCLKAMLFFNVGK
2878	TCFDRIMQDSVKFAKRIPGFSDLLPEDRMVLVQSGCFELACVIFSFYVDEESQTFCGPGNFTLSQSQ

MWLTFPMSKKFVNLLDFAFQVQSHRLEPLKGLLLAVLLVTPIREGLTNREEVTWLRDLICQAFRF
QLMVTHSDGVGLFNHLVSSIREELQ

3309 DTCIRRIIRVVKMLPYFNEIGKPAQLGLLRANIYGMIVLYSSFFEREIRKLRYPVKRADGSLTTVTVS
MLDDLAPSVVSDEKAFSAFLSGKHRHAASAAAAAASLREDFELYKANTLAAFNHLEELTGEDDILR
MTLLAIKLFSDDSLDELQSVVVSSKRIVLVFLWTYIRWRAGPKHLRQATELFARLHLAFIDLRSLR
MTEFAKLVSLLEGLSPLMREI

3395 NTSGFLVRKFINFAKKLADFSVLGQEGQICLLKGVVLNLFIRSASHYDVIKDVVWVTPKGEIPTSILKI
(EmNHR1) ATGMQNLVYEEHAKYCRNFADVVKRDSHLVALMQVLCLFAPDRPRLSDRQSVSNIDRYILLKHYL
EARHGFTRGRLLAAVLTNLAELQALT

3400 SMLEDCLFHMVDWVNRTEIFRVIRVEDKMQLLYSSWSEVIVIEFLQCIVILNRTEDRSDIMKAGAG
SPREPSNRDLHYLVKELMEYLLPPDENQRIRDLIARFNALNLSSEFTCLKFLVIFNPYKHDVNLTS
LEYVREVQADLCHFLRAARRAIKQRPLPPPTFPPTHAASLATAASERLGRLLSHLDEVKHVA

3425 GESVEVIRQYADLVPGFSSLEADREKIILLHSADLITFRMAFRTAKAAAERAQLNLIHPNTSQPNAY
FRSSTSADVSRTQQQTSTIMQHQQTGPFQSVENLSAWHTQPASLESSFRPFHTPLTPPPSSW
LRGGSGGSVPRPANFEAEENITAWELALSTPTEPVYIFENGSIPTDEELIRAGLGSWIRALTWF
GWQLELAMGDHSTIAGLSALVLINYQALSGRSDLENSSDIYTVHHRFVEMLKSHCCSPTSAVAIPT
GYPGCYVPEVDPAAATVATAATTTMVPPARADSTYFSQVFKKDTVHWIASQLL

3440 TDIQESIINLLWSQKIPLFSDSDRIFILLRAGCIELLVHFISRLANSLTESHSPTSLRSSNPPLQESS
TTSVTPUESTTPTPLNIPFVVVDVLPFHSAPKDILFSQQAECDLRNADRWHESRVLNMNIPVDV
DHPISITGVPNELNAQCLSRRLICRLFDLARLFKRLCLSVEAVGCLRMVILFNPDPDLTEATRERV
ESRRDEAFICLEHTFLKADKKTALGRMAQMCLHLADLSFVA

3442 NLADQRLYRIVRWSRALPVFSNLDLDDQILLQNCWADLLCLDCCWKS LPTPTEIRLTSTKINLDA
AREMGAEGLVDSLLRLTQDLKRLRFLIDFACLKVFLMQGDLTNLKA VRQVKQFQECVSQLLMD
YNSTSCADVDPDKFTELLVRIPELQRTS

A: For each NR, the encoding contig is depicted and the amino acid sequence of the LBD from N- to C-Terminus.

7.4. Putative amino acid sequence of EmNDK

MGSVSITASANVPVVGSHNRQVSLHVGDLHLLLECPIWGSNEGVPVHSEGESQPTSFLDGSLMNNVIYQWNIQGLPE
YAVAMDTFRFRFLEGGRRVVELTQPVTKSDAGIYQCSGVTGFGQKKVDFEVHVAVLCLMNPDLRPTIMTTEAELGS
AIDLSCEAIGREPIKYLWFMGNAVADWISSSQGVRGPILHIERVGREHIGQYVCQVKNPIGTLNITYRLTVKEPPSAIP
RIIGEVENQTLIAGSSGVLTCRVKCSCEPIIQWLKHVDPEDIDAYKAAGRSLVPLPAPRPAEAEFFYLALAKWEDAPA
YMERTVVQLHRTTSITATAAAAGEITVPEREFLSSRHEGEAEERLFVSRRLRGRPVSVPLHAGKYVVMTMSRSLKAI
DYAVAYVHIVPKSFNVTVHNIMVYCVPIALILLIAFVSLYCFLSRRNKDLEHPATRRGNVIFPPVVRGHSMSGVKKEY
RPIVRQTPQSSVFSNGNTVSNKSTSSRLPSYVAHSSPSQWNAATATASITSPSPHSNSFHNQSHVSPPTQLSPS
PSTFYNYSGLQSLSNQPTYWHPPAPSVATETSFDQYSAIMGNPPSASGGLSVSHSASSSQRPQLSFPNVMGSVSITA
SANVPVVGSHNRQVSLHVGDLHLLLECPIWGSNEGVPVHSEGESQPTSFLDGSLMNNVIYQWNIQGLPEYAVAMDT
RFRFLEGGRRVVELTQPVTKSDAGIYQCSGVTGFGQKKVDFEVHVAVLCLMNPDLRPTIMTTEAELGSAIDLSCEAI
GREPIKYLWFMGNAVADWISSSQGVRGPILHIERVGREHIGQYVCQVKNPIGTLNITYRLTVKEPPSAIPRIIGEVEN
QTLIAGSSGVLTCRVKCSCEPIIQWLKHVDPEDIDAYKAAGRSLVPLPAPRPAEAEFFYLALAKWEDAPAYMERTVV
QLHRTTSITATAAAAGEITVPEREFLSSRHEGEAEERLFVSRRLRGRPVSVPLHAGKYVVMTMSRSLKAI
DYAVAYVHIVPKSFNVTVHNIMVYCVPIALILLIAFVSLYCFLSRRNKDLEHPATRRGNVIFPPVVRGHSMSGVKKEYRPIVRQT
PQSSVFSNGNTVSNKSTSSRLPSYVAHSSPSQWNAATATASITSPSPHSNSFHNQSHVSPPTQLSPSPSTFYNY
SGLQSLSNQPTYWHPPAPSVATETSFDQYSAIMGNPPSASGGLSVSHSASSSQRPQLSFPNV

8. List of Abbreviations

aa	amino acid
AE	Alveolar Echinococcosis
AF 1	Activation Function 1
AF 2	Activation Function 2
aFGF	acidic Fibroblast Growth Factor
AKT	protein kinase B
APS	ammonium persulfate
Arg	arginine
AR-Smads	TGF- β /activin receptor regulated Smads
ATP	Adenosine triphosphate
BCL2	B-cell lymphoma 2
bFGF	basic Fibroblast Growth Factor
BIBF1120	„Vargatef“ (Z)-methyl3-(((4-(N-methyl-2-(4-methylpiperazin-1-yl)acetamido)phenyl)amino)(phenyl)methylene)-2-oxoindoline-6-carboxylate]
BMP	Bone Morphogenetic Protein
BMP2	Bone Morphogenetic Protein 2
BrdU	5-bromo-2'-deoxyuridine
BR-smad EmSmadE	BMP receptor regulated Smads
BS	bile salts
<i>C. elegans</i>	<i>Caenorhabditis elegans</i>
CA	cholic acid
CAR	Constitutive Androstane Receptor
CCND1	gene of G1/S-specific cyclin-D1
CDA	chenodesoxy acid
CDK inhibitors	Cyclin-dependent kinase inhibitors
cDNA	complementary Deoxyribonucleic Acid
CIP	calf intestinal phosphatase
<i>D. japonica</i>	<i>Dugesia japonica</i>
<i>D. melanogaster</i>	<i>Drosophila melanogaster</i>
DA	dafachronic acid
DAF12	abnormal dauer formation 12
DBD	DNA-binding domain
DCA	desoxycholic acid
DA	dafachronic acid
DjFGFR1	<i>Dugesia japonica</i> Fibroblast Growth Factor Receptor 1
DjFGFR2	<i>Dugesia japonica</i> Fibroblast Growth Factor Receptor 2
DjNDK	<i>Dugesia japonica</i> nou-darake
DMEM	Dulbecco's modified Eagle's medium
DmHNF4	<i>Drosophila melanogaster</i> Hepatocyte Nuclear Factor 4
DMSO	Dimethyl sulfoxide
DNA	deoxyribonucleic acid
DR5	Direct repeat 5

<i>E. multilocularis</i>	<i>Echinococcus multilocularis</i>
E2F1	human transcription factor E2F1
EGF	Epidermal Growth Factor
EGFR	Epidermal Growth Factor Receptor
EGL-15	<i>Caenorhabditis elegans</i> fibroblast growth factor receptor
ELISA	Enzyme-Linked Immunosorbent Assay
EmABP	<i>Echinococcus multilocularis</i> Apolipoprotein A-I Binding Protein
EmAlien	<i>Echinococcus multilocularis</i> Alien-like protein
Emelp	<i>Echinococcus multilocularis</i> ezrin-radixin-moesin-like protein
EmFR TkD-	<i>Echinococcus multilocularis</i> Fibroblast growth factor receptor tyrosine kinase mutant
EmFR	<i>Echinococcus multilocularis</i> Fibroblast Growth Factor-like Receptor
EmHNF4	<i>Echinococcus multilocularis</i> Hepatocyte Nuclear Factor 4-like
EmMPK1	<i>Echinococcus multilocularis</i> Mitogen-Activated Protein Kinase 1
EmMPK3	<i>Echinococcus multilocularis</i> Mitogen-Activated Protein Kinase 3
Emndk	<i>Echinococcus multilocularis</i> nou-darake-like
EmNHR1	<i>Echinococcus multilocularis</i> Nuclear Hormone Receptor 1
EmNHRs	<i>Echinococcus multilocularis</i> Nuclear Hormone Receptors
EmNIP1	<i>Echinococcus multilocularis</i> Normal Immunosuppressive Protein
EmSkip	<i>Echinococcus multilocularis</i> Ski-interacting protein
EmSmads	<i>Echinococcus multilocularis</i> Smads
EmTR1	<i>Echinococcus multilocularis</i> transforming growth factor- β receptor 1
Erk	extracellular signal-regulated kinases
ERM	ezrin-radixin-moesin
CESCKA	amino acid motif "Cysteine- Glutamic acid- Serine- Cysteine- Lysine- Alanine"
EST	expresses sequence tag
E-value	expect value
FBS	fetal bovine serum
FGF	Fibroblast growth factor
FGFR	Fibroblast growth factor receptor
FGFR-1, -2, and-3	human Fibroblast growth factor receptor-1, -2, -3
FGFRL1	fibroblast growth factor receptor like 1
Fig.	Figure
FRS2	fibroblast growth factor receptor substrate 2
Grb2	Growth factor receptor-bound protein 2
GTP	Guanidine triphosphate
GVBD	Germinal Vesicle Breakdown
HNF1	Hepatocyte Nuclear Factor 1
HNF4	Hepatocyte Nuclear Factor 4
<i>H. sapiens</i>	<i>Homo sapiens</i>
HR-96	<i>Drosophila</i> hormone receptor 96
HREs	Hormone responsive elements
Hs	<i>Homo sapiens</i>
IC50	half maximal inhibitory concentration

Ig	immunoglobulin
Igf	Insulin-like growth factor
IR	Insulin receptor
JM	juxtamembrane domain
JNK	juxtamembrane domain (JM)
LBD	ligand-binding domain
LCA	lithocholic acid
LXR	liver X receptor
MAP	mitogen-activated protein
MAPK	mitogen-activated protein kinase
Mc	Metacestod vesicle
MKK1	mitogen-activated protein kinase kinase 1
NDK	nou-darake
NHR	Nuclear Hormone Receptor
NHRs	Nuclear Hormone Receptors
NPC1	Niemann-Pick disease, type C1 protein
NR1	Nuclear Receptor 1 subfamily
Pa	activated protoscoleces
PAA	polyacrylamide
Pc	Primary cells
PCR	polymerase chain reaction
Pd	dormant protoscoleces
PDGFR	Platelet Derived Growth Factor
PIP3K/AKT	phosphatidylinositol 3,4,5-trisphosphate kinase/ protein kinase B pathway
PLC γ	Phospholipase C γ
PXR	pregnane X receptor
RACE	Rapid amplification of cDNA ends
Raf	rapidly growing fibrosarcoma or rat fibrosarcoma
RAP250	nuclear receptor-activating protein 250
Ras	Rat sarcoma
RH- cells	Rat hepatoma cells
RTK	receptor tyrosine kinases
RT-PCR	Reverse Transcription Polymerase Chain Reaction
RXR	Retinoid X receptor
<i>S. mansoni</i>	<i>Schistosoma mansoni</i>
SDS-PAGE	sodium dodecyl sulfate polyacrylamide gel electrophoresis
SEM	standard error of the mean
SER	<i>Schistosoma mansoni</i> epidermal growth factor receptor homologue
siRNA	small interference Ribonucleic acid
<i>S. japonicum</i>	<i>Schistosoma japonicum</i>
SKIP	Ski-interacting protein
SL	spliced leader
Sm	Schistosoma mansoni
SM	Skim milk

Sm2DBDba	<i>Schistosoma mansoni</i> nuclear receptor with 2 DNA-binding domains
SMART	Simple Modular Architecture Research Tool
SmDSF	<i>Schistosoma mansoni</i> homologue of <i>Drosophila</i> dissatisfaction gene
SmFTZ-F1 α	<i>Schistosoma mansoni</i> Fushi tarazu-factor 1 α
SmHR96a	<i>Schistosoma mansoni</i> homologue of <i>Drosophila</i> hormone receptor 96 alpha
SmNR1	<i>Schistosoma mansoni</i> nuclear receptor 1
SmPNR	<i>Schistosoma mansoni</i> homologue of photoreceptor-specific nuclear receptor
SmRAR-like receptors	<i>Schistosoma mansoni</i> retinoic acid receptor-like gene
SmRXR2	<i>Schistosoma mansoni</i> retinoid X receptor
SmTLL	<i>Schistosoma mansoni</i> homologue of <i>Drosophila</i> tailless gene
SmTRa	<i>Schistosoma mansoni</i> thyroid hormone receptor a
SmTRb	<i>Schistosoma mansoni</i> thyroid hormone receptor b
SNW/SKIP family	SKI-interacting protein family
SOS	Ras guanine nucleotide exchange factor SOS1/2
Src	sarcoma proto-oncogene tyrosine-protein kinase
SU5402	3-[3-(2-Carboxyethyl)-4-methylpyrrol-2-methylidenyl]-2-indolinone
tBLASTN	Search translated nucleotide database using a protein query Basic Local Alignment Search Tool
TEMED	<i>N,N,N',N'</i> -tetramethylethane-1,2-diamine (Merck)
TGF- β	Transforming Growth Factor- β
TM	Transmembrane Domain
TyrKc	Tyrosine Kinase Domain
VDR	Vitamin D3 Receptor
VEGFR-1,-2, and-3,	Vascular Endothelial Growth Factor Receptor-1, -2, -3

9. References

1. Gilbert SF (2000) *Developmental Biology*. Sunderland, MA: Sinauer Associates.
2. Gottstein B, Hemphill A (1997) Immunopathology of echinococcosis. *Chem Immunol* 66: 177-208.
3. Huttner M, Nakao M, Wassermann T, Siefert L, Boomker JD, et al. (2008) Genetic characterization and phylogenetic position of *Echinococcus felidis* (Cestoda: Taeniidae) from the African lion. *Int J Parasitol* 38: 861-868.
4. Thompson RC, McManus DP (2002) Towards a taxonomic revision of the genus *Echinococcus*. *Trends Parasitol* 18: 452-457.
5. Nakao M, McManus DP, Schantz PM, Craig PS, Ito A (2007) A molecular phylogeny of the genus *Echinococcus* inferred from complete mitochondrial genomes. *Parasitology* 134: 713-722.
6. Ito A, Nakao M, Sako Y (2007) Echinococcosis: serological detection of patients and molecular identification of parasites. *Future Microbiol* 2: 439-449.
7. Saarma U, Jogisalu I, Moks E, Varcasia A, Lavikainen A, et al. (2009) A novel phylogeny for the genus *Echinococcus*, based on nuclear data, challenges relationships based on mitochondrial evidence. *Parasitology* 136: 317-328.
8. Haag KL, Zaha A, Araujo AM, Gottstein B (1997) Reduced genetic variability within coding and non-coding regions of the *Echinococcus multilocularis* genome. *Parasitology* 115 (Pt 5): 521-529.
9. Rinder H, Rausch RL, Takahashi K, Kopp H, Thomschke A, et al. (1997) Limited range of genetic variation in *Echinococcus multilocularis*. *J Parasitol* 83: 1045-1050.
10. Craig P (2003) *Echinococcus multilocularis*. *Curr Opin Infect Dis* 16: 437-444.
11. Romig T, Dinkel A, Mackenstedt U (2006) The present situation of echinococcosis in Europe. *Parasitol Int* 55 Suppl: S187-191.
12. Deplazes P, Hegglin D, Gloor S, Romig T (2004) Wilderness in the city: the urbanization of *Echinococcus multilocularis*. *Trends Parasitol* 20: 77-84.
13. Eckert J, Deplazes P (2004) Biological, epidemiological, and clinical aspects of echinococcosis, a zoonosis of increasing concern. *Clin Microbiol Rev* 17: 107-135.
14. Lethbridge LC (1980) The biology of the oncosphere of cyclophyllidean cestodes. *Helminthological Abstracts, Series A* 49: 59-72.
15. Dixon JB (1997) Echinococcosis. *Comp Immunol Microbiol Infect Dis* 20: 87-94.
16. Rogan MT, Hai WY, Richardson R, Zeyhle E, Craig PS (2006) Hydatid cysts: does every picture tell a story? *Trends Parasitol* 22: 431-438.
17. Lanier AP, Trujillo DE, Schantz PM, Wilson JF, Gottstein B, et al. (1987) Comparison of serologic tests for the diagnosis and follow-up of alveolar hydatid disease. *Am J Trop Med Hyg* 37: 609-615.
18. Rausch RL, D'Alessandro A (1999) Histogenesis in the metacestode of *Echinococcus vogeli* and mechanism of pathogenesis in polycystic hydatid disease. *J Parasitol* 85: 410-418.
19. Ingold K, Bigler P, Thormann W, Cavaliero T, Gottstein B, et al. (1999) Efficacies of albendazole sulfoxide and albendazole sulfone against *In vitro*-cultivated *Echinococcus multilocularis* metacestodes. *Antimicrob Agents Chemother* 43: 1052-1061.
20. Brehm K (2010) The role of evolutionarily conserved signalling systems in *Echinococcus multilocularis* development and host-parasite interaction. *Med Microbiol Immunol*.
21. Kern P (2010) Clinical features and treatment of alveolar echinococcosis. *Curr Opin Infect Dis* 23: 505-512.
22. Kern P, Bardonnnet K, Renner E, Auer H, Pawlowski Z, et al. (2003) European echinococcosis registry: human alveolar echinococcosis, Europe, 1982-2000. *Emerg Infect Dis* 9: 343-349.
23. Gottstein B, D'Alessandro A, Rausch RL (1995) Immunodiagnosis of polycystic hydatid disease/polycystic echinococcosis due to *Echinococcus vogeli*. *Am J Trop Med Hyg* 53: 558-563.

24. Hubner MP, Manfras BJ, Margos MC, Eiffler D, Hoffmann WH, et al. (2006) *Echinococcus multilocularis* metacystodes modulate cellular cytokine and chemokine release by peripheral blood mononuclear cells in alveolar echinococcosis patients. *Clin Exp Immunol* 145: 243-251.
25. Kocherscheidt L, Flakowski AK, Gruner B, Hamm DM, Dietz K, et al. (2008) *Echinococcus multilocularis*: inflammatory and regulatory chemokine responses in patients with progressive, stable and cured alveolar echinococcosis. *Exp Parasitol* 119: 467-474.
26. Sturm D, Menzel J, Gottstein B, Kern P (1995) Interleukin-5 is the predominant cytokine produced by peripheral blood mononuclear cells in alveolar echinococcosis. *Infect Immun* 63: 1688-1697.
27. Brunetti E, Kern P, Vuitton DA (2011) Expert consensus for the diagnosis and treatment of cystic and alveolar echinococcosis in humans. *Acta Trop* 114: 1-16.
28. Reuter S, Jensen B, Buttenschoen K, Kratzer W, Kern P (2000) Benzimidazoles in the treatment of alveolar echinococcosis: a comparative study and review of the literature. *J Antimicrob Chemother* 46: 451-456.
29. Hemphill A, Spicher M, Stadelmann B, Mueller J, Naguleswaran A, et al. (2007) Innovative chemotherapeutical treatment options for alveolar and cystic echinococcosis. *Parasitology* 134: 1657-1670.
30. Buhl L (1856) Briefliche Mittheilungen: Ueber die zusammengesetzte Echinokokkengeschwulst der Leber. *Verh der physicalisch-medicinischen Gesellschaft* 6: 428-429.
31. Virchow R (1856) Die multiloculäre, ulcerirende Echinokokkengeschwulst der Leber. *Verh der physicalisch-medicinischen Gesellschaft* 6: 84-95.
32. Frosch PM, Frosch M, Pfister T, Schaad V, Bitter-Suermann D (1991) Cloning and characterisation of an immunodominant major surface antigen of *Echinococcus multilocularis*. *Mol Biochem Parasitol* 48: 121-130.
33. Frosch PM, Geier C, Kaup FJ, Muller A, Frosch M (1993) Molecular cloning of an echinococcal microtrichal antigen immunoreactive in *Echinococcus multilocularis* disease. *Mol Biochem Parasitol* 58: 301-310.
34. Gottstein B, Tschudi K, Eckert J, Ammann R (1989) Em2-ELISA for the follow-up of alveolar echinococcosis after complete surgical resection of liver lesions. *Trans R Soc Trop Med Hyg* 83: 389-393.
35. Ito A, Osawa Y, Nakao M, Horii T, Okamoto M, et al. (1995) Em18 and Em16, new serologic marker epitopes for alveolar echinococcosis in western blot analysis, are the only two epitopes recognized by commercially available weak positive (cut off) sera for Em2plus-ELISA. *J Helminthol* 69: 369-371.
36. Brehm K, Jensen K, Frosch P, Frosch M (1999) Characterization of the genomic locus expressing the ERM-like protein of *Echinococcus multilocularis*. *Mol Biochem Parasitol* 100: 147-152.
37. Hubert K, Zavala-Gongora R, Frosch M, Brehm K (2004) Identification and characterization of PDZ-1, a N-ERMAD specific interaction partner of the *Echinococcus multilocularis* ERM protein Elp. *Mol Biochem Parasitol* 134: 149-154.
38. Louvet-Vallee S (2000) ERM proteins: from cellular architecture to cell signaling. *Biol Cell* 92: 305-316.
39. Brehm K, Jensen K, Frosch M (2000) mRNA trans-splicing in the human parasitic cestode *Echinococcus multilocularis*. *J Biol Chem* 275: 38311-38318.
40. Borst P (1986) Discontinuous transcription and antigenic variation in trypanosomes. *Annu Rev Biochem* 55: 701-732.
41. Blumenthal T (1995) Trans-splicing and polycistronic transcription in *Caenorhabditis elegans*. *Trends Genet* 11: 132-136.
42. Nilsen TW (1993) Trans-splicing of nematode premessenger RNA. *Annu Rev Microbiol* 47: 413-440.
43. Nilsen TW (1995) trans-splicing: an update. *Mol Biochem Parasitol* 73: 1-6.

44. Brehm K, Wolf M, Beland H, Kroner A, Frosch M (2003) Analysis of differential gene expression in *Echinococcus multilocularis* larval stages by means of spliced leader differential display. *Int J Parasitol* 33: 1145-1159.
45. Brehm K, Hubert K, Sciuotto E, Garate T, Frosch M (2002) Characterization of a spliced leader gene and of trans-spliced mRNAs from *Taenia solium*. *Mol Biochem Parasitol* 122: 105-110.
46. Jura H, Bader A, Hartmann M, Maschek H, Frosch M (1996) Hepatic tissue culture model for study of host-parasite interactions in alveolar echinococcosis. *Infect Immun* 64: 3484-3490.
47. Hemphill A, Gottstein B (1995) Immunology and morphology studies on the proliferation of in vitro cultivated *Echinococcus multilocularis* metacestodes. *Parasitol Res* 81: 605-614.
48. Spiliotis M, Tappe D, Sesterhenn L, Brehm K (2004) Long-term in vitro cultivation of *Echinococcus multilocularis* metacestodes under axenic conditions. *Parasitol Res* 92: 430-432.
49. Spiliotis M, Brehm K (2009) Axenic in vitro cultivation of *Echinococcus multilocularis* metacestode vesicles and the generation of primary cell cultures. *Methods Mol Biol* 470: 245-262.
50. Spiliotis M, Lechner S, Tappe D, Scheller C, Krohne G, et al. (2008) Transient transfection of *Echinococcus multilocularis* primary cells and complete in vitro regeneration of metacestode vesicles. *Int J Parasitol* 38: 1025-1039.
51. Gelmedin V, Caballero-Gamiz R, Brehm K (2008) Characterization and inhibition of a p38-like mitogen-activated protein kinase (MAPK) from *Echinococcus multilocularis*: Antiparasitic activities of p38 MAPK inhibitors. *Biochem Pharmacol*.
52. Gelmedin V, Spiliotis M, Brehm K (2010) Molecular characterisation of MEK1/2- and MKK3/6-like mitogen-activated protein kinase kinases (MAPKK) from the fox tapeworm *Echinococcus multilocularis*. *Int J Parasitol* 40: 555-567.
53. Konrad C, Kroner A, Spiliotis M, Zavala-Gongora R, Brehm K (2003) Identification and molecular characterisation of a gene encoding a member of the insulin receptor family in *Echinococcus multilocularis*. *Int J Parasitol* 33: 301-312.
54. Spiliotis M, Brehm K (2004) *Echinococcus multilocularis*: identification and molecular characterization of a Ral-like small GTP-binding protein. *Exp Parasitol* 107: 163-172.
55. Spiliotis M, Konrad C, Gelmedin V, Tappe D, Bruckner S, et al. (2006) Characterisation of EmMPK1, an ERK-like MAP kinase from *Echinococcus multilocularis* which is activated in response to human epidermal growth factor. *Int J Parasitol* 36: 1097-1112.
56. Spiliotis M, Kroner A, Brehm K (2003) Identification, molecular characterization and expression of the gene encoding the epidermal growth factor receptor orthologue from the fox-tapeworm *Echinococcus multilocularis*. *Gene* 323: 57-65.
57. Spiliotis M, Tappe D, Bruckner S, Mosch HU, Brehm K (2005) Molecular cloning and characterization of Ras- and Raf-homologues from the fox-tapeworm *Echinococcus multilocularis*. *Mol Biochem Parasitol* 139: 225-237.
58. Zavala-Gongora R, Derrer B, Gelmedin V, Knaus P, Brehm K (2008) Molecular characterisation of a second structurally unusual AR-Smad without an MH1 domain and a Smad4 orthologue from *Echinococcus multilocularis*. *Int J Parasitol* 38: 161-176.
59. Zavala-Gongora R, Kroner A, Bernthaler P, Knaus P, Brehm K (2006) A member of the transforming growth factor-beta receptor family from *Echinococcus multilocularis* is activated by human bone morphogenetic protein 2. *Mol Biochem Parasitol* 146: 265-271.
60. Zavala-Gongora R, Kroner A, Wittek B, Knaus P, Brehm K (2003) Identification and characterisation of two distinct Smad proteins from the fox-tapeworm *Echinococcus multilocularis*. *Int J Parasitol* 33: 1665-1677.
61. Gelmedin V, Zavala-Gongora R, Fernandez C, Brehm K (2005) *Echinococcus multilocularis*: cloning and characterization of a member of the SNW/SKIP family of transcriptional coregulators. *Exp Parasitol* 111: 115-120.
62. Günthel D (2005) Molekulare Charakterisierung von Komponenten des Nukleären-Hormon-Rezeptor-Signallings in *Echinococcus multilocularis*. [MD]. Würzburg: University of Würzburg. 109 p.

63. Itoh N (2007) The Fgf families in humans, mice, and zebrafish: their evolutionary processes and roles in development, metabolism, and disease. *Biol Pharm Bull* 30: 1819-1825.
64. Itoh N, Ornitz DM (2004) Evolution of the Fgf and Fgfr gene families. *Trends Genet* 20: 563-569.
65. Dailey L, Ambrosetti D, Mansukhani A, Basilico C (2005) Mechanisms underlying differential responses to FGF signaling. *Cytokine Growth Factor Rev* 16: 233-247.
66. Ornitz DM (2000) FGFs, heparan sulfate and FGFRs: complex interactions essential for development. *Bioessays* 22: 108-112.
67. Ornitz DM, Itoh N (2001) Fibroblast growth factors. *Genome Biol* 2: REVIEWS3005.
68. Powers CJ, McLeskey SW, Wellstein A (2000) Fibroblast growth factors, their receptors and signaling. *Endocr Relat Cancer* 7: 165-197.
69. Schlessinger J, Plotnikov AN, Ibrahimi OA, Eliseenkova AV, Yeh BK, et al. (2000) Crystal structure of a ternary FGF-FGFR-heparin complex reveals a dual role for heparin in FGFR binding and dimerization. *Mol Cell* 6: 743-750.
70. Knights V, Cook SJ (2010) De-regulated FGF receptors as therapeutic targets in cancer. *Pharmacol Ther* 125: 105-117.
71. Wiedemann M, Trueb B (2000) Characterization of a novel protein (FGFRL1) from human cartilage related to FGF receptors. *Genomics* 69: 275-279.
72. Bertrand S, Somorjai I, Garcia-Fernandez J, Lamonerie T, Escriva H (2009) FGFRL1 is a neglected putative actor of the FGF signalling pathway present in all major metazoan phyla. *BMC Evol Biol* 9: 226.
73. Sleeman M, Fraser J, McDonald M, Yuan S, White D, et al. (2001) Identification of a new fibroblast growth factor receptor, FGFR5. *Gene* 271: 171-182.
74. Rieckmann T, Kotevic I, Trueb B (2008) The cell surface receptor FGFRL1 forms constitutive dimers that promote cell adhesion. *Exp Cell Res* 314: 1071-1081.
75. Trueb B, Zhuang L, Taeschler S, Wiedemann M (2003) Characterization of FGFRL1, a novel fibroblast growth factor (FGF) receptor preferentially expressed in skeletal tissues. *J Biol Chem* 278: 33857-33865.
76. Steinberg F, Gerber SD, Rieckmann T, Trueb B (2010) Rapid fusion and syncytium formation of heterologous cells upon expression of the FGFRL1 receptor. *J Biol Chem* 285: 37704-37715.
77. Steinberg F, Zhuang L, Beyeler M, Kalin RE, Mullis PE, et al. (2010) The FGFRL1 receptor is shed from cell membranes, binds fibroblast growth factors (FGFs), and antagonizes FGF signaling in *Xenopus* embryos. *J Biol Chem* 285: 2193-2202.
78. Gerber SD, Steinberg F, Beyeler M, Villiger PM, Trueb B (2009) The murine Fgfr1 receptor is essential for the development of the metanephric kidney. *Dev Biol* 335: 106-119.
79. Rieckmann T, Zhuang L, Fluck CE, Trueb B (2009) Characterization of the first FGFRL1 mutation identified in a craniosynostosis patient. *Biochim Biophys Acta* 1792: 112-121.
80. Luedi PP, Dietrich FS, Weidman JR, Bosko JM, Jirtle RL, et al. (2007) Computational and experimental identification of novel human imprinted genes. *Genome Res* 17: 1723-1730.
81. Greber B, Lehrach H, Adjaye J (2007) Silencing of core transcription factors in human EC cells highlights the importance of autocrine FGF signaling for self-renewal. *BMC Dev Biol* 7: 46.
82. Ogawa K, Kobayashi C, Hayashi T, Oritani H, Watanabe K, et al. (2002) Planarian fibroblast growth factor receptor homologs expressed in stem cells and cephalic ganglions. *Dev Growth Differ* 44: 191-204.
83. Ogawa K, Wakayama A, Kunisada T, Oritani H, Watanabe K, et al. (1998) Identification of a receptor tyrosine kinase involved in germ cell differentiation in planarians. *Biochem Biophys Res Commun* 248: 204-209.
84. Cebria F, Kobayashi C, Umesono Y, Nakazawa M, Mineta K, et al. (2002) FGFR-related gene *nou-darake* restricts brain tissues to the head region of planarians. *Nature* 419: 620-624.
85. DeVore DL, Horvitz HR, Stern MJ (1995) An FGF receptor signaling pathway is required for the normal cell migrations of the sex myoblasts in *C. elegans* hermaphrodites. *Cell* 83: 611-620.

86. Birnbaum D, Popovici C, Roubin R (2005) A pair as a minimum: the two fibroblast growth factors of the nematode *Caenorhabditis elegans*. *Dev Dyn* 232: 247-255.
87. Huang P, Stern MJ (2004) FGF signaling functions in the hypodermis to regulate fluid balance in *C. elegans*. *Development* 131: 2595-2604.
88. Roubin R, Naert K, Popovici C, Vatcher G, Coulier F, et al. (1999) let-756, a *C. elegans* fgf essential for worm development. *Oncogene* 18: 6741-6747.
89. Branda CS, Stern MJ (2000) Mechanisms controlling sex myoblast migration in *Caenorhabditis elegans* hermaphrodites. *Dev Biol* 226: 137-151.
90. Bulow HE, Boulin T, Hobert O (2004) Differential functions of the *C. elegans* FGF receptor in axon outgrowth and maintenance of axon position. *Neuron* 42: 367-374.
91. Burdine RD, Branda CS, Stern MJ (1998) EGL-17(FGF) expression coordinates the attraction of the migrating sex myoblasts with vulval induction in *C. elegans*. *Development* 125: 1083-1093.
92. Burdine RD, Chen EB, Kwok SF, Stern MJ (1997) egl-17 encodes an invertebrate fibroblast growth factor family member required specifically for sex myoblast migration in *Caenorhabditis elegans*. *Proc Natl Acad Sci U S A* 94: 2433-2437.
93. Lo TW, Branda CS, Huang P, Sasson IE, Goodman SJ, et al. (2008) Different isoforms of the *C. elegans* FGF receptor are required for attraction and repulsion of the migrating sex myoblasts. *Dev Biol* 318: 268-275.
94. Schäfer T (2006) Molekulare Charakterisierung einer Tyrosinkinase der fibroblas growth factor-Rezeptorfamilie des Fuchsbandwurms *Echinococcus multilocularis*. Würzburg: University of Würzburg.
95. Letunic I, Doerks T, Bork P (2009) SMART 6: recent updates and new developments. *Nucleic Acids Res* 37: D229-232.
96. Schultz J, Milpetz F, Bork P, Ponting CP (1998) SMART, a simple modular architecture research tool: identification of signaling domains. *Proc Natl Acad Sci U S A* 95: 5857-5864.
97. Laudet V, Gronemeyer H (2002) The nuclear receptors factsbook: London: Academic Press.
98. Lazar MA (1999) Nuclear hormone receptors: from molecules to diseases. *J Investig Med* 47: 364-368.
99. Love JD, Gooch JT, Nagy L, Chatterjee VK, Schwabe JW (2000) Transcriptional repression by nuclear receptors: mechanisms and role in disease. *Biochem Soc Trans* 28: 390-396.
100. Margolis RN, Evans RM, O'Malley BW (2005) The Nuclear Receptor Signaling Atlas: development of a functional atlas of nuclear receptors. *Mol Endocrinol* 19: 2433-2436.
101. Zhao X, Patton JR, Davis SL, Florence B, Ames SJ, et al. (2004) Regulation of nuclear receptor activity by a pseudouridine synthase through posttranscriptional modification of steroid receptor RNA activator. *Mol Cell* 15: 549-558.
102. Robinson-Rechavi M, Escriva Garcia H, Laudet V (2003) The nuclear receptor superfamily. *J Cell Sci* 116: 585-586.
103. Sluder AE, Mathews SW, Hough D, Yin VP, Maina CV (1999) The nuclear receptor superfamily has undergone extensive proliferation and diversification in nematodes. *Genome Res* 9: 103-120.
104. Berriman M, Haas BJ, LoVerde PT, Wilson RA, Dillon GP, et al. (2009) The genome of the blood fluke *Schistosoma mansoni*. *Nature* 460: 352-358.
105. Wu W, Loverde PT (2011) Nuclear hormone receptors in parasitic helminths. *Mol Cell Endocrinol* 334: 56-66.
106. Novac N, Heinzl T (2004) Nuclear receptors: overview and classification. *Curr Drug Targets Inflamm Allergy* 3: 335-346.
107. McKenna NJ, Lanz RB, O'Malley BW (1999) Nuclear receptor coregulators: cellular and molecular biology. *Endocr Rev* 20: 321-344.
108. Baniahmad A, Leng X, Burris TP, Tsai SY, Tsai MJ, et al. (1995) The tau 4 activation domain of the thyroid hormone receptor is required for release of a putative corepressor(s) necessary for transcriptional silencing. *Mol Cell Biol* 15: 76-86.

109. Bourguet W, Germain P, Gronemeyer H (2000) Nuclear receptor ligand-binding domains: three-dimensional structures, molecular interactions and pharmacological implications. *Trends Pharmacol Sci* 21: 381-388.
110. Picard D (1998) Molecular endocrinology. Steroids tickle cells inside and out. *Nature* 392: 437-438.
111. Wehling M (1997) Specific, nongenomic actions of steroid hormones. *Annu Rev Physiol* 59: 365-393.
112. Kouzarides T (2000) Acetylation: a regulatory modification to rival phosphorylation? *Embo J* 19: 1176-1179.
113. Perissi V, Rosenfeld MG (2005) Controlling nuclear receptors: the circular logic of cofactor cycles. *Nat Rev Mol Cell Biol* 6: 542-554.
114. Yanagisawa J, Yanagi Y, Masuhiro Y, Suzawa M, Watanabe M, et al. (1999) Convergence of transforming growth factor-beta and vitamin D signaling pathways on SMAD transcriptional coactivators. *Science* 283: 1317-1321.
115. Committee NRN (1999) A unified nomenclature system for the nuclear receptor superfamily. *Cell* 97: 161-163.
116. Baker AR, McDonnell DP, Hughes M, Crisp TM, Mangelsdorf DJ, et al. (1988) Cloning and expression of full-length cDNA encoding human vitamin D receptor. *Proc Natl Acad Sci U S A* 85: 3294-3298.
117. Bertilsson G, Heidrich J, Svensson K, Asman M, Jendeberg L, et al. (1998) Identification of a human nuclear receptor defines a new signaling pathway for CYP3A induction. *Proc Natl Acad Sci U S A* 95: 12208-12213.
118. Kliewer SA, Moore JT, Wade L, Staudinger JL, Watson MA, et al. (1998) An orphan nuclear receptor activated by pregnanes defines a novel steroid signaling pathway. *Cell* 92: 73-82.
119. Baes M, Gulick T, Choi HS, Martinoli MG, Simha D, et al. (1994) A new orphan member of the nuclear hormone receptor superfamily that interacts with a subset of retinoic acid response elements. *Mol Cell Biol* 14: 1544-1552.
120. Antebi A, Yeh WH, Tait D, Hedgecock EM, Riddle DL (2000) *daf-12* encodes a nuclear receptor that regulates the dauer diapause and developmental age in *C. elegans*. *Genes Dev* 14: 1512-1527.
121. Ogawa A, Streit A, Antebi A, Sommer RJ (2009) A conserved endocrine mechanism controls the formation of dauer and infective larvae in nematodes. *Curr Biol* 19: 67-71.
122. Wang Z, Zhou XE, Motola DL, Gao X, Suino-Powell K, et al. (2009) Identification of the nuclear receptor DAF-12 as a therapeutic target in parasitic nematodes. *Proc Natl Acad Sci U S A* 106: 9138-9143.
123. Fisk GJ, Thummel CS (1995) Isolation, regulation, and DNA-binding properties of three *Drosophila* nuclear hormone receptor superfamily members. *Proc Natl Acad Sci U S A* 92: 10604-10608.
124. Sladek FM, Zhong WM, Lai E, Darnell JE, Jr. (1990) Liver-enriched transcription factor HNF-4 is a novel member of the steroid hormone receptor superfamily. *Genes Dev* 4: 2353-2365.
125. Hayhurst GP, Lee YH, Lambert G, Ward JM, Gonzalez FJ (2001) Hepatocyte nuclear factor 4alpha (nuclear receptor 2A1) is essential for maintenance of hepatic gene expression and lipid homeostasis. *Mol Cell Biol* 21: 1393-1403.
126. Li J, Ning G, Duncan SA (2000) Mammalian hepatocyte differentiation requires the transcription factor HNF-4alpha. *Genes Dev* 14: 464-474.
127. Stoffel M, Duncan SA (1997) The maturity-onset diabetes of the young (MODY1) transcription factor HNF4alpha regulates expression of genes required for glucose transport and metabolism. *Proc Natl Acad Sci U S A* 94: 13209-13214.
128. Watt AJ, Garrison WD, Duncan SA (2003) HNF4: a central regulator of hepatocyte differentiation and function. *Hepatology* 37: 1249-1253.

129. Hertz R, Magenheim J, Berman I, Bar-Tana J (1998) Fatty acyl-CoA thioesters are ligands of hepatic nuclear factor-4 α . *Nature* 392: 512-516.
130. Chou WC, Prokova V, Shiraishi K, Valcourt U, Moustakas A, et al. (2003) Mechanism of a transcriptional cross talk between transforming growth factor- β -regulated Smad3 and Smad4 proteins and orphan nuclear receptor hepatocyte nuclear factor-4. *Mol Biol Cell* 14: 1279-1294.
131. Jiang G, Nepomuceno L, Yang Q, Sladek FM (1997) Serine/threonine phosphorylation of orphan receptor hepatocyte nuclear factor 4. *Arch Biochem Biophys* 340: 1-9.
132. Soutoglou E, Katrakili N, Talianidis I (2000) Acetylation regulates transcription factor activity at multiple levels. *Mol Cell* 5: 745-751.
133. Consortium SjGSaFA (2009) The *Schistosoma japonicum* genome reveals features of host-parasite interplay. *Nature* 460: 345-351.
134. Wu W, Niles EG, Hirai H, LoVerde PT (2007) Identification and characterization of a nuclear receptor subfamily I member in the Platyhelminth *Schistosoma mansoni* (SmNR1). *FEBS J* 274: 390-405.
135. de Mendonca RL, Escriva H, Bouton D, Zelus D, Vanacker JM, et al. (2000) Structural and functional divergence of a nuclear receptor of the RXR family from the trematode parasite *Schistosoma mansoni*. *Eur J Biochem* 267: 3208-3219.
136. Freebern WJ, Niles EG, LoVerde PT (1999) RXR-2, a member of the retinoid x receptor family in *Schistosoma mansoni*. *Gene* 233: 33-38.
137. Freebern WJ, Osman A, Niles EG, Christen L, LoVerde PT (1999) Identification of a cDNA encoding a retinoid X receptor homologue from *Schistosoma mansoni*. Evidence for a role in female-specific gene expression. *J Biol Chem* 274: 4577-4585.
138. Lu C, Wu W, Niles EG, LoVerde PT (2006) Identification and characterization of a novel fushi tarazu factor 1 (FTZ-F1) nuclear receptor in *Schistosoma mansoni*. *Mol Biochem Parasitol* 150: 25-36.
139. Hu R, Niles EG, LoVerde PT (2006) DNA binding and transactivation properties of the *Schistosoma mansoni* constitutive androstane receptor homologue. *Mol Biochem Parasitol* 150: 174-185.
140. Wu W, Niles EG, El-Sayed N, Berriman M, LoVerde PT (2006) *Schistosoma mansoni* (Platyhelminthes, Trematoda) nuclear receptors: sixteen new members and a novel subfamily. *Gene* 366: 303-315.
141. Wu W, Niles EG, Hirai H, LoVerde PT (2007) Evolution of a novel subfamily of nuclear receptors with members that each contain two DNA binding domains. *BMC Evol Biol* 7: 27.
142. Wahab MF, Warren KS, Levy RP (1971) Function of the thyroid and the host-parasite relation in murine schistosomiasis mansoni. *J Infect Dis* 124: 161-171.
143. Escobedo G, Larralde C, Chavarria A, Cerbon MA, Morales-Montor J (2004) Molecular mechanisms involved in the differential effects of sex steroids on the reproduction and infectivity of *Taenia crassiceps*. *J Parasitol* 90: 1235-1244.
144. Escobedo G, Roberts CW, Carrero JC, Morales-Montor J (2005) Parasite regulation by host hormones: an old mechanism of host exploitation? *Trends Parasitol* 21: 588-593.
145. Forster S, Gunthel D, Kiss F, Brehm K (2011) Molecular characterization of a serum-responsive, DAF-12-like nuclear hormone receptor of the fox-tapeworm *Echinococcus multilocularis*. *J Cell Biochem*.
146. Bethony JM, Cole RN, Guo X, Kamhawi S, Lightowers MW, et al. (2011) Vaccines to combat the neglected tropical diseases. *Immunol Rev* 239: 237-270.
147. Spiliotis M, Mizukami C, Oku Y, Kiss F, Brehm K, et al. (2010) *Echinococcus multilocularis* primary cells: improved isolation, small-scale cultivation and RNA interference. *Mol Biochem Parasitol* 174: 83-87.
148. Brehm K, Spiliotis M (2008) Recent advances in the in vitro cultivation and genetic manipulation of *Echinococcus multilocularis* metacestodes and germinal cells. *Exp Parasitol* 119: 506-515.

149. Hemphill A, Stettler M, Walker M, Siles-Lucas M, Fink R, et al. (2002) Culture of *Echinococcus multilocularis* metacestodes: an alternative to animal use. *Trends Parasitol* 18: 445-451.
150. Brehm K (2010) *Echinococcus multilocularis* as an experimental model in stem cell research and molecular host-parasite interaction. *Parasitology* 137: 537-555.
151. Bente M, Harder S, Wiesgigl M, Heukeshoven J, Gelhaus C, et al. (2003) Developmentally induced changes of the proteome in the protozoan parasite *Leishmania donovani*. *Proteomics* 3: 1811-1829.
152. Rabilloud T, Vuillard L, Gilly C, Lawrence JJ (1994) Silver-staining of proteins in polyacrylamide gels: a general overview. *Cell Mol Biol (Noisy-le-grand)* 40: 57-75.
153. Hubert K, Cordero E, Frosch M, Solomon F (1999) Activities of the EM10 protein from *Echinococcus multilocularis* in cultured mammalian cells demonstrate functional relationships to ERM family members. *Cell Motil Cytoskeleton* 42: 178-188.
154. Mojtahedi Z, Clos J, Kamali-Sarvestani E (2008) *Leishmania major*: identification of developmentally regulated proteins in procyclic and metacyclic promastigotes. *Exp Parasitol* 119: 422-429.
155. Browaeys-Poly E, Perdereau D, Lescuyer A, Burnol AF, Cailliau K (2009) Akt interaction with PLC(γ) regulates the G(2)/M transition triggered by FGF receptors from MDA-MB-231 breast cancer cells. *Anticancer Res* 29: 4965-4969.
156. Browaeys-Poly E, Cailliau K, Vilain JP (2000) Signal transduction pathways triggered by fibroblast growth factor receptor 1 expressed in *Xenopus laevis* oocytes after fibroblast growth factor 1 addition. Role of Grb2, phosphatidylinositol 3-kinase, Src tyrosine kinase, and phospholipase C γ . *Eur J Biochem* 267: 6256-6263.
157. Altschul SF, Gish W, Miller W, Myers EW, Lipman DJ (1990) Basic local alignment search tool. *J Mol Biol* 215: 403-410.
158. Altschul SF, Madden TL, Schaffer AA, Zhang J, Zhang Z, et al. (1997) Gapped BLAST and PSI-BLAST: a new generation of protein database search programs. *Nucleic Acids Res* 25: 3389-3402.
159. Letunic I, Copley RR, Schmidt S, Ciccarelli FD, Doerks T, et al. (2004) SMART 4.0: towards genomic data integration. *Nucleic Acids Res* 32: D142-144.
160. Spiliotis M, Mizukami C, Oku Y, Kiss F, Brehm K, et al. *Echinococcus multilocularis* primary cells: improved isolation, small-scale cultivation and RNA interference. *Mol Biochem Parasitol* 174: 83-87.
161. Spiliotis M (2006) Untersuchungen zur in vitro Kultivierung und Charakterisierung von MAP-Kinase-Kaskade-Komponenten des Fuchsbandwurmes *Echinococcus multilocularis* [PhD]. Würzburg: University of Würzburg. 273 p.
162. Arpin M, Chirivino D, Naba A, Zwaenepoel I (2011) Emerging role for ERM proteins in cell adhesion and migration. *Cell Adh Migr* 5: 199-206.
163. Tsukita S, Yonemura S (1997) ERM (ezrin/radixin/moesin) family: from cytoskeleton to signal transduction. *Curr Opin Cell Biol* 9: 70-75.
164. Rappaport AC, Krufka A, Olwin BB (1991) Requirement of heparan sulfate for bFGF-mediated fibroblast growth and myoblast differentiation. *Science* 252: 1705-1708.
165. Yayon A, Klagsbrun M, Esko JD, Leder P, Ornitz DM (1991) Cell surface, heparin-like molecules are required for binding of basic fibroblast growth factor to its high affinity receptor. *Cell* 64: 841-848.
166. Lambaerts K, Wilcox-Adelman SA, Zimmermann P (2009) The signaling mechanisms of syndecan heparan sulfate proteoglycans. *Curr Opin Cell Biol* 21: 662-669.
167. Choi SC, Kim SJ, Choi JH, Park CY, Shim WJ, et al. (2008) Fibroblast growth factor-2 and -4 promote the proliferation of bone marrow mesenchymal stem cells by the activation of the PI3K-Akt and ERK1/2 signaling pathways. *Stem Cells Dev* 17: 725-736.

168. Vicogne J, Cailliau K, Tulasne D, Browaeyts E, Yan YT, et al. (2004) Conservation of epidermal growth factor receptor function in the human parasitic helminth *Schistosoma mansoni*. *J Biol Chem* 279: 37407-37414.
169. Haccard O, Lewellyn A, Hartley RS, Erikson E, Maller JL (1995) Induction of *Xenopus* oocyte meiotic maturation by MAP kinase. *Dev Biol* 168: 677-682.
170. Gelmedin V (2008) Targeting flatworm signaling cascades for the development of novel antihelminthic drugs [PhD]. Würzburg: University of Würzburg. 133 p.
171. Chen Y, Li X, Eswarakumar VP, Seger R, Lonai P (2000) Fibroblast growth factor (FGF) signaling through PI 3-kinase and Akt/PKB is required for embryoid body differentiation. *Oncogene* 19: 3750-3756.
172. Yun YR, Won JE, Jeon E, Lee S, Kang W, et al. (2011) Fibroblast growth factors: biology, function, and application for tissue regeneration. *J Tissue Eng* 2010: 218142.
173. Hemer S (2008) Molekulargenetische und zellbiologische Untersuchungen zum Insulin-Signaling in *Echinococcus multilocularis* [Diploma]. Würzburg: University of Würzburg. 150 p.
174. Moore JM, Guy RK (2005) Coregulator interactions with the thyroid hormone receptor. *Mol Cell Proteomics* 4: 475-482.
175. Lonard DM, O'Malley BW (2006) The expanding cosmos of nuclear receptor coactivators. *Cell* 125: 411-414.
176. Epping K, Brehm K (2011) *Echinococcus multilocularis*: Molecular characterization of EmSmadE, a novel BR-Smad involved in TGF-beta and BMP signaling. *Exp Parasitol*.
177. Reiher C (2008) Molekulare Charakterisierung von Signalosom-Komponenten des Fuchsbandwurms *Echinococcus multilocularis* [Diploma]. Würzburg: University of Würzburg. 112 p.
178. Gelmedin V (2005) Molekulare Charakterisierung von Komponenten des nukleären Hormonrezeptor-Signaling beim Fuchsbandwurm *Echinococcus multilocularis* [Diploma]. Würzburg: University of Würzburg. 113 p.
179. Chauchereau A, Georgiakaki M, Perrin-Wolff M, Milgrom E, Loosfelt H (2000) JAB1 interacts with both the progesterone receptor and SRC-1. *J Biol Chem* 275: 8540-8548.
180. Shackleford TJ, Claret FX (2010) JAB1/CSN5: a new player in cell cycle control and cancer. *Cell Div* 5: 26.
181. Tian L, Peng G, Parant JM, Leventaki V, Drakos E, et al. (2010) Essential roles of Jab1 in cell survival, spontaneous DNA damage and DNA repair. *Oncogene* 29: 6125-6137.
182. Yanagi Y, Suzawa M, Kawabata M, Miyazono K, Yanagisawa J, et al. (1999) Positive and negative modulation of vitamin D receptor function by transforming growth factor-beta signaling through smad proteins. *J Biol Chem* 274: 12971-12974.
183. Shaffer PL, Gewirth DT (2004) Vitamin D receptor-DNA interactions. *Vitam Horm* 68: 257-273.
184. Nagaki M, Moriwaki H (2008) Transcription factor HNF and hepatocyte differentiation. *Hepatol Res*.
185. Fernandez C, Gregory WF, Loke P, Maizels RM (2002) Full-length-enriched cDNA libraries from *Echinococcus granulosus* contain separate populations of oligo-capped and trans-spliced transcripts and a high level of predicted signal peptide sequences. *Mol Biochem Parasitol* 122: 171-180.
186. Mangone M, Manoharan AP, Thierry-Mieg D, Thierry-Mieg J, Han T, et al. (2010) The landscape of *C. elegans* 3'UTRs. *Science* 329: 432-435.
187. Peri S, Pandey A (2001) A reassessment of the translation initiation codon in vertebrates. *Trends Genet* 17: 685-687.
188. Kozak M (1987) An analysis of 5'-noncoding sequences from 699 vertebrate messenger RNAs. *Nucleic Acids Res* 15: 8125-8148.
189. Hadzopoulou-Cladaras M, Kistanova E, Evagelopoulou C, Zeng S, Cladaras C, et al. (1997) Functional domains of the nuclear receptor hepatocyte nuclear factor 4. *J Biol Chem* 272: 539-550.

190. Ryffel GU (2001) Mutations in the human genes encoding the transcription factors of the hepatocyte nuclear factor (HNF)1 and HNF4 families: functional and pathological consequences. *J Mol Endocrinol* 27: 11-29.
191. Brehm K, Spiliotis M (2008) The influence of host hormones and cytokines on *Echinococcus multilocularis* signalling and development. *Parasite* 15: 286-290.
192. Ruddell RG, Mann DA, Ramm GA (2008) The function of serotonin within the liver. *J Hepatol* 48: 666-675.
193. Beaudry P, Hadengue A, Callebort J, Gaudin C, Soliman H, et al. (1994) Blood and plasma 5-hydroxytryptamine levels in patients with cirrhosis. *Hepatology* 20: 800-803.
194. Lesurtel M, Graf R, Aleil B, Walther DJ, Tian Y, et al. (2006) Platelet-derived serotonin mediates liver regeneration. *Science* 312: 104-107.
195. Konrad C (2007) Molecular analysis of insulin signaling mechanisms in *Echinococcus multilocularis* and their role in the host-parasite interaction in the alveolar echinococcosis. [PhD]. Würzburg: University of Würzburg.
196. Graf M (2006) Charakterisierung einer bisher noch unbekanntenen MAPK aus dem Fuchsbandwurm *Echinococcus multilocularis*. [Bachelor]. Würzburg: University of Würzburg.
197. Widmann C, Gibson S, Jarpe MB, Johnson GL (1999) Mitogen-activated protein kinase: conservation of a three-kinase module from yeast to human. *Physiol Rev* 79: 143-180.
198. Brehm K, Carlton JM, Hoffmann KF (2012) Parasite genomics and post-genomic activities: 21st century resources for the parasite immunologist. *Parasite Immunol* 34: 47-49.
199. Olson PD, Zarowiecki M, Kiss F, Brehm K (2012) Cestode genomics - progress and prospects for advancing basic and applied aspects of flatworm biology. *Parasite Immunol* 34: 130-150.
200. Sheng Z, Liang Y, Lin CY, Comai L, Chirico WJ (2005) Direct regulation of rRNA transcription by fibroblast growth factor 2. *Mol Cell Biol* 25: 9419-9426.
201. Kosako H, Gotoh Y, Nishida E (1994) Requirement for the MAP kinase kinase/MAP kinase cascade in *Xenopus* oocyte maturation. *EMBO J* 13: 2131-2138.
202. Hung KW, Kumar TK, Kathir KM, Xu P, Ni F, et al. (2005) Solution structure of the ligand binding domain of the fibroblast growth factor receptor: role of heparin in the activation of the receptor. *Biochemistry* 44: 15787-15798.
203. Roth GJ, Heckel A, Colbatzky F, Handschuh S, Kley J, et al. (2009) Design, synthesis, and evaluation of indolinones as triple angiokinase inhibitors and the discovery of a highly specific 6-methoxycarbonyl-substituted indolinone (BIBF 1120). *J Med Chem* 52: 4466-4480.
204. Hilberg F, Roth GJ, Krssak M, Kautschitsch S, Sommergruber W, et al. (2008) BIBF 1120: triple angiokinase inhibitor with sustained receptor blockade and good antitumor efficacy. *Cancer Res* 68: 4774-4782.
205. Eiselleova L, Matulka K, Kriz V, Kunova M, Schmidtova Z, et al. (2009) A complex role for FGF-2 in self-renewal, survival, and adhesion of human embryonic stem cells. *Stem Cells* 27: 1847-1857.
206. Thompson RC (2008) The taxonomy, phylogeny and transmission of *Echinococcus*. *Exp Parasitol* 119: 439-446.
207. Clark IB, Muha V, Klingseisen A, Leptin M, Muller HA (2011) Fibroblast growth factor signalling controls successive cell behaviours during mesoderm layer formation in *Drosophila*. *Development* 138: 2705-2715.
208. Murakami M, Nguyen LT, Zhuang ZW, Moodie KL, Carmeliet P, et al. (2008) The FGF system has a key role in regulating vascular integrity. *J Clin Invest* 118: 3355-3366.
209. Polanska UM, Fernig DG, Kinnunen T (2009) Extracellular interactome of the FGF receptor-ligand system: complexities and the relative simplicity of the worm. *Dev Dyn* 238: 277-293.
210. Lo TW, Bennett DC, Goodman SJ, Stern MJ (2010) *Caenorhabditis elegans* fibroblast growth factor receptor signaling can occur independently of the multi-substrate adaptor FRS2. *Genetics* 185: 537-547.

211. Coulier F, Pontarotti P, Roubin R, Hartung H, Goldfarb M, et al. (1997) Of worms and men: an evolutionary perspective on the fibroblast growth factor (FGF) and FGF receptor families. *J Mol Evol* 44: 43-56.
212. Huang P, Stern MJ (2005) FGF signaling in flies and worms: more and more relevant to vertebrate biology. *Cytokine Growth Factor Rev* 16: 151-158.
213. Czermak BV, Akhan O, Hiemetzberger R, Zelger B, Vogel W, et al. (2008) Echinococcosis of the liver. *Abdom Imaging* 33: 133-143.
214. Bohm F, Kohler UA, Speicher T, Werner S (2010) Regulation of liver regeneration by growth factors and cytokines. *EMBO Mol Med* 2: 294-305.
215. Kan NG, Junghans D, Izpisia Belmonte JC (2009) Compensatory growth mechanisms regulated by BMP and FGF signaling mediate liver regeneration in zebrafish after partial hepatectomy. *FASEB J* 23: 3516-3525.
216. Mooijaart SP, Brandt BW, Baldal EA, Pijpe J, Kuningas M, et al. (2005) *C. elegans* DAF-12, Nuclear Hormone Receptors and human longevity and disease at old age. *Ageing Res Rev* 4: 351-371.
217. Van Gilst MR, Hadjivassiliou H, Jolly A, Yamamoto KR (2005) Nuclear hormone receptor NHR-49 controls fat consumption and fatty acid composition in *C. elegans*. *PLoS Biol* 3: e53.
218. Escobedo G, Soldevila G, Ortega-Pierres G, Chavez-Rios JR, Nava K, et al. (2010) A new MAP kinase protein involved in estradiol-stimulated reproduction of the helminth parasite *Taenia crassiceps*. *J Biomed Biotechnol* 2010: 747121.
219. Bujold M, Gopalakrishnan A, Nally E, King-Jones K (2010) Nuclear receptor DHR96 acts as a sentinel for low cholesterol concentrations in *Drosophila melanogaster*. *Mol Cell Biol* 30: 793-805.
220. Horner MA, Pardee K, Liu S, King-Jones K, Lajoie G, et al. (2009) The *Drosophila* DHR96 nuclear receptor binds cholesterol and regulates cholesterol homeostasis. *Genes Dev* 23: 2711-2716.
221. Bernthaler P, Epping K, Schmitz G, Deplazes P, Brehm K (2009) Molecular characterization of EmABP, an apolipoprotein A-I binding protein secreted by the *Echinococcus multilocularis* metacestode. *Infect Immun* 77: 5564-5571.
222. McManus DP, Bryant C, editors (1986) *Biochemistry and physiology of Echinococcus*. London, United Kingdom: George Allen and Unwin Ltd. 114-136 p.
223. Motola DL, Cummins CL, Rottiers V, Sharma KK, Li T, et al. (2006) Identification of ligands for DAF-12 that govern dauer formation and reproduction in *C. elegans*. *Cell* 124: 1209-1223.
224. Antebi A, Culotti JG, Hedgecock EM (1998) *daf-12* regulates developmental age and the dauer alternative in *Caenorhabditis elegans*. *Development* 125: 1191-1205.
225. Ludewig AH, Kober-Eisermann C, Weitzel C, Bethke A, Neubert K, et al. (2004) A novel nuclear receptor/coregulator complex controls *C. elegans* lipid metabolism, larval development, and aging. *Genes Dev* 18: 2120-2133.
226. Sieber MH, Thummel CS (2009) The DHR96 nuclear receptor controls triacylglycerol homeostasis in *Drosophila*. *Cell Metab* 10: 481-490.
227. Monteiro KM, de Carvalho MO, Zaha A, Ferreira HB (2010) Proteomic analysis of the *Echinococcus granulosus* metacestode during infection of its intermediate host. *Proteomics* 10: 1985-1999.
228. Shostak Y, Van Gilst MR, Antebi A, Yamamoto KR (2004) Identification of *C. elegans* DAF-12-binding sites, response elements, and target genes. *Genes Dev* 18: 2529-2544.
229. Shostak Y, Yamamoto KR (2005) Overlapping but separable determinants of DNA binding and nuclear localization map to the C-terminal end of the *Caenorhabditis elegans* DAF-12 DNA binding domain. *J Biol Chem* 280: 6554-6560.
230. Voght SP, Fluegel ML, Andrews LA, Pallanck LJ (2007) *Drosophila* NPC1b promotes an early step in sterol absorption from the midgut epithelium. *Cell Metab* 5: 195-205.
231. Antonson P, Jakobsson T, Almlof T, Guldevall K, Steffensen KR, et al. (2008) RAP250 is a coactivator in the transforming growth factor beta signaling pathway that interacts with Smad2 and Smad3. *J Biol Chem* 283: 8995-9001.

-
232. MacDonald PN, Dowd DR, Zhang C, Gu C (2004) Emerging insights into the coactivator role of NCoA62/SKIP in Vitamin D-mediated transcription. *J Steroid Biochem Mol Biol* 89-90: 179-186.
233. Dhe-Paganon S, Duda K, Iwamoto M, Chi Yi, Shoelson SE (2002) Crystal structure of the HNF4 alpha ligand binding domain in complex with endogenous fatty acid ligand. *J Biol Chem* 277: 37973-37976.
234. Wisely GB, Miller AB, Davis RG, Thornquest AD, Jr., Johnson R, et al. (2002) Hepatocyte nuclear factor 4 is a transcription factor that constitutively binds fatty acids. *Structure* 10: 1225-1234.
235. Palanker L, Tennessen JM, Lam G, Thummel CS (2009) *Drosophila* HNF4 regulates lipid mobilization and beta-oxidation. *Cell Metab* 9: 228-239.
236. Jakobsson E, Alvite G, Bergfors T, Esteves A, Kleywegt GJ (2003) The crystal structure of *Echinococcus granulosus* fatty-acid-binding protein 1. *Biochim Biophys Acta* 1649: 40-50.
237. Lucas Sd S, Lopez-Alcorocho JM, Bartolome J, Carreno V (2004) Nitric oxide and TGF-beta1 inhibit HNF-4alpha function in HEPG2 cells. *Biochem Biophys Res Commun* 321: 688-694.
238. Ishikawa F, Nose K, Shibamura M (2008) Downregulation of hepatocyte nuclear factor-4alpha and its role in regulation of gene expression by TGF-beta in mammary epithelial cells. *Exp Cell Res* 314: 2131-2140.
239. Peiler G, Bockmann B, Nakhei H, Ryffel GU (2000) Inhibitor of the tissue-specific transcription factor HNF4, a potential regulator in early *Xenopus* development. *Mol Cell Biol* 20: 8676-8683.
240. Mosialou I, Zannis VI, Kardassis D (2010) Regulation of human apolipoprotein m gene expression by orphan and ligand-dependent nuclear receptors. *J Biol Chem* 285: 30719-30730.
241. Taubert S, Ward JD, Yamamoto KR (2011) Nuclear hormone receptors in nematodes: evolution and function. *Mol Cell Endocrinol* 334: 49-55.
242. Elsadek B, Kratz F (2011) Impact of albumin on drug delivery - New applications on the horizon. *J Control Release*.
243. Iwata K, Asawa Y, Nishizawa S, Mori Y, Nagata S, et al. (2012) The development of a serum-free medium utilizing the interaction between growth factors and biomaterials. *Biomaterials* 33: 444-454.
244. Abe MK, Kuo WL, Hershenson MB, Rosner MR (1999) Extracellular signal-regulated kinase 7 (ERK7), a novel ERK with a C-terminal domain that regulates its activity, its cellular localization, and cell growth. *Mol Cell Biol* 19: 1301-1312.
245. Abe MK, Saelzler MP, Espinosa R, 3rd, Kahle KT, Hershenson MB, et al. (2002) ERK8, a new member of the mitogen-activated protein kinase family. *J Biol Chem* 277: 16733-16743.
246. Bogoyevitch MA, Court NW (2004) Counting on mitogen-activated protein kinases--ERKs 3, 4, 5, 6, 7 and 8. *Cell Signal* 16: 1345-1354.
247. Zacharogianni M, Kondylis V, Tang Y, Farhan H, Xanthakis D, et al. (2011) ERK7 is a negative regulator of protein secretion in response to amino-acid starvation by modulating Sec16 membrane association. *EMBO J* 30: 3684-3700.

10. Acknowledgement – Danksagung

An dieser Stelle möchte ich mich bei einigen Personen herzlich bedanken:

Prof. Klaus Brehm für die Bereitstellung meines Promotionsthemas, die gute Betreuung und stetige Unterstützung, sowie die lebhaften Exkursionen in Sachen Evolution, Religion und Geschichte.

Prof. Dr. Roy Gross und Prof. Dr. Andrew Hemphill für die Übernahme der Gutachten als Mitglieder des Promotionskomitees.

Dr. Nicolai Siegel für die spontane Übernahme der Korrektur in Vertretung für Prof. Dr. Andrew Hemphill.

Prof. Dr. Matthias Frosch für die freundliche Aufnahme am Institut für Hygiene und Mikrobiologie.

PD Dr. Joachim Clos für die Möglichkeit die massenspektrometrischen Analysen am Bernard-Nocht-Institut für Tropenmedizin durchführen zu können.

Meiner Arbeitsgruppe möchte ich für die angenehme Arbeitsatmosphäre danken. Liebe Echis und Ex-Echis - Dankeschön: Moni Bergmann, Verena Gelmedin, Sarah Hemer, Ferenc Kiss, Markus Spiliotis, Dirk Radloff, Corinna Reiher, Clara Albani, Justin Nono, Kerstin Epping, und Steffie Riedl.

Dank auch an die Azubis für unzählige Western Blots, Proteinbestimmungen und Zellkulturversuche: Christin Staar, Romy Lorenz, Marie Dankworth und Astrid Dylida.

Insbesondere möchte ich an dieser Stelle Moni Bergmann erwähnen. Du hast mir mit deinem Wissen und deiner Erfahrung viele technische Details und Tricks näher gebracht. Vielen Dank bei der tatkräftigen Unterstützung im Labor – ohne dich würde ich noch heute Yeast-Two-Hybrids pipettieren.

Außerdem ein herzliches Dankeschön an die „Helfer im Hintergrund“ vom IHM: im Tierstall Rainer Brandner, wenn ich wieder mal Extrawünsche hatte; Michael Ullrich in allen Notsituationen und bei kaputten Zentrifugen; Stefan Simon, wenn Pipetten gerichtet werden mussten; Günther Troll von der Pforte mit immer guter Laune sowie Matthias Brandt, bei Softwareproblemen.

Natürlich möchte ich ebenfalls die guten Seelen vom Institut, Ida Paul und Edeltraud Rausch erwähnen – danke für die Hilfsbereitschaft und Geduld – wenn ich mal wieder Fußabdrücke morgens im Labor hinterlassen habe.

Ein lieber Gruß geht auch an die alte Mittagsrunde: Moni Bergmann, Steffie Dille, Tessa van Alen und Sarah Hemer. Beim Schafkopfen hatte ich immer viel Spaß. Danke!

Steffi Dille und Gabi Ommen möchte ich ins besondere für die tiefe Freundschaft danken. Außerdem danke ich Euch, für die unendliche Geduld und den großen Zuspruch. Ich vermisse die Kaffeepausen und Mädelsabende wirklich sehr!

Einen ganz besonderen Dank möchte ich meiner Familie, insbesondere meiner Mutter und meinem Mann Frank zukommen lassen. Ihr habt mich immer unterstützt; finanziell und besonders moralisch, gerade in Momenten, in denen ich alles hinschmeißen wollte.

11. Publications

Parts of this work have been or will be published in peer reviewed journals and have been presented on international meetings as oral or poster presentations (indicated by asterisk *).

11.1. Original Publications

***Förster S**, Schäfer T, Gelmedin V, Browaeys E, Cailliau K, Dissous C, Brehm K

“An Unusual Fibroblast Growth Factor (FGF)-Receptor of *Echinococcus multilocularis* interacts with host FGF and Regulates Parasite Development”

Manuscript in preparation

*Gelmedin V, **Förster S.**, Graf M, Brehm K

“Molecular Characterization of EmMPK3, a serum-responsive MAPK of *Echinococcus multilocularis*”

Manuscript in preparation

Chrobak M, **Förster S**, Meisel S, Pfefferkorn R, Förster F, Clos, J

“*Leishmania donovani* HsIV Does Not Interact Stably with HsIU Proteins”

Journal of Parasitology, **2012**, Feb 21. [Epub ahead of print]

Wenzel UA, Bank E, Florian C, **Förster S**, Zimara N, Steinacker J, Klinger M, Reiling N, Ritter U, van Zandbergen G.

“*Leishmania major* parasite stage-dependent host cell invasion and immune evasion”

FASEB Journal, **2012**, 26(1):29-39.

***Förster S**, Günthel D, Kiss F, Brehm K

“Molecular characterization of a serum-responsive, DAF-12-like nuclear hormone receptor of the fox-tapeworm *Echinococcus multilocularis*”

Journal of Cellular Biochemistry, **2011**, 112(6):1630-42.

Ommen G, **Lorenz S**, Clos J

“One-step generation of double-allele gene replacement mutants in *Leishmania donovani*”

International Journal of Parasitology, **2009**, 39(5):541-6.

Royer JF, Schratl P, **Lorenz S**, Kostenis E, Ulven T, Schuligoi R, Peskar BA, Heinemann A

“A novel antagonist of CRTH2 blocks eosinophil release from bone marrow, chemotaxis and respiratory burst”

Allergy, **2007**, 62(12):1401-9.

11.2. Conference Contributions

11.2.1. Talks

*Brehm K, **Förster S**, Schäfer T, Gelmedin V, Dissous C

“Host-derived FGF stimulates *Echinococcus multilocularis* development by activation of a biochemically unusual cestode FGF receptor”

Joint Meeting of the German Societies of Parasitology and Protozoology, Heidelberg, Germany, **2012**
March 14-17

Förster S, Wenzel UA, Bank E, Florian C, Zimara N, Steinacker J, Klinger M, Reiling N, Ritter U, van Zandbergen G.

“Leishmania major parasite stage-dependent host cell invasion and immune evasion”

Joint Meeting of the German Societies of Parasitology and Protozoology, Heidelberg, Germany, **2012**
March 14-17

***Lorenz S**, Schäfer T, Gelmedin V, Dissous C, Brehm K

“Host derived FGF stimulates *Echinococcus multilocularis* development by activation of a biochemically unusual cestode FGF receptor”

Molecular and Cellular Biology of Helminth Parasites VI, Hydra, Greece, **2010** Sep 5-10

*Brehm K, Gelmedin V, **Lorenz S**, Hemer S, Spiliotis M

“Targeting flatworm signaling cascades for the development of novel antihelminthics”

Molecular and Cellular Biology of Helminth Parasites VI, Hydra, Greece, **2010** Sep 5-10

***Lorenz S**, Günthel D, Brehm K

“Characterization of EmNHR1 – a serum-responsive nuclear hormone receptor in *Echinococcus multilocularis*”

Joint Meeting of the German Societies of Parasitology and Protozoology, Düsseldorf, Germany, **2010**
March 16-19

*Brehm K, Konrad C, Spiliotis M, Gelmedin V, Hemer S, Schäfer T, **Lorenz S**

„Hormonal host-parasite cross-communication during larval cestode infections”

XI. International Symposium on Flatworm Biology, Hasselt, Belgium, **2009** July 26-30

Chrobak M, **Lorenz S**, Clos J

Bacterial-like HSL-VU protease in *Leishmania donovani*: a potential new drug target? 4th World Congress on Leishmaniasis, Lucknow, India, **2009** February 6-8

***Lorenz S**, Günthel D, Brehm K

“Molecular Characterization of Nuclear Hormone Receptor Signaling Mechanisms in the Human Parasite *Echinococcus multilocularis*”

DGP 3rd Short Course for Young Parasitologists, Bernhard-Nocht-Institute for Tropical Medicine, Hamburg, Germany, **2008** March 1-4

11.2.2. Poster

*Hemer S, Gelmedin V, Konrad C, **Lorenz S**, Brehm K

Targeting *Echinococcus* signaling cascades for developing novel anti-infectives

Joint Meeting of the German Societies of Parasitology and Protozoology, Düsseldorf, Germany, **2010**
March 16-19

***Lorenz S**, Günthel D, Brehm K

“EmNHR1 – characterization of a serum-responsive nuclear hormone receptor in *Echinococcus multilocularis*”

XI. International Symposium on Flatworm Biology, Hasselt, Belgium, **2009** July 26-30

***Lorenz S**, Günthel D, Brehm K

“Nuclear hormone receptor signaling in the human parasite *Echinococcus multilocularis*”

4th International Symposium of the Graduate School of Life Sciences Würzburg, Würzburg, Germany,
2009 March 26-27

Clos J, Ommen G, **Lorenz S**

“One-step generation of double-allele gene replacement mutants in *Leishmania donovani*”

4th World Congress on Leishmaniasis, Lucknow, India, **2009** February 6-8

12. Curriculum Vitae

Name **Sabine Förster**

Place of Birth **Zeitz**

Date of Birth **07 February 1982**

- Dec 2011 - current Research Associate
Paul-Ehrlich-Institute, Federal Institute for Vaccines and Biomedicines,
Langen, Germany
- Feb 2011 – Nov 2011 Research Associate
University of Ulm, Germany
Institute of Medical Microbiology and Hygiene/ Institute of Molecular Virology
- May 2007 – Jan 2011 PhD Studies (Dr. rer. nat.)
University of Würzburg, Germany
Institute of Hygiene and Microbiology
Thesis: “Nuclear Hormone Receptors and Fibroblast Growth Factor Receptor Signaling
in *Echinococcus multilocularis*”
- Supervision: Prof. Klaus Brehm (Würzburg, Germany)
Prof. Roy Gross (Würzburg, Germany)
Prof. Andrew Hemphill (Bern, Switzerland)
Dr. Nicolai Siegel (Würzburg, Germany)
- Oct 2005 – Mar 2007 Graduate Studies (Master of Science)
University of Würzburg, Germany
Bernhard-Nocht-Institute for Tropical Medicine, Hamburg, Germany
Parasitology Section, Leishmaniasis
Thesis: “Characterisation of HSL-VU proteases in parasites of the genus *Leishmania* “
- Supervision: PD Joachim Clos (BNI, Hamburg, Germany)
Prof. Heidrun Moll (University of Würzburg, Germany)
- Oct 2002 – Sep 2005 Undergraduate Studies (Bachelor of Science)
University of Würzburg, Germany
Center for Infectious Diseases
Bachelor thesis: “Identification and characterization of anti-leishmanial compounds”
- Supervision: Prof. Heidrun Moll (Würzburg, Germany)
Prof. Alicia Ponte-Sucre (Würzburg, Germany)

Würzburg, March 7th 2012

Sabine Förster